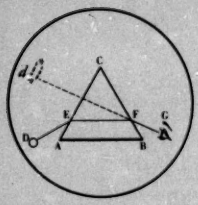

optics and spectroscopy

volume ix
number 3
september 1960

OPTICAL SOCIETY OF AMERICA

USSR ACADEMY OF SCIENCES

RUSSIAN EDITORIAL STAFF FOR
OPTIKA I SPEKTROSKOPIYA sponsored by
USSR ACADEMY OF SCIENCES

Editor: S. E. FRISH

Assistant Editor: P. P. FEOFILOV
Corresponding Secretary: L. S. SAZONOV

Associate Editors:

M. M. GUREVICH M. A. EL'IASHEVICH A. A. LEBEDEV V. P. LINNIK
S. L. MANDEL'SHTAM I. V. OBREIMOV V. K. PROKOF'EV
N. N. SOBOLEV A. N. TERENIN A. I. TUDOROVSKII

Translated from *OPTIKA I SPEKTROSKOPIYA* on the initiative of THE OPTICAL SOCIETY OF AMERICA, INC. with a grant-in-aid from THE NATIONAL SCIENCE FOUNDATION. *Optics and Spectroscopy* is a cover-to-cover translation of *Optika i Spektroskopiya* and no attempt is made to edit the material other than to correct obvious misprints. The views are those of the original authors and do not represent the Optical Society of America.

TRANSLATION EDITORIAL STAFF

Scientific Editors

CYRUS FELDMAN, *Oak Ridge National Laboratory*

CARL W. GARLAND, *Massachusetts Institute of Technology*

MATHEW G. GIBBONS, *Oakland, California*

Administrative Editor: PATRICIA R. WAKELING, *OSA*

Published monthly by the Optical Society of America, Inc. Executive office: 1155 Sixteenth Street, N.W., Washington, D.C. Subscriptions for one year to members of the Society: Associates $13.00; Regular members and Fellows $17.00. Subscriptions for non-members of the Society: One year U. S. and Possessions, $25.00; Foreign $28.00. Back numbers: $3.00 per copy. Subscriptions, changes of address and undeliverable copies should be referred to the Executive offices in Washington, D.C. The office of publication is 2500 South State Street, Ann Arbor, Michigan. Second class postage paid at Ann Arbor, Michigan.

Printed in the U.S.A. by Edwards Brothers, Inc., Ann Arbor, Michigan.

CONCENTRATION OF ATOMS IN THE ARC PLASMA AS DETERMINED BY THE PULSE ABSORPTION METHOD

L. D. Kondrasheva and I. V. Podmoshenskii

Received 17 October 1959

This paper describes a pulse method which gives the instantaneous absorption spectrum of a plasma at temperatures up to 6000°K. It was found that in the Fe-Cu direct current arc, the volume occupied by atoms excited to about 3 ev comprises only about 30% of the volume occupied by unexcited atoms. The instantaneous concentrations of Fe, Cr, and Mn were determined.

The main difficulty in the determination of atomic concentrations in plasma from absorption spectra is the plasma's own emission, which alters the absorption spectrum. This emission, according to Kirchhoff's law, always exists in the region of true absorption. Therefore, for photographic recording it is desirable to have a source of continuous radiation whose brightness exceeds that of the plasma investigated by not less than two orders of magnitude.* Commercially available gas discharge lamps are difficult to use under stationary or pulsed conditions, because of their insufficient brightness or the short duration of the high intensity pulse. Successful results were obtained only with special capillary lamps working under the conditions close to their limit of operation.[1]

*For smaller difference in brightness, it is necessary to correct for the emission of the plasma itself, but this is difficult to accomplish.

For this purpose, it appeared to be very convenient to use an EV-39 pulsed light source, whose emission spectrum is close to that of an absolute black body at about 40,000°K.[2,3] With this light source, it was possible to obtain the absorption spectra of plasmas up to 6000°K without correcting for the plasma's own emission. The energy of one flash from this source is sufficient for photographing the spectrum with a high dispersion spectrograph ($d\lambda/dl \approx 0.5$ A/mm; A = 1 : 50). This permits an almost instantaneous (about 10^{-4} sec) description of the space distribution of absorbing atoms in the plasma.

In this work the plasma of a direct current arc in air between vertically mounted metallic electrodes was investigated.

First of all, a picture of the radial distribution of atoms in the arc column was sought. The basic layout of the equipment is presented in Fig. 1. The discharge gap 1 of the pulsed source of continuous radiation, magnified three times, was projected onto the plasma of a direct current arc 2, which in turn was magnified 1.5 times and projected on the slit 3 of the ISP-51 spectrograph with an autocollimating UF-85 camera. In order to obtain the absorption spectrum of a cross section of the arc, its image was rotated 90° around the optical axis with the aid of a Dove prism 4. In front of the slit we placed a shutter 5 whose exposure time was slightly longer than the duration of the pulse. The opening of the shutter was synchronized with the trigger of the pulsed source by a signal from photocell 6 through a pulse amplifier 7. The photocell was illuminated by a 100 watt incandescent point source (lamp 8).

The absorption spectra of the arc were obtained under the following conditions: the lower electrode was made of samples of steel V of series UIM with small contents of Cr, Mn, Ni, W, Si, and other elements; the upper electrode was a copper bar machined to a truncated cone; the current was 5 amp and there was an electrode gap of 2 mm.

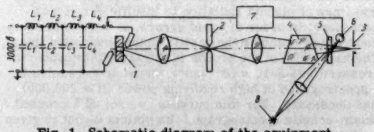

Fig. 1. Schematic diagram of the equipment.

The insufficient resolving power of the ISP-51 spectrograph did not permit the exact determination of either the concentration of the atoms or their radial distribution. Therefore, the visually determined length of spectral lines was chosen as characterizing these quantities. Low intensity lines were used for this purpose because they are more sensitive to changes in concentration, although experiment showed that even the use of high intensity lines does not alter the results appreciably.

Table 1 presents the wavelengths of several lines of Fe and Cr, the potentials of their lower levels, and the arc diameters as estimated from the observed length of these lines. Assuming axial symmetry of the arc, it can be concluded from the data in Table 1 that the part of the plasma volume occupied by atoms on the energy level of about 3 ev comprises about 30% of the volume occupied by atoms on the ground level.

Table 1

λ (A)	Lower level (ev)	Arc diameter (mm)	λ (A)	Lower level (ev)	Arc diameter (mm)
CrI 4254.3	0.00	4	FeI 4143.4	3.05	1.8
CrI 4274.8	0.00	4	FeI 4181.7	2.83	2.3
FeI 4271.7	1.48	3.8	FeI 4199.1	3.05	2.0
FeI 4307.9	1.56	3.5	FeI 4227.4	3.3	1.9
FeI 4325.7	1.60	4	FeI 4233.6	2.48	2.2
FeI 4375.9	0.00	4	FeI 4235.9	2.42	2.2
FeI 4404.7	1.56	3.5	FeI 4260.4	2.40	2.4
FeI 4427.3	0.05	4	FeI 4298.2	2.42	2.2

In a thermal light source, a necessary condition for the formation of nonhomogeneity appears to be a localized change of the factor $\exp(-h\nu/kT)$, which determines the ratio between the populations of the levels between which the transition occurs. At $\lambda = 4000$ A, this factor can differ tenfold between the center of the arc and its periphery which also results in absorption by the external layer. It is interesting to note that if only one transition in the atom is responsible for emitting the frequency ν, and all other conditions are unchanged, the radiation approaches closer to homogeneity as $h\nu/kT$ decreases. For this reason, a source tends to show greater homogeneity at longer wavelengths. For a given wavelength, better homogeneity is more probable with a source having a higher tempera-

ture. Good homogeneity can therefore be expected in the visible spectrum of a high temperature ($T > 10^5$ °K) plasma.

It is necessary to point out that the dimensions of the absorption zone and the concentration of atoms in it depend largely on the discharge conditions. A high-power pulsed arc (300-400 amp) between metallic electrodes has a fully reversed arc spectrum, which indicates appreciable optical thickness of the reversing layer.[4] In this case, the reversing layer is formed by the cooling of the plasma streams emerging from the cathode and anode.

Let us discuss the problem of the determination of the concentration of atoms in the plasma of an arc by the pulse absorption method. Since in the majority of the cases the available information on the profiles of spectral lines of plasma radiation is insufficient, it was necessary, in order to avoid errors, to work with equipment which resolves the profile of the absorption line. The half-width of the profile in the arc at atmospheric pressure was $2\text{-}10 \times 10^{-1}$ cm^{-1}. In order to resolve it, a spectrograph of high resolving power ($R \approx 200{,}000$) was necessary. For this purpose, we set up a crossed prism-echelle spectrograph.[5] Its optical layout is given in Fig. 2.*

*The authors are grateful to F. M. Gerasimov and G. P. Startsev for furnishing parts necessary for the building of the equipment with an echelle.

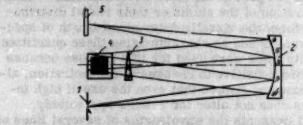

Fig. 2. Optical arrangement of the device with an echelle. 1—Entrance slit; 2—concave mirror; 3—prism; 4—echelle; and 5—spectral plane.

When an echelle is crossed with a prism, the spectra of different orders are located in strips one below the other. The spectrum between 2000 A (70th order) and 5000 A (28th order) was distributed over 42 strips. To avoid the superposition of orders, the height of the entrance slit (i.e., the height of the spectrum in a strip) was limited to 0.5 mm. The actual resolving power of the instrument was evaluated by the absorption spectrum of iodine vapor, and was found to be $R \approx 180{,}000$. The linear dispersion was 0.25 A/mm at 2000 A and 0.64 A/mm at 5000 A. Using this equipment, a single pulse of an EV-39 was sufficient to obtain the absorption spectrum of the whole photographic region.

Investigation of the spectrograms obtained shows that the pulsed source has a uniform continuous spectrum (Fig. 3) with a few absorption lines arising in its peripheral regions.

A direct determination of the concentrations of Cr, Mn, and Fe atoms was accomplished by measuring the total absorption of the lines of these elements which were excited by a 2 amp direct current arc having a 2 mm gap between the metal electrodes. The lower electrode, steel V of the series UIM, was the cathode, and the upper electrode, copper machined to a truncated cone, was the anode. In order to obtain darker exposures and some averaging, two pulses were photographed for each spectrum. The data on the resonance lines measured are given in Table 2.

Table 2

Element	λ (A)	Transition	f	Ratio of intensities in multiplet (theoretical)
Cr I	4254.3 4274.8 4289.7	$a^7S - z^7P^0$	0.035 0.025 0.019	9 : 7 : 5
Mn I	4030.7 4033.07 4034.5	$a^6S - z^6P^0$	0.062 0.046 0.031	8 : 6 : 4
Fe I	3719.9 2912.15	$a^5D_4 - z^5F_5^0$ $a^5D_4 - y^5F_5^0$	0.043 $8 \cdot 10^{-4}$	—

The concentrations were calculated using the formula

$$N_i = \frac{mc^2}{\pi e^2 f_{ik} \lambda^2} \int k_\lambda d\lambda,$$

where N_i is the concentration of atoms at the i-th level, m is the mass of an electron, e the electronic charge, c the velocity of light, f_{ik} the oscillator strength, and k_λ the coefficient of absorption.

The coefficient of absorption k_λ was determined from the logarithm of the ratio of the intensity of the continuous spectrum I_0 to its intensity at various points on the absorption profile, I_λ. The integral $\int k_\lambda d\lambda$ is numerically equal to the area of the profile of the absorption line.

Since the arc is a relatively high temperature (5000-6000 K) source, then according to the Boltzmann distribution, levels a little higher than the ground state can be populated. Consequently, when calculating the concentrations of atoms in the arc plasma, one must consider the sum function for states B(T), i.e.,

$$N = \frac{N_1}{g_1}\left(g_1 + g_2 e^{-\frac{\Delta E_{1,2}}{kT}} + g_3 e^{-\frac{\Delta E_{1,3}}{kT}} + \ldots\right) = \frac{N_1}{g_1} B(T),$$

where N is the total number of atoms of a given element, N_1 is the number of atoms in the ground state, $g_{1,2,3,\ldots}$ are the statistical weights, and $E_{1,2;1,3;\ldots}$ are the potentials of corresponding levels.

Fig. 3. Spectrum of pulsed source.

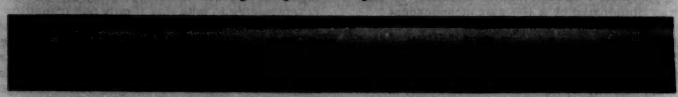

Fig. 4. Absorption spectrum of the arc.

The calculations showed that taking $T_{arc} = 5200°K$, we obtain $N \approx 1.5N_1$ for Cr I and $N \approx 3N_1$ for Fe I. For Mn I this correction appeared to be unimportant because of the absence of intermediate levels below 2 ev. Figure 4 shows the absorption spectrum of the arc which resembles a positive emission spectrum. The most intense lines of the emission spectrum (especially when they correspond to transitions to the ground state) give the most intense absorption. In addition to the arc lines, lines of Fe II are also observed. Figures 5-7 show the observed absorption profiles of Cr, Mn, and Fe lines. The evaluation of the influence of "ghosts" on the calculated concentrations of atoms showed that it is necessary to consider them only when the absorption is fairly intense (when $\Delta \log I \geq 0.025$-0.3).

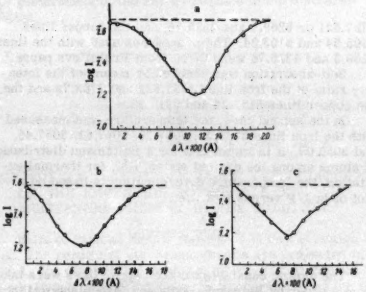

Fig. 5. Profiles of the absorption lines of the chromium triplet. λ (in A): a—4254.3; b—4274.8; and c—4289.7.

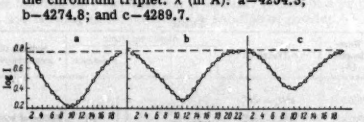

Fig. 6. Profiles of the absorption lines of the manganese triplet. λ (in A): a—4030.76; b—4033.07; and c—4034.5

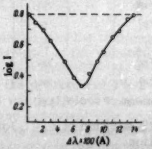

Fig. 7. Profile of the absorption of iron (λ 2912.1 A).

The data on the concentration measurements, corrected for the influence of the echelle's "ghosts," are presented in Table 3. The relative intensities of multiplet lines, obtained from these measurements, are also given in Table 3. In order to avoid consideration of the instrumental profile, spectra with very intense absorption were excluded.

Table 3

Element	No. of the steel sample and the value of the relative concentration of the element (%)	Relative intensities in the multiplet	Absolute concentration ($N \times 10^{-13}$)	Relative concentration of atoms in the plasma $\frac{C_{Cr}}{C_{Mn}}$ (%)
Cr	№ 57 — 5.05	9 : 7.0 : 5.0	1.47	—
	№ 57 — 5.05	9 : 7.03 : 5.3	1.7	1
	№ 57 — 5.05	9 : 6.8 : 4.6	2.8	—
	№ 56 — 2.1	9 : 7.1 : 5.0	0.93	1.2
	№ 55 — 0.58	9 : 7.0 : 4.8	0.7	0.51
		Mean 9 : 7.0 : 4.9		
Mn	№ 57 — 2.05	—	0.74	0.5
	№ 57 — 2.05	8 : 6.1 : 4.4	1.2	—
	№ 56 — 1.06	8 : 6.0 : 4.0	0.35	0.45
	№ 56 — 1.06	8 : 6.0 : 4.8	0.4	
	№ 55 — 0.57	8 : 5.7 : 3.7	0.4	0.3
		Mean 8 : 5.9 : 4.2		
Fe	№ 57	—	170	—
	№ 56	—	78	—
	№ 55	—	130	—

From the reproducibility of the multiplet ratios given in Table 3, and also from their close agreement with theoretical values, it can be concluded that the mean error in the determination of the relative concentrations of atoms was about ±5%. The accuracy in the measurement of the instantaneous absolute concentrations (excluding errors in the absolute values of f) depends on the reliability of our knowledge of the temperature distribution in the cross section of the arc. This last condition determines the change of the sum function B(T). For example, a temperature change from 4000° to 5200°K changes B(T) about 20% for Cr and about 12% for Fe.

The data in Table 3, as well as experience gained during this investigation, indicate that the composition of the direct current arc plasma between metal electrodes is subject to great changes which are determined by the influx of electrode matter into the gap. Unfortunately, this situation made it impossible to draw definite quantitative conclusions about the composition of the arc plasma.

REFERENCES

1. W. R. S. Garton and A. Rajaretnam, Proc. Phys. Soc. A70, 815 (1957).
2. I. V. Podmoshenskii and N. N. Ogurtsova, Opt. i Spektr. 4, 539 (1958).
3. M. I. Demidov, N. N. Ogurtsova, and I. V. Podmoshenskii, Zhur. Opt.-Mekh. Prom. 1, 1 (1960).
4. Yu. N. Denisyuk, Diplomnaya rabota (Thesis). LITMO, 1954.
5. G. Harrison, J. Opt. Soc. Am. 39, 522 (1949).

INVESTIGATION OF A HIGH-FREQUENCY DISCHARGE WITH HYDRODYNAMIC COMPRESSION

Zh. Zheenbaev

Received 21 December 1959

The temperature characteristics of a high frequency discharge with hydrodynamic compression have been investigated. This paper presents the results of a study of the effect of various discharge conditions on the temperature of the source and the intensities of spectral lines. Temperatures in the discharge were measured with the aid of iron and copper lines and found to be approximately 6800°K.

INTRODUCTION

In previous papers[1,2] we suggested a high frequency discharge with hydrodynamic compression as a light source for the spectral analysis of solutions. A UKV generator having a frequency of 11.2 Mck with two GK-3000 tubes was used for generating the high frequency electromagnetic oscillations. A quarter-wavelength, two-wire line was coupled to the oscillating circuit of the generator by means of a capacitance and an inductance; the high frequency discharge occurred on one end of the line. We used a water-cooled, permanent copper electrode as the upper electrode; the lower electrode was one of the cylindrical connected containers made of plexiglass.

This discharge was subjected to an intense hydrodynamic compression in order to stabilize the discharge, increase the temperature, and prolong the working life of the discharge gap. As was shown, this discharge shows adequate stability and high sensitivity for the analysis of solutions, as well as some properties not attainable in other types of light sources.

The present investigation made a study of the temperature characteristics of this discharge. These characteristics were determined by procedures similar to those used for the dc and ac arc, so that the results obtained and the mechanisms of excitation could be compared.

All investigations and measurements were made with the setup described previously.[1] The spectra were photographed with a DFS-2 spectrograph having a 600 line/mm grating; the spectrograph slit was 0.01 mm. A three lens illumination system was used. Only the central portion of the discharge was projected onto the spectrograph slit. The spectra were photographed on RF-3 film, using 5 to 20 sec exposures. The solution to be analyzed was prepared with distilled water. The method for introducing the solution and the shape of the electrodes remained unchanged. The measurement and determination of the discharge temperature were made by using the atomic lines of iron and copper.

DETERMINATION OF THE DISCHARGE TEMPERATURE

For determination of the temperature by means of the iron lines, ten lines were selected. Their transition probabilities were measured by various methods. The measurements were made by applying an algebraic formula to the intensities of two lines or by using a graph expressing the same relationship for several lines.

In the first case, the temperature was determined from the intensity ratios of the iron lines 3859.913 and 3727.621 or 5269.5 and 4325.76, and the copper lines 5105.54 and 5153.24. The procedures used with the lines 5269.5 and 4325.76 were taken from Prokof'evs paper.[3]

Self-absorption was checked by means of the intensity ratio of the iron lines 3727.621 and 3763.79 and the the copper lines 5153.24 and 5218.20.

In the second case, the temperature was measured with the iron lines 2999.52, 3037.39, 3047.61, 3057.45, and 3059.09. It is known that for a Boltzmann distribution of atoms among the excited states, i.e., for thermal excitation, the temperature determination is based on a plot of ln J/P versus E/k, i.e.,

$$\ln \frac{J}{Ah\nu N_{0g}} = -\frac{E}{kT} \cdot \frac{}{g_0}$$

The atomic constants for the copper lines were taken from a paper by Belyakov-Bodin and Mandelshtam;[4] those for the iron lines are given in Table 1.

Table 1

Wavelengths (Å)	Transition	Atomic constants			Methods of measurement
		f	P	Reference	
3859.913	$a^5D_4 - z^5D_4^0$	110	—	[5]	Method of hooks
3727.621	$a^5F_5 - y^5F_5^0$	210	—		
3763.79	$a^5F_5 - y^5F_5^0$	1280	—		
5269.5	$a^5F_5 - z^5D_4$	15	—	[6]	Total absorption
4325.76	$a^5F_2 - z^5G_3$	760	—		
3059.09	$a^5D_2 - y^5D_4^0$	—	206	[7]	DC arc, T° measured with tin lines
3057.45	$a^5F_4 - z^5D_4^0$	—	500		
3047.61	$a^5D_2 - y^5D_2^0$	—	236		
3037.39	$a^5D_1 - y^5D_2^0$	—	185		
2999.52	$a^5F_5 - z^5F_5^0$	—	240		

Notations: f – oscillator strength, $P = Ah\nu N_0 (g/g_0)$.

We used a 0.1% solution of $FeCl_3$ for obtaining the iron lines in question.

It was found that when ln J/P versus E/k plots were made, all of the points fell fairly consistently on a straight line (Fig. 1), which indicates the thermal character of the excitation of spectra in the source used.

The results of measurements are given in Table 2. As can be seen from this table, all of the lines give the same temperature (6800°K) within experimental error. The discharge temperature was measured while air was being blown in through the lower electrode, i.e., the discharge took place under suction and air blast. This was accomplished in the following manner: The auxiliary cone-shaped electrode,[1] which was immersed in the liquid, had an opening 1 mm in diameter and was con-

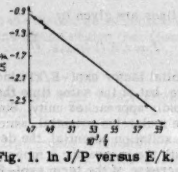

Fig. 1. ln J/P versus E/k.

nected to an air line by means of a little porcelain tube. In this case the measured temperature was 300 to 400°K higher. The increase in temperature is explained by increased heat removal from the discharge zone, that is, by a disturbance of the energy balance in the discharge column.

Table 2

Atoms	Wavelengths (A)			T °K
Fe	I 3859.913	I 3727.621	—	6852 ± 150
Fe	I 5269.5	I 4325.76	—	6781 ± 180
Cu	I 5105.54	I 5153.24	—	6908 ± 160
Fe	I 2999.52	I 3037.39	I 3047.61	—
	I 3057.45	I 3059.09	—	6800 ± 100

DEPENDENCE OF THE DISCHARGE TEMPERATURE ON THE IONIZATION POTENTIALS OF SUBSTANCES PRESENT IN THE SOLUTION

Salts of various metals were used in this investigation. The results of the measurements are presented in Fig. 2. The diagram shows that a linear relationship exists in this discharge between the temperature and the ionization potential of the added element. It can be concluded that the discharge mechanism is similar to that of a dc or ac arc burning in the vapors of a solution of powder.[8,9]

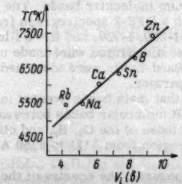

Fig. 2. Dependence of the temperature on the ionization potential of the substance.

In our setup, the presence of 1% of vapor of the element investigated was sufficient to make the conductivity of the discharge gap dependent only on the ionization of this element. This dependence can be explained as follows. The heat liberated in the discharge must keep the temperature high enough to produce enough ions to sustain the discharge. The higher the ionization potential of the elements in the solution, the higher the temperature necessary for the production of a sufficient number of ions, and vice versa.

DEPENDENCE OF THE DISCHARGE TEMPERATURE ON THE CONCENTRATION OF ALKALI ELEMENTS

For this investigation, salts of easily ionizable elements (NaCl and KCl) were used over a wide range of concentrations. As the measurements show (see Figs. 3 and 4), the discharge temperature drops sharply with increasing salt concentration, as in the case of the low frequency arc discharge. The temperature drop is explained as follows: introducing a substance with a low ionization potential into the discharge facilitates formation of the number of electrons and ions necessary to maintain the needed current through the discharge gap. This causes a decrease in the discharge temperature and the potential gradient.

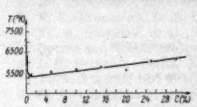

Fig. 3

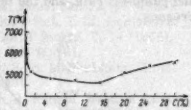

Fig. 4

Fig. 3. Temperature as a function of NaCl concentration.
Fig. 4. Temperature as a function of KCl concentration.

The temperature continues to decrease until almost all of the electrons and ions necessary for conduction are obtained from the potassium and sodium atoms. Saturation as a result of the increase in concentration of the salts of alkaline elements was not observed in our case.

Contrary to the situation in dc and ac arcs, a further increase in the concentration of alkalis causes an increase in the temperature. The lowest temperature is obtained at relatively low concentrations of the alkaline elements.

This difference can be explained only by the special features of this discharge which operates directly in the vapors of the solution. One may assume that with a further increase in temperature, the number of electrons decreases because of their capture by electronegative particles and neutral molecules. The probability of capture reaches a maximum[10,11] under certain conditions. Furthermore, the number of undissociated water molecules increases with decreasing temperature, which also greatly affects the electron concentration.[12] Finally, one may expect an increase of temperature when the energy balance is changed because of increased heat losses due to the presence of hydrogen, as the presence of large quantities of an alkaline element increases the yield of hydrogen.

DEPENDENCE OF THE DISCHARGE TEMPERATURE ON GENERATOR POWER AND ON THE RATE OF GAS WITHDRAWAL THROUGH THE ELECTRODES

We have studied the dependence of the discharge temperature on generator power and on the rate of gas withdrawal when the discharge occurred directly in the vapors of the solution. The generator power was taken to be the power supplied to the plate of the generator tube N, as was done in the paper by Khokhlov.[13] The voltage applied to the motor of the dust collector was considered a measure of the rate of gas withdrawal from the discharge gap. We have considered three cases of the abovementioned dependence: (1) the generator power and the rate of withdrawal change simultaneously; (2) the rate of withdrawal is constant and the generator power varies; (3) the rate of withdrawal varies and the generator power remains constant.

These relationships are depicted in Fig. 5, which shows that the temperature increases linearly in all three

cases. In the first case, when both the generator power and the rate of gas withdrawal increase simultaneously, the temperature increases faster, as would be expected. The increase of the rate of withdrawal through the channel in the upper electrode does not permit the discharge column to expand when the generator power is increased; but an increase in the rate of withdrawal increases the compression. As a result, the power density of the discharge increases sharply with increasing generator power and pump-off rate, and the temperature therefore increases.

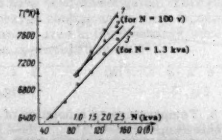

Fig. 5. Dependence of the discharge temperature on the generator power and on the intensity of gas removal. 1—power and gas-removal intensity varied, 2—removal intensity constant, 3—generator power constant.

In the second case, the linear dependence can be explained by the fact that the temperature depends on the power liberated per unit volume.

In our conditions, the power density apparently increased because of the limiting influence of the upper electrode, which resulted in a relatively slow increase in volume of the discharge with increasing power.

The increase of temperature with increasing pump-off rate can be explained in the following way: The drawing off of the air and vapors in the discharge region results in a flow of air toward the discharge axis. This creates considerable compression, leading to an increase in the current density in the center of the arc. Maintaining this high current density requires both a large longitudinal field gradient and a high degree of ionization, i.e., a high temperature.

Thus, a high frequency discharge with hydrodynamic compression is an efficient light source, offering smooth regulation over a wide range of powers and temperatures and permitting a choice of the most favorable conditions.

DEPENDENCE OF THE ABSOLUTE INTENSITIES OF SPECTRAL LINES ON DISCHARGE CONDITIONS

We have studied the dependence of the intensities of spectral lines on discharge conditions; i.e., on generator power and pump-off rate. As mentioned above, the dependence of the temperature on these factors is linear. In this case, we can consider the above-mentioned dependence as the relationship between the intensities of spectral lines and the temperature of the discharge.

The atomic lines of iron I 3719.935, I 3753.79, and I 3815.842, which have different excitation potentials, were selected for the investigation. The relationships obtained are shown in Figs. 6 and 7. Figure 6 depicts the logarithm of the line intensities versus the generator power (at a constant withdrawal rate), and Fig. 7 the logarithm of the intensity of spectral lines versus withdrawal rate (at constant generator power).

It can be seen from the figures that the intensity changes of some iron arc lines with temperature agree qualitatively with the data for arc and spark discharges. Under the conditions of thermal equilibrium, the intensities of spectral lines are given by

$$J = CN(1-x)e^{-\frac{K}{kT}}.$$

The exponential factor exp(−E/kT) increases rapidly with temperature, but at the same time the degree of ionization x rapidly approaches unity. Since the quantity x is given by the ionization potential, which is of course higher than the excitation potential, the decrease of the factor (1 − x) with the increasing temperature is more rapid than the increase of the term exp(−E/kt). As a result, the intensity of the spectral lines first increases up to a certain maximum, and then starts to decline.

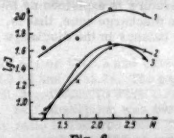

Fig. 6

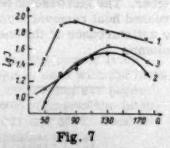

Fig. 7

Fig. 6. Intensity of spectral lines versus generator power. Wavelengths: curve 1—3719.935; curve 2—3763.79; curve 3—3815.842. Fig. 7. Intensity of spectral lines versus suction speed. Notations as in Fig. 6.

THE DISCHARGE SPECTRUM

As mentioned before, the high frequency discharge with hydrodynamic compression, burning directly in the vapor of the solution, differs from other light sources by certain characteristic features. We therefore consider it necessary to describe its spectra, because it is important in the spectroanalytical technique to know the regions which are free from molecular bands. The spectra were photographed with a DFS-2 spectrograph from 2000 to 10,000 A on type I-820, I-720, and RF-3 films. The solutions used in these discharges were made up in double-distilled water. Band-heads were identified with the aid of an IZA-2 comparator.

It was found that main bands present in this light source are the OH molecular bands between 3064 and about 3380 A and those of the O_2, H_2, and other molecules, which cover the region from 6121 to 6750 A and overlap each other.

With long exposures, the spectra of the N_2 molecule appear between 5620 and 6121 A. The spectra were identified from the tables of Pearse.[14] The rest of the spectrum is free of molecular bands and is usable for spectroanalytical purposes.

It should be mentioned that the molecular bands in the 6121-6750 A region completely disappear in acid solutions, and the OH band 3064 A is weakened considerably. Figure 8 shows the discharge spectra in the region 6121 A obtained under identical conditions, except that in one case the discharge took place in a concentrated HCl solution, and in the other case in a water solution.

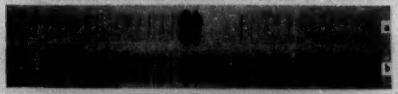

Fig. 8. Discharge spectra near 6121 A. a—spectrum obtained with concentrated acid, b—spectrum with aqueous solution.

Thus, when the discharge is maintained in acid solutions, one obtains a wide region free from molecular bands.

DETERMINATION OF THE TRANSITION PROBABILITY IN THE SOURCE

This discharge makes it feasible to determine transition probabilities between different atomic levels by measuring the relative intensities of lines of two different elements. The method consists essentially of the following procedure: By measuring the relative intensities of lines of two different elements, for one of which the transition probability is known, the unknown transition probability of the other element is determined.

However, this method is applicable only when the number of unexcited atoms of one element is the same at all times, or is proportional to the number of unexcited atoms of the other element, i.e., when the rate at which the different elements enter the discharge is the same.

It has been found that when the discharge burns directly in the vapors of the solution, the lines of the elements appear in the spectrum simultaneously, regardless of their position in the volatility series, and the absolute and relative intensities of the lines are practically constant. Because of the high stability of the discharge, and because of the continuous feeding of the sample directly into the discharge zone, the complex and uncontrollable processes of evaporation from the electrodes are eliminated. Furthermore, thermal equilibrium exists in this discharge.

By using high generator power and intense compression, one can raise the discharge temperature to 8000°K and higher.

In conclusion, I wish to express my deep gratitude to F. A. Korolev for suggesting the topic and for his great help given to me in the course of the work.

REFERENCES

1. F. A. Korolev and Zh. Zheenbaev, Izvest. Vuzov MVO (physics) No. 5, 136 (1959).
2. Zh. Zheenbaev, Inzh.-Fiz. Zhur. No. 12, 44 (1959).
3. V. K. Prokof'ev, D. B. Gurevitch, I. M. Belousova, Yu. A. Snigirev, et al., Opt. i Spektr. 7, 14 (1959), Optics and Spectroscopy 7, 7 (1959).
4. I. B. Belyakov-Bodin and S. L. Mandelstam, Zhur. Tekh. Fiz. 10, No. 4, (1940).
5. G. F. Parchevskii and N. P. Penkin, Vestnik Leningrad. Gosudarst. Univ. No. 11, 113 (1954).
6. R. B. King and A. S. King, Astrophys. J. 82, 377 (1935); ibid. 87, 24 (1938); ibid. 95, 78 (1942).
7. N. N. Sobolev, Zhur. Eksptl. i Teoret. Fiz. 13, 5, 137 (1943).
8. O. P. Semenova, Izvest. Akad. Nauk SSSR, Ser. Fiz. 9, 715 (1945).
9. L. V. Popov and I. S. Pominov, Uchenye Zapiski, Kazan. Univ., Fiz. 113, b.9, 5 (1953).
10. V. L. Granovskii, "Electricheskii tok v gase" (Electric Current in Gas). Moscow, 1952.
11. N. S. Buchel'nikova, Uspekhi Fiz. Nauk 65, No. 3 (1958).
12. V. D. Mikhalevskii and V. V. Prokof'eva, Zhur. Eksptl. i Teoret. Fiz. 20, No. 7 (1950).
13. M. Z. Khokhlov, Dissertation, Moscow, 1953.
14. P. Pearse and A. Gaydon (Russian translation) "Otoshdestvlenie molecularnykh spectrov" (Identification of Molecular Spectra). Moscow, 1949.

CALCULATION AND INTERPRETATION OF THE VIBRATIONAL SPECTRA OF BIPHENYL AND SOME OF ITS DEUTERIUM SUBSTITUTION PRODUCTS

G. V. Peregudov

Received 17 December 1959

On the basis of the V_{2h} model, a calculation of the vibrational spectra of the $C_{12}H_{10}$, $C_{12}H_6D_4$, $C_{12}H_4D_6$, and $C_{12}D_{10}$ molecules has been carried out. A complete interpretation of the fundamental frequencies of the Raman and infrared spectra is given. The fulfillment of the product rule and the sum rule for the frequencies of isotopic molecules has been verified. Data are presented for the first time on the infrared absorption spectra for $C_{12}H_6D_4$ and $C_{12}H_4D_6$ in the region from 700 to 3100 cm^{-1}.

The present investigation relates to a series of works on the study of the vibrational spectra of deuterium substitution products of the aromatic series. In previously published communications[1-3] we have presented Raman and infrared spectra of the biphenyl ($C_{12}H_{10}$), decadeuteriobiphenyl ($C_{12}D_{10}$), 2,5,2',5'-tetradeuteriobiphenyl ($C_{12}H_6D_4$), and 1,3,4,1',3',4'-hexadeuteriobiphenyl ($C_{12}H_4D_6$) molecules. In the present work, the results of calculation are presented and an interpretation is given for the vibrational spectra of all 4 of the molecules listed. In the interpretation of the spectrum of the $C_{12}H_4D_6$ and $C_{12}H_6D_4$ molecules, we have made use of the data obtained by us for the first time on the infrared absorption spectra of these molecules.

The investigation of the infrared absorption spectrum in the region from 700 to 3000 cm^{-1} was carried out with the help of an IKS-14 double-beam spectrophotometer with NaCl and LiF prisms. The spectrum of the $C_{12}H_6D_4$ molecule was studied in CCl_4 solution, the spectrum of $C_{12}H_4D_6$ in the melt. The infrared absorption spectra of the $C_{12}H_{10}$ and $C_{12}D_{10}$ molecules were also restudied. In doing so, we used narrower slits than in ref. 1, which in a number of cases enabled us to observe better the complex structure of the absorption bands. Thus, new absorption maxima were observed in $C_{12}H_{10}$ and $C_{12}D_{10}$ in the region from 2200 to 3100 cm^{-1}. The data on these spectra are presented in Tables 1 and 2.

The calculation and interpretation of the vibrational spectra of the $C_{12}H_{10}$ and $C_{12}D_{10}$ molecules were first accomplished by Kovner.[4] We have taken our model and the fundamental parameters of the $C_{12}H_{10}$ molecule from ref. 4. We used as force constants the set of force con-

Table 1. Infrared Absorption Spectra of the $C_{12}H_2D_4$ and $C_{12}H_4D_8$ Molecules (Frequencies in cm^{-1})*

Band No.	$C_{12}H_2D_4$ Solution in CCl_4	$C_{12}H_2D_4$ Melt	Band No.	$C_{12}H_4D_8$ Solution in CCl_4	$C_{12}H_4D_8$ Melt
1	885 s	680 m	21	1600 s	1390 s
2	894 s	722 m	22	1649 w	1420 s
3	912 m	738 m	23	1660 w	1430 s
4	974 m	758 m	24	1687 vw	1490 w
5	994 m	776 m	25	1710 vw	1560 w
6	1010 w	796 w	26	1738 vw	1593 s
7	1067 vw	820 s	27	1782 vw	1630 m
8	1109 w	838 s	28	1806 w	1718 vw
9	1222 m	863 w	29	1823 m	1754 vw
10	1251 w	916 s	30	1840 m	1840 s
11	1280 m	962 w	31	1855 m	1920 w
12	1391 w	1000 s	32	1880 vw	2254 s
13	1396 m	1054 vw	33	2242 m	2268 s
14	1408 w	1078 vw	34	2259 s	2967 m
15	1424 vw	1096 vw	35	2268 s	3047 s
16	1430 m	1146 vw	36	2291 m	—
17	1438 s	1238 vw	37	3002 m	—
18	1448 w	1280 s	38	3048 vs	—
19	1534 m	1286 vw	39	3092 vs	—
20	1568 s	1350 vw			

*Symbols: vs – very strong line, s – strong, m – medium, w – weak, vw – very weak.

Table 2. Infrared Absorption Spectra of the $C_{12}H_{10}$ and $C_{12}D_{10}$ Molecules in the Region 2200-3100 cm^{-1} (Frequencies in cm^{-1})*

Band No.	$C_{12}H_{10}$	$C_{12}D_{10}$	Band No.	$C_{12}H_{10}$	$C_{12}D_{10}$
1	—	2250 w	7	—	2947 (s)
2	—	2267 s	8	2982 m	—
3	—	2274 s	9	3010 s	—
4	—	2284 m	10	3047 s	—
5	—	2792 s	11	3069 m	—
6	—	2922 s	12	3086 w	—

*For symbols, see note to Table 1.

stants for benzene presented in ref. 5. However, in refs. 4 and 5 the choice of the force constant for the CCC angles external to the ring (force constant K_γ) cannot be recognized as adequately established. In the works just cited the force constant K_γ was taken as equal to that for propane, i.e., $K_\gamma = 1.10 \times 10^5$ cm^{-2}. We have varied this force constant between the limits of 0.71×10^5 cm^{-2} and 1.10×10^5 cm^{-2}. Comparison of the calculation with the experimental data has shown that the best result is obtained if $K_\gamma = 0.90 \times 10^5$ cm^{-2}.

The solution of the secular equations was carried out with the help of an "Arrow" electronic computer. The secular equations were solved by the method of progressive diagonalization,[8] and the forms of the normal vibrations were determined according to Mayants's method.[7] The atomic displacements were also computed. In Table 3, the results of the calculation are assembled and an interpretation of the vibrational spectra is given for all 4 molecules studied. In the column "ν_c" are presented the values of the frequencies observed in the spectra (in cm^{-1}), a visual estimate of the line intensity being indicated in parentheses on a 10-point scale for each substance separately. In the column "ν_c" are given the calculated frequency values. In view of the absence of certain frequencies from the observed spectra, well-known difficulties arise in comparing the experimental data with the calculated values. From the results of the calculation, we sometimes have to assign one and the same frequency to different symmetry classes. A discussion by symmetry classes of the results obtained is presented below.

SYMMETRY CLASS A_{1g}

To this class belong 11 frequencies which are active in the Raman spectrum. As was to be expected, these

Table 3. Results of Calculation, and Interpretation, of the Vibrational Spectra of the $C_{12}H_{10}$, $C_{12}H_8D_2$, $C_{12}H_4D_6$, and $C_{12}H_{10}$ Molecules (Frequency in cm^{-1})*

Band No.	$C_{12}H_{10}$		$C_{12}H_8D_2$		$C_{12}H_4D_6$		$C_{12}D_{10}$	
	ν_0	ν_c	ν_0	ν_c	ν_0	ν_c	ν_0	ν_c
				Symmetry class A_{1g}				
1	315 (1.5)	286	312 (0)	283	306 (1)	277	300 (1.5)	274
2	740 (4)	734	700 (4)	703	735 (5)	724	692 (3)	695
3	1003 (8)	997	1002 (8)	998	974 (8)	960	960 (10)	955
4	1032 (4)	1024	854 (6)	869	—	861	840 (0.5)	852
5	1185 (1.5)	1198	1088 (1)	1077	1080 (4)	1076	870 (4)	879
6	1280 (10)	1301	1264 (8)	1275	1260 (3)	1280	1188 (6)	1195
7	1504 (4)	1539	1452 (8)	1485	1452 (8)	1501	1412 (6)	1449
8	1611 (8)	1623	1595 (6 d)	1621	1590 (10)	1602	1574 (10)	1597
9	3047 **	3054	2278 (0)	2288	2275 (3)	2286	2272 (3)	2275
10	3060 (2d)	3061	3060 (2)	3061	2283 (3b)	2289	2286 (2)	2289
11	—	3089	3060 (2)	3062	3060 (2b)	3061	2297 (3)	2299
				Symmetry class B_{1g}				
12	407 (3b)	401	378 (2)	392	381 (2)	381	355 (2b)	373
13	612 (2,5)	599	599 (1)	589	604 (2)	588	589 (2,5)	577
14	1092 (0)	1087	1088 (1)	1100	833 (0)	835	835 (0.5)	847
15	1155 (2b)	1179	938 (1)	922	956 (10)	957	870 (4)	866
16	—	1300	1255 (0)	1271	—	1224	1070 (0)	1060
17	1326 (0)	1342	—	1338	1292 (0)	1328	—	1298
18	1452 (0)	1479	1452 (8)	1456	—	1398	1345 (0)	1352
19	1592 (6)	1619	1595 (6)	1600	1582 (10)	1606	1566 (3b)	1600
20	3047 **	3049	2278 (0)	2286	2283 (3b)	2287	2272 (3)	2268
21	—	3075	3060 (2)	3062	3060 (2b)	3062	2297 (3)	2307
				Symmetry class B_{2g}				
22	267 (2b)	241	254 (0)	241	249 (1)	223	248 (2b)	233
23	540 **	513	485 (0)	467	496 (0)	493	—	453
24	—	699	642 (0.5)	663	—	557	540 (0)	558
25	780 (1 b)	768	700 (4)	706	704 (4)	716	634 (4)	650
26	967 (0)	929	938 (1)	938	780 (0)	793	780 (0.5)	779
27	980 **	996	—	917	928 (1)	931	835 (0.5)	834
				Symmetry class B_{2g}				
28	407 (3)	405	386 (0)	377	—	377	355 (2)	355
29	838 (1.5)	858	—	728	735 (5)	728	654 (4)	675
30	965 (0.5)	985	938 (1)	939	928 (1)	939	780 (0.5)	803
				Symmetry class B_{1u}				
31	—	95	—	94	(100) ***	91	—	89
32	(430)	427	(400)	409	(400)	401	(340)	385
33	688 s	708	(600)	611	(550)	559	(560)	549
34	724 s	734	(700)	709	722 m	713	(680)	626
35	904 s	920	894 s	905	758 m	754	741 w	750
36	974 w	996	912 m	936	916 s	931	802 vs	830
				Symmetry class B_{2u}				
37	—	105	—	102	(100)	100	—	97
38	—	614	(800)	604	(800)	603	(560)	595
39	1080 s	1069	1088 w	1086	820 s	852	836 s	845
40	1170 m	1176	912 m	909	—	948	868 w	867
41	1280 w	1286	1222 m	1246	—	1186	10286 w	1027
42	1326 w	1341	—	1340	1260 s	1283	1278 m	1272
43	1440 s	1445	1396 m	1396	1360 s	1386	1326 w	1306
44	1580 m	1591	1588 s	1582	1560 w	1570	1570 m	1562
45	3047 s	3049	2268 s	2286	2258 s	2285	2250 w	2265
46	3096 w	3074	3092 vs	3062	3047 s	3062	2284 m	2306
				Symmetry class B_{2u}				
47	—	808	(800)	802	(800)	597	(560)	590
48	396 m	988	974 m	974	962 w	950	956 w	948
49	1018 s	1015	994 m	1004	1000 s	1013	988 s	988
50	1060 m	1049	885 s	854	838 s	850	818 s	834
51	1190 vw	1198	1100 w	1111	1096 vw	1108	868 w	876
52	1492 vs	1505	1438 s	1440	1434 s	1437	1380 vs	1346
53	1600 s	1586	1600 s	1588	1562 s	1581	1586 vs	1569
54	3010 s	3053	2291 m	2288	2258 s	2286	2287 s	2275
55	3047 s	3081	3002 s	3060	2268 s	2289	2284 m	2299
56	3069 m	3069	3048 vs	3062	3047 s	3061	2274 s	2258

*In parentheses: visual intensities on a 10-point scale. Symbols: b – broad line, d – double line; for the remaining symbols, see note to Table 1.

**These frequencies were observed in ref. 8.

***Determined approximately, on the basis of combination tones.

are the most intense lines in the spectra and, according to the selection rules, must be polarized.[1] As follows from Table 3, the calculated frequency values agree well with the observed ones (the average deviation does not exceed 10-12 cm^{-1} and reaches 30-40 cm^{-1} only in isolated cases). Making use of the data of Table 3, it is easy to verify the fulfillment of the product rule[2-3] and the sum rule[3] for the frequencies of isotopic molecules. In this case, when a given frequency was not observed in the spectrum, we used its calculated value. Thus we obtain the following values for the product rule:

$$\frac{\prod_{i=1}^{11}\nu_i(C_{12}H_{10})}{\prod_{i=1}^{11}\nu_i(C_{12}H_8D_4)}=1.98\ (\text{theor. } 2.00);$$

$$\frac{\prod_{i=1}^{11}\nu_i(C_{12}H_{10})}{\prod_{i=1}^{11}\nu_i(C_{12}H_4D_6)}=2.83\ (\text{theor. } 2.82);$$

$$\frac{\prod_{i=1}^{11}\nu_i(C_{12}H_{10})}{\prod_{i=1}^{11}\nu_i(C_{12}D_{10})}=5.51\ (\text{theor. } 5.64).$$

The values of the frequency ratios calculated according to formula 2.313 of ref. 8 are given in parentheses. It is easy to see that the agreement of the two values is entirely satisfactory. The sum rule in our case has the form

$$\sum_{i=1}^{k}\nu_i^2(C_{12}H_{10})+\sum_{i=1}^{k}\nu_i^2(C_{12}D_{10})=\sum_{i=1}^{k}\nu_i^2(C_{12}H_6D_4)+\sum_{i=1}^{k}\nu_i^2(C_{12}H_4D_6). \quad (1)$$

for each symmetry class.

If we substitute into (1) the data for the class A_{1g}, we find that the difference Δ between the right and left sides of the equality (1) equals $0.095\times10^6\ cm^{-2}$, while the entire left side equals $63.183\times10^6\ cm^{-2}$.

From the analysis of the forms of the normal vibrations and of the values of the atomic displacements, it follows that the displacements of the hydrogen and deuterium atoms, and also the frequencies related to the deformation vibrations of the CCH angles, change most markedly on deuteration. The displacements of the carbon atoms and the frequencies associated with the ring vibrations undergo smaller changes. These questions will be discussed in more detail in a separate article.

SYMMETRY CLASS B_{1g}

The frequencies of this class are active in the Raman spectrum. Our interpretation of the frequencies for this symmetry class differs in a number of cases from the interpretation given in ref. 4. We have obtained the following values for the product rules and the sum rule:

$$\frac{\prod_{i=1}^{10}\nu_i(C_{12}H_{10})}{\prod_{i=1}^{10}\nu_i(C_{12}H_8D_4)}=1.84\ (\text{theor. } 1.94);$$

$$\frac{\prod_{i=1}^{10}\nu_i(C_{12}H_{10})}{\prod_{i=1}^{10}\nu_i(C_{12}H_4D_6)}=2.72\ (\text{theor. } 2.74);$$

$$\frac{\prod_{i=1}^{10}\nu_i(C_{12}H_{10})}{\prod_{i=1}^{10}\nu_i(C_{12}D_{10})}=5.29\ (\text{theor. } 5.33).$$

The difference $\Delta = 0.011\times10^6\ cm^{-2}$ while the right side of expression (1) equals $49.565\times10^6\ cm^{-2}$. It is easy to see that in this case also the product rule and the sum rule are well satisfied.

SYMMETRY CLASS B_{2g}

Six nonplanar vibrations, active in the Raman spectrum, constitute the class B_{2g}. These, as a rule, are the weakest lines. Therefore some frequencies were not observed in the spectra. Nevertheless, the sum rule and the product rule are well satisfied:

$$\frac{\prod_{i=1}^{6}\nu_i(C_{12}H_{10})}{\prod_{i=1}^{6}\nu_i(C_{12}H_8D_4)}=1.45\ (\text{theor. } 1.38);$$

$$\frac{\prod_{i=1}^{6}\nu_i(C_{12}H_{10})}{\prod_{i=1}^{6}\nu_i(C_{12}H_4D_6)}=1.94\ (\text{theor. } 1.95);$$

$$\frac{\prod_{i=1}^{6}\nu_i(C_{12}H_{10})}{\prod_{i=1}^{6}\nu_i(C_{12}D_{10})}=2.63\ (\text{theor. } 2.69).$$

The difference $\Delta = 0.010\times10^6\ cm^{-2}$, the left side of (1) equals $5.516\times10^6\ cm^{-2}$. Hence weak lines with frequencies close to the calculated values must be present in the spectra of the molecules studied. Analysis of the form of the normal vibrations shows that the whole molecule is strongly deformed during nonplanar vibrations.

SYMMETRY CLASS B_{3g}

To this symmetry class belong 3 frequencies in the Raman spectrum, corresponding to nonplanar vibrations. Here

$$\frac{\prod_{i=1}^{3}\nu_i(C_{12}H_{10})}{\prod_{i=1}^{3}\nu_i(C_{12}H_8D_4)}=1.32\ (\text{theor. } 1.35);$$

$$\frac{\prod_{i=1}^{3}\nu_i(C_{12}H_{10})}{\prod_{i=1}^{3}\nu_i(C_{12}H_4D_6)}=1.28\ (\text{theor. } 1.35);$$

$$\frac{\prod_{i=1}^{3}\nu_i(C_{12}H_{10})}{\prod_{i=1}^{3}\nu_i(C_{12}D_{10})}=1.82\ (\text{theor. } 1.82).$$

The difference $\Delta = 0.126\times10^6\ cm^{-2}$, the right side of (1) equals $2.961\times10^6\ cm^{-2}$; i.e., in this case the sum rule is somewhat less well satisfied than for the other symmetry classes.

SYMMETRY CLASS B_{1u}

The frequencies of this class are active in the infrared absorption spectrum and lie, according to our calculation, in the region from 100 to 1000 cm^{-1}. In our case, the observations of the infrared absorption spectrum were limited to the region from 700 to 3100 cm^{-1}, so that we have determined the lower frequencies from analysis of combination tones. The frequencies of this class correspond to nonplanar vibrations. Here the following values are obtained for the product rule and the sum rule:

$$\frac{\prod_{i=1}^{6} \nu_i(C_{12}H_{10})}{\prod_{i=1}^{6} \nu_i(C_{12}H_8D_4)} = 1.23 \text{ (theor. 1.39)};$$

$$\frac{\prod_{i=1}^{3} \nu_i(C_{12}H_{10})}{\prod_{i=1}^{3} \nu_i(C_{12}H_4D_6)} = 1.62 \text{ (theor. 1.96)};$$

$$\frac{\prod_{i=1}^{6} \nu_i(C_{12}H_{10})}{\prod_{i=1}^{6} \nu_i(C_{12}D_{10})} = 2.36 \text{ (theor. 2.74)}.$$

The difference $\Delta = -0.013 \times 10^8$ cm^{-2} while the left side of (1) equals 5.082×10^8 cm^{-2}. Such good agreement of both the sum and product rules permits us to expect the presence, in the infrared absorption spectra in the region below 700 cm^{-1}, of bands with frequencies close to the calculated values.

SYMMETRY CLASS B_{2u}

The bands (corresponding to planar vibrations) which belong to this class lie in the region from 100 to 3050 cm^{-1}. Just as for class B_{1g}, the interpretation of certain frequencies differs from the interpretation given in ref. 4. In this case also we observe an entirely satisfactory fulfillment of the product and sum rules:

$$\frac{\prod_{i=1}^{10} \nu_i(C_{12}H_{10})}{\prod_{i=1}^{10} \nu_i(C_{12}H_8D_4)} = 1.92 \text{ (theor. 1.97)};$$

$$\frac{\prod_{i=1}^{10} \nu_i(C_{12}H_{10})}{\prod_{i=1}^{10} \nu_i(C_{12}H_4D_8)} = 2.76 \text{ (theor. 2.77)};$$

$$\frac{\prod_{i=1}^{10} \nu_i(C_{12}H_{10})}{\prod_{i=1}^{10} \nu_i(C_{12}D_{10})} = 5.10 \text{ (theor. 5.47)}.$$

The difference $\Delta = -0.127 \times 10^8$, the left side of (1) equals 48.489×10^8 cm^{-2}.

SYMMETRY CLASS B_{3u}

The frequencies of this class are most fully represented in the infrared absorption spectrum. Only one frequency, no. 47 in the 600 cm^{-1} region, was not observed. A check of the sum and product rules shows them to be well fulfilled:

$$\frac{\prod_{i=1}^{10} \nu_i(C_{12}H_{10})}{\prod_{i=1}^{10} \nu_i(C_{12}H_8D_4)} = 1.79 \text{ (theor. 1.97)};$$

$$\frac{\prod_{i=1}^{10} \nu_i(C_{12}H_{10})}{\prod_{i=1}^{10} \nu_i\ C_{12}H_4D_8)} = 2.61 \text{ (theor. 2.77)};$$

$$\frac{\prod_{i=1}^{10} \nu_i(C_{12}H_{10})}{\prod_{i=1}^{10} \nu_i(C_{12}D_{10})} = 5.07 \text{ (theor. 5.47)}.$$

The difference $\Delta = -0.208 \times 10^8$ cm^{-2} while the left side of (1) equals 60.566×10^8 cm^{-2}.

We did not calculate the frequencies of symmetry class A_{1u}, which are inactive in both the Raman and infrared spectra. In the spectra of the molecules investigated there appear a number of frequencies which cannot be assigned to fundamentals. We interpret them as combination tones (see, for example, refs. 1 and 2). It is not impossible that some of these frequencies belong to the spectra of an admixture of another kind of deuterium-substituted biphenyl molecule.

The calculations carried out have made it possible to interpret completely the observed spectra of the molecules studied by us. The set of force constants used by us enables us to explain the experimentally observed frequency values better than was done in ref. 4. The data obtained on the forms of the normal vibrations and the magnitudes of the atomic displacements enable us to trace unequivocally the frequency change on replacement of hydrogen atoms by deuterium.

In conclusion I express my thanks to P. A. Bazhulin for his continuing interest in the work, to M. A. Kovner for consultation during the performance of the calculations, and to A. M. Bogomolov for his courtesy in providing a program for the calculations on the "Arrow" machine.

REFERENCES

1. G. S. Landsberg, A. I. Shatenshtein, G. V. Peregudov, E. A. Izrailevich, and L. A. Novikova, Izvest. Akad. Nauk SSSR, Ser. Fiz. 18, 669 (1954).
2. G. S. Landsberg, A. I. Shatenshtein, G. V. Peregudov, E. A. Izrailevich, and L. A. Novikova, Opt. i Spektr. 1, 34 (1956).
3. A. I. Shatenshtein, G. V. Peregudov, E. A. Izrailevich, and V. R. Kalinichenko, Zhur. Fiz. Khim. 32, 146 (1958).
4. M. A. Kovner, Opt. i Spektr. 1, 734 (1956).
5. M. A. Kovner and A. M. Bogomolov, Opt. i Spektr. 4, 301 (1958).
6. M. V. Vol'kenshtein, M. A. El'yashevich, and B. I. Stepanov, "Kolebaniya molekul" (Molecular Vibrations), Vol. I. Gosudarst. Izd. Tekh.-Teoret. Lit., Moscow-Leningrad, 1949.
7. L. S. Mayants, Trudy Fiz. Inst. Akad. Nauk SSSR 5, 63 (1950).
8. G. Herzberg, "Kolebatel'nye i vrashchatel'nye spektry mnogoatomnykh molekul" (Vibrational and Rotational Spectra of Polyatomic Molecules). Izd. Inostrannoi Lit., Moscow, 1949.

9. L. M. Sverdlov, Doklady Akad. Nauk SSSR 86, 513 (1952).

Note added in proof. In the journal Spectrochim. Acta 8, 627 (1959), there is an article by Lippincott devoted to the interpretation of the vibrational spectra of the $C_{12}H_{10}$ and $C_{12}D_{10}$ molecules. The interpretation proposed by the author gives rise to serious objections. It should be noted that the isotopic purity of the $C_{12}D_{10}$ preparation investigated appears to have been insufficient.

VIBRATIONAL SPECTRA OF UNSATURATED HYDROCARBONS
VIII. Vibrational Spectra and Rotational Isomerism of 1,3-Butadiene

L. M. Sverdlov and N. V. Tarasova

Received 4 December 1959

In order to clarify the question of the structure of the 1,3-butadiene molecule, a calculation of the normal vibration frequencies of the trans- and cis-isomers of 1,3-butadiene has been carried out. As a result of detailed analysis of the experimental data and comparison with the calculated frequency values, it has been shown that all the frequencies in the Raman and infrared spectra relate to the trans-form of 1,3-butadiene.

1. In the preceding works,[1,2] we studied the effect on the vibrational spectra of including in the molecule several double bonds with various relative positions in the chain: molecules with two double bonds separated by several single bond (1,4-pentadiene, diallyl) and molecules with cumulated double bonds (allene, 1,1-dimethylallene).

It is interesting to consider also the vibrational spectra of molecules with conjugated double bonds, especially 1,3-butadiene. In this molecule, the existence of two rotational isomers (the cis- and trans-forms) with a planar arrangement of the double bonds is possible in principle. Clarification of the structural peculiarities of the simplest representative of the class of compounds with conjugated double bonds is important for the theory of chemical structure, for polymer chemistry, and also for the calculation of thermodynamic functions.

2. Many works have been devoted to the study of the structure of 1,3-butadiene; however, in the literature there is no unanimity concerning the structure of the molecule. Some authors[3-5] consider that butadiene has the trans-form; others[6-8] assign the cis-form to it, and, finally, certain authors[9-12] adhere to the viewpoint that butadiene represents a mixture of the two forms. For example, Godnev and Morozov[8] have carried out a calculation of the thermodynamic functions starting from the cis-configuration. Certain authors,[6,7] having carried out quantum-mechanical calculations on 1,3-butadiene, arrive at the conclusion that the cis-form is the more stable; others[3] draw the opposite conclusion.

Price and Walsh,[4] on the basis of a study of the ultraviolet spectra, also consider that butadiene is represented only by the trans-form. Rasmussen and Brattain,[9,10] starting from the coincidences observed in a number of cases for frequency values in the infrared and Raman spectra, supposed that butadiene consists of a mixture of the two forms with the trans-form predominating at room temperature, the cis-form at low temperatures.

Aston and collaborators[11] arrive at the same conclusion on the basis of an investigation of the thermodynamic properties of gaseous 1,3-butadiene, and Ricarde and Nielsen[12] do likewise as a result of a study of the Raman spectra of gaseous and liquid 1,3-butadiene, and also the impossibility of interpreting certain weak lines satisfactorily as either overtones or combination frequencies. However, the authors[12] point out that, for a final demonstration of the existence of the cis-form, an investigation of intensities over a broad temperature range is necessary.

Vol'kenshtein and collaborators[13] carried out an investigation of the influence of temperature change on the intensity of lines in the Raman spectrum, with the purpose of clarifying the presence of rotational isomerism and estimating the difference in the energies of the isomers. The authors[13] established the fact that the distribution of the relative intensities of the lines 509, 912, 1197, 1272, and 1434 cm^{-1} was invariant in the temperature interval from −60 to +75°C. Two possible explanations were put forward in order to interpret the results obtained: (1) the difference in the energies of the isomers is very small, and therefore in the liquid phase the equilibrium of the rotational isomers of butadiene does not change with temperature; (2) there is no rotational isomerism at all in liquid butadiene—only the trans-isomer is present. Inasmuch as an unequivocal answer to the question posed was not obtained, the authors rightly point out that "a final solution of the question requires a theoretical calculation which fully explains all the coincidences in the infrared and Raman spectra."

In the present work, a calculation of the frequencies of the normal vibrations of the cis- and trans-forms of 1,3-butadiene has been carried out according to the procedure of El'yashevich and Stepanov[14] with the aim of a complete interpretation of the Raman and infrared spectra of 1,3-butadiene. We note that a theoretical calculation of the vibrational spectra of 1,3-butadiene has not been carried out up to the present time.

The vibrational spectra of 1,3-butadiene have been repeatedly studied. The infrared absorption spectrum of gaseous 1,3-butadiene has been studied by Bartolomé and Karweil[15] in the 500-1800 cm^{-1} region and by Rasmussen and Brattain[10] in the 650-4500 cm^{-1} region. The infrared spectrum of liquid 1,3-butadiene has also been studied.[16] The Raman spectrum of liquid 1,3-butadiene has been investigated in refs. 12, 13, 17, and 18. In the works of Bradacs and Kohovec[17] and of Richarde and Nielsen,[12] polarization measurements were also carried out. The Raman spectrum of gaseous 1,3-butadiene is presented in ref. 12 (without intensity measurements, to be sure).

3. The trans- and cis-1,3-butadiene molecules belong respectively to the symmetry point groups C_{2h} and

C_{2v}. The 24 normal vibrations of these molecules belong to the following symmetry types:

$\Gamma = 9A_g + 8B_u + 4A_u + 3B_g$ (trans-1,3-butadiene),
$\Gamma = 9A_1 + 8B_1 + 4A_2 + 3B_2$ (cis-1,3-butadiene).

The trans-1,3-butadiene molecule has a center of symmetry, and for it the rule of mutual exclusion must be satisfied. In the Raman spectrum of cis-1,3-butadiene all the fundamental frequencies are allowed, but in the infrared spectrum lines belonging to the representation A_2 are forbidden.

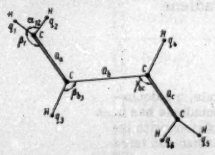

Fig. 1

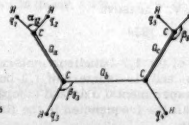

Fig. 2

Fig. 1. Vibrational coordinates of trans-1,3-butadiene.
Fig. 2. Vibrational coordinates of cis-1,3-butadiene.

For the calculation, we introduce 28 internal vibrational coordinates—the changes in the bond lengths and angles (see Figs. 1 and 2): q_1, β_1 (i = 1 – 6), Q_a, Q_b, Q_c, β_{b3}, β_{b4}, α_{12}, α_{23}, γ_{ab}, γ_{bc}, ρ_{12}^{t}, ρ_{23}^{t}, ρ_{23}^{c}, ρ_{64}^{c}, χ_{12}^{cc}, χ_{34}^{bb}, χ_{12}^{cc}.

Here ρ_{12}^{t} and ρ_{23}^{c} are the angles determining the departure of the bond (C=C)$_a$ from the plane of the CH_2 and CCH groups: χ_{12}^{bb} is the angle of twist of the two groups CH_2 and CCH relative to one another; χ_{12}^{cc} is the angle of twist of the two groups relative to the C—C single bond. There are 4 supplementary conditions among the internal coordinates.

For the evaluation of the kinematic coefficient matrices, the following geometric parameters[19] were used: r(C=C) = 1.337 A, r(C—C) = 1.483 A, r(C—H) = 1.082 A, ∠C=C—C = 122.4°, ∠C=C—H = 119.8°. Anharmonicity was taken into account by the introduction of "spectroscopic masses" for hydrogen.

The force coefficients necessary for the evaluation of the potential energy matrices were taken from the calculation for propylene[20]; some of the coefficients were evaluated by the method of variation of constants. In particular, the force coefficient k(C—C) = 8.02, while in the paraffins k(C—C) = 7.02 (in units of 10^5 cm^{-2}).

4. Comparison of the calculated values of the vibration frequencies of trans- and cis-1,3-butadiene shows a great similarity in their vibrational spectra. Let us con-

Table 1. Interpretation of the Vibrational Spectra of 1,3-Butadiene (Frequencies in cm^{-1})

Band No.	Coordinate	Symmetry	Calculation	Trans-1,3-butadiene: Experiment: Raman spectrum according to ref. 12: Gas	Raman spectrum according to ref. 12: Liquid*	Infrared spectrum: Gas according to refs. 10, 15*	Interpretation: According to ref. 11	According to ref. 21	According to ref. 12	Cis-1,3-butadiene: Symmetry	Calculation
1	$\varphi_{CH_2}^{+}$(C—H)	A_g	3088	3101	3093 (m) 0.8		3088	3088	3101	A_1	3099
2	$\varphi_{CH_2}^{-}$(C—H)	A_g	3013	3014	3004 (vs) 0.1		3000	3000	3014	A_1	3007
3	φ_{CH}(C—H)	A_g	2997	3014	3004 (vs) 0.1		3000	3000	3014	A_1	3023
4	Q (C=C)	A_g	1640	1643	1638 (vs) 0.1		1635	1635	1643	A_1	1652
5	α (HCH)	A_g	1434	1442	1439 (vs) 0.3		1437	1437	1442	A_1	1426
6	β_{CH} (CCH)	A_g	1327	1279	1279 (vs) 0.2		1303	1303	1302	A_1	1324
7	Q (C—C)	A_g	1154	1205	1202 (vs) 0.3		1200	1200	1205	A_1	1012
8	$\beta_{CH_2}^{c}$(CCH)	A_g	831		890 (w)**		1276	1276	1279	A_1	859
9	γ (CCC)	A_g	520	513	514 (s) 0.1		513	513	513	A_1	210
10	$\varphi_{CH_2}^{+}$(C—H)	B_u	3098			3095 (vs)	3000		3100	B_1	3098
11	$\varphi_{CH_2}^{-}$(C—H)	B_u	3007			3000 (s)***	3000		3000	B_1	3012
12	φ_{CH}(C—H)	B_u	3016			3030 (s)	3000		3080	B_1	2996
13	Q (C=C)	B_u	1580			1599 (vs)	1602	1590	1599	B_1	1568
14	α (HCH)	B_u	1382			1385 (m)	1490	1470	1484	B_1	1396
15	β_{CH} (CCH)	B_u	1320			1285 (m)	1385	1285	1379	B_1	1309
16	$\beta_{CH_2}^{c}$(CCH)	B_u	986			987 (s)	1282	1385	1290	B_1	1116
17	γ (CCC)	B_u	311			309****	326	520	320	B_1	572
18	$\chi_{CH_2}^{CH_2}$	B_g	987		987 (w) 0.8		667		686	B_2	974
19	ρ_{CH_2}	B_g	909	910	911 (m) 0.7**		914	914	911	B_2	909
20	ρ_{CCH}	B_g	660	686	686 (vw)		899	899	890	B_2	482
21	$\chi_{CCH}^{CH_2}$	A_u	1044			1013 (vs)	520	340	520	A_2	1042
22	ρ_{CH_2}	A_u	907			909 (vs)	1014	1010	909	A_2	913
23	ρ_{CCH}	A_u	517			520 (m)	910	912	1014	A_2	662
24	$\chi_{43}^{C_1}$	A_u	223				170		170	A_2	285

*Symbols: vs – very strong line; s – strong; m – medium; w – weak; vw – very weak; number to right of parentheses – degree of depolarization of the line.
**According to the data of ref. 17, depolarized.
***According to the data of ref. 16.
****The weak line 618 cm^{-1} in the Raman spectrum may be interpreted as an overtone of ν_{17}. Hence ν_{17} = 309 cm^{-1}.

Table 2. Interpretation of the Overtones and Combination Frequencies of Trans-1,3-Butadiene (Frequencies in cm^{-1})

Infrared absorption spectrum (gas from ref. 10)	Interpretation	Raman spectrum according to ref. 12		Interpretation
		Gas*	Liquid*	
687 (w)	$\nu_{13} - \nu_{18} = 689\ (A_u)$		320 (vw)	$\nu_7 - \nu_9 = 315\ (A_g)$
739 (vw)	$\nu_4 - \nu_{21} = 734\ (A_u)$		618 (vw)	$2\nu_{17} = 618\ (A_g)$
758 (vw)	$\nu_9 - \nu_{23} = 759\ (A_u)$		752 (vw)	$\nu_8 - \nu_9 = 766\ (A_g)$
1416 (vw)	$\nu_9 + \nu_{23} = 1410\ (A_u)$		1025 (vw)**	$2\nu_9 = 1026\ (A_g)$
1439 (vw)	$\nu_{18} + \nu_{23} = 1430\ (B_u)$		1130 (vw)	$\nu_4 - \nu_9 = 1130\ (A_g)$
1481 (w)	$\nu_{18} + \nu_{22} = 1487\ (B_u)$	1302	1303 (s) P	$\nu_{13} - \nu_{17} = 1290\ (A_g)$ ***
1497 (w)	$\nu_{16} + \nu_9 = 1500\ (B_u)$		1401 (vw)	$\nu_{18} + \nu_{17} = 1296\ (A_g)$
1661 (vw)	$\nu_{18} + \nu_{20} = 1673\ (A_u)$			$\nu_9 + \nu_8 = 1403\ (A_g)$
	$\nu_{16} - \nu_9 = 1653\ (B_u)$	1659 (vw)		$\nu_1 - \nu_9 = 1659\ (A_g)$
1757 (w)	$\nu_3 + \nu_{17} = 1751\ (B_u)$		1678 (vw)	$\nu_{18} + \nu_{20} = 1653\ (A_g)$
1823 (m)	$\nu_{18} + \nu_{22} = 1819\ (B_u)$	1780	1779 (w) P	$\nu_{21} + \nu_{17} = 1694\ (A_g)$
1883 (vw)	$\nu_{18} + \nu_{23} = 1876\ (B_u)$	2092	2089 (vw)	$2\nu_8 = 1780\ (A_g)$
1965 (w)	$\nu_3 + \nu_{23} = 1962\ (A_u)$	2256 (vw)		$\nu_7 + \nu_8 = 2095\ (A_g)$
1975 (w)	$\nu_{18} + \nu_{21} = 1980\ (B_u)$		2327 (vw)	$\nu_8 + \nu_{18} = 2246\ (B_g)$
2105 (vw)	$\nu_9 + \nu_{15} = 2112\ (B_u)$		2401 (vw)	$\nu_4 + \nu_{20} = 2329\ (B_g)$
2265 (vw)	$\nu_8 + \nu_{14} = 2275\ (B_u)$		2523 (vw)	$2\nu_7 = 2410\ (A_g)$
2515 (vw)	$\nu_{13} + \nu_{19} = 2509\ (A_u)$	2842	2838 (vw)	$\nu_4 + \nu_8 = 2533\ (A_g)$
2595 (vw)	$\nu_7 + \nu_{14} = 2590\ (B_u)$	2879	2874 (vw)	$\nu_4 + \nu_7 = 2848\ (A_g)$
3955 (vw)	$\nu_{13} + \nu_{19} = 3940\ (A_u)$		3187 (vw)	$2\nu_9 = 2884\ (A_g)$
4100 (vw)	$\nu_1 + \nu_{21} = 4114\ (A_u)$		3287 (vw)	$2\nu_{13} = 3198\ (A_g)$
4290 (w)	$\nu_2 + \nu_{15} = 4299\ (B_u)$			$2\nu_4 = 3286\ (A_g)$
4485 (w)	$\nu_1 + \nu_{14} = 4486\ (B_u)$			
4695 (vw)	$\nu_1 + \nu_{13} = 4700\ (B_u)$			

*Symbols: P—polarized line; for the remaining symbols, see note to Table 1.
**According to the data of ref. 17.
***Fermi resonance with ν_8.

sider first of all the totally symmetric planar vibrations of symmetry types A_g and A_1. The two molecules have closely-agreeing frequencies for the vibrations q(C—H), Q(C=C), α(HCH), β_4(CCH), and β^-(CCH). Only the frequencies of the vibrations Q(C—C) and γ(CCC) differ markedly. These lines must be intense and polarized in the Raman spectrum. The values of the nonplanar vibrational frequencies ρ_{CH_2}, $\chi^{CH}_{CH_2}$, and ρ_{CCH} (symmetry type B_g) of the trans-form, which are active in the Raman spectrum, are close to the corresponding vibration frequencies ρ_{CH_2}, $\chi^{CH}_{CH_2}$ (B_2) and ρ_{CCH} (A_2) of the cis-form. The frequencies of the antisymmetric planar vibrations q(C—H), Q(C=C), α(HCH), and β_4(CCH) of the trans-form (symmetry type B_u), which are active in the infrared spectrum, differ comparatively little from the corresponding frequencies of the cis-form (symmetry type B_1). Only the frequencies of the vibrations γ(CCC) and β^-(CCH) are markedly different. The frequency ρ_{CH_2} (A_u), which is active in the infrared spectrum, is close to the frequency ρ_{CH_2} (B_2), while the frequencies ρ_{CCH} and $\chi^{CH}_{CH_2}$ (A_u) differ markedly from the corresponding frequencies of the cis-form (symmetry type B_2).

In order to demonstrate the existence of one or the other form, it is necessary first of all to consider the Raman and infrared spectra in those regions where the spectra of the two designated isomers must differ markedly. The intense polarized lines 1202 and 514 cm^{-1} can be assigned only to the vibrations Q(C—C) and γ(CCC) of the trans-form, inasmuch as the frequency values of these observed lines are closest to the calculated frequencies of trans-butadiene. The intense infrared bands 1013 and 520 cm^{-1} are to be assigned to the same isomer (to the vibrations $\chi^{CH}_{CH_2}$ and ρ_{CCH} (A_u)). The line 1013 cm^{-1} cannot be assigned to the vibration $\chi^{CH}_{CH_2}$ of the cis-form, symmetry type A_2, since this vibration is inactive in the infrared spectrum. As for the line 520 cm^{-1}, it is to be assigned to the vibration ρ_{CCH} (A_u), since the calculated value for the frequency of this vibration (517 cm^{-1}) is closer to the experimental quantity than in the case of the cis-form (462 cm^{-1}).

The indicated assignment of the four above-named lines unequivocally indicates the presence of the trans-form of 1,3-butadiene. It is now necessary to carry out the assignment of the other trans-butadiene frequencies. The intense polarized lines 1643 and 1442 cm^{-1} are to be assigned to the vibrations Q(C=C) and α(HCH), symmetry type A_g. If these lines belonged to the cis-form, they would have to be observed in the infrared spectrum also, with medium intensity (as, for example, in the case of propylene and other molecules of the type RCH=CH_2 which contain the CH=CH_2 group). However, this is not observed—in the region around 1640 cm^{-1} there are no infrared absorption bands at all, while in the 1440 cm^{-1} region there is a line of insignificant intensity, which may be interpreted as a combination frequency. By analogous considerations, the intense infrared band 1599 cm^{-1} and the medium-intensity band 1385 cm^{-1} are to be assigned to the antisymmetric vibrations Q(C=C) and α(HCH) (symmetry type B_u) of the trans-form, since these frequencies do not manifest themselves in the Raman spectrum. Thus the most intense lines in the Raman spectrum (1643, 1442, 1205, and 513 cm^{-1}) and in the infrared absorption spectrum (1599, 1385, 1013, and 520 cm^{-1}) may be interpreted only as vibration frequencies of the trans-form. When one takes into account, furthermore, that in the region around 200 and 1000 cm^{-1} there are in the Raman spectrum no intense polarized lines which, according to the calculation, should correspond to the frequencies of the vibrations Q(C—C) and γ(CCC) of the cis-form, then one may draw the conclusion that, if the cis-isomer of 1,3-butadiene is present, it is only in negligible concentration. Therefore the remaining weaker lines are also to be assigned to the trans-form, for it is unlikely that the strongest lines Q(C=C), Q(C—C), γ(CCC), α(HCH), and others should not appear in the spectrum while weaker lines were found.

On the basis of the foregoing, we have carried out the interpretation of the vibrational spectra of 1,3-butadiene. The results of the interpretation are presented in Tables 1 and 2. From the data presented it follows that, by assuming the existence of the trans-form alone, all the frequencies in the Raman and infrared spectra may be interpreted as fundamental frequencies, overtones, and combination frequencies. Here we should dwell particularly on the interpretation of the intense polarized line around 1303 cm^{-1} in the Raman spectrum. As is shown by the calculation, it cannot be assigned to the fundamental frequencies of the trans-form. This line must be interpreted as a combination frequency. The high intensity of this line may be explained by Fermi resonance between the fundamental frequency 1279 and the combination frequencies 1290 cm^{-1} (1599 – 309) and 1296 cm^{-1} (987 + 309), which belong to the same symmetry type (A_g) as the 1279 cm^{-1} line. If the 1303 cm^{-1} line belonged to the cis-form, it would be incomprehensible why this one line should appear with considerable intensity while the other lines Q(C=C), Q(C—C), and γ(CCC) do not appear at all.

As can be seen from Table 1, the agreement between the calculated and observed frequency values is quite good—the maximum error amounts to 59 cm^{-1}, the average error equals 16 cm^{-1}. This indicates that the set of force coefficients used in the calculation reflects quite well the peculiarities of the force field of the 1,3-butadiene molecule. In particular, the results of the calculation lead to a conclusion concerning the increase in stiffness of the C—C single bond in comparison with the paraffins, which agrees with the diminution in the length of this bond in 1,3-butadiene.

The results obtained in this work may be used for the calculation and interpretation of the vibrational spectra of other dienes. At the present time, the calculation of isoprene and 2,3-dimethyl-1,3-butadiene is underway.

REFERENCES

1. L. M. Sverdlov, Opt. i Spektr. 2, 540 (1957).
2. L. M. Sverdlov, M. G. Borisov, and N. V. Tarasova, Opt. i Spektr. 5, 354 (1958).
3. R. S. Mulliken, Revs. Modern Phys. 14, 265 (1942); C. Moser, J. Chem. Soc. 3455 (1954); J. Fain and F. Matsen, J. Chem. Phys. 26, 376 (1957).
4. W. C. Price and A. D. Walsh, Proc. Roy. Soc. A174, 220 (1940).
5. T. Anno, J. Chem. Phys. 28, 944 (1958).
6. Ya. K. Syrkin, M. E. Dyatkina, and A. A. Zhukhovitskii, Uspekhi khim. 10, 121 (1941).
7. I. Pople, Trans. Faraday Soc. 49, 1375 (1953); R. Berry, J. Chem. Phys. 26, 1660 (1957).
8. I. N. Godnev and V. P. Morozov, Zhur. Fiz. Khim. 21, 799 (1947).
9. R. S. Rasmussen, D. Tunnicliff, and R. Brattain, J. Chem. Phys. 11, 432 (1943).
10. R. S. Rasmussen and R. Brattain, J. Chem. Phys. 15, 131 (1947).
11. J. Aston, G. Szasz, H. Woolley, and F. Brickwedde, J. Chem. Phys. 14, 67 (1946).
12. C. Richarde and J. Nielsen, J. Opt. Soc. Am. 40, 438 (1950).
13. M. V. Vol'kenshtein, V. N. Nikitin, and T. V. Yakovleva, Izvest. Akad. Nauk SSSR, Ser. Fiz. 14, 471 (1950).
14. M. V. Vol'kenshtein, M. A. El'yashevich, and B. I. Stepanov, "Kolebaniya molekul" (Molecular Vibrations), Vol. I. Gosudarst. Izd. Tekh.-Teoret. Lit., Moscow, 1949.
15. E. Bartolomé and J. Karweil, Z. physik. Chem. 35, 442 (1937).
16. E. Greitz and F. Smith, J. Res. Natl. Bur. Standards 43, 305 (1949).
17. K. Bradacs and Z. Kohovec. Z. physik. Chem. 48, 63 (1940).
18. A. Dadieu and K. Kohlrausch, Ber. deut. chem. Ges. 63, 1657 (1930).
19. A. Almeuningen, O. Bastiansen, and M. Tractteberg. Acta Chem. Scand. 12, 1221 (1958).
20. L. M. Sverdlov, Doklady Akad. Nauk SSSR 106, 80 (1956).
21. Landolt-Börnstein Tabellen, Molekeln, 1, 2 Teil. 1951.

VIBRATIONAL SPECTRA OF AROMATIC COMPOUNDS
VII. Characteristic Vibrations of Monosubstituted Benzenes

A. M. Bogomolov

Received 22 December 1959

A scheme has been realized for calculating the characteristic vibrations of the substitution products of benzene with the use of electronic computers. A classification of the characteristic vibrations of monosubstituted benzenes has been completed on the basis of a calculation of the frequencies, vibration forms, and atomic displacements of toluene during its vibrations.

SCHEME FOR CALCULATING THE CHARACTERISTIC VIBRATIONS

In the present work, the general theory of characteristic or specific frequencies[1] is used to determine the characteristic vibrations of the substitution products of benzene. The application of this theory to the substitution products of benzene has been worked out in refs. 2 and 3. The scheme of concrete calculations planned in these articles has been realized by us on an electronic computer of the "Arrow" type. This scheme contains a number of stages, to which the following programs which we have set up correspond.

1. A program for the method of progressive diagonalization[4] for finding the roots of the secular equations. The program enables us to find simultaneously the roots of a submatrix of the equation which has a lower order than the matrix of the equation itself. In its application to aromatic compounds, the roots of the submatrix for the benzene ring were first separated out (they do not interact with the submatrix for the substituent), then the diagonal elements of the remaining matrix emerged, after which its roots were found. Operation of the program in such a pattern made it possible to determine immediately the frequencies which are characteristic with respect to frequency and form, and to study the influence of the radical on the nonspecific vibrations.

2. A program for the Mayants method[1] of refining the roots of the secular equation and of finding the vibration forms at the same time. The computed form coefficients served as confirmation for the characteristic vibrations found in the first program and made it possible to estimate the degree of nonspecificity of the vibrations associated with the substituent.

3. A program for the Leverrier-Faddeeva method[5] of transforming the secular equation into a polynomial and of finding the eigenvalues and eigenvectors of the matrix of the secular equation. The program was used as a check on the calculations.

4. A program for computing the normalizing factors[4] for the form coefficients of the vibrations; these were necessary to calculate the atomic displacements and the intensities.

5. A check of the computation of the form coefficients of the vibrations according to the relationship: $LL' = A$, where L is the matrix of the normalized form coefficients (the prime is the sign of transposition) and A is the matrix of the kinematic coefficients.

6. As a supplement to refs. 1-3, we have set up a program for the computation of the atomic displacements during the normal vibrations of the molecule. It is thoroughly evident that the atomic displacements during each normal vibration enable us to obtain a far clearer picture of this vibration than do the vibration forms even in internal coordinates, and all the more so in symmetry coordinates.

In order to investigate the problem of specificity, it

is especially important to establish the fraction to which the atoms of the substituent participate in each normal vibration. The atomic displacements are calculated according to the formula:[6]

$$\mathbf{d}_a = \mu_a \sum_{ij} S^i_a g_{ij} R^j,$$

where $\mathbf{d}_a$ is the displacement vector of the atom numbered a, μ_a is a quantity reciprocal to the mass of the atom, R^j are the symmetry coordinates, $\| g_{ij} \|$ is the kinetic energy matrix in these coordinates, which is obtained by a program for the transformation of the matrix of the kinematic coefficients, and S^i_a are vectors with the help of which the coordinates R can be expressed in terms of d.[6] The realization of the program just described enabled us, for the first time, to obtain graphical representations, based on the results of calculation, of the atomic displacements of toluene during its vibrations. The graphical depictions of vibrations based only on considerations of symmetry, which are widely distributed in the literature, have a qualitative character.

In the computation of the frequencies and normalized forms of the vibrations of toluene, we used the force constants for benzene and toluene[7,8] with the changes described in refs. 9 and 10.

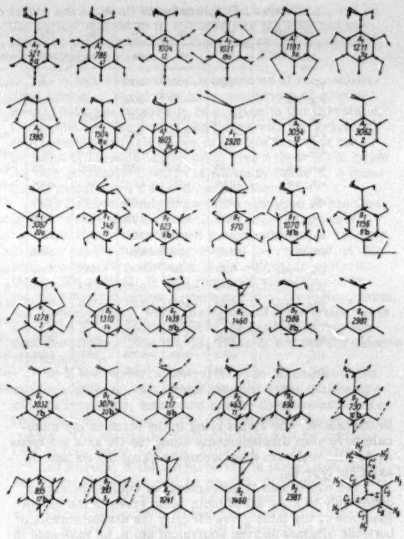

RESULTS OF THE CALCULATION

From experimental data, the characteristic frequencies[11,12] of monosubstituted benzenes and the lines which are characteristic in the Raman spectra[13] are well known. In the present work these experimental data receive a confirmation based on theoretical calculations, which in turn testifies to the applicability of our procedure to the theoretical study of the characteristic vibrations of substituted benzenes of other types. The fundamental results of the calculations are presented in Tables 1-4 and in the figure. The atomic displacements in toluene for vibrations of symmetry types A_1, B_1, and B_2 are presented in Tables 1-3. For type A_2, such displacements coincide completely with the corresponding displacements in benzene, and therefore they are not shown in the figure.

The symbols for the atoms of toluene and the positive directions of the coordinate axes are indicated in the last diagram of the figure. The origin is located in the center of the ring. The atoms of the methyl group are marked by primes, and H'_2 is located in the plane of the ring. In Tables 1-3 are presented the values of the atomic displacements (in Å) along the coordinate axes (the general displacement of any atom is obtained by vector addition of the displacements along the coordinate axes). The atoms lying on the C_s symmetry axis (H_1, C_1, C'_4, C_4) have zero displacements along the Ox axis for type A_1, and zero displacements along the Oy axis for type B_1; consequently, for the sake of brevity, these are not included

Table 1. Displacements (in A) of the Atoms of Toluene During Normal Vibrations of type A_1

$\nu_{obs.}$ (cm^{-1})	521	790	1004	1030	1181	1211	1380	1504	1605	2920	3057	3067	3077
$\nu_{calc.}$ (cm^{-1})	490	775	997	1014	1172	1232	1380	1502	1601	2950	3054	3061	3069
$zC_2, -zC_6$ . .	0.010	−0.012	−0.003	−0.017	0.003	−0.005	0	0.008	0.003	0	0.008	0	−0.003
$zC_3, -zC_5$ . .	0.010	−0.016	−0.016	0.011	0.003	0.002	0	−0.006	0.005	0	−0.001	−0.004	0.001
$xH_2, -xH_6$ . .	0.004	0.001	−0.005	−0.033	0.028	0.008	−0.001	−0.015	−0.007	0	0.031	0.001	0.029
$xH_3, -xH_5$ . .	0.003	−0.016	−0.015	0.026	0.030	−0.013	0	0.010	−0.010	0	0.011	0.038	−0.014
xH'_1, xH'_2 . .	0	0	0	0	0	0	−0.010	0	0	−0.020	0	0	0
xH'_3	0	0	0	0	0	0	0.021	−0.001	0	0.040	0	0	0
yC_1	−0.025	0.011	−0.022	−0.007	−0.001	0.003	0	0.008	0.005	0	0.004	−0.003	−0.004
yC_2, yC_6 . . .	−0.009	−0.008	−0.001	−0.003	−0.004	−0.006	0	−0.010	−0.011	0	−0.002	0	−0.001
yC_3, yC_5 . . .	−0.005	−0.003	0.012	0.002	0.004	0.004	0	−0.003	0.013	0	0	0.002	−0.001
yC_4	0.018	−0.007	0.002	0.002	−0.002	0.023	−0.001	0.011	−0.011	0	0	0	0
yH_1	−0.024	0.010	−0.023	−0.008	−0.001	0.003	0	0.010	0.004	0	−0.044	0.029	0.045
yH_2, yH_6 . . .	0.001	−0.028	0.003	0.023	−0.045	−0.029	0.002	0.031	0.006	0	0.018	0.001	0.018
yH_3, yH_5 . . .	−0.018	−0.003	0.015	0.026	0.050	−0.022	0.001	0.027	−0.013	0	−0.007	−0.022	0.008
yC'_4	0.031	0.016	−0.002	−0.001	0.001	−0.010	0.015	−0.003	0.002	−0.004	0	0	0
yH'_1, yH'_2, yH'_3	0.032	0.017	−0.002	−0.001	0	−0.013	−0.052	−0.002	0.003	0.012	0	0	0
$xH'_1, -xH'_2$ . .	0	0	0	0	0	0	−0.018	0.001	0	−0.035	0	0	0

Table 2. Displacements (in A) of the Atoms of Toluene during Normal Vibrations of type B_1

$\nu_{obs.}$ (cm^{-1})	340	423	970	1021	1155	1270	1311	1439	1480	1580	2920	3032	3074
$\nu_{calc.}$ (cm^{-1})	347	408	975	1023	1154	1300	1317	1441	1467	1599	2976	3049	3075
xC_1	0.010	−0.008	0.004	0.007	0.010	−0.001	0.014	0.008	0.005	−0.015	0	0	0
xC_2, xC_6 . . .	0.002	−0.017	−0.003	−0.005	−0.004	−0.005	−0.005	0	−0.002	0.008	0	−0.003	−0.003
xC_3, xC_5 . . .	−0.019	0.013	−0.007	−0.003	−0.002	0	−0.008	−0.003	0.001	−0.008	0	0.002	−0.003
xC_4	−0.037	0.008	0.022	0	0.002	0.012	0.008	0.010	0	0.014	0	0	0
xH_1	0.019	0.015	0.015	0.050	0.077	0.018	−0.032	−0.042	−0.018	0.015	0	0	0
xH_2, xH_6 . .	0.009	−0.020	0.002	0.005	−0.026	0.019	0.004	−0.019	−0.008	0.001	0	0.030	0.029
xH_3, xH_5 . .	−0.026	0.017	−0.007	0.016	−0.008	−0.024	0.015	−0.015	−0.010	0	0	−0.030	0.030
xC_4'	0.029	0.005	0.020	−0.005	−0.002	−0.005	−0.002	−0.005	0.004	−0.001	0.007	0	0
xH_1'	0.038	0.003	−0.038	0.006	0.003	0.011	0.008	0.024	−0.010	−0.004	0.016	0	0
xH_2'	0.053	0.005	−0.030	0.005	0.003	0.009	0.008	0.023	−0.008	−0.005	−0.011	0	0
xH_3'	0.051	0.004	−0.015	0.002	0.001	0	0	−0.007	−0.044	0.003	−0.053	0	0
yC_2, $-yC_6$ . .	−0.011	−0.017	−0.002	−0.008	0.006	0.006	0.008	−0.009	−0.044	−0.004	0	−0.001	−0.002
yC_3, $-yC_5$ . .	−0.008	−0.016	0.001	0.012	−0.002	0.003	−0.011	0.007	0.014	−0.004	0	−0.002	0.002
yH_2, $-yH_6$ . .	−0.024	−0.010	−0.011	−0.026	0.043	−0.038	−0.008	0.019	0.005	0.008	0	0.017	0.017
yH_3, $-yH_5$ . .	−0.021	−0.009	0.001	0.046	−0.011	−0.038	0.028	−0.011	−0.013	0.009	0	0.017	−0.017
yH_1'	0.034	0	−0.035	0.006	0.002	0.003	0.001	−0.006	0.019	0.005	−0.009	0	0
yH_2'	0.023	−0.001	−0.038	0.007	0.002	0.004	0.001	−0.005	0.018	0.006	0.010	0	0
yH_3'	−0.068	−0.001	0.069	−0.012	−0.004	−0.006	−0.002	0.013	−0.037	−0.011	0.018	0	0
zH_1', $-zH_2'$ . .	−0.028	−0.003	0	0.001	0	−0.003	−0.004	−0.015	0.033	0.005	−0.022	0	0

in the tables. The atoms lying in the plane of the molecule have zero displacements along the Oz axis for types A_1 and B_1, and zero displacements along the Ox and Oy axes for type B_2.

The coordinate displacements of equivalent atoms differ only in sign, all of them being given in the tables (one line of the table gives directly the displacements of both the original and the equivalent atom, as indicated in the first column of the table).

In the figure are shown the displacement vectors of the atoms of toluene during the normal vibrations. Inside each ring are shown the experimental frequency value and the number of the corresponding benzene vibration in the standard numbering. The scales of the displacement vectors and of the bond lengths are different.

In Table 4 are represented the frequencies of monosubstituted benzenes, divided into three groups: (1) frequencies of vibrations which are specific in frequency, form, and atomic displacements for the C_6H_5 group of coordinates; (2) frequencies of vibrations which are specific with respect to frequency; and (3) frequencies of nonspecific vibrations, for which the spectral ranges are

Table 3. Displacements (in A) of the Atoms of Toluene During Normal Vibrations of Type B_2

$\nu_{obs.}$ (cm^{-1})	217	485	630	720	885	993	1041	1440	2960
$\nu_{calc.}$ (cm^{-1})	207	445	636	726	904	979	1022	1434	2975
zC_1	0.032	−0.023	−0.013	0.014	0.011	−0.012	0	0	0
zC_2, zC_6 . .	0.003	0.015	0.018	0	0.002	0.010	0	0	0
zC_3, zC_5 . .	−0.030	0.045	−0.013	0.010	−0.011	−0.003	0.003	0	0
zC_4	−0.046	−0.043	0.015	−0.021	0.006	0.001	0.004	−0.002	0
zH_1	0.071	−0.041	−0.054	−0.050	−0.052	0.070	0.099	0	0
zH_2, zH_6 . .	0.016	0.042	0.003	−0.063	−0.014	−0.056	−0.003	0	0
zH_3, zH_5 . .	−0.034	0.035	−0.051	−0.018	0.056	0.023	−0.009	0	0
zC_4'	0.081	0.016	0	0.010	−0.004	0	−0.014	−0.050	−0.007
zH_1', zH_2' . .	−0.054	−0.013	0.001	−0.011	0.005	0	0.021	0.008	0.039
zH_3'	−0.055	−0.015	0.002	−0.012	0.008	0	0.039	0.072	−0.003
yH_1', $-yH_2'$ . .	0.001	0.001	0	0.001	−0.002	0	−0.011	−0.038	0.025
yH_3', $-yH_2'$ . .	−0.042	−0.029	0.012	−0.036	0.013	0	0.063	−0.036	−0.017

indicated. The CH valence vibrations are of no interest for analytical purposes, and therefore they are not included in Table 4.

The coefficient of nonspecificity[1] is a criterion for the specificity of a vibration with respect to frequency. In order to confirm the specificity with respect to fre-

Table 4. Vibrations of Monosubstitution Products of Benzene, their Correlation with Benzene Vibrations, and their Specificity Properties

Band No.	$\nu_{obs.}$ (cm^{-1})* IR	$\nu_{obs.}$ (cm^{-1})* Ram.	$\nu_{calc.}$ (cm^{-1})	Symmetry	$\nu_{benzene}$** (cm^{-1})
Vibrations specific in frequency, form, and atomic displacements for the C_6H_5 group of coordinates					
1	—	406 ± 8	405	A_2	405 (18a)
2	620 ± 3	618 ± 4	608	B_1	606 (6b)
3	695 ± 5	—	695	B_2	704 (4)
4	838 ± 8	838 ± 10	844	A_2	849 (10a)
5	904 ± 8	—	904	B_2	970 (17b)
6	970 ± 10	970 ± 10	970	A_2	970 (17a)
7	—	993	979	B_2	985 (5)
8	1000 ± 4	1000 ± 5	997	A_1	1010 (12)
9	1030 ± 4	1028 ± 3	1014	A_1	1037 (18a)
10	1156 ± 4	1156 ± 5	1154	B_1	1178 (9b)
11	1178 ± 3	1180 ± 4	1172	A_1	1178 (9a)
12	1310 ± 7	1315 ± 10	1317	B_1	1310 (14)
13	1500 ± 5	1500 ± 2	1502	A_1	1485 (19a)
14	1605 ± 7	1607 ± 10	1605	A_1	1596 (8a)
Vibrations specific with respect to frequency					
15	1070 ± 10	1060 — 1070	1073	B_1	1037 (18b)
16	1450 ± 10	1445 ± 6	1441	B_1	1485 (19b)
17	1588 ± 9	1585 ± 6	1599	B_1	1596 (8b)

Nonspecific vibrations

	Toluene $\nu_{obs.}$	Toluene $\nu_{calc.}$	Symmetry	First group of substituents $\nu_{obs.}$ (cm^{-1})	Second group of substituents $\nu_{obs.}$ (cm^{-1})	$\nu_{benzene}$** (cm^{-1})
18	217	207	B_2	180—240	140—300	849 (10b)
19	348	347	B_1	290—350	250—400	1150 (15)
20	465	445	B_2	435—480	415—480	405 (16b)
21	521	499	A_2	480—500	270—535	606 (6a)
22	730	726	B_2	702—730	690—750	671 (11)
23	786	775	A_1	730—780	650—800	992 (1)
24	1211	1232	A_1	1205 specific for the C_6H_5C group	1060—1080 1190—1270	3047 (7a)
25	1331	1300	B_1	1275—1295	1255—1275	1326 (3)

*Symbols: IR – infrared absorption spectrum; Ram. – Raman spectrum.
**In parentheses – the number of the corresponding benzene vibration in the standard numbering.

quency, calculations were also carried out for more complex substituents (ethylbenzene) and the diagonal elements were compared after diagonalization of the ring and final solution of the secular equation. If, for the two molecules (toluene and ethylbenzene), the coefficient of nonspecificity does not exceed 10% for some one vibration, that vibration is considered to be specific with respect to frequency for the given substitution type.

The experimental frequency values in Table 4 are based on a synthesis of the data of all the numerous literature sources known to us.[11-21] From them it follows in particular that, with regard to the frequency of the nonspecific vibrations, the substituents may be divided into 2 groups: (1) alkyl radicals with a normal or branched structure, and radicals of arbitrary structure but attached to the ring through a CH_2 group, and (2) substituents connected to the ring through an N, O, S, F, Cl, Br, or I atom, a quanternary C atom, a CH group or a CO group.

We make the following comments on individual normal vibrations.

No. 21. Vibration of the internal ring angles γ. If the substituent belongs to the first group (alkyl radicals of normal structure), the vibration is specific with respect to frequency, beginning with ethylbenzene—495 ± 6 cm^{-1}. For branched alkyl radicals with the branch at the point of attachment to the ring, the vibration has a constant frequency—460 ± 2 cm^{-1}—and no longer depends on the length of the branched chains.

No. 22. Totally symmetric vibration corresponding to A_{1g} of benzene. The substitution distorts the vibration; it interacts strongly with the radical and is nonspecific with respect to the vibration form and the atomic displacements. In the first group of substituents—the normal alkyl radicals—a lowering of the frequency from 786 to 740 cm^{-1} is observed as the chain is lengthened. When the radical is branched at the point of attachment to the ring, the frequency lowering is more pronounced (to 730 cm^{-1}).

No. 24. Valence vibration of the bond joining the ring with the radical, involving the external CCH angles, β, of the ring. In the case of the first group of substituents, the vibration is specific in frequency and form for the C_6H_5 group of coordinates. An explanation for this is given in our ref. 2. The frequencies of the C—C valence vibrations of the subsituent chains lie in the interval 1200-740 cm^{-1}, only bands with extreme values of the frequency being intense. The vibration with the frequency 1200 cm^{-1} is localized at the beginning of the chain, at the point of attachment of the radical to the ring. For substituents of the second group, the vibration is nonspecific in both frequency[14] and form.

CONCLUSIONS

From the data of Tables 1-4 and from the figure the following conclusions may be drawn.

1. A deep-seated connection is found between the specificity of a vibration and the atomic displacements in that vibration, namely: (a) if the vibration is specific in frequency and form for the C_6H_5 group of coordinates or specific in frequency for the C_6H_5C group of coordinates, then the atom linking the benzene ring with the substituent and the atoms of the substituent itself undergo insignificant displacements during the given vibration, and the vibration itself is localized, as a rule, on the atoms of the benzene ring which are remote from the point of substitution; (b) vibrations which are specific neither in frequency nor in form are essentially localized on the bond joining the ring with the substituent, and on the angles nearest to it; the atoms of the ring and the radical near this bond and these angles undergo considerable displacements.

2. A correlation of the frequencies of monosubstituted benzenes based only on a comparison of experimental data has repeatedly been given in the literature. Comparison of the data of the figure with the graphical representations (well known in the literature) of the vibrations of benzene allows us to give a theoretical basis for this correlation, which is shown in Table 4. A number of conclusions follow from this table:

(a) To each doubly degenerate vibration of benzene, in accordance with the established correlation, there correspond two vibrations of a monosubstituted benzene. In practice, the degeneracy may not be removed, if this doubly degenerate vibration is not subject to perturbation by the radical. In this case both vibrations of the monosubstituted benzene are specific in frequency, form, and displacements, while the values of their frequencies are close to one another and to the corresponding benzene frequency. (Nos. 10, 11, Table 4, and the CH valence vibrations).

(b) If the perturbation referred to takes place, but is not large, then only one of the vibrations will be specific in frequency, form, and atomic displacements, its frequency being close to the corresponding benzene frequency. The second benzene vibration will be specific only in frequency (Nos. 14, 17; 9, 13; 15, 16, Table 4).

(c) Finally, if the perturbation is large, then only one of the vibrations will be specific in frequency, form, and atomic displacements. Its frequency is close to the corresponding benzene frequency. The second vibration will be entirely nonspecific—its frequency is sharply lowered, depending on the nature and mass of the substituent (Nos. 1, 18; 2, 21; 4, 22; Table 4).

In conclusion, the author thanks M. A. Kovner for his interest in the work and for discussion.

REFERENCES

1. L. S. Mayants, Trudy Fiz. Inst. Akad. Nauk SSSR 5, 65 (1950).
2. M. A. Kovner and A. M. Bogomolov, Opt. i Spektr. 1, 364 (1956).
3. M. A. Kovner and A. M. Bogomolov, Uchenye Zapiski Saratovsk. Univ., Fiz. 56, 100 (1957).
4. M. V. Vol'kenshtein, M. A. El'yashevich, and B. I. Stepanov, "Kolebaniya molekul" (Molecular Vibrations). Gosudarst. Izd. Tekh.-Teoret. Lit., Moscow, 1949.
5. V. N. Faddeeva, "Vychislitel'nye metody lineinoi algebry" (Computational Methods of Linear Algebra). Gosudarst. Izd. Tekh.-Teoret. Lit., Moscow, 1950.
6. S. M. Ferigle and A. Weber, Can. J. Phys. 32, 799 (1954).
7. M. A. Kovner, Zhur. Eksptl. i Teoret. Fiz. 26, 598 (1954).
8. M. A. Kovner, Doklady Akad. Nauk SSSR 97, 65 (1954).
9. M. A. Kovner and A. M. Bogomolov, Opt. i Spektr. 4, 301 (1958).
10. M. A. Kovner and G. V. Peregudov, Opt. i Spektr. 5, 134 (1958).
11. G. S. Landsberg, P. A. Bazhulin, and M. M. Sushchinskii, "Osnovnye parametry spektrov kombinatsionnogo rasseyaniya uglevodorodov" (Fundamental Parameters of the Raman Spectra of Hydrocarbons). Izd. Akad. Nauk SSSR, 1956.

12. R. R. Randle and D. H. Whiffen, Mol. Spectrosc. 111 (1955).
13. M. M. Sushchinskii, Izvest. Akad. Nauk SSSR, Ser. Fiz. 17, 608 (1953).
14. R. R. Randle and D. H. Whiffen, Trans. Faraday Soc. 52, 9 (1956).
15. G. S. Landsberg, B. A. Kazanskii, P. A. Bazhulin, T. F. Bulanova, A. L. Liberman, E. A. Mikhailova, A. F. Plate, Kh. E. Sterin, M. M. Sushchinskii, G. A. Tarasova, and S. A. Ukholin, "Opredelenie individual'nogo uglevodorodnogo sostava benzinov pryamoi gonki kombinirovannym metodom" (Determination of the Individual Hydrocarbon Composition of Straight-Run Gasolines by the Raman Method). Izd. Akad. Nauk SSSR, 1959.
16. K. Kohlrausch, "Spektry kombinirovannogo rasseyania" (Raman Spectra). Izd. Inostrannoi Lit., Moscow, 1952.
17. Landolt-Börnstein, Zahlenwerte und Funktionen aus Phys.-Chem. Vol. 1, chap II, 1951.
18. H. M. Randall, R. G. Fowler, N. Fuson, and I. R. Dangl, "Infrared Determinations of Organic Structures." New York, London, 1949.
19. R. B. Barnes, R. C. Gore, U. Liddel, and V. Z. Williams, "Infrared Spectroscopy." New York, 1944.
20. M. R. Fenske, W. G. Braun, R. V. Wiegand, D. Quiggle, R. H. McCormick, and R. H. Rank, Anal. Chem. 19, 700 (1947).
21. E. A. Glebovskaya, A. A. Zakharov, I. K. Lapina, and Z. G. Kaplan. Trudy Vsesoyuz. Nauch.-Issledovovatel, Geol.-Razved. Inst., Geokhim. sb., No. 4, 23 (1957).

THEORY OF THE VIBRATIONAL SPECTRA OF POLYMERS
II. Torsional Skeletal Vibrations in Syndiotactic Polymer Chains

Yu. Ya. Gotlib

Received 23 December 1959

A derivation of the equations of motion for skeletal torsional vibrations of planar syndiotactic chains is presented, in the case where the center of mass of the side group does not coincide with a carbon atom of the skeleton. The frequencies of the two infrared-active torsional skeletal vibrations have been computed. The form of the vibrations has been investigated and expressions have been obtained for the intensities in the zeroth approximation of the valance-optical scheme. The experimental data for polyvinyl chloride, polyvinylidene chloride, and polyacrylonitrile are discussed and the values of the force constants are estimated.

1. The experimental investigations carried out in recent years on the infrared spectra of high polymers encompass in particular the 100-300 cm^{-1} low-frequency region.[1-4] This frequency interval corresponds to the frequencies of torsional vibrations around single C—C bonds in a number of low-molecular-weight compounds (haloethanes, low-molecular-weight paraffins, etc.).[4-7] One may therefore suppose that the frequencies of the skeletal torsional vibrations of polymer chains also fall into the above-mentioned interval. The investigation of the skeletal torsional vibrations may be of considerable interest for the determination of the structure of the chains, since the frequencies and intensities of these vibrations are directly determined by the structure of the underlying carbon chain, and one may expect marked differences between the torsional vibrations of the planar segments of syndiotactic polymers and the helical segments of isotactic polymer chains.

In the present work, we shall consider the vibration frequencies and intensities for infinite chains (cf. ref. 8), limiting ourselves for the present to the case of planar syndiotactic chains. Isotactic chains will be considered later.

In solving the problem of the skeletal torsional vibrations in a syndiotactic chain of the type (—CU_2—CVW—CU_2—CWV—), we shall consider the entire mass of the CU_2 and CVW groups to be concentrated on the respective centers of inertia of these groups. The centers of inertia of the CU_2 and CVW groups, naturally, do not coincide with C atoms of the skeleton. In ref. 7 this circumstance was not taken into account, which, as we shall see below, exerts a substantial influence on the frequency values if the masses of the atoms or groups U, V, and W (m_U, m_V, m_W) are comparable in magnitude with m_C. Furthermore, we note that the results presented without derivation in ref. 7 relate to the case $m_{CU_2} = m_{CVW}$. The calculation of the torsional skeletal vibrations carried out in the present work may be used in the theory of the vibrational heat capacity of polymers, in the theory of dielectric losses for polymers with rigid side groups, and so on.

2. Let us introduce a Cartesian coordinate system associated with the equilibrium configuration of the infinitely long planar syndiotactic chain under consideration (Fig. 1). The atoms of the carbon skeleton lie in the XY plane, the Y axis coinciding with the long axis of the chain. For small torsional vibrations with respect to the equilibrium configuration, the displacements of the C atoms of the skeleton, z_l, are normal to the XY plane (cf. ref. 7).

We shall associate the CU_2 groups with the odd C atoms of the skeleton and the CVW groups with the even ones. Let us introduce the unit vectors $n_{\parallel}^{(l)}$ and $n_{\perp}^{(l)}$, where $n_{\parallel}^{(l)}$ is located in the plane $C_{l-1}C_lC_{l+1}$ and is directed along the bisectrix of the angle $C_{l-1}C_lC_{l+1}$, while $n_{\perp}^{(l)}$ is perpendicular to the plane $C_{l-1}C_lC_{l+1}$ (see Fig. 1).

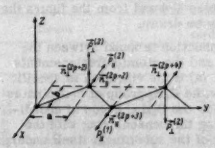

Fig. 1

Fig. 2

Fig. 1. Coordinate system, unit vectors, and distances for a planar syndiotactic chain.
Fig. 2. Position of the center of mass in the side groups.

The potential energy of the torsional vibrations, V_{tors}, is a function of the angles φ formed by the planes $C_lC_{l+1}C_{l+2}$ and $C_{l+1}C_{l+2}C_{l+3}$. Each angle φ equals $(n_\perp^{(l)} \wedge n_\perp^{(l+1)})$. Limiting outselves to terms of the second order in the displacements z_l, it is easy to obtain expressions for the components of the vectors $n_\perp^{(l)}$ and $n_\parallel^{(l)}$ (for the distances a and b, see Fig. 1):

$$n_\perp^{(l)} = \begin{pmatrix} -\left(\frac{1}{b}\right)(-1)^l\left[z_l - \frac{1}{2}(z_{l-1}+z_{l+1})\right] \\ -\left(\frac{1}{2a}\right)[z_{l+1}-z_{l-1}] \\ 1-\left(\frac{1}{b^2}\right)\left[z_l-\frac{1}{2}(z_{l-1}+z_{l+1})\right]^2-\left(\frac{1}{8a^2}\right)(z_{l+1}-z_{l-1})^2 \end{pmatrix}, \quad (1)$$

$$n_\parallel^{(l)} = \begin{pmatrix} \left\{1-\left(\frac{1}{2b^2}\right)\left[z_l-\frac{1}{2}(z_{l-1}+z_{l+1})\right]^2\right\}(-1)^l \\ 0 \\ \left(\frac{1}{b}\right)\left[z_l-\frac{1}{2}(z_{l-1}+z_{l+1})\right] \end{pmatrix} \quad (2)$$

The angles φ, if they are small, may be connected with z_l by means of the relation $\cos\varphi \cong 1-(\varphi^2/2) = (n_\perp^{(l)}, n_\perp^{(l+1)})$, using the equalities (1) and (2):

$$\varphi_l(C_{l-1}C_lC_{l+1};\ C_lC_{l+1}C_{l+2}) = \frac{1}{2}\sqrt{\frac{1}{a^2}+\frac{1}{b^2}}(z_{l-1}-z_l-z_{l+1}+z_{l+2}). \quad (3)$$

The expression for the potential energy of the torsional vibrations, neglecting intermolecular interactions, has the form

$$V = \frac{1}{2}K_\varphi\sum_{l=-\infty}^{+\infty}\varphi_l^2 + K'_\varphi\sum_{p=-\infty}^{p=+\infty}\varphi_{2p}\varphi_{2p+1}. \quad (4)$$

in the simplest case.

The second term in (4) is determined by the presence of a correlation between the vibrations around the bonds $C_{2p}C_{2p+1}$ and $C_{2p+1}C_{2p+2}$ on account of the interaction of the heavy "pendants" CVW and CWV. Thus we have

$$V = \left(\frac{K}{2}\right)\sum_{l=-\infty}^{+\infty}(z_{l+3}-z_{l+2}-z_{l+1}+z_l)^2 + K'\sum_{p=-\infty}^{p=+\infty}(z_{2p}-z_{2p-1}-z_{2p-2}+z_{2p-3})(z_{2p+1}-z_{2p}-z_{2p-1}+z_{2p-2}). \quad (5)$$

The constant factors $\frac{1}{2}\sqrt{1/a^2+1/b^2}$ from (3) are included in the constants K and K'.

3. For the symmetrical CU_2 groups, the radius vector of the center of inertia may be represented in the form

$$R = r_{C_l} + c'n_\parallel^{(l)} \quad (l = \ldots 2p-1,\ 2p+1,\ldots), \quad (6)$$

while for the unsymmetrical CVW groups, assuming that the center of mass lies in the $(n_\parallel^{(l)}, n_\perp^{(l)})$ plane, we obtain

$$R_{2p} = r_{C_{2p}} + c''n_\parallel^{(2p)} + d''n_\perp^{(2p)}, \quad (7)$$

$$R_{2p+2} = r_{C_{2p+1}} + c''n_\parallel^{(2p)} - d''n_\perp^{(2p)}. \quad (8)$$

The distances c', c'', and d'' are shown in Fig. 2. The total kinetic energy of the torsional vibrations of the chain is then written in the form

$$T = \frac{1}{2}\left\{m\sum_{p=-\infty}^{+\infty}\dot{R}_{2p+1}^2 + M\sum_{p=-\infty}^{+\infty}\dot{R}_{2p}^2\right\} = \sum_{l=-\infty}^{+\infty}T_l;$$

$$m = m_{CU_2};\ M = m_{CVW}. \quad (9)$$

Taking account of the fact that for small torsional vibrations of planar chains $x_l = 0$ and $y_l = 0$, as well as expressions (1) and (2) which connect $n_\parallel^{(l)}$ and $n_\perp^{(l)}$ with z_l, and retaining quadratic terms in $\dot{z}_l$, we obtain for the contributions of the separate groups to the kinetic energy

$$T_{2p-1} = \frac{m}{2}\left[\alpha'^2\dot{z}_{2p-1}^2 - 2\alpha'\beta'\dot{z}_{2p-1}(\dot{z}_{2p}+\dot{z}_{2p-2}) + \beta'^2(\dot{z}_{2p}+\dot{z}_{2p-2})^2\right], \quad (10)$$

$$T_{2p} = \frac{M}{2}\left[\alpha''^2\dot{z}_{2p}^2 - 2\alpha''\beta''\dot{z}_{2p}(\dot{z}_{2p-1}+\dot{z}_{2p+1}) + \beta''^2(\dot{z}_{2p-1}+\dot{z}_{2p+1})^2\right] + \frac{M}{2}\gamma^2\left[\dot{z}_{2p} - \frac{1}{2}(\dot{z}_{2p-1}+\dot{z}_{2p+1})\right]^2 + \frac{M}{2}\delta^2(\dot{z}_{2p+1}-\dot{z}_{2p-1})^2, \quad (11)$$

and

$$\alpha' = 1+\frac{c'}{b};\ \beta' = \frac{c'}{2b};$$
$$\alpha'' = 1+\frac{c''}{b};\ \beta'' = \frac{c''}{2b};\ \gamma = \frac{d''}{b};\ \delta = \frac{d''}{2a}. \quad (12)$$

The expressions for the pairs $(T_{2p+1}$ and $T_{2p-1})$ and (T_{2p}, T_{2p+2}) for $x_l = y_l = 0$ are respectively of the same type.

Let us set up the equations of motion according to Lagrange's method, for instance, with the Lagrangian function $L = T - V$:

$$\frac{d}{dt}\frac{\partial L}{\partial \dot{z}_l} - \frac{\partial L}{\partial z_l} = 0. \quad (13)$$

Thus we obtain for the repeating unit of the syndiotactic chain, which includes 4 groups (the groups CVW and CWV, and two CU_2 groups), a set of equations of motion:

$$\ddot{z}_{2p}\left(2m\beta'^2 + M\gamma^2 + M\alpha''^2\right) - (\ddot{z}_{2p-1}+\ddot{z}_{2p+1})\left(m\alpha'\beta' + M\alpha''\beta'' + \frac{1}{2}M\gamma^2\right) + (\ddot{z}_{2p-2}+\ddot{z}_{2p+2})\,m\beta'^2 - (K-K')\times(4z_{2p} - z_{2p+1} - z_{2p-1} - 2z_{2p-2} - 2z_{2p+2} + z_{2p-3} + z_{2p+3}) = 0; \quad (14)$$

$$\ddot{z}_{2p+1}\left(2M\beta''^2 + \frac{1}{2}M\gamma^2 + m\alpha'^2 + 2M\delta^2\right) - (\ddot{z}_{2p}+\ddot{z}_{2p+2})\left(m\alpha'\beta' + M\alpha''\beta'' + \frac{1}{2}M\gamma^2\right) + (\ddot{z}_{2p-1}+\ddot{z}_{2p+3})\left(M\beta''^2 + \frac{1}{2}M\gamma^2 - M\delta^2\right) + K(4z_{2p+1} - z_{2p} - z_{2p+2} - 2z_{2p-1} - 2z_{2p+3} + z_{2p-2} + z_{2p+4}) + K'(2z_{2p+1} + z_{2p-3} + z_{2p+5} + z_{2p} + z_{2p+2} - 2z_{2p-1} - 2z_{2p+3} - z_{2p-2} - z_{2p+4}) = 0. \quad (15)$$

The equations for z_{2p+3} and z_{2p+4} are identical with the equations for z_{2p} and z_{2p+1} respectively. For sufficiently long chains, only those vibrations will be optically active in the spectrum for which adjacent repeating units vibrate in phase; i.e., $z_1 = z_{1+4}$, for all l and s. Let us denote $z_{2p+4s} = \xi_1$, $z_{2p+1+4s} = \xi_2$, $z_{2p+2+4s} = \xi_3$, and $z_{2p+3+4s} = \xi_4$, and, using the conditions for being in phase, we obtain from Eqs. (14) and (15) (and also from the equations for z_{2p+2} and z_{2p+3}) the equations for ξ_1:

$$\ddot{\xi}_1(2m\beta'^2 + M\gamma^2 + M\alpha''^2) - (\ddot{\xi}_2+\ddot{\xi}_4)\left(m\alpha'\beta' + M\alpha''\beta'' + \frac{1}{2}M\gamma^2\right) + \ddot{\xi}_3 2m\beta'^2 + 4(K-K')(\xi_1-\xi_3) = 0, \quad (16)$$

$$\ddot{\xi}_3\left(2M\beta''^2 + \frac{1}{2}M\gamma^2 + m\alpha'^2 + 2M\delta^2\right) - (\ddot{\xi}_1+\ddot{\xi}_3)\left(m\alpha'\beta' + M\alpha''\beta'' + \frac{1}{2}M\gamma^2\right) + 2\ddot{\xi}_4\left(M\beta''^2 + \frac{1}{4}M\gamma^2 - M\delta^2\right) + 4(K+K')(\xi_3-\xi_1) = 0. \quad (17)$$

$$\xi_3(2m\beta^2 + M\gamma^2 + M\alpha'^2) - (\xi_2 + \xi_4)\left(ma'\beta' + Ma''\beta'' + \frac{1}{2}M\gamma^2\right) + \xi_1 2m\beta^2 + 4(K - K')(\xi_3 - \xi_1) = 0, \quad (18)$$

$$\xi_4\left(2M\beta''^2 + \frac{1}{2}M\gamma^2 + ma'^2 + 2M\beta^2\right) - (\xi_3 + \xi_1)\left(ma'\beta' + Ma''\beta'' + \frac{1}{2}M\gamma^2\right) + 2\xi_2\left(M\beta''^2 + \frac{1}{4}M\gamma^2 - M\beta^2\right) + 4(K + K')(\xi_4 - \xi_2) = 0. \quad (19)$$

Let us introduce symmetric and antisymmetric combinations of ξ_i:

$$\nu_1 = \frac{1}{\sqrt{2}}(\xi_1 + \xi_3); \quad \nu_3 = \frac{1}{\sqrt{2}}(\xi_1 - \xi_3);$$

$$\nu_2 = \frac{1}{\sqrt{2}}(\xi_2 + \xi_4) \text{ and } \nu_4 = \frac{1}{\sqrt{2}}(\xi_2 - \xi_4). \quad (20)$$

Then we obtain

$$\left.\begin{aligned}\nu_1(M\gamma^2 + 4m\beta'^2 + Ma''^2) - 2\nu_2\left(ma'\beta' + Ma''\beta'' + \frac{1}{2}M\gamma^2\right) = 0,\\ \nu_2(4M\beta''^2 + M\gamma^2 + ma'^2) - 2\nu_1\left(ma'\beta' + Ma''\beta'' + \frac{1}{2}M\gamma^2\right) = 0.\end{aligned}\right\} \quad (21)$$

$$\nu_3(M\gamma^2 + Ma''^2) + 8(K - K')\nu_3 = 0. \quad (22)$$

$$\nu_4(ma'^2 + 4M\beta^2) + 8(K + K')\nu_4 = 0. \quad (23)$$

Hence (frequencies in cm^{-1})

$$\nu_1 = \nu_2 = 0;$$

$$\nu_3 = \frac{1}{2\pi c}\sqrt{\frac{8(K - K')}{M}}\frac{1}{\sqrt{\gamma^2 + \alpha''^2}}; \quad (24)$$

$$\nu_4 = \frac{1}{2\pi c}\sqrt{\frac{8(K + K')}{m}}\frac{1}{\sqrt{\alpha'^2 + 4\left(\frac{M}{m}\right)\beta^2}} \quad (25)$$

For $m = M$, $K' = 0$, $c' = c'' = d' = d'' 0$ ($\alpha' = \alpha'' = 1$; $\gamma = \delta = 0$), Eqs. (14) and (15) go over into Pitzer's equation,[7] and (24) and (25) give the corresponding solution.

From (23) it can be seen that, in active in-phase torsional vibrations with nonzero frequency, the CVW groups of each repeating unit vibrate in opposite phase (the same also applies to the CU_2 groups).

In the ν_3 vibrations, the displacements which take place involve only the even C atoms of the skeleton, those associated with the CVW groups (mass M), while in the ν_4 vibrations only the odd C atoms with the CU_2 groups (mass m) move; but since, during this process, a displacement of the center of mass of the unsymmetrical CVW group takes place, M also enters into the expression for ν_4. We note also that the factors $\sqrt{\gamma^2 + \alpha''^2}$ and $\sqrt{\alpha'^2 + 4(M/m)\delta^2}$, which take account of the mass distribution in the CU_2 and CVW groups, are fairly large. Thus for polyvinyl chloride $(-CH_2-CHCl-)_n$, $\sqrt{\gamma^2 + \alpha''^2} = 1.97$ and $\sqrt{\alpha'^2 + 4(M/m)\delta^2} = 1.1$; for polyacrylonitrile $(-CH_2-CHCN-)_n$, $\sqrt{\gamma^2 + \alpha''^2} = 2.32$ and $\sqrt{\alpha'^2 + 4(M/m)\delta^2} = 1.17$; for polyvinylidene chloride $(-CH_2-CCl_2-)_n$, $\gamma = \delta = 0$, $\alpha'' = 1.97$, and $\alpha' = 1.1$. Consequently, the frequency values will differ substantially from the values which may be obtained according to Pitzer's formula[1,7] with the same values of the force constant K, even if we modify it for the case $m \neq M$.

4. In order to calculate the changes in the dipole moment during torsional vibrations, we shall make use of the zeroth approximation of the valence-optical scheme.[6] For the dipole moments of the "even" CVW groups and of the "odd" CU_2 groups of the syndiotactic chain, the equalities

$$\left.\begin{aligned}p_{2j+1} = p_{\parallel}^{(1)}u_{\parallel}^{(2j+1)}; \quad p_{2j+3} = p_{\parallel}^{(1)}u_{\parallel}^{(2j+3)};\\ p_{2j} = p_{\parallel}^{(2)}u_{\parallel}^{(2j)} + p_{\perp}^{(2)}u_{\perp}^{(2j)};\\ p_{2j+2} = p_{\parallel}^{(2)}u_{\parallel}^{(2j+2)} - p_{\perp}^{(2)}u_{\perp}^{(2j+2)}.\end{aligned}\right\} \quad (26)$$

hold.

Using the relations (1) and (2) and introducing $\eta_i^{(n)}$ according to (20) (n is the number of the repeating unit), we obtain for the components of the dipole moment vector during torsional vibrations

$$\left.\begin{aligned}\partial P_x = \frac{\sqrt{2}}{b}(p_{\parallel}^{(1)} - p_{\parallel}^{(2)})\sum_n(\nu_1^{(n)} - \nu_3^{(n)});\\ \partial P_z = -\frac{\sqrt{2}}{b}p_{\perp}^{(2)}\sum_n\nu_3^{(n)}; \quad \partial P_y = -\frac{\sqrt{2}}{a}p_{\perp}^{(2)}\sum_n\nu_4^{(n)}.\end{aligned}\right\} \quad (27)$$

For infinitely long chains, in the case of active in-phase vibrations, the radiation intensity is proportional to the radiation intensity of one repeating unit (cf. ref. 9). Then, according to the usual theory of intensities, we have for the intensity of a given normal vibration Q (cf. ref. 6):

$$I(Q) = \frac{\pi}{3m_0\varphi^2}\cdot\frac{1}{1 - e^{-\frac{h\nu(Q)}{kT}}}\left(\frac{\partial P}{\partial Q}\right)^2 I_0, \quad (28)$$

where m_0 is the effective mass for the given normal vibration and I_0 is the initial radiation intensity at the given frequency. Then for the intensities of the active torsional vibrations ν_3 and ν_4 we obtain from (27) and (28):

$$I(\nu_3) = A\left[p_{\perp}^{(2)}\right]^2\left[b^2\left(1 - e^{-\frac{h\nu_3}{kT}}\right)\sqrt{M(\gamma^2 + \alpha''^2)}\right]^{-1}. \quad (29)$$

$$I(\nu_4) = A\left[p_{\perp}^{(2)}\right]^2\left[a^2\left(1 - e^{-\frac{h\nu_4}{kT}}\right)\sqrt{m\left(\alpha'^2 + 4\frac{M}{m}\beta^2\right)}\right]^{-1}. \quad (30)$$

$$\frac{I(\nu_3)}{I(\nu_4)} = \frac{a^2}{b^2}\sqrt{\frac{m\left(\alpha'^2 + 4\frac{M}{m}\beta^2\right)}{M(\gamma^2 + \alpha''^2)}}\cdot\frac{1 - e^{-\frac{h\nu_4}{kT}}}{1 - e^{-\frac{h\nu_3}{kT}}}. \quad (31)$$

5. A detailed comparison with experimental data entails considerable difficulties at the present time for the following reasons: (1) there are no data on infrared dichroism and band polarization in the 100-300 cm^{-1} region for polymers; (2) bands of other vibration types may fall into the frequency interval under consideration (torsional vibrations of flexible "pendants," certain deformation vibrations), and in the long-wavelength part of the interval the appearance of intermolecular vibration bands is possible; (3) the presence of disturbances of stereospecificity and rotational isomerism may lead to a change in the frequency of the torsional vibrations, to other selection rules, etc.

We shall consider the data for three polymers (polyvinyl chloride, polyvinylidene chloride,[3] and polyacrylonitrile[4]) which possess the simplest structure and rigid side groups.

In the spectra of polyvinyl chloride, the bands 102 (very weak), 160, and 182 cm^{-1} (weak, but far more intense than the 102 cm^{-1} band) fall into the frequency region under consideration, as well as the band 315 cm^{-1} (a weak, but sharp line) which is ascribed[2] to the wagging CCl deformation vibration in which the two CCl groups of the repeating unit of the chain vibrate in opposite phase. It is unlikely that the latter frequency should be associated with a torsional vibration, since it leads to too high values of the torsional force constant K. In ref. 3 it is assumed that the bands 160 and 182 cm^{-1} correspond to torsional vibrations of the chain (i.e., to ν_3 and ν_4 in our symbols).

From a comparison of the calculated quantities $I(\nu_3)/I(\nu_4)$ for all possible combinations ($\nu_3 = 102$, $\nu_4 = 160$ or $\nu_3 = 160$, $\nu_4 = 102$, etc.) with the intensity ratio observed in the experiments, there results the most probable assignment of the bands: $\nu_3 = 102$ cm^{-1} and $\nu_4 = 160$ or 182 cm^{-1}. The use of (24) and (25) enables us in this case to determine the values of the force constants K and K′ (for $\nu_3 = 102$ and $\nu_4 = 160$ cm^{-1}): $K = 0.14 \times 10^5$ dynes/cm, $K' = 0.3\,K \approx 0.05 \times 10^5$ dynes/cm ($\nu_3 = 102$ and $\nu_4 = 182$ cm^{-1} gives nearly the same values of K and K′). It should be noticed that the values of K turn out to be larger than the values of the torsional constant K for polyethylene[10] and the normal paraffins,[2] in which $K = 0.02 \times 10^5$ dynes/cm or 0.034×10^5 dynes/cm. The large values of K and K′ in the case of polyvinyl chloride are probably associated with the presence of the strongly interacting heavy polar CHCl groups. If we suppose that the band 102 cm^{-1} corresponds to the vibration ν_4, and that $\nu_3 < \nu_4$ and does not fall into the experimentally investigated region of the spectrum (which is in general unlikely, since the origin of the stronger bands 160 and 182 cm^{-1} then remains unclear), then only the one equation (25) remains for the determination of K and K′. Then, if we set $K' = 0$, we obtain $K = 0.098 \times 10^5$ dynes/cm, while if we consider $K'/K = 0.3$ as before, then $K = 0.055 \times 10^5$ dynes/cm.

The chains of polyvinylidene chloride in the crystalline form are not planar, although the deviation from a planar configuration is evidently not great (see refs. 3, 11). The repeating unit of the chain contains two CCl_2 groups, in agreement with Fuller's model, which corresponds better to the polarized-spectrum data than does Reinhart's alternative model.[3,11] By virtue of what has been said, we may expect that the torsional frequencies for polyvinylidene chloride will differ little from the frequencies calculated for a planar trans-conformation of the chain, whereas the activity of the bands in the infrared spectrum and their intensities will be determined by the deviations of the conformation of the chain from the planar trans-conformation. In the spectrum of polyvinylidene chloride there are found,[3] in the region of interest to us, weak bands at 102, 113, and 185 cm^{-1}. Supposing that the band 102 (or 113) cm^{-1} corresponds to ν_4, then we may determine K and K′. Taking for example, $\nu_3 = 113$ cm^{-1} and $\nu_4 = 185$ cm^{-1}, we get $K = 0.17 \times 10^5$ dynes/cm and $K'/K = -0.74$, which is generally regular, since the replacement of CHCl by CCl_2 increases the magnitude of the intramolecular interactions.

In the spectra of polyacrylonitrile,[4] bands are found at 127 and 86 cm^{-1}. From the data of ref. 4, it is impossible to draw conclusions with any reliability concerning the stereospecific structure of the chain (the polymer is probably atactic). If we assume that syndiotactic sequences predominate in the chain, the assignment $\nu_3 = 86$ cm^{-1} and $\nu_4 = 127$ cm^{-1} leads to the values $K = 0.08 \times 10^5$ dynes/cm and $K' = 0.2\,K$. In ref. 4 it is assumed that the 127 cm^{-1} band relates to the rocking CN deformation vibration. Then we may consider another variant, setting $\nu_4 = 86$ cm^{-1} and $\nu_3 < \nu_4$. In this case, if $K' = -0.23$ K, we get $K = 0.04 \times 10^5$ dynes/cm, and if $K' = 0$, then $K = 0.03 \times 10^5$ dynes/cm. It is easy to see that (as also in the case of polyvinyl chloride) the assumption that the smallest frequencies correspond to ν_4 and $\nu_3 < \nu_4$ leads to values of K which are closer to those for polyethylene.

In conclusion, I take the opportunity to express my sincere gratitude to M. V. Vol'kenshtein for his valuable comments during discussion of this work.

REFERENCES

1. C. Y. Liang, S. Krimm, and G. B. B. M. Sutherland, J. Chem. Phys. 25, 543 (1956).
2. S. Krimm and C. Y. Liang, J. Chem. Phys. 25, 563 (1956).
3. S. Krimm and C. Y. Liang, J. Polymer Sci. 27, 95 (1956).
4. C. Y. Liang and S. Krimm, J. Polymer Sci. 31, 513 (1958).
5. S. Mizushima, "Stroenie molekul i vnutrennee vrashchenie" (Molecular Structure and Internal Rotation). Izd. Inostrannoi Lit., Moscow, 1957.
6. M. V. Vol'kenshtein, M. A. El'yashevich, and B. I. Stepanov, "Kolebaniya molekul" (Molecular Vibrations). Gosudarst. Izd. Tekh.-Teoret. Lit., Moscow-Leningrad, 1949.
7. K. S. Pitzer, J. Chem. Phys. 8, 711 (1940).
8. Yu. Ya. Gotlib, Opt. i Spektr. 7, 294 (1959), Optics and Spectroscopy 7, 191 (1959).
9. P. W. Higgs, Proc. Roy. Soc. 220, 472 (1953).
10. O. Theimer, J. Chem. Phys. 27, 408 (1957).
11. "Volokna iz sinteticheskikh polimerov" (Synthetic Polymer Fibers). Izd. Inostrannoi Lit., Moscow, 1957.

THE VIBRATIONAL SPECTRA OF PYROPHOSPHATES

A. N. Lazarev and V. S. Aksel'rod

Received 14 November 1959

The state of polarization of the Raman lines of an aqueous solution of $K_4P_2O_7$ was studied. Interpretation of the internal vibration frequencies of ions of the X_2O_7 type in spectra of the pyrophosphates and some other compounds was discussed.

The interpretation of the infrared spectra of pyrosilicates,[1] which one of us proposed, can be confirmed by means of a study of the degree of depolarization of the Raman lines of these substances. For Si_2O_7, in the frequency region of valence vibrations, two polarization lines at about 650-700 and 850 cm^{-1} (instead of one line at about 750-800 cm^{-1} in the $[SiO_4]^{4-}$ ion spectrum) can be expected. However, a study of the vibrations of ions of the $[Si_2O_7]^{6-}$ type by the method of Raman spectra was fraught with great experimental difficulties—the absence of large single crystals, on the one hand, and the impossibility of obtaining $[Si_2O_7]^{6-}$ ions in solution without contamination of other silicon oxide anions, on the other. Therefore, we have been faced with the expedient of studying the Raman spectra of $[P_2O_7]^{4-}$ ions, which would give a direct confirmation of the validity of the interpretation of the spectra of pyrosilicates. A comparison of of the vibrational spectra of different ions of the X_2O_7 type was also of interest from the point of view of the concepts of the structure and spectra of oxygen acids developed by Siebert.[2]

We obtained the Raman spectrum of a saturated aqueous solution of $K_4P_2O_7$ and determined the state of polarization of the lines see Fig. 1 and the Table .*

*The spectra were obtained by means of an ISP-51 spectrograph with an FEP-1 attachment for the photoelectric recording of spectra. Photographing of the spectra was carried out immediately after preparation of the solution, and measures were taken for cooling the cells during the photographing process.

Frequency of line (cm^{-1})	1090	1012	715	515	325
Relative intensity	2	10	3	1	2
Degree of polarization	0.71	0.18	0.22	0.84	0.86

On the basis of the resulting data, it could apparently be concluded at once that the general form of the spectrum (number and position of polarization lines) corresponds to that expected for an ion of the X_2O_7 type. In ref. 3, two more polarization lines were observed, extremely weak, of course) in the 850-900 and 900-950 cm^{-1} regions in the Raman spectra of pyrophosphate solutions. In our opinion, these lines cannot be attributed to vibrations of the $[P_2O_7]^{4-}$ ion. It could be assumed that they correspond to completely symmetrical vibrations of hydrated pyrophosphate ions or, more likely, "monomeric" $[PO_4]^{3-}$ and $[PO_3OH]^{2-}$ or $[PO_2(OH)_2]^{-}$ ions formed as a result of partial hydrolytic cleavage of the P—O—P bonds in solution.

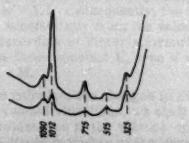

Fig. 1. Raman spectrum of an aqueous solution of $K_4P_2O_7$ (strong and weak components).

In the interpretation of the spectrum we considered the $[P_2O_7]^{4-}$ ion (similar to the $[Si_2O_7]^{6-}$ ion) as two PO_4 tetrahedra, joined by a mutual oxygen atom. According to Siebert's concepts,[2] the pentavalent P atom produces in the $[P_2O_7]^{4-}$ ion a nonequivalent bond, in contrast to the tetravalent Si atom, which forms Si—O(—Si) and Si—O^- bonds of approximately the same order. Since the O atom in the P—O—P "bridge" can form only two simple bonds, the order of the P—O bonds should increase to 4/3. The difference in the lengths of the bonds, $r_{P-O(P)} > r_{P-O^-}$,[4] corresponds to this. However, this change is small and should not essentially affect the character of the vibration spectrum.

For the purpose of facilitating the recording of frequencies, we calculated the vibrations of the P_2O_7 group by the formulas derived by Matossi[4] for frequencies of the X_2O_7 group (D_{3d} symmetry; $\angle XOX = 180°$), consisting of two regular XO_4 tetrahedra. Since the POP angles in $[P_2O_7]^{4-}$ ions usually differ appreciably from 180°,[5] it is difficult to expect good agreement between the calculated frequencies and those observed.* Sufficiently satisfactory results (see Fig. 2) were obtained with $k_{P-O^-} = 5.6 \times 10^5$ dynes/cm, $k_{P-O(P)} = 4.6 \times 10^5$ dynes/cm and $d_{OPO} = 1.0 \times$

*The obvious observance of an alternative prohibition in the Raman spectrum of the P_2O_7 ion can hardly serve as an argument favoring D_{3d} symmetry. In absorption spectra of crystalling pyrophosphates the frequencies of completely symmetrical vibrations display considerable intensity. Also, recent investigations of the absorption spectra of pyrophosphate solutions[6] indicate a bent configuration for the P_2O_7 groups.

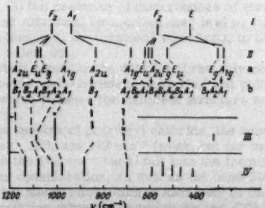

Fig. 2. Scheme of frequencies in the vibrational spectra of the pyrophosphates (the polarization lines in the spectra are indicated by crosses). I—$[PO_4]^{3-}$; II—$[P_2O_7]^{4-}$ (a—D_{3d} symmetry, b—C_{2v} symmetry); III—$K_4P_2O_7$ (Raman spectrum, solution); IV—$K_4P_2O_7$ (infrared absorption spectrum, crystal).

10^5 dynes/cm. The value of the $k_{P-O'}/k_{P-O(P)}$ ratio was approximately 4/3, as should be expected, since the dynamic coefficients are approximately proportional to the multiplicity of the bond. However, as a result of the very approximate character of the calculation, the absolute values of the dynamic coefficients have no intrinsic physical meaning. It should also be noted that vibrations, degenerate for the D_{3d} model, should actually be split, since with $\angle POP \neq 180°$ the symmetry group of P_2O_7 can be no higher than C_{2v}; but the value of this splitting is apparently small.

In Fig. 2 is presented an attempt to interpret the valence vibration frequency regions in the Raman spectrum of an aqueous solution of $K_4P_2O_7$ and in the absorption spectrum of crystalline $K_4P_2O_7$ (data on the absorption spectrum were taken from ref. 7). Moreover, we observe that the assignment of the absorption bands in the 1000-1150 cm^{-1} region is only of a tentative character, since the complex structure of these bands can be caused partially by a change in the internal vibrations of the $[P_2O_7]^{4-}$ ion in the crystal lattice. Just as in the transition $SiO_4 - Si_2O_7$, the splitting of the completely symmetrical valence vibration of the PO_4 group is clearly seen on consideration of the spectra of the PO_4 and P_2O_7 ions. The appearance of the polarization Raman line close to 700 cm^{-1} and the strong absorption bands at about 900 cm^{-1}, corresponding to the pulsation vibrations "in phase" and "out of phase" of the two PO_4 groups bonded by a mutual oxygen atom, is a result of this splitting. These vibrations can also be described as a symmetrical and antisymmetrical P—O—P vibration which, in particular, was done in ref. 8, where in the interpretation of the spectra of the pyrophosphates the vibrations of the PO_3 and P—O—P "bridge" groups were separated. The interpretation of the spectra of the pyrophosphates which they proposed differed little in principle from the assignment of frequencies which we made (with the exception of the weak polarization lines mentioned above).

In conclusion we compare the spectra of ions of the X_2O_7 type in relation to the nature of the X atom. As seen from Fig. 3, in the $SiO_4 - Si_2O_7$ transition the completely symmetrical valence vibration is split into two symmetrically positioned components. For the $PO_4 - P_2O_7$ transition (and to a still greater extent, for the $CrO_4 - Cr_2O_7$ transition) both these frequencies are much lower than the $\nu_{XO_4}(A_1)$ vibration frequency. On the other hand, the frequency values into which the $\nu_{XO_4}(F_2)$ vibration breaks down, have a tendency to increase for the pyrophosphates and pyrochromates.

We repeat that the order (multiplicity) of the X—O(—X) bond in X_2O_7 ions always amounts to approximately 1; whereas bonds of the X—O^- type in XO_4 and X_2O_7 ions can have a multiplicity value close to 1 only for an element of the fourth group—silicon. For elements of groups V and VI (P and Cr), the following relationship apparently holds for bond multiplicity values $N: N_{X-O^-}(X_2O_7) > N_{X-O^-}(XO_4) > N_{X-O(X)}(X_2O_7)$. Analogous relationships are obviously also valid for the dynamic coefficients of the bonds indicated. Moreover, the difference in the values of the dynamic coefficients of the

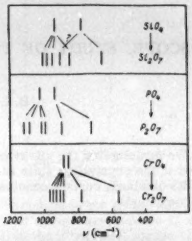

Fig. 3. The $XO_4 - X_2O_7$ transition for X = Si, P, Cr (valence vibrations). Spectra of Si_2O_7 ions were taken from ref. 1; P_2O_7—from the present report and from ref. 7; Cr_2O_7—from refs. 9 and 10.

X—O X) and X—O^- bonds for chromium are higher than for phosphorus. Therefore, the effect of a decrease in the values of the vibrational frequencies which occur on splitting $\nu_{XO_4}(A_1)$ and which appear to be principally vibrations of the XOX bonds in the X_2O_7 groups can be directly related to a decrease in the values of the dynamic coefficients. At the same time, the phenomenon of an increase in the frequencies which occur on splitting $\nu_{XO_4}(F_2)$ and which correspond to the fundamental vibrations of the XO_3 groups in X_2O_7 ions is explained by an increase in the values of the dynamic coefficients of the X—O^- bonds. Thus, vibrations of the XO_3 and X—O—X groups, to a great extent, are "separated" in $[Cr_2O_7]^{2-}$ ions and are "combined" in $[Si_2O_7]^{6-}$ ions.

REFERENCES

1. A. N. Lazarev, Opt. i Spektr. 9, 195 (1960), Optics and Spectroscopy 9, 103 (1960).
2. H. Siebert, Z. anorg. und allgem. Chem. 275, 225 (1954).
3. T. J. Hanwick and P. O. Hoffman, J. Chem. Phys. 19, 708 (1951).
4. F. Matossi, J. Chem. Phys. 17, 679 (1949).
5. G. R. Levi and G. Peironel, Z. Krist. 92, 190 (1935); G. Peironel, Z. Krist. 94, 311 (1936); D. M. McArthur and C. A. Beevers, Acta Cryst. 10, 428 (1957).
6. A. Simon and H. Richter, Z. annorg. und allgem. Chem. 301, 154 (1959).
7. A. Mutschin and K. Maennchen, Z. anal. Chem. 160, 81 (1958).
8. W. Bues and H. W. Gehrke, Z. anorg. und allgem. Chem 288, 291 (1958).
9. T. Dupuis, Compt. Rend. Acad. Sci. 248, 3332 (1958).
10. H. Stammreich, D. Bassi, O. Sala, and H. Siebert, Spectrochim. Acta 13, 192 (1958).

SPECTROSCOPIC STUDY OF THE MOLECULAR STRUCTURE OF GUANYL-UREA AND BIURET

B. I. Sukhorukov and A. I. Finkel'shtein

Received 14 November 1959

We investigated the ultraviolet and infrared absorption spectra of guanyl-urea and of biuret in the crystalline state and in aqueous solutions at different pH. On the basis of the results obtained, certain conclusions were reached regarding the molecular structure of the two compounds.

Biuret and guanyl-urea belong to the compounds whose molecular structure is obscure and which have not been thoroughly investigated spectroscopically. The papers found in the literature, on the ultraviolet spectra of biuret and guanyl-urea,[1,2] and the infrared spectra of N-substituted guanyl-ureas,[3] do not examine the molecular structure of these compounds in any detail.

We investigated the ultraviolet and infrared spectra of these compounds with the aim of a more detailed understanding of their molecular structure.

The infrared absorption spectra were measured on an IKS-12 single-beam spectrophotometer, using lithium fluoride (2-4μ) and sodium chloride (4-15μ) prisms. The ultraviolet spectra were measured on an SF-4 quartz spectrophotometer. The potassium bromide pressed pellet technique[4] was used to study the compounds in the crystallines state. The aqueous solutions in light and heavy water were investigated by placing the solution between two Teflon plates 10μ thick placed in a special mounting, consisting of two metallic plates with a rectangular opening. Since Teflon absorbs in the region 7.7-8.4μ, we used identical polyethylene sheets in this region. The attempt to deuterate guanyl-urea by means of direct exchange was not successful because of the slowness of the reaction.

Figure 1 shows the absorption spectra of crystalline guanyl-urea salts. It must be noted that the band in the region 2500-2800 cm^{-1}, corresponding to hydrogen-bonded HCl, is absent in the spectra of the guanyl-urea salts. This indicates that the proton is completely transferred to the nitrogen atom, forming a true salt. In the region of NH valence vibrations a number of bands are observed, which are analyzed as follows:

1. The absorption bands with maxima at 2.9μ (3450 cm^{-1}) and at 3.07μ (3260 cm^{-1}) are assigned to the NH_2 valence vibrations of the amide group (ν_{as} and ν_s), because their frequencies correspond closely to those in the spectra of amides[5,6] and or urea.[7]

2. The absorption band at 3.15μ (3180 cm^{-1}), belongs to the NH group.[5]

3. The three overlapping bands at 3.33μ (3000 cm^{-1}), 3.37μ (2970 cm^{-1}) and 3.40μ (2945 cm^{-1}) are tentatively assigned to the guanidine group. The presence of three bands is apparently due to the formation of an intramolecular hydrogen bond $\overset{(+)}{HN}—H—NH_2$. Such hydrogen bonding should weaken the interaction between the nitrogen atom of the amide group and the carbonyl group leading to an increase in the frequency of the C—O group The ν_{CO} is 1735 cm^{-1}. The increase in the frequency $\nu_{C=O}$ relative to urea[7] and acetamide[6] is here caused by the same circumstances as in the case of molecules containing the grouping —CO—NH—CO,[5] and the case of formation of the intramolecular hydrogen bond.

The strong absorption band at 6.0μ (1670 cm^{-1}) most probably belongs to the deformation vibration of the NH_2-group of the amide part of the molecule. In the case of urea δ_{NH_2} = 1600 cm^{-1}.[7] The absorption bands at 6.3μ (1590 cm^{-1}), 6.8μ (1470 cm^{-1}), and 7.4μ (1350 cm^{-1}) belong to the vibrations of the guanidine-ionic part of the molecule.[9]

It is easy to locate the bands due to the anions from comparison of the salt spectra. Thus the bands at 1390 (ν_{as}), 1099 (ν_s), and 813 cm^{-1} (δ) belong to the nitrate ion; the strong band at 1087 cm^{-1} and probably the weak band at 971 cm^{-1} belong to the sulfate ion. The remaining bands in the spectra of the salts are not characteristic and require a detailed calculation for their assignment.

As a result of the above considerations, it is possible to write down the following formula (I) for the guanyl-urea cation (using the notation developed in ref. 8):

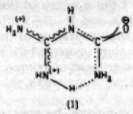

(I)

Guanyl-urea is a relatively strong base.[1] From a spectrophotometric determination of its dissociation constant, we found that the inflection point (Fig. 4, curve 1) occurs at pH = 8.3, which correspond to $K_b = 2 \times 10^{-6}$. Hence, in the region of pH < 7 guanyl-urea must exist as a cation. Figure 2 shows the infrared spectra of aqueous solutions of guanyl-urea at various pH values. As can be seen from the figure, in the region of pH < 7, $\nu_{C=O}$ = 1690 cm^{-1}, i.e., the frequency of the carbonyl group is lowered by 45 cm^{-1} relative to its value in the crystalline state. The absorption band at 1670 cm^{-1} observed in spectra of crystals is shifted to 1655 cm^{-1} in aqueous solutions. The frequencies of two other bands is also lowered somewhat: from 1590 and 1470 cm^{-1} for the crystal to 1570 and 1430 cm^{-1} in the aqueous solution at pH < 7. These shifts in going from the crystalline state to the saturated aqueous solution are apparently due to change in the hydrogen bonding.

Since the absorption spectrum of guanyl-urea in the ultraviolet and infrared regions is constant over the range of pH values from 0 to 7, it must be the spectrum of the guanyl-urea ion (I). Both spectra vary in the region of pH 7 to 10 and then become constant at pH 10 to 14. The change in the spectra is caused by the process of removal of a proton from the molecule. Thus, in the region of pH from 9 to 14, the guanyl-urea must be a free base.

The infrared spectrum of an aqueous solution of guanyl-urea at pH = 11 is shown in Fig. 2,d. The absence of an absorption band $\nu_{C=O}$ with frequency higher than 1600 cm^{-1} indicates the absence of a carbonyl group in the free guanyl-urea. This fact can be explained by the

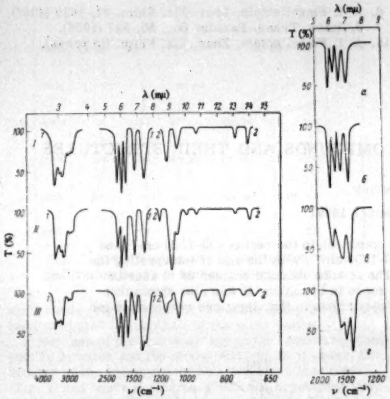

Fig. 1

Fig. 2

Fig. 1. The infrared spectra of crystalline guanyl-urea salts. I—chloride; II—sulfate; III—nitrate. Percent concentration of guanyl-urea in the pellet: curves 1—0.33; curves 2—1.

Fig. 2. The infrared spectra of aqueous solutions of guanyl-urea at various pH. a—Ph = 5; b—pH = 7; c—pH = 8; d—pH = 11.

formation of the zwitter-ion (II):

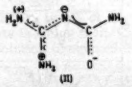

(II)

It is interesting to compare the characteristic frequencies of biuret and guanyl-urea. With this aim in mind, let us examine in more detail, the infrared spectrum of crystalline biuret (Fig. 3). The N—H frequencies of the NH_2 group in the spectrum of biuret (ν_{as} = 3450 and ν_s = 3310 cm^{-1}) are very close to the corresponding frequencies in urea[6,7] (ν_{as} = 3444 cm^{-1} and ν_s = 3348 cm^{-1}). The bands at 1430 and 1370 cm^{-1} can be assigned to the vibrations of the bond H_2N—C (in urea, 1476 cm^{-1}). The appearance of two bands is explained by strong interaction between the H_2N—C groups through the chain of CN bonds. The C=O frequency in biuret is 1680 cm^{-1}. Apparently, the increase in the frequency of the C=O bond is due to the increase in the bond order of C=O, which

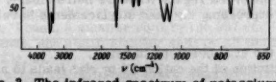

Fig. 3. The infrared spectrum of potassium bromide pellets of crystalline biuret. Percent concentration of biuret in the pellet: curves 1—0.33; curves 2—1.

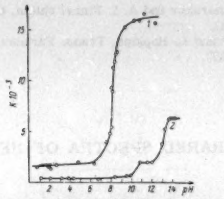

Fig. 4. Variation in the molar absorption coefficients of guanyl-urea (curve 1) and biuret (curve 2) in the ultraviolet region (225 mμ) as function of the pH of the solution.

in urea is 1.5,[10] resulting from the decrease in the order of the internal bonds C=N relative to urea. The strong bands at 1122 and 1087 cm^{-1} can be tentatively assigned to the ν_{as} vibrations of N—C—N. The assignment of other frequencies is vague. Thus, the spectrum of biuret is quite similar to the spectrum of urea if we take into account the evident structural differences. The molecular structure of biuret can be written down (using the above-mentioned notation) as follows (III):

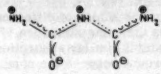

(III)

Figure 4 (curve 2) shows the variation in the absorption coefficient of urea in the ultraviolet region* as a function of pH (from 0 to 15). We found two inflections in the curve instead of only one,[1] corresponding to $K_{a1} = 63 \times 10^{-11}$ and to $K_{a2} = 10^{-13}$. We measured the spectrum of biuret down to pH = 2, but did not observe any variation. The dissociation of biuret can be represented as follows:

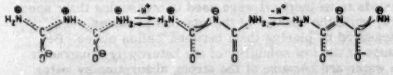

Since guanyl-urea is a stronger base than biuret, it must be more weakly acidic, as a result of which, the dissociation constant of guanyl-urea must have a value $K_a \ll 6.3 \times 10^{-11}$, which supports the assumption that in the region of pH from 9 to 11, guanyl-urea exists as the free base.

*The ultraviolet spectra were measured with the help of T. G. Kornienko.

REFERENCES

1. R. C. Nirt and R. G. Schmitt, Spectrochim. Acta 12, 127 (1958).
2. J. C. Gage, J. Chem. Soc. 221, 1949; ibid., 60, 68 (1956).
3. P. A. Bawin, W. Bridgeo and J. L. Bawin, Can. J. Chem. 32, 242 (1954).
4. A. I. Finkel'shtein, F. L. Malachevskaya, A. M. Fisher, and B. G. Rabovskii, Opt. i Spektr. 6, 415 (1959), Optics and Spectroscopy, 6, 260 (1959).
5. L. Bellamy, "Infrared Spectra of Molecules," Izd. Inostrannoi Lit., Moscow, 1957.

6. B. I. Sukhorukov and A. I. Finkel'shtein, Opt. i Spektr. (in press).
7. M. Davis and L. Hopkins, Trans. Faraday Soc. 53, 1563 (1957).
8. A. I. Finkel'shtein, Zhur. Fiz. Khim. 31, 1659 (1957).
9. J. Jones, Trans. Faraday Soc. 55, 527 (1959).
10. A. I. Finkel'shtein, Zhur. Fiz. Khim. (in press).

INFRARED SPECTRA OF HETEROPOLY-COMPOUNDS AND THEIR STRUCTURES

G. V. Yukhnevich

Received 26 December 1959

We investigated the spectra of six heteropoly-compounds in the region 400-1300 cm^{-1} and of three of their aqueous solutions in the region 660-1200 cm^{-1}, with the aim of interpreting the infrared absorption spectra of heteropoly-anions. The results obtained enabled us to ascribe the observed absorption bands to vibration of three zones in the anion. It was also shown that the complexing (central) atom of the anion does not participate in the vibrations responsible for the absorption bands in this region.

The recent infrared spectral investigations of the structure of heteropoly-compounds,[1-3] were qualitative in nature. The absence of interpretation of the observed absorption bands has hindered the full exploitation of the available experimental results.

It is known that the anions of different heteropoly-compounds possess the same structure,[4,5] as a result of which they must exhibit similar absorption spectra. However, the difference between the complexing atoms leads to shifts in the positions of the absorption bands. Investigation and analysis of these shifts should aid the interpretation of the spectrum of any heteropoly-anion.

EXPERIMENTAL RESULTS

We investigated the spectra of six heteropoly-compounds and of three of their aqueous solutions. The measurements were performed on spectrophotometers IKS-1 and IKS-11 in the region 400-1300 cm^{-1} using KBr and NaCl prisms. The error in the positions of the absorption band maxima is 1-2 cm^{-1}. Mulls of the heteropoly-compounds in an inert oil were used in measuring their spectra, while the spectra of the aqueous solutions were measured by placing them between Teflon plates. Because of the low solubility of the heteropoly-compounds in water and because of the strong absorption by water itself, we investigated the spectra of the solutions only in the region 660-1200 cm^{-1}.

Figures 1 and 2 show the spectra observed and the frequencies of the absorption bands of phosphorus-sodium molybdate, phosphorus-sodium tungstate, silicon-sodium tungstate, silicon-calcium tungstate, silico-tungstic acid and metatungstic acid.* The spectra of solutions of heteropoly-compounds are given in Fig. 3. Comparison of the spectra of the crystalline hydrates of the heteropoly-compounds and of metatungstic acid (Fig. 1) shows that they are all equivalent. All the strong and medium bands appear in the spectra of all the compounds and their half-widths and relative intensities remain constant. The difference between the spectra consists only of shifts in the positions of the observed bands and of their splitting into two or three components in some cases.

*From now on, for the sake of brevity, we will use the abbreviated formulas of the heteropoly-compounds instead of their names (for example, phosphorus-sodium molybdate—PMoNa, silico-tungstic acid—SiWH, etc.).

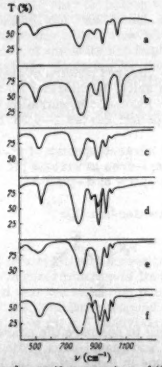

Fig. 1. The absorption spectra of the crystalline heteropoly-compounds. a—phosphorus-sodium molybdate; b—phosphorus-sodium tungstate; c—silicon-sodium tungstate; d—silicon-calcium tungstate; e—silico-tungstic acid; f—metatungstic acid.

Let us examine now the variations in the spectra occurring when an atom in the anion is substituted by another. When the molybdenum atom in PMoNa is substituted by a tungsten atom, all the observed bands shift by 1-2%* towards larger frequencies (Fig. 1, a,b), analogously to the shift observed in ref. 1.

*In connection with the fact that the absorption bands considered are located in the range from 500 to 1100 cm^{-1}, the observed regularities are more clearly illustrated by expressing the band displacements in relative units.

Substitution of the cation K^+ by Na^+ leads to a shift of the 545 cm^{-1} band and a decrease in the intensity of the 878 cm^{-1} band (Fig. 1, b,c). Substitution of K^+ by H^+ leads to a further shift of the above-mentioned bands in the same direction and also to a shift in the 790 and 924

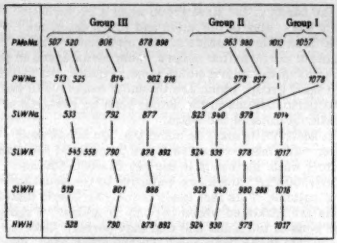

Fig. 2. Identification and classification of the absorption bands of heteropoly-compounds.

cm^{-1} bands (Fig. 1, c,d). At the same time, the 924 cm^{-1} band is shifted by only half of the other shifts.

Because of the low solubility of the heteropoly-compounds in water and the strong absorption of water, the spectra of the aqueous solutions are much less clear (Fig. 3) and hence comparison with the crystalline spectra is possible only for the strongest bands (Table 1). It can be seen from Fig. 3 that the general appearance of the spectrum remains unchanged in going from the crystalline to the solution state, although some of the bands are shifted to a certain extent (Table 1). The bands that experience the largest shift are the 790 cm^{-1} (SiWK), 792 cm^{-1} (SiWNa) and the 814 cm^{-1} (PWNa) bands. A shift half as large is experienced by the 877 cm^{-1} (SiWNa) and the 916 cm^{-1} (PWNa) bands. An even smaller shift (4-5 times less) is experienced by the 924 cm^{-1} (SiWK), the 923 cm^{-1} (SiWNa), and the 978 cm^{-1} (PWNa) bands.

Table 1. The Shift in the Positions of the Absorption Bands of Heteropoly-Compounds in Going from Crystal to Aqueous Solution (frequencies in cm^{-1})

SiWK	$\nu_{cryst.}$	790	878	924	978	1017
	$\nu_{soln.}$	807	—	928	977	1015
	$\Delta\nu$	+17	—	+4	−1	−2
SiWNa	$\nu_{cryst.}$	792	877	923	978	1014
	$\nu_{soln.}$	810	886	927	977	1013
	$\Delta\nu$	+18	+9	+4	−1	−1
PWNa	$\nu_{cryst.}$	814	916	978	—	1078
	$\nu_{soln.}$	838	928	983	—	1079
	$\Delta\nu$	+24	+12	+5	—	+1

When the central phosphorus atom in PWNa is substituted by silicon, all the bands are shifted so far that their identification, at first glance, seems impossible. However, consideration of the general appearance of the spectra (Fig. 1) and the behavior of the various bands in solution in water (Table 1), enables the identification of the bands of PWNa and SiWNa (shown by dotted line in Fig. 2). Analysis of the spectra of PWNa and SiWNa shows that the largest shift on substitution is experienced by the 1078 cm^{-1} band, a smaller shift by the 997 cm^{-1} and 978 cm^{-1} bands, and a still smaller shift by all the remaining bands (Fig. 2).

It is interesting to note that a weak band near 1015 cm^{-1} occurs in the spectra of all the heteropoly-compounds and their aqueous solutions. This band shifts its position by only 4 cm^{-1} in going from one compound to another (Fig. 2, Table 1).

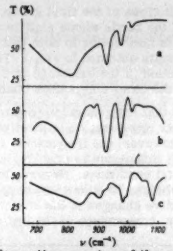

Fig. 3. Absorption spectra of the aqueous solutions of heteropoly-compounds. a—silicon-calcium tungstate; b—silicon-sodium tungstate; c—phosphorus-sodium tungstate.

DISCUSSION OF EXPERIMENTAL RESULTS

The similarity between the spectra of the anions of the heteropoly-compounds investigated, their aqueous solutions, and the metatungstic acid (Figs. 1, 3) indicates the following: firstly, the anions of all the heteropoly-compounds and of metatungstic acid have the same structure and hence, the metatungstic acid must be considered a heteropoly-compound (this result is in complete agreement with the conclusions obtained in refs. 4, 5; and secondly, the heteropoly-anions in solution and in the crystalline states have similar structures.

All the absorption bands of the heteropoly-compounds can be divided into three groups (Fig. 2) depending on the magnitude of the relative shift in the position of the absorption bands occurring when one of the central (complexing) atoms of the anion is substituted by another (Table 2). The first group comprises the bands that exhibit the strongest shift, the second group the bands

Table 2. Relative Shift (in %) of the Position of the Absorption Bands of Heteropoly Compounds Caused by Substitution of the Central Atom

Nature of substitution	Compound	Spectral region (cm^{-1})						
		1000	900		800		600	520
P by Si	Phosphorus-sodium tungstate	— 9.0	−5.7	−5.6	−3.2	−2.7	−2.6	+2.8
	Phosphorus-ammonium tungstate	−10	—	−5.7	—	−1.5	−2.0	—
	Phosphoro-tungstic acid	— 9.0	—	−5.7	—	−1.8	−2.0	—
	Phosphorus-ammonium molybdate	−11	—	−6.0	—	−1.5	−1.5	—
P by As	Phosphorus-ammonium tungstate	— 9.0	—	−7.1	—	−1.8	−2.3	—
	Phosphorus-ammonium molybdate	−11	—	−7.5	—	−2.7	−2.0	—
P by B	Phosphorus-ammonium tungstate	— 1	—	0	—	+1	+0.5	—
P by Ti	Phosphorus-ammonium molybdate	0	—	0	0	0	+0.5	—
Si by 2H	Silico-tungstic acid	0 (band 980)	−1.0 (band 940)	−0.4 (band 928)		0	−1.4	+1.7

whose shift is half those of the first group, and the third group consists of the bands whose shift is half that of the second group. It is interesting to note that when we recalculated the results obtained in ref. 1 (Table 2), we obtained an indication of the existence of similar groups in the spectra of the other compounds studied in ref. 1.*

*It must be noted that the general appearance of the spectra obtained in this investigation is identical to that obtained in ref. 1; however, the frequencies of separate bands differ. This difference is probably caused by different experimental conditions. Nevertheless, since the experimental conditions in either investigation remained constant, the relative changes in the spectra should be comparable. Thus, comparison of the two sets of results is quite justified.

When a silicon atom is substituted for a central phosphorus atom, the magnitude of the shift in the position of the bands was found to be the same in both investigations. Substitution of an arsenic atom for a central atom of phosphorus leads to similar shifts (with the exception of the 980 cm^{-1} band whose shift is slightly larger than on substitution of a silicon atom for a phosphorus atom). The spectral manifestations occurring when other central (complexing) atoms are substituted will be examined below.

It is easily seen that when a sodium cation is substituted for a calcium cation, only two bands of the third group are sensitive to this perturbation (the substitution of cations in the molecule can be regarded as a perturbation) (Figs. 1, 2). When a hydrogen cation is substituted for a calcium cation, i.e., the case of a stronger perturbation, the shift in the positions of the 545 cm^{-1} and 878 cm^{-1} bands is larger relative to the one occurring on substitution of Na^+ for the K^+ cation. Furthermore, the third band (790 cm^{-1}) of the third group is also shifted and, to a lesser extent, so is the 924 cm^{-1} band of the second group.

The bands of the third group with frequencies around 800 cm^{-1} were found to be the most sensitive to the process of solution in water (Table 1); the bands of the third group with frequencies around 880 cm^{-1} were less sensitive, and the bands of the second group were the least sensitive.

Since, at present, it is an established fact that the complexing atom is located at the center of the anion while the cations and the solvent molecules are located at the "surface" of the anion,[4-7] we can interpret our experimental results in the following manner: Let us visualize a spherically symmetrical anion consisting of fifty-three atoms. All the constituent atoms of the anion participate in its vibrations, during which all the bonds existing in the anion are deformed. However, the deformation of the separate bonds in the anion will be different for every single vibration of the anion. Let us now arbitrarily divide the anion into three zones: interior, intermediate, and exterior. Then, all the vibrations of the anion can be divided, as a first approximation, into vibrations of the interior zone, the intermediate zone, and the exterior zone, depending on which zone contains the bond undergoing the largest deformation. Since perturbations in the center of the anion must influence primarily the vibrations of the interior zone of the anion, while perturbations in its periphery should influence the vibrations of the exterior zone of the anion, then it is natural to make the following assignment. The bands of the first group, which exhibit the largest shifts in their positions when the central atom of the anion is perturbed and which are not influenced by peripheral perturbations, are assigned to the vibrations of the interior zone of the anion. The bands of the second group, which are shifted less than the bands of the first group when a perturbation occurs at the center of the anion and which again are shifted less than the bands of the third group when a peripheral perturbation occurs, must be assigned to the vibrations of the intermediate zone. Finally, the bands of the third group, which are the most sensitive to peripheral perturbations in the anion, must be assigned to the exterior zone of the anion.

In addition, it must be noted that the bands near 800 cm^{-1} are more sensitive to the process of solution in water, while the bands in the regions 500-550 cm^{-1} and 880-900 cm^{-1} are more sensitive to the substitution of cations. This fact leads to the conclusion that the cations are localized within certain "regions" of the exterior zone of the anion and that they perturb most the bonds within these "regions." On the other hand, when the heteropoly-compounds are dissolved in water, these "regions" of the exterior zone and hence the bonds contained within them, are screened by the cations from the influence of the solvent molecules. In agreement with this conclusion, the bands in the regions 500-550 cm^{-1} and 880-900 cm^{-1} must be assigned to the vibrations of the anion with preponderant deformation of the bonds found within these "regions" of the exterior zone of the anion.

The behavior of the weak band around 1015 cm^{-1} is slightly peculiar. This band is found in all the heteropoly-compounds, with the exception of phosphorus-sodium tungstate, where it is probably masked by the strong doublet band (978, 997 cm^{-1}) (Fig. 1, b). This band is not affected by any kind of perturbation and can be considered to be a characteristic band of the whole heteropoly-anion. However, the weak intensity of this band precludes its use for analytic purposes.

Comparison of the spectra of silico-tungstic acid (Si-central atom) and of metatungstic acid (the central atom is absent or its place is occupied by two hydrogen atoms, Fig. 1, e,f) shows that a fourteenfold change in the mass of the central atom does not affect the anion spectrum. The absence of a spectroscopic manifestation of such a large change in mass leads to the conclusion that the central atom of the heteropoly-anion only influences but does not participate in the vibrations of the anion which determine the observed absorption bands. The nature of the influence has been discussed above in great detail.

The data shown in Table 2 indicate that substitution of the central P atom by a B or Ti atom does not affect the spectrum. An analogous phenomenon is observed on substitution of the central Si atom by As or 2H. Nevertheless, substitution of any one of the three atoms (P, B, Ti) by any of the following (Si, As, 2H), is accompanied by a large shift in the positions of all the observed bands. This phenomenon cannot be explained either by the atomic weight, or the valencies, or the coordination numbers, or the ionic or covalent radii of the atoms under consideration. It is thus impossible to determine the nature of the influence exerted by the central atom on the anion vibrations. As a result, the only valid conclusion is that the central atom remains practically immobile during the anion vibrations resulting in the observed absorption bands.

In the present work, we investigated six different heteropoly-compounds. As shown in Table 2, our conclusions fully substantiate the results of ref. 1, where ten other heteropoly-compounds were studied. Hence, our conclusions concerning the assignment of absorption bands to one or another anion zone, can be extended to all the heteropoly-compounds and metatungstates whose anions can be considered as heteropoly-compounds. The proposed interpretation cannot be considered as incon-

trovertible and definite. Its reliability can be proven only by strict calculation. Nevertheless, it permits an estimate of the location and magnitude of the anion deformation.

During our investigation, we found that the spectra of silico-tungstic acid and phosphorus-sodium molybdate were identical with the spectra of their reduction products. That there was reduction was indicated by the following color changes: silico-tungstic acid—from white to dark-blue, and in the case of phosphorus-sodium molybdate—from yellow to dark-green. That the change in the valency of the tungsten and molybdenum exerted no effect on the spectra is a surprising phenomenon for which we have no explanation.

In conclusion, we want to thank A. V. Karyakin and L. S. Mayants for helpful discussions of the experimental results.

REFERENCES

1. N. Sharpless and I. Munday, Anal. Chem. **29**, 1619 (1957).
2. A. A. Babushkin, G. V. Yukhnevich, Yu. F. Berezkina, and V. I. Spitsyn, Zhur. Neorg. Khim. **4**, 823 (1959).
3. G. V. Yukhnevich, A. A. Babushkin, and I. D. Kolli, Zhur. Neorg. Khim. **5**, 1176 (1960).
4. R. Signer and H. Gross, Helv. chim. Acta **17**, 1076 (1934).
5. J. W. Illingworth and J. F. Keggin, J. Chem. Soc. 409 (1935).
6. E. A. Nikitina, Sbornik Statei Obshchei Khim. **1**, 44 (1953).
7. V. I. Spitsyn, Zhur. Neorg. Khim. **2**, 502 (1957).

THE KINETICS OF THE CONCENTRATION DEPOLARIZATION OF LUMINESCENCE AND OF THE INTERMOLECULAR TRANSFER OF EXCITATION ENERGY

P. I. Kudryashov, B. Ya. Sveshnikov, and V. I. Shirokov

Received 9 December 1959

According to the migration theory of the concentration depolarization of the fluorescence of solutions, in the concentration depolarization region, the decay time for that component of the radiation which is parallel to the electric vector of exciting light ($\tau_{\parallel}$) is shorter, and the decay time of the perpendicular component ($\tau_{\perp}$) larger, than the average fluorescence time (τ_0). The dependence of $\tau_{\perp} - \tau_{\parallel}/\tau_0$ on the concentration of the fluorescing material and the maximum value of this ratio are determined by the kinetics of the energy transfer. Calculations based on Vavilov's theory, which assumes that the frequency of energy transfer does not depend on the interaction time, show that the maximum value of this ratio is 0.225 for a limiting polarization of 0.42 (fluorescein). According to the theory of Foerster and Galanin, which states that the frequency of the energy transfer is inversely proportional to $\sqrt{t}$, this same ratio has a value of 0.142. The experimental value is 0.12, which is approximately equal to the value calculated from the Foerster-Galanin theory. Validity and accuracy of the method were tested by investigating the change of $\tau_{\parallel}$ and $\tau_{\perp}$ that occurs as a result of rotational Brownian motion.

1. INTRODUCTION

The current theory of the concentration depolarization of solutions proceeds, as is well known, from assumptions concerning the transfer of excitation energy from an excited to an unexcited molecule. This mechanism of the phenomenon leads to the result that concentration depolarization is a function not only of the distance between molecules (i.e., of their concentration) but also of the time of interaction between an excited and an unexcited molecule. The latter was demonstrated by (1) the experiments of Feofilov and Sveshnikov,[1] which showed that, in the concentration depolarization range, the polarization is a function of the duration of the excited state of the molecule; (2) the experiments of Sevchenko,[2] who observed that in uranium glasses with high activator concentrations the degree of polarization decreases during the decay process; and (3) by the fluorometric experiments of Galanin.[3] The latter showed that for solutions of fluorescein in glycerine which were in the concentration depolarization range, but not within the concentration quenching range, when luminescence is excited by polarized light the decay time of that component of radiation parallel to the electric vector of the exciting light ($\tau_{\parallel}$) is smaller, while that of the perpendicular component ($\tau_{\perp}$) is larger than the average duration of the fluorescence (τ_0).

The experiments cited above also served as experimental proof of the migration theory of concentration phenomena proposed by Vavilov.[4] Vavilov considered that the direct fluorometric experiments of Galanin were especially conclusive, since the results of these experiments were not only in qualitative agreement with the theory but, bearing in mind the relative inaccuracy of the measurements, he felt that they also agreed quantitatively with the theory. During the past 10 years, however, Vavilov's theory has undergone some revisions.

In Vavilov's theory, in order to explain how the yield and τ depend on concentration in highly viscous solutions, it must be assumed that, along with the quenching that occurs during the transfer of excitation energy, which has a constant probability throughout the lifetime of the excited state, an instantaneous quenching also occurs.

Later, Foerster[5] and Galanin[6] pointed out that owing to fluctuations in the positions of the molecules of the fluorescing substance in solutions, the assumption of a time-independent transfer frequency was invalid. They proposed a new migration theory, according to which the transfer frequency was inversely proportional to the square root of the time elapsed from the instant of excitation. The new theory satisfactorily explained how the yield and luminescence time depend on concentration in viscous solutions without the rather artificial assumption that an instantaneous quenching occurs.[6]

The deviations of $\tau_{\parallel}$ and $\tau_{\perp}$ from τ_0 in the concentration depolarization range, as studied by Galanin, should also depend on the way the excitation energy transfer process depends on time.

As is shown below (see Section 2), the results predicted by the old and new theories are esentially different. The difference is such that in view of the accuracy now attained by fluorometric measurements, experimental values of $\tau_{\parallel}$ and $\tau_{\perp}$ can serve as conclusive evidence for the correctness of one or the other of these theories. This also prompted us to repeat Galanin's experiments.

2. THEORETICAL PART

Assume that all of the excited molecules comprise a set of virtual oscillators oriented along three axes, one of which is parallel to the electric vector of the exciting light, and the other two perpendicular to the first axis and to each other.

Let us call $n_{\parallel}$ the number of oscillators oriented along the first axis, $n_{\perp}$ the number of oscillators oriented along each of the other two axes, and n the total number of oscillators.

The changes of $n_{\parallel}$ and $n_{\perp}$ with time will be determined by the system of differential equations

$$\frac{dn_{\parallel}}{dt} = -\frac{1}{\tau_0} n_{\parallel} - \frac{2}{3} a n_{\parallel} + \frac{2}{3} a n_{\perp}, \tag{2.1}$$

$$\frac{dn_{\perp}}{dt} = -\frac{1}{\tau_0} n_{\perp} - \frac{1}{3} a n_{\perp} + \frac{1}{3} a n_{\parallel}. \tag{2.2}$$

The second and third terms take account of changes in $n_{\parallel}$ and $n_{\perp}$ which occur as a result of the transfer of excitation energy to oscillators oriented along the other axes.

The coefficient a, which determines the rate of this transfer, should be proportional to the transfer frequency. The number of oscillators oriented along each of the axes is proportional to the intensity of radiation polarized along the axes. Therefore, the initial conditions for (2.1) and (2.2) will be

$$n_{\parallel}(0) = \frac{1 + p_0}{3 - p_0} n(0), \tag{2.3}$$

$$n_{\perp}(0) = \frac{1 - p_0}{3 - p_0} n(0), \tag{2.4}$$

where p_0 is the limiting polarization of luminescence in the solution being investigated.

Let us now derive equations for $\tau_{\parallel}$ and $\tau_{\perp}$, first on the basis of Vavilov's migration theory and then on the basis of the Foerster-Galanin theory.

(a) according to S. I. Vavilov's theory, the transfer frequency is independent of time, and consequently

$$a = a_1 = \text{const}. \tag{2.5a}$$

The solution of Eqs. (2.1) and (2.2) with condition (2.5a) gives

$$n_{\parallel} = \frac{n(0)}{3}\left[e^{-\frac{t}{\tau_0}} + A_{\parallel} e^{-t\left(\frac{1}{\tau_0} + a_1\right)}\right], \tag{2.6a}$$

$$n_{\perp} = \frac{n(0)}{3}\left[e^{-\frac{t}{\tau_0}} - A_{\perp} e^{-t\left(\frac{1}{\tau_0} + a_1\right)}\right], \tag{2.7a}$$

where

$$A_{\parallel} = \frac{4p_0}{3 - p_0} \text{ and } A_{\perp} = \frac{2p_0}{3 - p_0}. \tag{2.8}$$

By using the equation which defines the average luminescence time

$$\tau = \frac{\int_0^{\infty} t n(t)\, dt}{\int_0^{\infty} n(t)\, dt}, \tag{2.9}$$

we obtain

$$\frac{\tau_{\parallel}}{\tau_0} = \frac{1 + A_{\parallel} \frac{1}{(1 + a_1\tau_0)^2}}{1 + A_{\parallel} \frac{1}{1 + a_1\tau_0}}, \tag{2.10a}$$

$$\frac{\tau_{\perp}}{\tau_0} = \frac{1 - A_{\perp} \frac{1}{(1 + a_1\tau_0)^2}}{1 - A_{\perp} \frac{1}{1 + a_1\tau_0}}. \tag{2.11a}$$

(b) In the Foerster-Galanin theory, the transfer frequency is inversely proportional to the square root of the time elapsed from the instant of excitation (t), and consequently

$$a = \frac{a_2}{\sqrt{t}}, \tag{2.5b}$$

where a_2 is a constant.

The solution of Eqs. (2.1) and (2.2) with the condition (2.5b) leads to

$$n_{\parallel} = \frac{n(0)}{3}\left[e^{-\frac{t}{\tau_0}} + A_{\parallel} e^{-\left(\frac{t}{\tau_0} + 2a_2\sqrt{t}\right)}\right], \tag{2.6b}$$

$$n_{\perp} = \frac{n(0)}{3}\left[e^{-\frac{t}{\tau_0}} - A_{\perp} e^{-\left(\frac{t}{\tau_0} + 2a_2\sqrt{t}\right)}\right], \tag{2.7b}$$

$$\frac{\tau_{\parallel}}{\tau_0} = \frac{1 + A_{\parallel}\left[1 + q^2 - (3 + 2q^2) q e^{q^2} \int_q^{\infty} e^{-x^2} dx\right]}{1 + A_{\parallel}\left(1 - 2q e^{q^2} \int_q^{\infty} e^{-x^2} dx\right)}, \tag{2.10b}$$

$$\frac{\tau_{\perp}}{\tau_0} = \frac{1 - A_{\perp}\left[1 + q^2 - (3 + 2q^2) q e^{q^2} \int_q^{\infty} e^{-x^2} dx\right]}{1 - A_{\perp}\left(1 - 2q e^{q^2} \int_q^{\infty} e^{-x^2} dx\right)}, \tag{2.11b}$$

where

$$q = a_2\sqrt{\tau_0}. \tag{2.12}$$

Curves calculated from Eqs. (2.10a), (2.11a) and (2.10b), (2.11b) for $p_0 = 0.42$ (the limiting polarization for fluorescence in fluorescein[7]), are shown in Fig. 1.

Generally speaking, it is necessary to know how the coefficients a_1 and a_2 depend on the concentration of the luminescing substance if one wishes to make a comparison with theory. The latter is not required if one limits oneself to a comparison of the maximum values of the difference $\tau_{\perp} - \tau_{\parallel}/\tau_0|_{max}$ with the values calculated from the theory.

3. COMPARISON OF GALANIN'S EXPERIMENTAL RESULTS WITH THEORY

Figure 2 shows the experimental values of $\tau_{\perp} - \tau_{\parallel}/\tau_0$ taken from Galanin's publication.[3] For comparison, horizontal lines are drawn at levels corresponding to the maximum values of the difference $\tau_{\perp} - \tau_{\parallel}/\tau_0$ calculated from the Vavilov theory (line 1) and from the Foerster-Galanin theory (line 2) for $p_0 = 0.5$, which was the limiting polarization in Galanin's experiments.

The experimental results of Galanin are about 20% higher than the theoretical results based on Vavilov's theory, and about 80% higher than those based on the Foerster-Galanin theory, i.e., they show better agreement with the first theory.

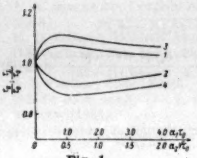

Fig. 1

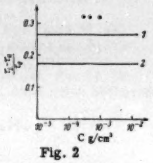

Fig. 2

Fig. 1. Curves for $\tau_\perp/\tau_0$ and $\tau_\parallel/\tau_0$. Curves 1 and 2—calculated from the Foerster-Galanin theory; curves 3 and 4—calculated from the Vavilov theory.

Fig. 2. $\tau_\perp - \tau_\parallel/\tau_0|_{max}$ for $p_0 = 0.5$. Calculated from the Vavilov theory (Line 1); from the Foerster-Galanin theory (Line 2). The points are the values of $\tau_\perp - \tau_\parallel/\tau_0$ from Galanin's measurements.

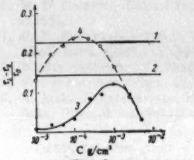

Fig. 3

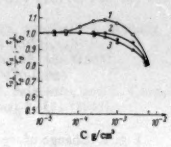

Fig. 4

Fig. 3. $\tau_\perp - \tau_\parallel/\tau_0|$ for $p_0 = 0.42$. Calculated from the Vavilov Theory (Line 1); from the Foerster-Galanin theory (Line 2). The experimental dependence of $\tau_\perp - \tau_\parallel/\tau_0$ on C from measurements on thin layers (curve 3) and on thick layers (curve 4).

Fig. 4. Experimental dependence of $\tau_\perp/\tau_0$ (curve 1), $\tau_{\perp\parallel}/\tau_0$ (curve 2), and $\tau_\parallel/\tau_0$ (curve 3) on concentration.

4. EXPERIMENTAL PART

Following Galanin, we also chose to experiment with solutions of fluorescein in glycerine. The luminescence was excited by the mercury line at 436 mμ. The observations were made from the side on which the exciting light was incident. Polaroids were used as polarizer and analyzer. The measurements were made on an IF-39 phase fluorometer. The modulation frequency of the exciting light was 12.8 Mc/s. In order to exclude depolarization caused by rotatory Brownian motion, the experiments were conducted at 0°C.

In order to increase the accuracy of measurement of the difference $\tau_\perp - \tau_\parallel$, the experimental values of which were to be compared with the theoretical values, this difference was calculated from direct measurements of the phase difference $\varphi_\perp - \varphi_\parallel$ which appeared when the analyzer was rotated by 90°. In order to lessen the errors introduced by secondary fluorescence, which gives the same kind of effect as the migration of excitation energy, the measurements were made on thin layers. Furthermore, in order to decrease reabsorption as a result of multiple reflections, the back wall of the vessel was made of black glass.

At each concentration, the measurements were made for three luminescence intensities (in three layers of different thicknesses) and the final results were obtained by extrapolating to zero intensity.

The concentration dependence of the difference calculated from the values of $\tau_\perp - \tau_\parallel/\tau_0$ corresponding to zero intensity are shown in Fig. 3 (curve 3). Here, also for comparison with theory, we show horizontal lines at levels corresponding to the maximum values of the difference $\tau_\perp - \tau_\parallel/\tau_0$, calculated for $p_0 = 0.42$ (the limiting polarization in our solutions) from Vavilov's theory (line 1) and the Foerster-Galanin theory (line 2).

The theoretical and experimental values of $\tau_\perp - \tau_\parallel/\tau_0|_{max}$ were as follows:

Calculated from Vavilov	0.225
Calculated from Foerster-Galanin	0.142
Experimental	0.12

The value of $\tau_\perp - \tau_\parallel/\tau_0|_{max}$ calculated from Vavilov is 1.9 as large as the experimental value, while that calculated from Foerster-Galanin is only 1.2 as large.

Figure 4 shows the dependence of $\tau_\perp/\tau_0$, $\tau_\parallel/\tau_0$, and the duration of luminescence observed from the side exposed to excitation by unpolarized light $\tau_{\perp\parallel}/\tau_0$; $\tau_\perp/\tau_0$ and $\tau_{\perp\parallel}/\tau_0$ were measured directly and $\tau_\parallel/\tau_0$ was calculated from $\tau_\perp/\tau_0$ and $\tau_\perp - \tau_\parallel/\tau_0$. These curves differ somewhat from the theoretical curves. There is practically no minimum visible in the experimental curves. This can be explained by assuming that reabsorption of luminescence, which contributes toward a lifting of all the curves for large concentrations, has not been taken into account with sufficient accuracy.

Let us evaluate the possible distortion of the fundamental result (the magnitude of $\tau_\perp - \tau_\parallel/\tau_0|_{max}$) resulting from reabsorption, which leads to a lifting of the $\tau_\parallel/\tau_0$ curve in the region of $\tau_\parallel/\tau_0|_{min}$ to a value equal to $\tau_\parallel/\tau_0|_{theor.\ min}$. In the Appendix, an expression for $\tau_\parallel/\tau_0$ and $\tau_\perp/\tau_0$ is derived for simultaneous excitation energy transfer and reabsorption (Eqs. (6.6) and (6.7)). The value of $\tau_\perp - \tau_\parallel/\tau_0|_{max}$ calculated from (6.6) and (6.7), corresponding to $\tau_\parallel/\tau_0|_{min} = 1$, is equal to 0.161, i.e., it differs by 13% from the value calculated without considering reabsorption.

In order to explain why our data differ from those of Galanin by a factor of 2.6, we repeated the measurements with complete absorption of the exciting radiation (the condition prevailing in Galanin's experiment). The results are shown in Fig. 3 (curve 4). In comparing the results it must be kept in mind that in our case $\tau_{\parallel\perp}$ increased by almost 70% as a result of reabsorption, whereas in Galanin's case it increased by only 30%.

In order to check the validity and accuracy of our experimental method, we investigated the viscosity dependence of the deviation of the duration of the parallel and perpendicular components of luminescence from the average duration during depolarization, which deviation was caused by rotational Brownian motion in solutions of fluorescein in glycerine (1×10^{-5} gm/cm³).* Since in this case the rate of depolarization was constant with time,[9] the maximum value of $\tau_\perp - \tau_\parallel/\tau_0$ should be determined by Eqs. (2.10a) and (2.11a). We increased the rate of depolarization by heating the solution and thus decreasing its viscosity.

*The changes of $\tau_\perp$ and $\tau_\parallel$ as a result of Brownian rotational motion were first demonstrated by Szymanowsky.[8]

Figure 5 shows the dependence of $\tau_\perp - \tau_\parallel/\tau_0$ on temperature for layers 0.5 mm and 1.0 mm thick. It follows from these curves that rotational depolarization finally dies out only at temperatures below 0°C. Because of the high degree of reabsorption, the curve for the 1 mm layer lies somewhat higher than the curve for the 0.5 mm layer. Linear extrapolation to zero thickness leads to a maximum effect equal to 0.2, which differs from the theoretical value by only 10%.

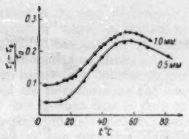

Fig. 5. Change of $\tau_\perp - \tau_\parallel/\tau_0$ with temperature as a result of rotational Brownian motion.

5. CONCLUSIONS

The results of the fluorometric experiments described in Section 4 showed that the kinetics of concentration depolarization and, consequently, the kinetics of the resonance migration of energy from an excited molecule to an unexcited one are described better by the Foerster-Galanin theory than by the Vavilov theory.

6. APPENDIX

(a) Calculation of $\tau_\parallel$ and $\tau_\perp$, including the effect of secondary fluorescence

Let $P'_\parallel$ represent the fraction of the oscillators excited by reabsorption which are oriented along the axis parallel to the direction of the primary oscillators, and let $P'_\perp$ represent the same parameter for each of the two axes perpendicular to the first axis and to each other.

The differential equations for $n_\parallel$ and $n_\perp$ will be:

$$\frac{dn_\parallel}{dt} = -\frac{1}{\tau_0} n_\parallel + \frac{1}{\tau_0} qB_a P'_\parallel n_\parallel + \frac{2}{\tau_0} qB_a F'_\perp n_\perp - \frac{2}{3}\frac{a_2}{\sqrt{t}} n_\parallel + \frac{2}{3}\frac{a_2}{\sqrt{t}} n_\perp, \tag{6.1}$$

$$\frac{dn_\perp}{dt} = -\frac{1}{\tau_0} n_\perp + \frac{1}{\tau_0} qB_a (P'_\parallel + P'_\perp) n_\perp + \frac{1}{\tau_0} qB_a P_\perp n_\parallel - \frac{1}{3}\frac{a_2}{\sqrt{t}} n_\perp + \frac{1}{3}\frac{a_2}{\sqrt{t}} n_\parallel, \tag{6.2}$$

where q is the fraction of primary radiation absorbed secondarily, and B_a is the quantum yield of luminescence associated with reabsorption. The solution of this system of equations with the initial conditions (2.3) and (2.4) is given by

$$n_\parallel = \frac{n(0)}{3}\left[e^{-\frac{t}{\tau_0}(1-qB_a)} + A_\parallel e^{-\frac{t}{\tau_0}(1-qB_aP')-2a_2\sqrt{t}}\right], \tag{6.3}$$

$$n_\perp = \frac{n(0)}{3}\left[e^{-\frac{t}{\tau_0}(1-qB_a)} - A_\perp e^{-\frac{t}{\tau_0}(1-qB_aP')-2a_2\sqrt{t}}\right], \tag{6.4}$$

where

$$P' = P'_\parallel - P'_\perp \tag{6.5}$$

and $A_\parallel$ and $A_\perp$ were evaluated previously (see Eq. (2.8)).

$$\frac{\tau_\parallel}{\tau_0} = \frac{1}{(1-qB_a)(1-qB_aP')} \cdot \frac{(1-qB_aP')^3 + A_\parallel(1-qB_a)^3[1+b^2-(3+2b^2)B]}{(1-qB_aP') + A_\parallel(1-qB_a)(1-2B)}, \tag{6.6}$$

$$\frac{\tau_\perp}{\tau_0} = \frac{1}{(1-qB_a)(1-qB_aP')} \cdot \frac{(1-qB_aP')^3 - A_\perp(1-qB_a)^3[1+b^2-(3+2b^2)B]}{(1-qB_aP') - A_\perp(1-qB_a)(1-2B)}, \tag{6.7}$$

where

$$b = a_2\sqrt{\tau_0}\cdot\frac{1}{\sqrt{1-qB_aP'}}, \tag{6.8}$$

$$B = be^{b^2}\int_b^\infty e^{-x^2}dx. \tag{6.9}$$

(b) Calculation of $P'_\parallel$ and $P'_\perp$

The parameters $P'_\parallel$ and $P'_\perp$ can be evaluated in the same way as the polarization of the secondary fluorescence. The latter was calculated by Galanin for the case of spherically symmetrical absorption of radiation.[3] We shall start with this same model.*

*In the paper by Budo, Ketskemety, Salkovits and Gargya,[10] the effect on fluorescence polarization of secondary radiation was calculated for the case in which the molecule excited by the primary radiation is located along the axis of a cylindrical luminor.

At the center of the absorption sphere, let there be n_Z excited oscillators oriented parallel to the OZ axis. The intensity of the radiation directed along an angle ϑ from the oscillator axis is given by

$$dJ_\vartheta \sim n_z \sin^2\vartheta\, d\Omega, \tag{6.10}$$

where $d\Omega = \sin\vartheta\, d\vartheta\, d\varphi$.

The components of the secondary radiation excited by linearly polarized primary radiation polarized along the meridian (dJ'_ϑ), the parallel (dJ'_φ), and the radius (dJ'_r), will be

$$dJ'_\vartheta = dJ_\vartheta \frac{1+p_0}{3-p_0} = dJ_\vartheta \cdot P^0_\parallel, \tag{6.11}$$

$$dJ'_\varphi = dJ'_\varphi = dJ_\vartheta \frac{1-p_0}{3-p_0} = dJ_\vartheta \cdot P^0_\perp. \tag{6.12}$$

If we project dJ'_ϑ, dJ'_φ, and dJ'_r onto the OZ and OX axes, we obtain

$$dJ'_z = dJ'_\vartheta \sin^2\vartheta + dJ'_r \cos^2\vartheta, \tag{6.13}$$

$$dJ'_x = (dJ'_\vartheta \cos^2\vartheta + dJ'_r \sin^2\vartheta)\cdot\cos^2\varphi + dJ'_\varphi \cdot \sin^2\varphi, \tag{6.14}$$

$$J'_z \sim \int_{\varphi=0}^{2\pi}\int_{\vartheta=0}^{\pi} dJ'_z = \frac{8\pi}{15}(4P^0_\parallel + P^0_\perp), \tag{6.15}$$

$$J'_x \sim \int_{\varphi=0}^{2\pi}\int_{\vartheta=0}^{\pi} dJ'_x = \frac{4\pi}{15}(P^0 + 9P^0_\perp), \tag{6.16}$$

$$P'_\parallel = \frac{J'_z}{J'_z + 2J'_x} = \frac{1}{5}\frac{4P^0_\parallel + P^0_\perp}{P^0_\parallel + 2P^0_\perp}, \tag{6.17}$$

$$P'_\perp = \frac{J'_x}{J'_z + 2J'_x} = \frac{1}{10}\frac{P^0_\parallel + 9P^0_\perp}{P^0_\parallel + 2P^0_\perp}. \tag{6.18}$$

For $p_0 = 0.42$, we have $P'_\parallel = 0.485$ and $P'_\perp = 0.2575$.

REFERENCES

1. P. P. Feofilov and B. Ya. Sveshnikov, Zhur. Eksptl. i Teoret. Fiz. 10, 1372 (1940).

2. A. A. Sevchenko, Doklady Akad. Nauk SSSR **42**, 349 (1944).
3. M. D. Galanin, Doklady Akad. Nauk SSSR **57**, 883 (1947); Trudy Fiz. Inst., Akad. Nauk SSSR **5**, 341 (1950).
4. S. I. Vavilov, Zhur. Eksptl. i Teoret. Fiz. **13**, 13 (1943); Sobr. soch, Vol. 2, Izd. Akad. Nauk SSSR, Moscow (1954).
5. Th. Foerster, Z. Naturforsch. **4a**, 321 (1949).
6. M. D. Galanin, Zhur. Eksptl. i Teoret. Fiz. **28**, 485 (1955).
7. P. P. Kudryashov and B. Ya. Sveshnikov, Doklady Akad. Nauk. SSSR **115**, 894 (1957).
8. W. Szymanowsky, Z. Physik **95**, 466 (1935).
9. F. Perrin, Ann. Phys, **12**, 169 (1929).
10. A. Budo, I. Ketskemety, E. Salkovits, and L. Gargya, Acta. Phys. Acad. Sci. Hung. **8**, 181 (1957).

STUDY OF THE PHOSPHORESCENCE LIFETIMES OF SOLUTIONS OF ORGANIC COMPOUNDS AT −196°

E. N. Viktorova, I. A. Zhmyreva, V. P. Kolobkov, and A. A. Saganenko

Received 22 December 1959

The study of the relative quantum yields of phosphorescence and of fluorescence (δ)[1-13] (at −180° and −196° in most investigations), is one of the fundamental methods of investigating the influence of various extra- and intramolecular factors on the probability of transition of excited organic molecules to a metastable state (r). In the case of long wavelength phosphorescence,[3]

$$\delta = \frac{r}{p} \cdot \frac{\pi}{\pi + q_2},$$

where p is the probability of the fluorescence transition, π is the probability of emission from the metastable to the ground state, and q_2 is the probability of quenching of the metastable state.

The problem in the present investigation of phosphorescence lifetimes $\tau_{phosph.}$,* was to find out whether quenching of the metastable state occurred at −196°. This would enable us to determine the extent, under the specified conditions, to which variation in r determined the variation in δ occurring as a result of a change in the solvent. The experimental results are presented in Tables 1 and 2.

It is easily seen that there exists a large group of solvents (1-8) (see Table 1 for numbering of solvents), differing in their chemical nature and in their state at −196°, for which the $\tau_{phosph.}$ of the majority of the compounds investigated vary within a rather narrow interval. Moreover it must be noted that these values of $\tau_{phosph.}$ are the maximal values for the corresponding compounds. On the other hand, the magnitude of δ varies widely in these solvents. For example, $\tau_{phosph.}$ of compound IV (Table 1), in ten solvents out of the twenty used, varies between 0.5 and 0.7 sec while δ in these solvents varies from 0.4 to 1.75. An analogous effect on the magnitude of

*The determination of $\tau_{phosph.}$ was performed using the apparatus of B. Ya. Sveshnikov[14] and P. I. Kudryashov, to whom the authors express their deep gratitude.

Table 1. The Values of $\tau_{phosph.}$ and δ of 3-Acetylamino-(I), 4-Acetylamino-(II), 3,6-Diacetylamino-(III), and 3-Methylacetylamino-6-(IV) Acetylamino-N-Phthalimides in Various Solvents* at −196°

Solvent No.	I		II		III		IV	
	$\tau_{phos.}$	δ	$\tau_{phos.}$	δ	$\tau_{phos.}$	δ	$\tau_{phos.}$	δ
1	0.90	1.26	0.90	—	0.55	0.12	0.70	0.39
2	1.25	—	1.1	0.09	0.70	—	0.7	1.34
3	0.90	1.1	1.1	—	0.55	0.165	0.60	1.07
4	1.0	—	1.0	—	0.55	—	0.40	0.39
5	1.1	—	1.1	—	0.65	—	0.55	0.84
6	0.95	—	1.0	—	0.65	—	0.50	—
7	1.25	2.2	1.25	0.1	0.60	0.195	0.50	1.36
8	1.05	3.0	1.1	0.12	0.65	0.29	0.50	1.75
9	0.90	2.3	0.75	—	0.45	—	0.50	0.58
10	1.05	0.5	0.70	0.09	0.50	0.06	0.50	0.62
11	0.85	—	0.80	—	0.35	—	0.45	—
12	0.75	—	0.75	0.09	0.40	—	0.50	1.49
13	0.90	0.36	0.50	0.01	0.35	—	0.45	0.25
14	1.2	0.32	0.60	—	0.35	—	0.25	—
15	0.50	—	0.30	—	—	—	0.25	—
16	0.50	0.32	—	0.02	—	—	0.30	0.04
17	0.95	0.37	0.30	0.04	0.1	0.02	0.25	0.17
18	0.55	0.14	0.50	0.005	0.1	0.01	0.25	0.12
19	0.75	3.3	0.80	0.15	—	—	0.15	—
20	0.20	—	0.40	—	—	—	0.35	0.70
21	0.15	10	0.20	—	0.17	—	0.15	—

*Key to the numbering of solvents (in Tables 1 and 2): 1 – acetic acid; 2 – acetic anhydride; 3 – acetone; 4 – diisopropyl ether; 5 – propylacetate; 6 – isopropyl formate; 7 – methyl alcohol; 8 – ethyl alcohol; 9 – toluene; 10 – anisole; 11 – isopropyl chloride; 12 – chloroform; 13 – carbon tetrachloride; 14 – n-octane; 15 – dioxane; 16 – crystalline state; 17 – benzene, 18 – water; 19 – pyridine; 20 – triethylamine; 21 – propyl bromide.

Table 2. The Values of $\tau_{phosph.}$ and δ of 3-Methylacetylamino-(V), 4-Methylacetylamino-(VI), 3-Hydroxy-(VII), 4-Hydroxy-(VIII), 3-Amino-6-nitro-(IX), 3-Dimethylamino-6-Methylacetylamino-(X), 3-Dimethylamino-6-Acetylamino-(XI), and 3-Dipheylamino-(XII), N-methylphthalimides, Anthranilic acid (XIII), p-Dimethyl-aminobenzoic acid (XIV), α-Naphthol (XV), β-Naphthol (XVI), and β-Naphthylamine (XVII) in Various Solvents* at −196°

Compound No.	Solvent No.	$\tau_{phos.}$	δ	Compound No.	Solvent No.	$\tau_{phos.}$	δ	Compound No.	Solvent No.	$\tau_{phos.}$	δ
V	3	0.35	—	VIII	5	1.1	0.1	XIII	8	1.50	0.21
	5	0.35	—		8	1.1	0.05		9	1.35	0.13
	8	0.55	—		12	0.7	0.08		12	0.50	0.39
	9	0.50	—		17	0.45	0.005		17	0.45	0.01
	12	0.30	—	IX	3	0.14	0.45		18	0.855	0.02
	13	0.15	—		5	0.11	3.3				
					8	0.10	—				
					12	0.12	0.27	XIV	8	0.30	—
VI	5	0.55	—	X	6	0.45	—		12	0.30	0.82
	8	0.70	—		8	0.45	0.08				
	9	0.55	—					XV	8	1.15	—
	12	0.50	—	XI	6	0.2	2.7		12	1.0	—
					12	0.35	3.7	XVI	8	1.45	0.06
VII	8	0.80	0.25						12	0.90	0.13
	12	0.55	7.3	XII	8	0.07	0.13				
	13	0.62	0.03		12	0.06	0.06	XVII	8	1.4	0.06
	19	0.15	0.045		17	0.10	—		12	1.2	0.84

*The key to the numbering of the solvents is given in the footnote to Table 1.

$\tau_{phosph.}$ and δ is obtained in the cases of compounds I-III in the same solvents. The lack of correspondence between the variations in δ and $\tau_{phosph.}$ is also evident from the results obtained for the other compounds investigated. A particularly striking case is that of compound V (Table 2) whose $\tau_{phosph.}$ decreases slightly in going from carbon tetrachloride to chloroform, while δ increases by more than 200 times.

The observed variation in δ as opposed to the constancy of $\tau_{phosph.}$, is most naturally explained by assuming that the variation in the δ in the above-mentioned solvents (1-8), is mainly determined by the variation in r. At the same time, the solvent does not influence the probability of deactivation of the metastable state. The fact that the $\tau_{phosph.}$ of the compounds investigated in the solvents (1-8) have maximal values indicates that the quenching of the metastable state is either absent or very weak.

In some of the other solvents used (11-18), the $\tau_{phosph.}$ are smaller than in solvents 1-8 and vary over a much wider interval. Apparently, this decrease in the magnitude of $\tau_{phosph.}$ is due to an increase in q_3. At the same time, the magnitude of δ in solvents 11-18, is, as a rule, smaller than in solvents 1-8. One could think that the lowering of the magnitude of δ in these cases is due mainly to quenching of the metastable state. However, it can be seen from Tables 1 and 2 that the decrease in $\tau_{phosph.}$ in solvents 11-18 relative to the maximal values is considerably smaller than the corresponding decrease in δ (for example, the δ of IV in solvents 17 and 18 is approximately 10 times smaller than in solvent 8, while the $\tau_{phosph.}$ is only 2 times smaller). Thus, it can be considered that even in solvents where the $\tau_{phosph.}$ is smaller than the maximal value it is the variation in r which determines the variation in δ and not the appearance of quenching of the metastable state. Let us note that we specifically omit from the present discussion any consideration of the results obtained for halogen-containing and certain aromatic solvents[9,10,21] which act in a specific manner on the probability of intercombinational transitions.[9,15-19]

Comparison of the $\tau_{phosph.}$ obtained with the magnitudes of the absolute luminescence yields of similar compounds also leads to the conclusion that the variation in the fraction of the total emitted radiation due to phosphorescence is mainly determined by the variation in r. As an example, let us compare the results obtained for 4-acetylamino-N-methylphthalimide (II) and 4-acetylamino-N-phenylphthalimide (XVIII). In methyl alcohol, these compounds have equal phosphorescence lifetimes $\tau_{phosph.}$ = 1.1 sec. At the same time, the total yield of luminescence ($\eta_{tot.\ emit.\ rad.}$) at −196° is 0.75 for compound (II) and 0.06 for compound (XVIII). There is also a large difference in δ values: for compound (II) δ = 0.12 and for compound (XVIII) δ = 1.0. Let us assume that the differences in δ and in $\eta_{tot.\ emit.\ rad.}$ of the two compounds is entirely due to the difference in the quenching of their metastable states. The deactivation of the excited state can be represented in the following manner (in percent of the total number of excited molecules):

$$\text{II}\quad S' \to S^0 - 68\%;\ S' \longrightarrow T - 32\%;$$

$$T \to S^0 - 7\%;\ T \longrightarrow S^0 - 25\%;$$

$$\text{XVIII}\quad S' \to S^0 - 3\%;\ S' \longrightarrow T - 97\%;$$

$$T \to S^0 - 3\%;\ T \longrightarrow S^0 - 94\%.$$

Here S^0 is the ground state, S′ are the excited singlet states, and T is the triplet state of the molecule

The following probabilities of deactivation of the metastable state were calculated: for (II) $q_3 = 0.59\ sec^{-1}$, $\pi = 0.185\ sec^{-1}$ and for (XVIII), $q_3 = 0.75\ sec^{-1}$, $\pi = 0.025\ sec^{-1}$. Thus, the natural lifetime of the metastable state $\tau^{nat.}_{phosph.} = 1/\pi$ must be very different for the two compounds so similar in their structure: for (II) $\tau^{nat.}_{phosph.} = 5.4$ sec and for (XVIII) $\tau^{nat.}_{phosph.} = 40$ sec. Such a divergence between the $\tau^{nat.}_{phosph.}$ values seems very improbable in view of the fact that the $\tau_{phosph.}$ of the two related compounds are equal. Much more natural seems to be the assumption that the proximity of the $\tau_{phosph.}$ values is determined by the small difference between the π and q_3 of different luminescent compounds. In the case of compounds whose $\eta_{tot.\ emit.\ rad.}$ and δ are very different, this assumption leads to the conclusion that quenching of T at −196° is either absent or very improbable.

Thus, the results of our investigation show that at −196°, quenching of the metastable state T is either absent or too small to affect δ substantially in the majority of the compounds investigated, in the solvents where the $\tau_{phosph.}$ have their maximal values and are almost all equal. Consequently, in this series of solvents, the variation occurring in going from one solvent to another reflects rather accurately the variation in r. Let us note in particular that ethyl alcohol is included in the series of solvents in which, at −196°, the majority of the compounds investigated exhibit absence of quenching of T. Sveshnikov noted this fact[3,20] based on the results in refs. 20 and 21. Hence, the use of ethyl alcohol as a solvent in the investigation of deactivation of the excited state at −196° possesses, in the majority of cases, the advantage of being able to neglect the quenching of the metastable state. The variation in r also determines the variation in δ even in solvents in which, judging from the lower values of $\tau_{phosph.}$, quenching of T does take place.

Thus, it can be concluded that in the majority of compounds in a wide selection of solvents, the variation in δ accurately reflects the variation in the transition probability to the metastable state caused by change in solvent.

REFERENCES

1. D. C. McClure, J. Chem. Phys. 17, 905 (1949).
2. P. Juster and S. I. Weissman, J. Chem. Phys. 17, 1183 (1949).
3. B. Ya. Sveshnikov, Dokt. Diss. Gosudarst. Opt. Inst.-Fiz. Inst. Akad. Nauk SSSR, 1951.
4. P. P. Dikun, Kand. Diss. Gosudarst. Opt. Inst., 1952.
5. E. H. Gilmore, G. E. Gibson, and D. S. McClure, J. Chem. Phys. 20, 829 (1952).
6. B. S. Neporent and A. I. Inyushin, Doklady Akad. Nauk SSSR 98, 197 (1954).
7. V. V. Zelinskii and V. P. Kolobkov, Doklady Akad. Nauk SSSR 101, 241 (1955).
8. V. V. Zelinskii, N. P. Emets, V. P. Kolobkov, and L. G. Pikulik, Izvest. Akad. Nauk SSSR, Ser. Fiz. 20, 507 (1956).
9. E. C. Clementy and M. Kasha, J. Chem. Phys. 26, 856 (1957).
10. V. V. Zelinskii and V. P. Kolobkov, Doklady Akad. Nauk SSSR 119, 922 (1958).
11. L. E. Golikova, V. V. Zelinskii, and V. P. Kolobkov, Opt. i Spektr. 5, 480 (1958).
12. V. V. Zelinskii, V. P. Kolobkov, and I. I. Reznikova, Izvest. Akad. Nauk SSSR, Ser. Fiz. 23, 1269 (1959).
13. V. L. Ermolaev and K. K. Svitashev, Opt. i Spektr. 7, 664 (1959), Optics and Spectroscopy 7, 399 (1959).
14. V. A. Pilipovich and B. Ya. Sveshnikov, Opt. i Spektr. 4, 116 (1958).
15. B. B. Zelinskii, V. P. Kolobnikov, and N. D. Krasnitskaya, Opt. i Spektr. 6, 417 (1959), Optics and Spectroscopy, 6, 261 (1959).

16. O. Padhye, O. McClyun, and M. Kasha, J. Chem. Phys. 24, 588 (1956).
17. V. V. Zelinskii and V. P. Kolobkov, Opt. i Spektr. 1, 560 (1956).
18. V. V. Zelinskii, V. P. Kolobkov, and N. A. Kondaraki, Doklady Akad. Nauk SSSR 117, 391 (1958).
19. V. A. Borgman, I. A. Zhmyreva, V. V. Zelinskii, and V. P. Kolobkov, Doklady Akad. Nauk SSSR 131, 781 (1960).
20. B. Ya. Sveshnikov and A. A. Petrov, Doklady Akad. Nauk SSSR 71, 461 (1950).
21. O. G. Zinov'eva, Doklady Akad. Nauk SSSR 68, 265 (1949).

INFLUENCE OF THE HYDROGEN BOND ON THE PROBABILITY OF INTERNAL CONVERSION TO THE TRIPLET LEVEL IN THE QUINOLINE MOLECULE

V. L. Ermolaev and I. P. Kotlyar

Received 28 December 1959

A solution of quinoline in a pure hydrocarbon solvent at 77°K shows only phosphorescence. Addition to the solution of small amounts of alcohol (~1%) leads to the appearance of fluorescence. These facts are ascribed to the influence of the hydrogen bond that is formed between the nitrogen atom of the quinoline and the hydrogen of the OH group of the alcohol on the probability of internal conversion of the quinoline molecule from the fluorescent to the phosphorescent state. A quantitative evaluation of the probability of internal conversion in quinoline has been carried out.

In ref. 1 the present authors and Svitashev showed that the ratio of the quantum yields of phosphorescence and fluorescence in a series of 1-substituted naphthalenes at 77°K is little changed on going from a nonpolar solvent (petroleum ether = p. e.) to a polar one (a mixture of ethyl alcohol and diethyl ether in 2:1 ratio by volume = al. + eth.).* Another possibility is found in the case of the heteroanalog of naphthalene—quinoline: a solution of quinoline in p. e. at 77°K only phosphoresces, but in al. + eth. fluorescence also appears in it. In ref. 1 we expressed the hypothesis that this effect is due to the presence of a hydrogen bond* between the nitrogen atom of the quinoline and the hydrogen of the OH group of the alcohol.* In the present communication we present new data confirming this hypothesis.

*Both solvents freeze at 77°K to a solid glass.

*The important role of the hydrogen bond in the phenomenon of fluorescence in organic compounds was indicated by Terenin in 1943.[2]

*Zelinskii and Kolobkov previously observed[3] great changes in the ratio of quantum yields of phosphorescence and fluorescence of organic molecules in different solvents at 77°K. These changes were associated by the authors of ref. 3 with a shift in the position of the fluorescence spectrum of the compounds considered in the solvent under investigation. In our case the phosphorescence and absorption spectra of quinoline did not change position within the limits of error of the measurements on going from p. e. to al. + eth.

The apparatus and the methods of measuring the luminescence spectra and the ratios of the quantum yields of phosphorescence and fluorescence used in this investigation were the same as those described in ref. 1. The fluorescence spectra were measured in a third order monochromator with a diffraction grating, and the phosphorescence in a second order one. The absorption spectra at 293°K were measured by means of an SF-4 spectrophotometer, and at 77°K by means of our spectrometric apparatus. The quinoline was purified by distillation in air and under vacuum, the p. e. was freed of contamination with unsaturated compounds by shaking it with highly concentrated sulfuric acid and subsequently washing it with sulfuric acid and water. Before use, the p. e. was distilled in a column over metallic sodium and the fraction boiling at 60-70°C was collected (lighter fractions did not freeze at 77°K). All the other solvents used were carefully dried and distilled in a column. The concentration of quinoline in the solution used for measurement of the luminescence was approximately 2×10^{-4} mole/liter. Excitation was accomplished through the monochromator by the light of the 3030 A mercury line. The time required for quenching the phosphorescence was measured in an apparatus with a loop oscillograph described by Sveshnikov and Pilipovich.[4]**

**The authors are deeply thankful to B. Ya. Sveshnikov and V. A. Pilipovich, who kindly permitted us to make our measurements on their apparatus.

The phosphorescence spectra of quinoline in p. e. and in al. + eth. are very similar to the spectra of naphthalene, but are shifted to higher frequencies by 600 cm^{-1}

Luminescence of Quinoline in Solutions at 77°K

Solvent	$\nu_{absorp.}$ (cm^{-1})	$\nu_{fluor.}$ (cm^{-1})	$\nu_{phosph.}$ (cm^{-1})	fl. (absol.)	$\eta_{phosph.}$ (absol.)	$\frac{\eta_{fl.}}{\eta_{phosph.}}$	$\frac{1}{\tau}$ $^1\pi\pi^* \rightarrow s$ (sec^{-1})	$^1\pi\pi^* \rightarrow {}^3\pi$ (sec^{-1})	$\tau_{phosph.}$ (sec)
p. e.	33000**	—	21875	—	—	<0.005	$4.5 \cdot 10^7$	$> 9 \cdot 10^9$	1.13 ± 0.06
p. e. + 1% Isopropyl alcohol	32000	31950	21875	~0.10	~0.19	0.55 ± 0.04	$6.6 \cdot 10^7$	$(1.2-6) \cdot 10^9$	1.34 ± 0.02
Isopropyl alcohol (absol.)	32000	31950	21875	~0.11	~0.19	0.60 ± 0.03	$6.6 \cdot 10^7$	$(1.1-5.4) \cdot 10^9$	1.36 ± 0.04
al.+ eth.	32000	31950	21850	0.10 ± 0.01	0.19 ± 0.02	0.53 ± 0.02	—	—	—

**The accuracy of measurement of the position of the first band of absorption and luminescence was ±25 cm^{-1}.

(see Table). The fluorescence spectrum of quinoline is very close in its structure to the spectra of the 1-substituted naphthalenes, since in naphthalene the electron shift corresponding to the fluorescence emission is forbidden. The O′–O″ shift is allowed in quinoline and in the 1-substituted naphthalenes (methyl-, hydroxy-, and halogenonaphthalenes). The fluorescence spectrum of quinoline is also shifted to higher frequencies in comparison with the fluorescence spectrum of naphthalene, but only by 175 cm^{-1}. The distribution of the quantum intensity in the fluorescence (I) and phosphorescence (II) spectra of quinoline in al. + eth. and in the phosphorescence spectrum of quinoline in p. e. (III) at 77°K is shown in Fig. 1. It can be seen from the figure that the phosphorescence spectrum has a more clearly developed structure in p. e. than in al. + eth.

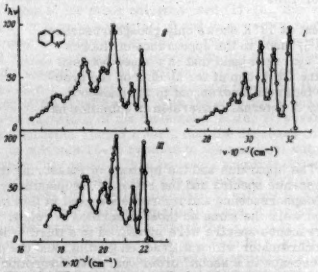

Fig. 1. Fluorescence and phosphorescence spectra of quinoline in solutions at 77°K. Curve I—fluorescence in al. + eth.; curve II—phosphorescence in al. + eth.; curve III—phosphorescence in p. e. On the ordinate axis are values proportional to the spectral quantum intensity; excitation by 3030 A line; concentration of quinoline ~2×10^{-4} mole/liter.

In order to ascertain the reasons for the change in the ratio of the quantum yields of fluorescence and phosphorescence of the quinoline molecule on going from a nonpolar solvent to a polar one, we investigated the luminescence of quinoline in p. e. in the presence of small added amounts of polar molecules. It was shown that the addition to the p. e. of such polar molecules as pyridine, diethyl ether, diethylamine, and formamide in 1-2% concentration did not result in any appreciable change in the structure and intensity of the phosphorescence spectrum of quinoline. No luminescence appeared in the ultraviolet part of the spectrum in this process. Quinoline in pure, dry diethyl ether also showed only phosphorescence. However, if small amounts of the order of 1-2% or less) of dry aliphatic alcohols (methyl, ethyl, isopropyl, or isoamyl) were added to a solution of quinoline in p. e., then the phosphorescence was immediately quenched, and a quinoline fluorescence appeared in the ultraviolet region of the spectrum. To obtain the maximum yield of quinoline fluorescence in pure alcohol, it was sufficient to add 1-2% of alcohol to p. e. The phosphorescence spectrum of quinoline in p. e. + 1% of alcohol was somewhat diffuse and became identical with the spectrum in al. + eth. (see Fig. 1, curve II).

The relation of the ratio of the quantum yields of fluorescence and phosphorescence of quinoline in p. e.

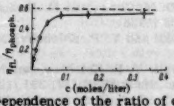

Fig. 2. Dependence of the ratio of quantum yields of fluorescence and phosphorescence of quinoline in p. e. at 77°K on concentration of isopropyl alcohol. Vertical lines through experimental points indicate the uncertainty of experimental values; excitation by 3030 A line; quinoline concentration 2×10^{-4} mole/liter.

to the concentration of isopropyl alcohol was determined. In this process it was established that the ratio of the yields increased rapidly for small concentrations of alcohol, but quickly reached saturation (Fig. 2). The behavior of the curve for the dependence of the ratios of the quantum yields on the concentration shown in Fig. 2 seems to indicate the formation of complexes between the molecules of the alcohol and the quinoline

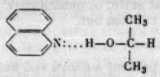

A study of the form of the curve for the ratios of the quantum yields of fluorescence and phosphorescence as functions of the concentration of isopropyl alcohol does not permit answering the question of how many molecules of isopropyl alcohol are bound in the complex with the quinoline molecule.

If instead of isopropyl alcohol, compounds that are stronger proton donors (ethyl and methyl alcohol, water, acetic acid) are added to p. e., then along with the appearance of the characteristic bands of the ultraviolet fluorescence of quinoline there appears the violet-blue luminescence of the quinolinium ion $C_9H_8N^+$, which has a diffuse spectrum. The addition of small amounts of phenol completely quenches any quinoline luminescence. The latter phenomenon can be explained from the point of view of the concepts of the interaction of the π-electron systems of the two different molecules through the hydrogen bond, which were developed in a series of publications by Mataga and his co-workers.[5]

Let us note that in solid solutions of quinoline in p. e. at 77°K in the presence of 0.5-2% of methyl or ethyl alcohol (higher concentrations of these alcohols precipitate out in the process of freezing the p. e.) during exposure to light of λ 3030 A a photochemical reaction takes place, which is manifested in a decrease in intensity of the fluorescence and phosphorescence characteristic of quinoline. At the same time, the violet-blue luminescence of the quinoline ion appears in the solution; i.e., apparently the photochemical transfer of a proton from the alcohol to the quinoline molecule occurs.* Two facts attract attention: first, the photochemical reaction develops at higher concentrations of alcohol (~1-2%) than the fluorescence (~0.25-0.5%), and secondly, the photochemical reaction scarcely takes place in pure, dry ethanol. The explanation of this probably should be sought in the formation in p. e. of dimers (or higher aggregates) of molecules of the alcohols mentioned at concentrations of 1-2%. Such dimers should have stronger proton-donor

*Photochemical transfer of a proton under the influence of light has been observed for other systems previously by Terenin, Karyakin, and Shablya.[6]

properties. The existence of such dimers of ethyl alcohol at 293°K has been suggested on the basis of data for the infrared spectra in the work of Becker.[7] The transfer of a proton is caused by an intensification of the basic properties of nitrogen heterocycles in the fluorescent state, as shown for acridine in Waller's work.[8] Thus, it is logical to assume the presence in the solution of the following photochemical reaction:

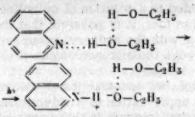

The reverse dark reaction was hindered, probably, because of the low temperature of the experiment. Quinoline in p. e. does not react photochemically with added isopropyl alcohol, although the molecules of the latter form a hydrogen bond with the nitrogen of the ring and in this way promote the appearance of the ultraviolet fluorescence of quinoline. In this connection it is possible that the formation of dimers in isopropyl alcohol is hindered sterically. Therefore, in order to ascertain more clearly the effect of the hydrogen bond on the probability of internal conversion to the triplet state in quinoline, uncomplicated by photochemical reactions, we just investigated the effect of additions of isopropyl alcohol.

The value of the ratio of the quantum yields of fluorescence and phosphorescence in the molecule is determined by the ratio of the probability of the emission of fluorescence to the probability of conversion to the triplet state. The minimum and maximum values of the latter can be estimated by measuring the absolute quantum yields of fluorescence and phosphorescence of the molecule at a low temperature. First of all we attempted to estimate the probability of emission of fluorescence and the effect on it of the hydrogen bond by determining the absorption integral in the first electron band of quinoline. Since it is difficult to distinguish the contour of the band related to the electron transfer to the first singlet excitation level, because of the superposition of the second electron band, we used the following method. Assuming the presence of approximate mirror symmetry of the first electronic band of the absorption spectrum with the fluorescence spectrum, it was possible, by comparing the intensities of the O—O vibration bands in the fluorescence and absorption spectra, to estimate the value of the absorption integral over the area of the fluorescence spectrum thus standardized. To determine $1/\tau_s$ we used the formula for the absorption integral proposed by Förster:[9]

$$\frac{1}{\tau_s} = 2.88 \cdot 10^{-9} n^2 \int_0^{\infty} \frac{(2\nu_0 - \nu)^2}{\nu} \varepsilon(\nu)\, d\nu, \qquad (1)$$

assuming that $\nu = \nu_0 + \nu_\nu$ for absorption and $\nu = \nu_0 - \nu_\nu$ for fluorescence, where ν_0 is the frequency of the purely electronic transfer, which almost coincides with the position of the maximum of the first band of the absorption and fluorescence spectra of quinoline, and ν_ν is the vibration frequency superimposed on the electronic frequency. Further, employing the relationship between the absorption spectra and the fluorescence spectra[9]

$$\frac{\varepsilon(\nu_0 + \nu_\nu)}{\nu_0 + \nu_\nu} = \text{const} \cdot \frac{I_{h\nu}(\nu_0 - \nu_\nu)}{(\nu_0 + \nu_\nu)^3},$$

and setting $I_{h\nu}(\nu_0) = \varepsilon(\nu_0)$, as we do in practice, we obtain const. $= \nu_0^2$. Substitution in (1), we obtain the formula

$$\frac{1}{\tau_s} = 2.88 \cdot 10^{-9} n^2 \nu_0^2 \int_{-\infty}^{\infty} I_{h\nu}(\nu_0 - \nu_\nu)\, d\nu_\nu,$$

which we also used. This method permits evaluation of the natural lifetime of the fluorescent state for aromatic compounds, where their long wavelength absorption band is formed by the superposition of transitions to two or more electronic levels, which makes it impossible to distinguish the contour of the band resulting from the excitation of the molecule to a lower electronic excitation state. For the employment of the method that we used it was necessary that the vibration frequencies appearing in the absorption spectrum be distinctly different from the frequencies observed in the fluorescence spectrum. The results of such an evaluation are given in the table (eighth column).

A study of the absorption spectra showed that the intensity of the first absorption band of quinoline increased when small amounts of alcohol were added to the p. e., as can be seen in Fig. 3. The latter fact is in agreement with observations made by Mataga and Tsuno.[5] The data given in the eighth column of the table indicate a magnitude of the probability of an electronic transition corresponding to the fluorescent luminescence of the quinoline molecule approximately 1.5 times as great when 1% of isopropyl alcohol was added to the p. e. (77°K). However, this change in the probability of an emission transition corresponding to fluorescence cannot explain the change of more than a hundredfold in the magnitude of the ratio of the quantum yields of fluorescence and phosphorescence of quinoline that took place upon the addition of alcohol to the p. e. (see the seventh column of the table). It therefore must be assumed that the hydrogen bond also strongly influences the probability of internal conversion of the quinoline molecule from the fluorescent to the triplet state.

Knowing the frequency of the emission transition from the fluorescent state to the ground state, and the absolute quantum yields of fluorescence and phosphorescence of quinoline, we can also determine the probability of internal conversion to the triplet state (r_{S^*-T}). Assuming the absence of quenching in the triplet state, we obtain the minimum value for r_{S^*-T}, but considering, on the other hand, that all quenching takes place in the phosphorescent state, we obtain the maximum value for r_{S^*-T} The values mentioned are given in the next to last column

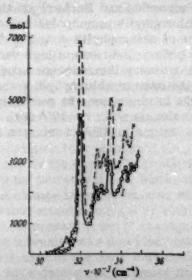

Fig. 3. Absorption spectra of quinoline in solutions at 77°K. Curve I—in p. e.; curve II—in p. e. + 1% isopropyl alcohol. On ordinate axis: molar absorption coefficients; concentration of quinoline 5×10^{-3} mole/liter.

of the table. From a comparison of the values of r_{S^*-T} in p. e. and in p. e. + 1% alcohol, it can be seen how greatly the probability of internal conversion of the quinoline molecule to the triplet state decreases if the nitrogen atom of the molecule enters into a hydrogen bond. At the same time, the value of τ for the phosphorescence of quinoline is little changed in this transfer (last column of table).

Comparison of r_{S^*-T} for quinoline with the values of the probability of internal conversion for the simplest naphthalene derivatives previously obtained by us[1] indicates the essential role that the unbound electrons of the nitrogen atom (p-electrons) must play in the spin-orbital interaction in the fluorescent state of quinoline. The participation of these electrons in the hydrogen bond decreases their effect on the π-cloud of the molecule, and in particular in the fluorescent state. The small change in τ for the phosphorescence of quinoline in comparison with naphthalene[1] and the weak influence of the hydrogen bond on τ for the phosphorescence of quinoline indicate the smaller reaction of the p- and π-electrons of quinoline in the lower triplet state in comparison with the fluorescent state.

Different points of view have previously been expressed in a monograph by Förster[9] and in a book by Bowen and Wokes[10] on the reason for the small yield (or complete absence) of fluorescence in pyridine, quinoline, acridine, and phenazine in contrast to their hydrocarbon analogs (benzene, naphthalene, and anthracene). Förster interpreted this phenomenon in the case of pyridine as predissociation of the C—N bond and the quenching associated with this. Bowen and Wokes[10] in their turn suggested that this effect was due to the strengthening of the spin-orbital bond in heteroatoms, although they did not present any experimental evidence confirming this point of view. Mataga[5] ascribed the small yield of fluorescence of the heterocycles to quenching due to the reaction of the p- and π-electrons, but he did not agree with Bowen and Wokes that this reaction caused a transition to the triplet state. Our experiments permit resolution of the question (at least in the case of quinoline) in favor of an explanation of the quenching of fluorescence in nitrogen heterocycles as a result of the strengthening of the spin-orbital interaction due to the effect of the unbound electrons of the nitrogen atom in the fluorescent state.

It is also interesting to compare the results obtained in our investigation with the data that appeared in a recent article by Fernandez and Becker[11] on the unusual luminescence of chlorophylls in nonpolar solvents at 77°K. The luminescence of chlorophylls a and b dissolved in 3-methylpentane under conditions of high vacuum differ sharply from the ordinary fluorescence spectrum in polar solvents. In the case of chlorophyll a the authors of ref. 11 ascribe the luminescence to $p\text{-}\pi^*$ triplet-singlet emission in the molecule with $\tau \sim 10^{-3}$ sec. At the same time, in frozen solutions in EPA (a mixture of ether, isopentane, and alcohol in the ratio 5:5:2) it was not possible to observe any afterglow from chlorophyll a.[12,13] It is characteristic that the phosphorescence spectrum of chlorophyll a completely disappears, but the normal fluorescence spectrum appears when alcohol is added in 0.1-0.2% concentration to the hydrocarbon solvent. A similar redistribution of the intensity of phosphorescence and fluorescence is observed in our case when 0.1-0.5% of alcohol is added to a solution of quinoline in p. e. Proceeding from this fact, it is possible that the interaction of chlorophyll a with the hydroxyl groups of the alcohol takes place through the nitrogen atoms present in the frame of the molecule.

In conclusion, we consider it our pleasant duty to express our deep appreciation to Academician A. N. Terenin for his constant interest in this research.

REFERENCES

1. V. L. Ermolaev and K. K. Svitashev, Opt. i Spektr. 7, 664 (1959), Optics and Spectroscopy 7, 399 (1960); V. L. Ermolaev, I. P. Kotlyar, and K. K. Svitashev, Izvest. Akad. Nauk SSSR, Ser. Fiz. 24, 492 (1960).
2. A. N. Terenin, Acta Phys. Chim. 18, 210 (1943); Zhur. Fiz. Khim. 18, 1 (1944).
3. V. V. Zelinskii and V. P. Kolobkov, Doklady Akad. Nauk SSSR 119, 922 (1958); V. V. Zelinskii, V. P. Kolobkov, and I. I. Reznikova, ibid. 121, 315 (1958); L. E. Golikova, V. V. Zelinskii, and V. P. Kolobkov, Opt. i Spektr. 5, 480 (1958).
4. V. A. Pilipovich and B. Ya. Sveshnikov, Opt. i Spektr. 4, 116 (1958).
5. N. Mataga and Sh. Tsuno, Bull. Chem. Soc. Japan 30, 368 (1957); N. Mataga, Ibid. 31, 459, 487 (1958).
6. A. N. Terenin and A. V. Karyakin, Doklady Akad. Nauk SSSR 58, 425 (1947); A. V. Shablya and A. N. Terenin, Doklad na VIII soveshch. po lyuminests (Report on Eighth Conference on Luminescence), Minsk, October 1959.
7. R. S. Becker, J. Mol. Spectroscopy 3, 1 (1959).
8. A. Weller, Z. Elektrochem. 61, 956 (1957).
9. Th. Förster, Fluorescenz organischer Verbindungen, Göttingen, 1951.
10. E. J. Bowen and F. Wokes, "Fluorescence of Solution(s)." London-New York, 1953.
11. J. Fernandez and R. S. Becker, J. Chem. Phys. 31, 467 (1959).
12. A. N. Terenin, Doklad na II Bsesoyuzn. konf. po fotosintezu (Report on Second All-Union Conference on Photosynthesis), Moscow, January 1957.
13. R. S. Becker and M. Kasha, J. Am. Chem. Soc. 77, 3669 (1955).

AN ELECTRON PARAMAGNETIC RESONANCE INVESTIGATION OF THE VALENCE CHANGE OF THE ACTIVATOR DURING EXCITATION OF THE PHOSPHOR SrS-Eu,Sm*

*Preliminary report in Ref. 1.

V. G. Dubinin and Z. A. Trapeznikova

Received 14 January 1960

Upon photoexcitation of the phosphor SrS-Eu,Sm in the absorption band of Eu^{++}, a decrease in the paramagnetic resonance absorption of the Eu^{++} is detected. It is concluded that upon excitation of the phosphor SrS-Eu,Sm ionization of the activator from Eu^{++} to Eu^{+++} takes place.

One of the unresolved questions of luminescence is that of direct ionization of the activator on excitation of the phosphor, with subsequent deionization during natural or externally produced quenching. To solve this question, it is obviously necessary, first of all, to know the valence state of the given activator in the crystal phosphor.

Attempts to determine the valency of the activator by chemical means do not give reliable results, since the activator is usually present in very small amounts, namely 10^{-5} to 10^{-3} gram atoms per mole of the host substance. Study of the luminescence spectra of crystalline phosphors likewise does not always yield information about the valency of the activator.

In recent years, the analysis of paramagnetic resonance absorption spectra, due to the presence of the activator in the crystalline phosphor, has been applied to the determination of the valence of the activator.[2-6] (The paramagnetic resonance absorption spectrum is characteristic for an ion in a given valence state.)

If the activator is ionized when a phosphor is excited, then the quantity of ions producing a given paramagnetic absorption spectrum decreases, so that one should observe a decrease in the intensity of the paramagnetic absorption line of the activator. However, the decrease in line intensity caused by a change in the valence state of some of the activator ions during excitation of the phosphor does not of itself give direct evidence for ionization of the activator. A change in valence can also be produced by deionization of the activator ion, if the latter traps an electron produced as a result of the absorption of light by the crystalline phosphor. Evidence for ionization of the activator is given when the activator thereby makes a transition to a valence state that possesses paramagnetic absorption. On the other hand, if the activator has paramagnetic absorption in its initial state, then the ionization of the activator during excitation of the phosphor can be considered to be proven by a decrease in the intensity of the paramagnetic absorption line when the phosphor is excited by light in the region of the fundamental absorption of the activator, in which case the accumulation of the light sum by the phosphor is dependent on the introduction of a second activator.

In order to be able to observe the appearance of paramagnetic absorption in the activator, or the decrease in its line intensity when the phosphor is excited, it is necessary to have samples which will store large light sums during excitation. It is well known that phosphors of strontium sulfide activated by cerium and samarium, or by europium and samarium, can store large light sums during irradiation. The properties of such phosphors are described in numerous papers, in which it is shown, in particular, that cerium and samarium exist in the trivalent state in strontium sulfide and europium in the divalent state.

Divalent europium has a paramagnetic resonance absorption spectrum at room temperature, since the ground state of Eu^{2+} is $^8S_{7/2}$. As is well known, S-state ions are but weakly affected by the internal electrical field of the crystal, thus leading to long relaxation times and allowing the observation of paramagnetic resonance even at room temperature. The paramagnetic resonance absorption spectra of Ce^{3+} and Sm^{3+} can be seen only at low temperatures.

In order to investigate the ionization of activators during excitation, we chose the phosphor SrS-Eu,Sm, which, as was indicated above, has a paramagnetic resonance absorption spectrum (Eu^{++}) at room temperature and is excited by light in the Eu^{++} absorption band.

As has been shown,[2-6] the paramagnetic resonance spectrum of Eu^{++} in SrS consists of twelve lines. These lines belong to the single electronic transition $M = \frac{1}{2} \rightarrow -\frac{1}{2}$, which is split into twelve hyperfine structure components by the interaction of the nuclear spins of the two stable isotopes of Eu with the electronic spin. On excitation of the phosphor, one should observe only a decrease in the intensity of the spectral lines of Eu^{2+} (if the excitation leads to an ionization of the Eu^{2+}), since the Eu^{3+} formed in this process does not have a paramagnetic resonance spectrum, its ground state being the nonmagnetic state $^7F_0$.

Attempts have been made[4-6] to detect a change in the paramagnetic absorption of Eu^{2+} in crystals of the phosphor SrS-Eu,Sm during excitation; however, well-defined results have not been obtained.

The fact that activator ionization was not detected in refs. 5 and 6, was felt by the authors to be due to the smallness of the light sums stored by their phosphors. In connection with this, it should be noted that their method of measuring the line intensity in the absorption spectrum of Eu^{2+} could not have provided sufficient accuracy. (The intensity was measured by the magnitude of the signal-to-noise ratio, which does not remain constant and is a function of spectrometer adjustment.)

In a later experiment,[4] the intensity of the Eu^{2+} absorption lines in excited and nonexcited phosphors was determined in relation to a standard; i.e., to the absorption line intensity of the diphenylpicrylhydrazyl radical. Such a relative measurement eliminates the error associated with a change in spectrometer adjustment and provides a measurement accurate to within 5 per cent. In this case, no decrease in the paramagnetic resonance absorption line intensity was detected, indicating that not more than 5 per cent of the Eu^{2+} ions could have changed their valence state during excitation of the phosphor. This result, however, is inconsistent with the >10 per cent change observed in the coefficient of the optical absorption caused by the presence of the activator when this substance was excited. The authors proposed that if one assumes that there are no systematic errors in the measurements, then it is possible that on excitation it is

not the activator ion that ionizes, but an ion of strontium sulfide which has been disturbed by the introduction of the activator.

The present investigation, which uses the same method of detecting the change in valency of Eu^{2+} (i.e., through the change in intensity of the paramagnetic absorption spectrum on excitation of the phosphor), was undertaken in order to arrive at a definite conclusion as to whether it is the activator itself or the luminescence center which ionizes in the phosphor. In order to obtain more reliable results, we increased the stability of the apparatus and also improved the conditions under which the crystalline phosphors were investigated.

EXPERIMENTAL PART

The measurements were carried out with the aid of a spectrometer of the type described previously,[7] in which the following modifications were introduced: (1) automatic stabilization of the klystron frequency on the natural frequency of the cavity was effected; (2) a cylindrical cavity of high Q was used in place of the rectangular cavity; (3) an IF amplifier of improved design was constructed, and its output was connected to a synchronous detector and a recorder. By virture of these changes, we realized at least a fifteenfold gain in the stability and sensitivity of the apparatus. Excitation of the phosphor was carried out in the cavity itself. The intensity of the Eu^{2+} paramagnetic absorption lines was determined relative to the intensity of the paramagnetic absorption line of Cu^{2+} in a monocrystal of $CuSO_4 \cdot 5H_2O$. It should be mentioned that the absorption line of Cu^{2+} did not overlap the absorption spectrum of Eu^{2+}, which was not the case with respect to the hydrazyl line in ref. 4; this also increased the accuracy of the measurement.

Fortunately, the Cu^{2+} line is wider and hence more stable than the narrow lines of hydrazyl and Eu^{2+}. In order to diminish the effects of fluctuations, we measured the intensities of six well-resolved lines in the Eu^{2+} spectrum. The measurement of the ratio of the intensity of the Eu^{2+} lines to the intensity of the reference line was accurate to within 1 per cent.

To obtain the absorption spectrum of Eu^{2+} in the nonexcited phosphor, the latter was given a preliminary de-excitation treatment. A quartz tube containing the phosphor was enclosed in an aluminum casing, placed in a muffle furnace, and heated to 400°C. After this temperature was reached, the heat was turned off and the sample cooled. It was then placed in the cavity in complete darkness. To avoid exposing the phosphor, the cavity was covered with a curtain. After adjustment of the spectrometer, numerous scans of the absorption spectrum of Eu^{2+} in the nonexcited phosphor were made.

The phosphor was excited directly in the cavity without disturbing the sample tube. For excitation we used a projection lamp provided with a filter made of a saturated solution of copper sulfate, which isolated the Eu^{2+} absorption band, and also served as a heat filter (in the excitation process the heating of the cavity did not exceed 1°).

To obtain the absorption spectrum of Eu^{2+} in the excited phosphor, the latter was first irradiated for 10 min to attain complete excitation. The spectrum was then observed during excitation. In both cases, the spectrum of Cu^{2+} was recorded simultaneously with that of Eu^{2+}. The monocrystal of $CuSO_4 \cdot 5H_2O$ was attached to the end of the cavity in a location corresponding to a maximum in the magnetic component. The intensities of six well-resolved lines of the Eu^{2+} paramagnetic resonance absorption spectrum in the de-excited and excited phosphor were determined relative to the intensity of the reference line. We then calculated the difference between the values of these ratios, which indicated the number of ionized Eu^{2+} ions. The value of this difference could be determined with an accuracy of 2 per cent.

RESULTS

The paramagnetic resonance absorption spectrum of Eu^{2+} was investigated in the following phosphors: SrS-Eu,Sm; SrS-Eu,Sm($CrCl_3$); SrS-Eu,Sm(LiF)(1); SrS-Eu,Sm(LiF)(2), both completely de-excited and excited in the absorption region of Eu^{2+}.

It was found that during excitation of these phosphors, the intensity of the Eu^{2+} paramagnetic resonance lines decreases: for SrS-Eu,Sm(LiF)(1), by 14 per cent; for SrS-Eu,Sm(LiF)(2), by 12 per cent; for SrS-Eu,Sm($SrCl_2$), by 16 per cent; and for SrS-Eu,Sm, by 16 per cent. Assuming that the decrease in the intensity of the Eu^{2+} paramagnetic resonance lines during photoexcitation is to a first approximation directly proportional to the decrease in the quantity of Eu^{2+} ions, it can be concluded that in these phosphors, under the given conditions of excitation (powdered phosphor in quartz tube placed in cavity), 12-16 per cent of the activator ions are ionized. It is interesting to note that Title[8] also observed an ionization of 13 per cent of the Eu^{2+} ions in the same type of phosphor, based on the change in paramagnetic absorption.

In parallel with this, we made measurements of the coefficient of diffuse reflection as a function of wavelength of the incident light for the three phosphors, SrS-Eu,Sm, SrS-Eu,Sm($SrCl_2$), and SrS-Eu,Sm(LiF)(2), both in the de-excited and the excited states. Similar measurements had been made earlier by Urbach[9] and Anikina.[10] The relative coefficient of absorption k was calculated from the well-known formula

$$k \sim \frac{(1-R)^2}{2R}$$

where R is the coefficient of diffuse reflection.

Curves showing the dependence of the relative absorption coefficient k on the wavelength of the incident light for the phosphors mentioned in the de-excited and excited states are shown in the Figure. As can be seen from the Figure, an absorption caused by the presence of Eu^{2+} occurs in the wavelength region 410-550 mμ. (In phosphors which do not contain Eu^{2+}, or in those containing Sm only, there is no absorption in this region of the

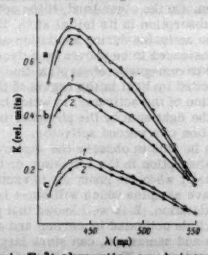

Change in Eu^{2+} absorption on photoexcitation of the phosphors: SrS-Eu,Sm(LiF)—a; SrS-Eu,Sm($SrCl_2$)—b; SrS-Eu,Sm—c. curves 1—unexcited phosphor; curves 2—excited phosphor. (The scales on the ordinate axis are different for a, b, and c.)

spectrum.) A comparison of the coefficients of absorption of the excited and nonexcited phosphors shows that on excitation a decrease in the intensity of absorption in the region 410-550 mμ is observed: for SrS-Eu,Sm, 13 per cent; for SrS-Eu,Sm($SrCl_2$), 12 per cent; and in the phosphor SrS-Eu,Sm(LiF)(2), 8 per cent. The decrease in absorption coefficient is obviously caused by the decrease in the quantity of nonionized centers during excitation of the phosphor.

This conclusion is easily seen to agree with the data obtained from paramagnetic resonance. It should also be taken into account that the measurements of absorption coefficient are carried out 20 min after excitation has been discontinued, whereas the change in paramagnetic absorption relates directly to the moment of excitation of the phosphor. Our measurements of the time dependence of the paramagnetic absorption after turning off the excitation showed that the number of ionized centers decreases by approximately one-fifth in the 30 min after excitation ceases.

The degree of ionization was also determined by measuring the absolute number of quanta emitted by the excited phosphor when it is illuminated by infrared light. In each recombination of an ionized center with an electron freed from a trapping level (in the absence of quenching), one quantum of light should be emitted. Hence, from the absolute number of quanta emitted by the excited phosphor under the influence of infrared light one can, on the one hand, determine the approximate number of ionized centers (lower limit). On the other hand, one can determine the approximate number of Eu^{2+} activator ions from the weight of the phosphor and the proportion of components. On the basis of results we have obtained for various phosphors, it has been found that some phosphors of the SrS-Eu,Sm type can emit 1.2×10^{16} quanta. At the same time these phosphors, in the quantities investigated, contained about 1.3×10^{17} activator ions, which indicates that on excitation of the phosphor some 10 per cent of the activator ions are ionized.

Thus, three independent methods have given concordant results, on the basis of which it can be stated that on excitation of crystalline phosphors of the SrS-Eu, Sm type, 12-16 per cent of the activator (europium) ions are ionized.

REFERENCES

1. V. V. Antonov-Romanovskii, V. G. Dubinin, A. M. Prokhorov, Z. A. Trapeznikova, and M. V. Fok, Zhur. Eksptl. i Teoret. Fiz. 37, 1466 (1959).
2. W. D. Hershberger and H. N. Leifer, Phys. Rev. 88, 714 (1952).
3. A. A. Manenkov and A. M. Prokhorov, Doklady Akad. Nauk SSSR 107, 402 (1956).
4. A. A. Manenkov, A. M. Prokhorov, Z. A. Trapeznikova, and M. V. Fok, Opt. i Spektr. 2, 470 (1957).
5. W. Low, Phys. Rev. 98, 426 (1955).
6. B. Bleaney and W. Low, Proc. Phys. Soc. (London) A68, 55 (1955).
7. A. A. Manenkov and A. M. Prokhorov, Radiotekh. i Elektron. 1, 469 (1956).
8. R. S. Title, Quantum Electronics-Resonance Phenomena Symposium, New York, 1959.
9. F. Urbach, H. Hemmendinger, and D. Pearlman, Preparation and Characteristics of Solid Luminescent Materials (Symposium), New York, 1948.
10. L. I. Anikina, Trudy Fiz. Inst. Akad. Nauk SSSR 7, 3 (1956).

THE KINETICS OF THE SHORT-LIVED PHOTOLUMINESCENCE OF SOME ACTIVATED ALKALI HALIDE CRYSTALS*

*Presented at the Conference on the Physics of Alkali Halide Crystals, Tartu, July, 1959.

I. K. Vitol and I. K. Plyavin'

Received 28 December 1959

This investigation considers the influence of the two lowest excited levels of the activator ions Ga^+, In^+, and Tl^+ on the kinetics of the short-lived photoluminescence of crystals of KI-Ga, KI-In, and KI-Tl. Good agreement is obtained between the calculated and experimental results, confirming the validity of the initial assumptions of the calculation and permitting the determination of certain of the parameters of the luminescence centers.

Investigations of the spectral characteristics[1-3] and the time-dependent behavior[4,5] of the photoluminescence of alkali halide crystals activated by mercurylike ions have shown conclusively that there are two closely spaced levels (corresponding to the $^3P_0$ and $^3P_1$ levels of the free mercurylike ions[2]) in the lower excited state of the activator which take part in the luminescence of the crystal. The quantities characterizing luminescence, including the decay time of photoluminescence and the temperature dependence of the decay time, are determined by the following factors: (1) the distribution of the excited ions between the two levels, which, according to the data of Lushchik,[1] is in thermal equilibrium; (2) the energy spacing between the levels; (3) the ratio of the emission transition probabilities.

As is well known,[2] the ratio of the emission transition probabilities from the $^3P_1$ and $^3P_0$ levels varies considerably among the mercurylike activators Tl, In, and Ga; the probability of transition from the $^3P_1$ level decreases with decreasing atomic number of the activator (which also occurs in the free ions[2]), while the probability of transition from the $^3P_0$ level increases (on account of the influence of the electrical field[2] of the crystalline lattice).

In order to study the kinetics of short-lived photoluminescence, we examined the effect of the ratio of the emission transition probabilities from the two excited levels on the time characteristics of photoluminescence. This was done by measuring the photoluminescence decay time as a function of temperature in a series of KI crystals activated by Ga, In, and Tl.

Before presenting the experimental results, let us

consider systems with two excited levels, taking account of all possible transitions from each level (i.e., emissive and radiationless transitions from the excited levels to the ground state and thermal transitions between the excited levels). According to a calculation by Stepanov,[6] the number of systems in each level, under conditions of thermal redistribution of the systems between the two excited levels, is given by the following approximate expressions* (excitation ceasing at the time t = 0):

*In expressions (1) and (2) the rapidly decaying components are neglected.

$$n_2 = \frac{n_0}{1+e^{-\frac{\varepsilon}{kT}}} e^{-\frac{t}{\tau}} \quad (1)$$

and

$$n_3 = \frac{n_0}{1+e^{\frac{\varepsilon}{kT}}} e^{-\frac{t}{\tau}}, \quad (2)$$

where

$$\tau = \frac{e^{-\frac{\varepsilon}{kT}}+1}{f_{21}+f_{31}e^{-\frac{\varepsilon}{kT}}+(p_2'+p_3')e^{-\frac{\varepsilon+U}{kT}}} \quad (3)$$

n_2 and n_3 are the numbers of systems in the lower and upper excited levels, respectively, n_0 is the total number of excited systems at t = 0, ε is the energy difference between the minima of the excited levels, and f_{21} and f_{31} are the emission transition probabilities from the lower and upper excited levels to the ground level, respectively. The quantity

$$(p_2'+p_3')e^{-\frac{\varepsilon+U}{kT}}$$

is the probability of radiationless transitions from both excited levels to the ground state, and U is the activation energy of a radiationless transition.

Knowing the number of excited systems in each level, it is easy to determine the intensity of luminescence from both levels I(t), the decay time of the emission τ, and the net quantum yield B:

$$I(t) = n_2 f_{21} + n_3 f_{31} = \frac{n_0\left(f_{21}+f_{31}e^{-\frac{\varepsilon}{kT}}\right)}{1+e^{-\frac{\varepsilon}{kT}}} e^{-\frac{t}{\tau}}, \quad (4)$$

$$B = \frac{f_{21}+f_{31}e^{-\frac{\varepsilon}{kT}}}{f_{21}+f_{31}e^{-\frac{\varepsilon}{kT}}+(p_2'+p_3')e^{-\frac{\varepsilon+U}{kT}}}. \quad (5)$$

From Eqs. (3) and (5) it follows that the time constant of the decay of luminescence is

$$\tau = B\frac{e^{-\frac{\varepsilon}{kT}}+1}{f_{21}+f_{31}e^{-\frac{\varepsilon}{kT}}}. \quad (6)$$

Let us compare the experimentally measured values of the decay constants of photoluminescence or photoscintillation* with the calculated ones, taking into account

*The experimental method is similar to that described in ref. 5.

that in our concrete case, the probabilities f_{21} and f_{31} correspond to the emission transition probabilities from the levels $^3P_0$ and $^3P_1$, and ε is the energy difference between the minima of the $^3P_0$ and $^3P_1$ levels in mercury-like activators.

Equation (4) indicates that the intensity of photoluminescence decays exponentially, which agrees fairly well with experiment. (For the entire series of alkali halide crystals activated by mercurylike ions, including KI-Ga, KI-In, and KI-Tl, the decay of photoluminescence appears to be exponential over an intensity range of thirty to fifty fold.[4])

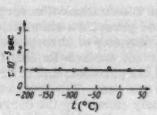

Fig. 1

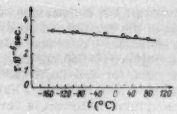

Fig. 2

Fig. 1. Temperature dependence of photoscintillation decay time of KI-Ga.
Fig. 2. Temperature dependence of photoscintillation decay time of KI-In.

We will now consider the dependence of the photoluminescence decay time on temperature. Between −160°C and +20°C, the photoluminescence decay time of the crystal KI-Ga is practically constant (Fig. 1), and for the crystal KI-In (Fig. 2), the change is insignificant. For these crystals, the areas under the long-wavelength activator absorption curves, corresponding to the transitions $^1S_0 \rightarrow {}^3P_0$ and $^1S_0 \rightarrow {}^3P_1$ in the free ions, are approximately the same.[2] From this it follows that the values of the probabilities f_{21} and f_{31} in Eq. (6) can also be considered equal. In this case, the equation for τ in the case of the activators Ga and In has the form

$$\tau = B\frac{1}{f_{21}} = B\frac{1}{f_{31}}. \quad (7)$$

Since temperature quenching is not observed in the temperature interval we are considering, for the crystals mentioned,[7] the value of B in Eq. (7) is a constant (we will take it equal to unity). The value of τ should therefore be independent of temperature, which obviously agrees with the experimental data. If Eq. (7) determines magnitude of the photoluminescent decay time in crystals activated by In and Ga, then the experimentally measured τ should be equal to the reciprocals of the transition probabilities for emission. There are no data on the absolute magnitudes of f_{21} and f_{31} which have been obtained independently of our method, so it is not possible to establish a quantitative agreement between the calculated and experimental values. However, the good agreement between the decay times of the resonant fluorescence from the $^3P_1$ levels in Cd and Zn (respectively 1×10^{-5} and 2.3×10^{-8} sec[8]) and the decay times of photoscintillation in crystals of KI-Ga and KI-In (respectively 1×10^{-5} and 3×10^{-8} sec) leads one to think that such agreement does indeed exist.

We turn now to a consideration of KI crystals activated by Tl. It is known that the time of decay of photoscintillation in crystals activated by Tl depends strongly on temperature in the region where there is no temperature quenching.[4,5,7] This indicates that in the case of Tl activation, the decay time of photoscintillation does not characterize the decay time of an emissive transition. We shall assume that Eq. (6) also approximates the photoscintillation in crystals activated by Tl (in particular, KI-Tl).

In order that the calculated dependence of the decay time of photoscintillation on temperature shall coincide with the experimental curves, it is necessary to assume that $f_{21} \ll f_{31}$.* Then

*This approximation is well substantiated. From absorption spectra it can be estimated that in crystals activated

by Tl, the transition $^1S_0 \rightarrow {}^3P_1$ is more probable than the transition $^1S_0 \rightarrow {}^3P_0$ by several orders of magnitude.

$$\tau = \frac{B}{f_{31}}\left(e^{\frac{\varepsilon}{kT}} + 1\right) \quad (8)$$

or

$$\ln \tau = \ln \frac{B}{f_{31}} + \ln\left(e^{\frac{\varepsilon}{kT}} + 1\right). \quad (9)$$

For numerical agreement of the calculated and experimental data in the case of the KI-Tl crystal, ε in Eq. (9) should be 0.03 ev, and $\ln(1/f_{31}) = -16.54$. Under these conditions, the experimental points lie on the calculated curve over a wide range of temperatures (Fig. 3). It thus follows that the decay time of the emissive transition $1/f_{31} \approx 6 \times 10^{-8}$ sec. The time of decay of emission from the $^3P_1$ level for KI-Tl was determined by another method by Kravets's formula. The result obtained in this manner (2×10^{-8} sec) agrees in order of magnitude with the values presented above.* In ref. 5, along with the mechanism of photoluminescence considered in the present investigation, another mechanism was proposed, according to which

$$\ln \tau = \ln A + \frac{\varepsilon}{kT}. \quad (10)$$

However, as can be seen in Fig. 3, the experimental points for KI-Tl for temperatures higher than room temperature deviate from the line described by (10), so that this mechanism of photoluminescence must be rejected.

Considering the published data and the results of this investigation, one can conclude that the kinetics of the short-lived photoluminescence of alkali halide crystals of the luminescence centers between the two lowest excited levels. Besides this, the conclusion can be drawn that the characteristic parameters of the luminescence—intensity, decay time, and quantum yield—are described by Eqs. (4), (3), and (5), respectively.

When the luminescence bands corresponding to the individual excited levels do not overlap, there is a possibility of determining the energy separation between them, as well as the absolute magnitude of the probabilities of radiative transitions from each electronic level, if one knows the decay time or the quantum yield of a single band as a function of temperature and the ratio of the quantum yield of each luminescence band to the decay time of the photoluminescence at any temperature.

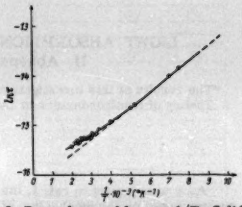

Fig. 3. Dependence of $\ln \tau$ on $1/T$. Solid line—calculated from Eq. (9) with $\ln(1/f_{31}) = -16.54$ and $\varepsilon = 0.03$ ev; dashed line—calculated from Eq. (10) with $\ln A = -16.2$ and $\varepsilon = 0.027$ ev; points—experimental values.

*The decay time of the radiative transition from the $^3P_1$ level of Tl ion in NaF was determined by Kravets's formula to be equal to 4.5×10^{-8} sec.[6] The values obtained in an investigation of the growth of scintillation from deuterons and gamma rays were 5.9×10^{-8} sec[10] and 6×10^{-8} sec,[9] respectively.

REFERENCES

1. N. E. Lushchik, Kand. diss., Tartu, 1959; Trudy Inst. Fiz. i Astron., Akad. Nauk Eston.SSR No. 10, 68 (1959).
2. Ch. B. Lushchik and N. E. Lushchik, Trudy Inst. Fiz. i Astron., Akad. Nauk Eston.SSR No. 6, 5 (1957).
3. Ya. Ya. Kirs and A. I. Laisaar, Trudy Inst. Fiz. i Astron., Akad. Nauk Eston.SSR, No. 8, 51 (1959).
4. I. K. Plyavin', Opt. i Spektr. 4, 266 (1958).
5. I. K. Plyavin', Opt. i Spektr. 7, 71 (1959), Optics and Spectroscopy 7, 41 (1959).
6. B. I. Stepanov, "Lyuminestsentsiya slozhnykh molekul" (Luminescence of Complex Molecules). Izd. Akad. Nauk Byeloruss.SSR, Minsk, 1955.
7. K. K. Shvarts, Trudy Inst. Fiz. i Astron., Akad. Nauk Eston.SSR No. 7, 253 (1958).
8. P. Pringsheim, "Fluorestsentsiya i fosforestsentsiya" (Fluorescence and Phosphorescence). Izd. Inostrannoi Lit., Moscow, 1951.
9. I. K. Plyavin', Opt. i Spektr. 2, 384 (1957).
10. F. S. Eby and W. K. Jentschke, Phys. Rev. 96, 911 (1954).

LIGHT ABSORPTION BY EXCITONS IN THE Cu_2O CRYSTAL
II. Absence of Constant External Fields*

*The results of this investigation were presented at the Third All-Union Conference on the Theory of Semiconductors in Lvov, April, 1959.

S. A. Moskalenko

Received 20 August 1959

As a complement to ref. 1, the present paper considers p-type hole bands, the exciton spectra based on the mechanism of excitation of the oxygen ions, and the characteristic frequencies of lattice vibrations in Cu_2O.

INTRODUCTION

In the publications of Gross and his collaborators,[2] two hydrogenlike series of bands were observed, which were named the yellow (y.s.) and the green (g.s.) series. The intense bands of the series are characterized by the numbers $n \geq 2$. The Stark and Zeeman effects in the y.s. have been studied,[3] and the behavior of the bands during compression of the samples was also investigated.[3]

At low temperatures, "new lines" and a very weak narrow line $\lambda_0 = 6125$ Å are found in the y.s. Gorban'[4] made detailed quantitative measurements of the bands in the y.s. and g.s., established that they were independent of impurities and confirmed that the spectrum was of an exciton character. Nikitin,[5] in addition to the usual two series, also found weak lines which he grouped into a red series along with the λ_0 line. These additional lines were not reproduced by other investigators, and therefore we refrain from discussing them. Nevertheless, the problem of the nature of the λ_0 line merits careful study. Recently this line was found to be polarized.[6,7] Pastrnyak[8] and Gorban'[9] studied the nature of the heavy background on which the bands of the y.s. and g.s. are superimposed. This noise, and also the weak noise under the line λ_0, belong to the ideal lattice and are related to band-band transitions. A number of hypotheses[2,5,10,11] have been proposed to explain the experimental data. None of these has been sufficiently substantiated. We have already discussed this point in ref. 1. We will now continue our consideration of the structure of the electronic, hole, exciton, and phonon states of the Cu_2O crystal which was begun in ref. 1. In the last of this paper, we will compare theory with experiment.

p-TYPE HOLE BANDS AND THE CHARACTERISTIC LATTICE VIBRATION FREQUENCIES

According to ref. 1, the space symmetry group of the Cu_2O crystal is denoted by O_h^4 and has the following generating elements:

$$P\,\{\varepsilon_3(111)\,|\,\mathbf{p}_0\}\,\{\varepsilon_4(001)\,|\,\mathbf{p}_1\}\,\{\varepsilon_2(110)\,|\,\mathbf{p}_2\}.$$

The elementary cell consists of two equivalent oxygen ions and four equivalent copper ions (see Fig. 1 in ref. 1.) The positions of the former are given by the vectors $\mathbf{q}_j$ where $j = 1,2$ and of the latter by the vectors $\mathbf{p}_i$, where $i = 0, 1, 2, 3$. The lattice vector is denoted by $\mathbf{h}$. A simple Bravais lattice is formed by performing the translation $\mathbf{h}$ from each of the ions in the elementary cell. There are six such lattices. Let us denote them by $\mathbf{p}_i$ and $\mathbf{q}_j$. In ref. 1, the local groups S_{p_i} and S_{q_j}, which reduce to simple Bravais lattices by themselves, were determined. These subgroups have the following generating elements:

$$S_{q_1} = S_{q_2} = S_q = P\,\{\varepsilon_3(111)\,|\,\mathbf{p}_0\}\,\{\varepsilon_4(001)\,|\,\mathbf{p}_1\}\,\{\varepsilon_2(110)\,|\,\mathbf{p}_3\}. \quad (1)$$

The group translation factor from the subgroup S_q is isomorphous with the group T_d, whose single-valued and double-valued representations are well known.[12] The symmetry elements of the O_h^4 group, which do not belong to the local symmetry group, transform the equivalent simple Bravais lattices into each other. The O_h^4 group can be represented in various ways as direct products of two subgroups

$$O_h^4 = V \times S_p = C_i \times S_q,$$

where

$$C_i = \{I, I^2\} = \{I^j\}, \quad (2)$$

where I is the space inversion operation; $j = 1, 2$; the V and S_{p_i} groups were determined in ref. 1. Note that $Iq_1 = q_2$ and $Iq_2 = q_1$, since

$$q_1 = -q_2. \quad (3)$$

The splitting of energy levels of the Cu^{2+} ion in the crystal field of local symmetry S_p and the symmetry properties of the corresponding single electron functions are given by Eqs. (6-9) of ref. 1. There are 5 twofold degenerate crystallographic terms E_{ξ} with wave functions $\psi_{E_{\xi}f_{\xi}}$, where f_{ξ} assumes the values 1 and 2. The terms E_1, E_2, and E_3 possess symmetry of type E_2^1, while E_4 and E_5 possess E_1^1 type symmetry.

The oxygen ion O^-, which finds itself in a crystalline field with local symmetry T_d, has two crystal terms with the same degree of degeneracy as the free ion. The irreducible representations Γ_7 and Γ_8 of group T_d^1 correspond to these terms. The single electron functions of the oxygen ions O^- are denoted by $\psi_{\Gamma_c f_c}[\mathbf{r} - \mathbf{h} - \mathbf{q}_j, S_z]$ where f_c can take on the values 1 and 2 when $\Gamma_c = \Gamma_7$, and the values 1, 2, 3, and 4 when $\Gamma_c = \Gamma_8$.

For symmetry elements $I^j\{G_q\,|\,\tau_q\}$, we obtain the following rule for the transformation of p-type functions:

$$I^j\,\{G_q\,|\,\tau_q\}\,\psi_{\Gamma_{p'_s}f_s}[\mathbf{r} - \mathbf{h} - \mathbf{q}_j S_z] = (-1)^j \sum_{f_s} (G_q)^{(\Gamma_s)}_{f'_s f_s}$$

$$\times\,\psi_{\Gamma_{p'_s}f'_s}[\mathbf{r} - I^j G_q \mathbf{h} - I^j G_q \mathbf{q} - I^j \tau_{q_j} S_z]. \quad (4)$$

Given the symmetry properties of the single electron functions, let us study the p-type hole bands in the Cu_2O lattice. In the ground state of the crystal, the crystallographic terms originating from the d and p-shells of the Cu^+ and O^- ions are filled. There are 52 valence electrons in the unit cell. The hole states arising from the d-shells and the electron states arising from the 4s shells of the copper ions were discussed in ref. 1, Eqs.

(12)-(20). Let us consider in a similar way a crystal with one electron missing from the F state in the crystallographic term T of the oxygen ion Q in the cell H. The wave function which corresponds to this crystalline state is

$$\Psi_F[H+Q,\ T,\ F] = (-1)^F \sum_\gamma (-1)^\gamma P_\gamma \prod_h \prod_{p_h} \prod_{\delta_p} \prod_{f_\delta} \prod_{q_f} \prod_{\Gamma_\tau} \prod_{f_\tau} \times \psi_{hp\delta_p f_\delta}(r_{hp\delta_p f_\delta}, S_{\sigma hp\delta_p f_\delta}) \psi_{hq\Gamma_\tau f_\tau}(r_{hq\Gamma_\tau f_\tau}, S_{\sigma hq\Gamma_\tau f_\tau}), \quad (5)$$

where

$$(hq\Gamma_\tau f_\tau) \neq (HQTF),$$

The parameter T may assume either of the two values Γ_7 or Γ_8^-; F is equal to one of the values which f_C can have. From the function (5), which describes a trapped hole, we pass over to a function which describes a hole distributed over the simple Bravais lattice:

$$\Psi_F[K,\ Q,\ T,\ F] = \sum_H \exp[iK,\ H+Q]\, \Psi_F[H+Q,\ T,\ F]. \quad (6)$$

Under the action of the symmetry operation $\{G \mid \tau\} = I^l\{G_Q \mid \tau_Q\}$ the function (6) is transformed into:

$$\{G \mid \tau\}\, \Psi_F[K,\ Q,\ T,\ F]$$

$$= \exp[-iGK,\ \tau] \sum_{F'} (-1)^l (G_Q^{-1})_{FF'} \Psi_{F'}[GK,\ l'Q,\ T,\ F']. \quad (7)$$

At the point K = 0, eight functions $\Psi_F[0, Q, \Gamma_8, F]$ form the reducible representation D_8 and four functions $\Psi_F[0, Q, \Gamma_7, F]$ form the reducible representation D_7. The characters of these representations are expressed through the characters of the irreducible representations of the groups T_d', Γ_7, and Γ_8; namely:

$$\chi_{D_\tau}(G \mid \tau) = \chi_{\Gamma_\tau}(G)\, m_G \text{ and } \chi_{D_\tau}(G \mid \tau) = \chi_{\Gamma_\tau}(G)\, m_G, \quad (8)$$

and they are shown in Table 1, Appendix I.[1] The numbers m_G indicate the number of local symmetry groups S_q to which the symmetry operator $\{G \mid \tau\}$ is applicable, i.e.,

$$m_G = \sum \delta_{KP_\gamma}[\{G \mid \tau\},\ S_q] \quad (9)$$

These numbers can assume two values: 0 and 2.

The characters of the other irreducible representations of the groups of a cube at the point K = 0 is given in ref. 13. Let us perform the reduction:

$$D_7 = \Gamma_8^- + \Gamma_7^+; \quad D_8 = \Gamma_8^- + \Gamma_8^+. \quad (10)$$

Thus, the p-shells of the oxygen ions at the point K = 0 give rise to four hole bands which belong to the irreducible representations Γ_8^-, Γ_8^-, Γ_7^+ and Γ_8^+. Because of the weak spin-orbit splitting of the p-shells in O^- (160 cm^{-1}) two of the crystallographic terms of the O^- ion are nearly equal.

The four hole bands are divided into two groups in Fig. 1—the even and odd hole bands. They are enclosed in squares. The odd hole bands, according to ref. 10, have an excitation energy which is 0.2 ev greater than that of the even bands. For $K \neq 0$, Eqs. (6) form the large representation of the $O_h^7 D_{\frac{1}{2}}^{|K|}$ group, which is characterized by the irreducible star {K}.[14] The subgroup of

Table 1. Characters of the Irreducible Representations of the Group Q_{110}'

	E	Q	$\{I\sigma_h(z) \mid p_h\}$	$\{I c_2 \ (1-1/2) \mid p_h\}$	$\chi(l_1, l_2, l_3)$
Γ_7^+	1	1	ε	1	$\exp[-ik_1(l_1+l_2)]$
Γ_8^-	1	1	$-\varepsilon$	+1	"
Γ_7^-	1	1	$-\varepsilon$	+1	"
Γ_8^+	1	1	ε	−1	"
Γ_5^+	2	−2	0	0	$2\exp[-ik_1(l_1+l_2]$

Note: In this table $\varepsilon = \exp(-ik_1)$; $k_1 = (ka_1) = (ka_2) = k_z$.

Fig. 1. Electron and hole bands in the Cu_2O crystal. The p-type hole bands are contained within the rectangles.

the space group, composed of the elements $[G \mid \tau]$ whose dyad parts G leave the vector K unchanged (GK = K) or transforms it into its equivalent, is called the group of the wave vector Q_K'.[14] Functions (6), with the same vector K form the little representation $d_{\Gamma_C}^K$ of the group Q_K'. The little representations determine a single-valued large representation.[15] The character of the representation $d_{\Gamma_C}^K$, according to Eq. (7), is equal to

$$\chi_{d_{\Gamma_C}^K}(G \mid \tau) = \exp(-iK\tau)\, \chi_{\Gamma_\tau}(G)\, m_G \delta_{KP_\gamma}[\{G \mid \tau\},\ Q_K']. \quad (11)$$

In order to reduce the representation $d_{\Gamma_C}^K$, we constructed irreducible representations of certain groups of wave vectors Q_{110}', Q_{111}', Q_{100}' and $Q_{k_1 k_2 k_3}'$ according to the the method proposed by Seitz.[14] The group Q_{111} does not contain any screw axes, and the characters of its irreducible representations are given in ref. 16. For the group Q_{110}' the construction of representations is shown in Table 1, and the same is done for the group Q_{100}' in ref. 1. For an arbitrary vector k there are two one-dimensional irreducible representations of the groups $Q_{k_1 k_2 k}'$ and τ_k'. Recently,* Zhilich[17] also constructed the irreducible representation of the group O_h^7. We, however, considered the binary group $O_h^{7'}$ and constructed additional irreducible representations in addition to the usual ones.

*The work of Zhilich appeared several months after my paper was submitted.

Thus far, however, we have not taken account of the symmetry of the problem with respect to an inversion of the sign of the time. Because of this symmetry, the Hamiltonian commutes with the nonlinear operator R, whose form is different in the relativistic and nonrelativistic cases.[18,19] The amplitudes of the function (6), which form the irreducible representation Γ_i^k of the wave vector Q_k' will be denoted by the symbol $S(\Gamma_i^k)$. According to refs. 18 and 19, the amplitude of the functions $RS(\Gamma_i^k)$ belong to the same energy values. Three cases can be differentiated as follows:

a) $RS(\Gamma_i^k) = S(\Gamma_i^k)$; b) $RS(\Gamma_i^k) = S(\Gamma_j^k)$, $\Gamma_i^k \neq \Gamma_j^k$;

c) $RS(\Gamma_i^k) = S'(\Gamma_j^k)$, where $S'(\Gamma_j^k) \neq S(\Gamma_i^k)$.

In the first case, there is no additional degeneracy (there may be accidental degeneracy); in the remaining cases additional degeneracy sets in. In order to establish in what case a given irreducible representation is applicable, it is necessary to use the criterion:[15]

$$\sum_{G} \chi_{\Gamma_i^k}(G^2) = \begin{cases} n_k, & \text{(a)}, \\ 0 & \text{(b)}, \\ -n_k, & \text{(c)}, \end{cases} \qquad \sum_{G} \chi_{\Gamma_i^k}(G^2) = \begin{cases} -n_k', \\ 0 \\ n_k'. \end{cases} \qquad (12)$$

$G\mathbf{k} = -\mathbf{k}$ $\qquad$ $G\mathbf{k} = -\mathbf{k}$

The expression on the left is written for the usual representations of the group $\mathbf{Q}_k$, while that on the right is for the complementary representations of the group $\mathbf{Q}_k'$. The parameters n_k and n_k' denote the number of elements in the two factor-groups $\mathbf{Q}_k/\Gamma$ and $\mathbf{Q}_k'/\Gamma$. By using criterion (12), we can convince ourselves that all of the irreducible representations in Table 1 correspond to case (a). Representation τ_k corresponds to case (a), whereas τ_k' corresponds to case (b). Thus, at an arbitrary point in K-space, there exists a double spin degeneracy in the band. Similar results were found for the directions [111], etc.

We effected the reduction of the representation $d^k_{\Gamma_c}$ with the help of Eq. (11) and Table 1 and also considered the degeneracy which arises because of the existence of the operator R. These results are also shown in Fig. 1. Besides the p-type hole bands we also reduced the s-type electron bands and d-type hole bands.

Let us now discuss the lattice vibration frequencies at the point K = 0 neglecting long range interactions and time lag. The displacement of the ions from their equilibrium positions is denoted by U (h + p, ξ) and U (h + q, ξ), where ξ assumes the three values x, y, and z. Following ref. 20, let us transform to the translation coordinates U (k, p, ξ) and U (kqξ).

As a result of action by the symmetry operator

$$\{G \mid \tau\} = \{G_s \mid \tau_s\} \times \{G_p \mid \tau_p\} = U\{G_q \mid \tau_q\}$$

the translation coordinates transform according to the following rules:

$$\left.\begin{aligned} \{G \mid \tau\}\, U(\mathbf{k}, p, \xi) &= \exp(-iG\mathbf{k}, \tau)\, U(G\mathbf{k}, \{q, (\tau_s)_p, G\xi), \\ \{G \mid \tau\}\, U(\mathbf{k}, q, \xi) &= \exp(-iG\mathbf{k}, \tau)\, U(G\mathbf{k}, l/q, G\xi). \end{aligned}\right\} \qquad (13)$$

It must be remembered that

At the point K = 0, 18 translational coordinates U (0, p, ξ); U (0, q, ξ) make up the representations F_1 and F_2. Their characters are determined by the equations:

$$\chi_{F_1}(G \mid \tau) = \chi_{\Gamma_4}(G)\, n_G \text{ and } \chi_{F_1}(G \mid \tau) = \chi_{\Gamma_4'}(G)\, n_G \qquad (14)$$

and they are shown in Table 2. The number m_G is determined by Eq. (9) and the numbers n_G are given by Eq. (15) of ref. 1.

$$n_G = \sum_p \chi_{\mathrm{rep.}}[(G \mid \tau),\ S_p]. \qquad (15)$$

Given the character of the irreducible representation of the O_h group, we can make the reduction of the F_1 and F_2 representations.

Table 2. Characters of the Reducible Representations D_7, D_8, F_1 and F_2

	E	Q	$4\{C_3 \mid \tau\}$ $4\{C_3^2 \mid \tau\}$	$4\{C_3 \mid \tau\}Q$ $4\{C_3^2 \mid \tau\}Q$	$6\{C_4 \mid \tau\}I$ $6\{C_4 \mid \tau\}IQ$	$3\{C_2^2 \mid \tau\}$ $3\{C_2^2 \mid \tau\}Q$	$3\{C_4 \mid \tau\}I$ $3\{C_4^3 \mid \tau\}IQ$	$3\{C_4^3 \mid \tau\}I$ $3\{C_4 \mid \tau\}QI$	I
D_7	4	−4	2	−2	0	0	$-2\sqrt{2}$	$2\sqrt{2}$	0
D_8	8	−8	−2	2	0	0	0	0	0
F_1	12	12	0	0	−2	0	0	0	−12
F_2	6	6	0	0	2	−2	−2	−2	0

Using Bethe's symbols, we write

$$F_1 = \Gamma_2' + \Gamma_3' + 2\Gamma_4' + \Gamma_5' \text{ and } F_2 = \Gamma_4' + \Gamma_5'.$$

To sum up, at the point K = 0 there are seven limiting frequencies, six optical and one acoustic which correspond to the irreducible representations

$$\Gamma_2', \ \Gamma_3', \ 3\Gamma_4', \ \Gamma_5', \ \Gamma_5. \qquad (16)$$

In dipole transitions, two optical and one acoustic frequency are active. Similar results were found by Pastrnyak.[22]

THE ENERGY SPECTRUM OF EXCITONS AT THE POINT K = 0. COMPARISON OF THEORY WITH EXPERIMENT

Let us dwell on three principal problems: (1) the origin of the two series, (2) the nature of the noise under them, and (3) the nature of the line λ_0.

The mechanism of excitation of the oxygen ion gives a unique answer to these three questions. The y.s. arises from the even pair of hole bands ($\Gamma_7^+ + \Gamma_8^+$) and the conduction band Γ_6^+, while the g.s. arises from the same pair of hole bands and the pair of electron bands ($\Gamma_7^+ + \Gamma_8^+$). Because of the weak spin-orbit interaction, the two pairs of bands must be considered almost touching. In both series, intense bands with n = 1 are absent, which both demonstrates our statement and refutes the hypothesis of ref. 10. Two other groups of bands should be expected in the shorter wavelength region of the spectrum. According to ref. 1, the number and symmetry type of exciton hydrogenlike levels with a given value of n and $0 \leq l \leq n-1$ which arise from a definite pair of electron and hole bands is found from the equation

$$\Gamma_g \times \Gamma_e \times \sum_{l=0}^{n-1} D_l, \qquad (17)$$

where Γ_g, Γ_e, and D_l are representations characterizing the band at the point K = 0 and functions of relative motion. In Table 3, we determined the number of representations of the type Γ_1, Γ_3, Γ_5, and Γ_4' in products of type (17). Levels of type Γ_4' are active in dipole transitions, and levels of type Γ_1, Γ_3, and Γ_5 are active in quadrupole transitions from the ground state. The exciton level scheme of the two series is shown in Fig. 2, divided approximately into singlet and triplet levels. We limited ourselves to the values l = 0, 1, 2, 3 and n = 1, 2, 3, 4. The groups of levels which correspond to higher values of n for these same values of l have the same form. The level scheme of the y.s. is explained by the presence of one quadrupole line (comparatively more intense than the other two lines) in the region n = 1. In order to explain the noise which starts under the line λ_0, it is necessary to assume a decrease in the width of the forbidden band as one moves away from the point K = 0. This scheme does not explain two important facts: (1) the splitting of the main y.s. band into doublets in a magnetic field and (2) the sharp increase in the noise at the boundary between the first and the second steps. A fur-

Table 3. The Number of Representations of the Type Γ_1, Γ_3, Γ_5 and Γ_4' in the Direct Products of the Representations $\Gamma_g \times \Gamma_e \times D_l$

$\Gamma_g \times \Gamma_e \times$	$D_0 = \Gamma_1$	$D_1 = \Gamma_4'$	$D_2 = \Gamma_3 + \Gamma_5$	$D_3 = \Gamma_2' + \Gamma_4' + \Gamma_5'$
$\Gamma^+ \times (\Gamma_7^+ + \Gamma_8^+)$	Γ_3 $2\Gamma_5$	$4\Gamma_4'$	$3\Gamma_1$ $5\Gamma_3$ $7\Gamma_5$	$11\Gamma_4'$
$(\Gamma_7^+ + \Gamma_8^+) \times$ $\times (\Gamma_7^+ + \Gamma_8^+)$	$2\Gamma_1$ $3\Gamma_3$ $4\Gamma_5$	$14\Gamma_4'$	$7\Gamma_1$ $15\Gamma_3$ $23\Gamma_5$	$31\Gamma_4'$

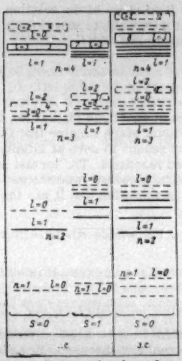

Fig. 2. Two exciton series based on the mechanism of excitation of the oxygen ion. Solid lines—levels of type Γ_4^+; dashed lines—quadrupole active. Levels with l = 2 and l = 3 are contained in the rectangles.

ther study of this problem is necessary.

In conclusion I wish to express my deep gratitude to K. B. Tolpygo for discussions of this work.

REFERENCES

1. S. A. Moskalenko, Fiz. Tver. Tela, 2, No. 8 (1960).
2. E. F. Gross, Uspekhi. Fiz. Nauk 63, 575 (1957).
3. V. V. Eremenko, Opt. i Spektr. (in press).
4. I. S. Gorban', Proceedings of the Plenary Session of the Semiconductor Commission, Akad. Nauk USSR, Odessa, 1959.
5. S. Nikitine, Phil. Mag. 4, 37 (1959).
6. E. F. Gross and A. A. Kaplyanskii, Fiz. Tver. Tela. 2, 379 (1960).
7. I. S. Gorban' and V. B. Timofeev, Fiz. Tver. Tela, 2, No. 8, (1960).
8. I. Pastrnyak, Fiz. Tver. Tela. 1, 970 (1959).
9. I. S. Gorban' and V. B. Timofeev, Fiz. Tver. Tela. 2, 1111 (1960).
10. A. G. Zhilich and P. P. Pavinskii, Vestnik Leningrad. Gosudarst. Univ. No. 4, 50 (1957).
11. R. T. Elliott, Phys. Rev. 108, 1384 (1954).
12. L. D. Landau and E. Lifshits, "Quantum Mechanics" (in Russian) part 1, pp. 386, 402. Gosudarst. Izd. Tekh.-Teoret. Lit., Moscow, 1948.
13. Collection "Problems in the Physics of Semiconductors" (in Russian) p. 471. Izd. Inostrannoi Lit., Moscow (1957).
14. F. Seitz, Ann. Math. 37, 17 (1936).
15. G. Ya. Lyubarskii, "Group Theory and its Application in Physics" (in Russian), paragraph 30. Gosudarst. Izd. Tekh.-Teoret. Lit., Moscow, 1957.
16. L. R. Bouckaert, R. Smoluchowsky, and E. Wigner, Phys. Rev. 50, 58 (1936).
17. A. G. Zhilich, Vestnik Leningrad. Gosudarst. Univ. 22, No. 4, 5 (1959).
18. E. Wigner, Gött. Nachr. p. 546 (1932).
19. D. F. Jonston, Proc. Roy. Soc. A243, 546 (1958).
20. Ianagawa Sodaaki, Progr. Theoret. Phys. (Kyoto) 10, 3 (1953).
21. H. A. Bethe, Ann. Phys. 3, 133 (1929).
22. I. Pastrnyak, Opt. i Spektr. 6, 107 (1959), Optics and Spectroscopy 6, 64 (1959).

Note added in proof: Recently E. F. Gross and A. A. Kaplyanskii studied the behavior of the line λ_0 under pressure. Calculations showed that a level of the type Γ_5, under pressure along [1 – 10], is divided into three levels. If light travels along [110] then one of these levels with a polarization $\perp$ to P is activated: if the direction of propagation is k [001] two levels, with mutually perpendicular polarizations are active; for k [111] and other directions with k perpendicular to P, all three levels are active. For two of them, the polarization is perpendicular to P; for one of them, it is parallel to P. Comparison of theory with experiment shows that the line λ_0 corresponds to a quadrupole of type Γ_5.

RADIATION TRANSFER IN A HOMOGENEOUS MEDIUM FOR THE NONCONSERVATIVE CASE

V. I. Barkov

Received 28 December 1959

A solution is given for the integro-differential equation of radiation transfer. The case of a point source located within a homogeneous medium filling all space is examined. A general expression for the average intensity and flux of radiation is obtained in the n-th approximation.

The transfer of radiant energy in an infinite homogeneous medium which is illuminated by a point source of radiation has been considered in papers by Ambartsumyan[1] and Chandrasekhar.[2] A similar problem concerning the diffusion of neutrons in homogeneous spheres has been solved in neutron physics. Marshak's work,[3] in which the Milne problem was examined for a sphere, borders on this question. This is the sort of problem that has to be dealt with in evaluating the dangerous effects of atomic detonations.[4]

The method of solving the integro-differential equation of transfer used in this paper is based on the replacement of integrals by finite sums. The particular merit of this method, which is essentially equivalent to the spherical harmonic method, is its rapid convergence in approximations of low order.

Let us analyze the problem in its usual form, considering the indicatrix of scattering as spherical and the optical characteristics of the medium as known. One must calculate the radiation field inside the medium at any finite distance from a point source of known power. We arrange to separate from the total radiation that direct radiation which arrives at the point under consideration directly from the source, and which has not under-

gone any scattering or absorption in that portion of the medium through which it has passed. What remains after this kind of separation is the diffuse radiation arising as a result of single or multiple scattering of the radiation in the medium. Denoting the intensity of the diffuse radiation field as $I(r, \mu)$, we write the equation of radiation transfer for a medium having spherical symmetry in the form

$$\mu \frac{\partial I}{\partial r} + \frac{1-\mu^2}{r} \frac{\partial I}{\partial \mu} = -\varkappa\rho I(r, \mu) + \frac{\sigma\rho}{2} \int_{-1}^{+1} I(r, \mu')\, d\mu' + \frac{\varkappa\rho}{4\pi} \frac{Q a_0 e^{-\varkappa r}}{4\pi r^2}, \quad (1)$$

where Q^0 is the power of an isotropically radiating source located at the origin of coordinates, α is the absorption coefficient, σ is the scattering coefficient, ρ is the density of the medium, and $\mu = \cos\vartheta$, where ϑ is the angle between the radius vector and the direction under consideration. We must emphasize that the radiation transfer equation pertains to a specific frequency ν.

Because of the homogeneity of the medium in which the radiant energy is propagated, the values of α, σ, and ρ are constant in all space. If there is a center of symmetry, the solution must have axial symmetry with respect to the radius vector r. For this reason the intensity of the diffuse radiation must depend entirely on the distance r and the angle ϑ. In place of r, we introduce the value

$$\tau = \varkappa\rho r, \quad (2)$$

considered as an optical distance calculated from the origin. The transfer equation can then be given some form such as

$$\mu \frac{\partial I}{\partial \tau} + \frac{1-\mu^2}{\tau} \frac{\partial I}{\partial \mu} = -I(\tau, \mu) + J(\tau), \quad (3)$$

where

$$J(\tau) = \frac{\lambda}{2} \left[\int_{-1}^{+1} I(\tau, \mu')\, d\mu' + Q \frac{e^{-\tau}}{\tau^2} \right] \quad (4)$$

is called the source function or output. The designation

$$Q = \frac{Q a_0 \varkappa^2}{8\pi} \quad (5)$$

is introduced in formula (4), along with $\lambda = \sigma/\rho$, which characterizes the scattered radiant energy as a fraction of the total quantity of radiant energy absorbed by the volume. It proves convenient to represent the term corresponding to direct radiation by an integral over the interval (0, +1), making use of the equality

$$Q \frac{e^{-\tau}}{\tau^2} = Q \int_0^1 \frac{e^{-\frac{\tau}{\mu}}}{\tau} \frac{d\mu}{\mu^2} = Q \sum_{j=1}^{n} \frac{a_j}{\mu_j^2} \frac{e^{-\frac{\tau}{\mu_j}}}{\tau}, \quad (6)$$

where μ_j are zeros of fourth order Legendre polynomials, and a_j are the corresponding Gaussian weights.

The significance of transformation (6) is that the action of a real point source of radiation is replaced by an equivalent action of a system of spatially distributed fictitious sources, each of which generates an intensity at the point under consideration equal to

$$\frac{Q}{\mu_j^2} \frac{e^{-\frac{\tau}{\mu_j}}}{\tau}.$$

Formula (4) can be rewritten with the help of equality (6) in the form

$$J(\tau) = \frac{\lambda}{2} \left[\int_{-1}^{+1} I(\tau, \mu)\, d\mu + \frac{Q}{\tau} \int_0^1 e^{-\frac{\tau}{\mu}} \frac{d\mu}{\mu^2} \right]. \quad (7)$$

We note in passing that the integrals can be replaced by sums at the final stage of the solution of the problem, operating at all intermediate stages with integrals over the intervals mentioned above.

I

The system of equations (3) and (4), together with the boundary conditions which require that the functions $I(\tau, \mu)$ and $J(\tau)$ reduce to zero at infinity, fully determine the desired functions. The formal solution of Eq. (3) can be found by standard procedures. It is easy to show by direct substitution that it has the form

$$I(\tau, \mu) = \int_0^\infty J\left(\sqrt{t^2 - 2t\tau\mu + \tau^2}\right) e^{-t}\, dt, \quad (-1 \leqslant \mu \leqslant +1). \quad (8)$$

For convergence of the integral, it is sufficient to require that

$$J\left(\sqrt{t^2 - 2t\tau\mu + \tau^2}\right) e^{-t} \to 0 \quad \text{for} \quad t \to \infty. \quad (9)$$

Expression (8) is not a solution of the transfer equation in the true sense of the word. However, using the method of moments, an explicit form of the source function $J(\tau)$ can be found without having recourse to replacement of the transfer equation by the integral equation pertaining to the source function.

We multiply Eq. (3) by $P_l'(\mu)$, where $P_l(\mu)$ is the Legendre polynomial of order l and the prime denotes differentiation with respect to the argument μ. We then integrate the equation over μ between the limits (−1) and (+1). We obtain

$$\frac{\partial}{\partial\tau} \int_{-1}^{+1} \mu P_l'(\mu) I(\tau, \mu)\, d\mu + \frac{1}{\tau} \int_{-1}^{+1} (1-\mu^2) P_l'(\mu) \frac{\partial I}{\partial \mu}\, d\mu = -\int_{-1}^{+1} P_l'(\mu) I(\tau, \mu)\, d\mu + J(\tau) \int_{-1}^{+1} P_l'(\mu)\, d\mu. \quad (10)$$

The source function $J(\tau)$ is taken out from behind the integral sign, since it is assumed that the source of radiation is isotropic. Both members on the left-hand side of the equation can be transformed if one takes advantage of the known properties of Legendre polynomials and integrates by parts. As a result, we have in place of (10)

$$\frac{l}{\tau^{2l+1}} \frac{d}{d\tau} \tau^{2l+1} \int_{-1}^{+1} P_l(\mu) I(\tau, \mu)\, d\mu + \frac{d}{d\tau} \int_{-1}^{+1} P_{l-1}'(\mu) I(\tau, \mu)\, d\mu = -\int_{-1}^{+1} P_l'(\mu) I(\tau, \mu)\, d\mu + J(\tau) \int_{-1}^{+1} P_l'(\mu)\, d\mu. \quad (11)$$

Forming an equation differing from the given one by 2 in the value of l, and taking their difference, we obtain the infinite system of equations

$$\frac{l}{\tau^{2l+1}} \frac{d}{d\tau} \tau^{2l+1} \int_{-1}^{+1} P_l(\mu) I(\tau, \mu)\, d\mu + (l-1)\, \tau^{l-2} \frac{d}{d\tau} \frac{1}{\tau^{l-2}} \int_{-1}^{+1} P_{l-2}(\mu) I(\tau, \mu)\, d\mu = -(2l-1) \int_{-1}^{+1} P_{l-1}(\mu) I(\tau, \mu)\, d\mu + 2J(\tau)\, \delta(l-1), \quad (l = 1, 2, \ldots) \quad (12)$$

where $\delta(l-1)$ is Dirac's delta function.

We introduce the functions

$$M_l(\tau) = \int_{-1}^{+1} P_l(\mu)\, I(\tau, \mu)\, d\mu. \qquad (13)$$

which can be called generalized moments of order 1 of the function $I(\tau, \mu)$. The physical meaning of the first two moments is obvious. The zero order moment

$$M_0(\tau) = \int_{-1}^{+1} I(\tau, \mu)\, d\mu = 2J(\tau), \qquad (14)$$

i.e., is equal to twice the average intensity. The first order moment

$$M_1(\tau) = \int_{-1}^{+1} \mu I(\tau, \mu)\, d\mu = \frac{1}{2\pi} F(\tau), \qquad (15)$$

i.e., is equal to $1/2\pi$ times the flux of radiant energy. The second order moment can be expressed in terms of the K-integral and the average intensity $J(\tau)$. After replacing the source function by its value from (7), we obtain a system of an infinite number of differential equations written in terms of generalized moments.

$$\frac{l}{2l+1}\frac{d}{d\tau}\left[\tau^{l+1}M_l(\tau)\right] + (l-1)\,\tau^{l-2}\frac{d}{d\tau}\left[\frac{M_{l-2}(\tau)}{\tau^{l-2}}\right] = -(2l-1)\,M_{l-1}(\tau)$$

$$+\lambda\left[M_0(\tau) + \frac{1}{\tau}\int_0^1 \frac{Q}{\mu^2}\, e^{-\frac{\tau}{\mu}}\, d\mu\right]\delta(l-1) \quad (l = 1, 2, \ldots). \qquad (16)$$

In order to have a solution to the n-th order approximation, we consider a system with a finite number of equations, terminating system (16) at the equation with $l = 2n$. We assume the generalized moment $M_{2n}(\tau)$ in the last equation to be zero.[5] This condition is equivalent to the P_{2n-1} approximation in the spherical harmonic method.[3]

The system of 2n linear differential equations of first order which we obtain can be reduced to a single differential equation of 2n-th order relative to any of the functions $M_l(\tau)(i = 1, 2, \ldots, 2n - 1)$. It is more important for us to have an equation written in explicit form with respect to the function $M_0(\tau)$. By substitution and successive transformation from equations with moments of higher order to equations of lower order, we eliminate from the final system of equations all the generalized moments $M_l(\tau)$ of order greater than zero.

The result of the indicated transformations will be a linear nonhomogeneous differential equation of order 2n relative to the function M_0:

$$\sum_{\alpha=0}^{n} (-1)^{\alpha} a_{\alpha}\left(\frac{1}{\tau}\frac{d^2}{d\tau^2}\tau\right)^{\alpha} M_0(\tau) = \frac{1}{\tau}\sum_{\alpha=0}^{n-1}(-1)^{\alpha} b_{\alpha}\int_0^1 e^{-\frac{\tau}{\mu}}\frac{d\mu}{\mu^{2(\alpha+1)}}. \qquad (17)$$

where a_α and b_α are constant coefficients which depend on the parameter λ and are associated in pairs. The coefficient associated with the most significant derivative a_n is normalized to 1. We represent Eq. (17) as a differential operator of the form

$$\left(\frac{1}{\tau}\frac{d^2}{d\tau^2}\tau - \omega_{\alpha}^2\right),$$

applied n times to the function M_0, namely:

$$\prod_{\alpha=1}^{n}\left(\frac{1}{\tau}\frac{d^2}{d\tau^2}\tau - \omega_{\alpha}^2\right) M_0(\tau) = \frac{1}{\tau}\sum_{\alpha=0}^{n-1}(-1)^{\alpha+n} b_{\alpha}\int_0^1 e^{-\frac{\tau}{\mu}}\frac{d\mu}{\mu^{2(\alpha+1)}}. \qquad (18)$$

Here the constants ω_α^2 are determined from the coefficients a_α by the Vieta formulas, and are consequently functions of the parameter λ. It will be shown below that ω_α is a root of the characteristic equation figuring in the theory of radiation transfer in plane-parallel atmospheres[6] with a spherical indicatrix of diffusion.

Equation (18) is a linear nonhomogeneous differential equation of order 2n. The general solution of a homogeneous equation can be expressed in the form

$$\frac{1}{\tau}\sum_{\alpha=-n}^{+n} C_{\alpha} e^{-\omega_{\alpha}\tau}, \qquad (19)$$

where the C_α are constants of integration depending on the parameter λ. Solution (19) must reduce to zero at infinity. In order to satisfy this requirement, all terms containing $\exp(+\omega_\alpha\tau)$ must be discarded in solution (19). A particular solution of the nonhomogeneous equation can be found by the method of variation of constants of integration. Application of this method to Eq. (18) yields

$$\frac{1}{\tau}\int_0^1 \frac{\sum_{\alpha=0}^{n-1}(-1)^{\alpha+n} b_{\alpha}\mu^{2(n-\alpha)}}{\prod_{k=1}^{n}(1-\omega_k^2\mu^2)}\, e^{-\frac{\tau}{\mu}}\frac{d\mu}{\mu^2}. \qquad (20)$$

Solution (20) satisfies the boundary condition at an infinitely distant point, converging to zero exponentially as $\tau \to \infty$.

Combining solutions (19) and (20), we obtain a general solution to the nonhomogeneous equation (18), which takes the form

$$M_0(\tau) = \frac{1}{\tau}\sum_{\alpha=1}^{n} C_{\alpha} e^{-\omega_{\alpha}\tau} + \frac{1}{\tau}\int_0^1 \frac{\sum_{\alpha=0}^{n-1}(-1)^{\alpha+n} b_{\alpha}\mu^{2(n-\alpha)}}{\prod_{k=1}^{n}(1-\omega_k^2\mu^2)}\, e^{-\frac{\tau}{\mu}}\frac{d\mu}{\mu^2}. \qquad (21)$$

Substituting (21) into (7), we obtain

$$J(\tau) = \frac{\lambda}{2}\left[\frac{1}{\tau}\sum_{\alpha=1}^{n} C_{\alpha} e^{-\omega_{\alpha}\tau} + \frac{1}{\tau}\int_0^1 \varphi(\mu)\, e^{-\frac{\tau}{\mu}}\frac{d\mu}{\mu^2}\right] \qquad (22)$$

where

$$\varphi(\mu) = Q + \frac{\sum_{\alpha=0}^{n-1}(-1)^{\alpha+n} b_{\alpha}\mu^{2(n-\alpha)}}{\prod_{k=1}^{n}(1-\omega_k^2\mu^2)} \qquad (23)$$

It can be shown that $\varphi(\mu)$ must be identically equal to zero; hence, instead of the equalities written above we have

$$\frac{\sum_{\alpha=0}^{n-1}(-1)^{\alpha+n} b_{\alpha}\mu^{2(n-\alpha)}}{\prod_{k=1}^{n}(1-\omega_k^2\mu^2)} = -Q, \qquad (24)$$

$$J(\tau) = \frac{\lambda}{2}\sum_{\alpha=1}^{n} C_{\alpha}\frac{e^{-\omega_{\alpha}\tau}}{\tau}, \qquad (25)$$

$$M_0(\tau) = \sum_{\alpha=1}^{n} C_{\alpha}\frac{e^{-\omega_{\alpha}\tau}}{\tau} - Q\frac{e^{-\tau}}{\tau}. \qquad (26)$$

Expressions (25) and (26) differ from the corresponding functions in the problem of radiation transfer in semi-infinite plane atmospheres[6] by the factor $1/\tau$, which is characteristic of the problem involving a point source.

The source function obviously satisfies condition (9) if τ in (25) is replaced by $\sqrt{\tau^2 - 2t\tau\mu + t^2}$. A descriptive physical interpretation can be given to solution (26). The second term in this solution corresponds to the direct radiation intensity. This conclusion follows from a com-

parison of this term with the nonintegral term of transfer equation (1), which takes the direct radiation into account in the radiant energy balance. At the same time, the partial solution (20) of Eq. (19) acquires an obvious physical content. On the other hand, the general solution (19) of the homogeneous equation must be considered as the average intensity of the total radiation of the source, which we obtain by adding the direct radiation intensity of the diffuse radiation (26).

II

The over-all nature of the dependence of the source function on τ was established in the preceding section. Let us now formulate an equation determining the constants C_α and ω_α. Integrating equation (8) over μ between the limits (−1) and (+1), we obtain

$$M_0(\tau)=\int_{-1}^{+1}\left[\int_0^\infty J\left(\sqrt{t^2-2t\tau\mu+\tau^2}\right)e^{-t}dt\right]d\mu. \tag{27}$$

The limits of integration in integral (27) include all of space. For this reason the integrand (25) goes to infinity when the variable point of integration coincides with the point at which the radiation intensity is determined. Consequently, integral (27) is an improper integral. This integral does have a meaning, however, inasmuch as $J(\tau)$, as a continuous function, satisfies the conditions sufficiently well in the neighborhood of a singular point so that the integral converges.[7] We make a change in the order of integration and introduce a new variable $x=\sqrt{t^2-2t\tau\mu+\tau^2}$. Two cases must then be distinguished: if $t<\tau$, then on varying μ from (−1) to (+1) the value of x changes from $(\tau+t)$ to $(\tau-t)$; if $t>\tau$, then x is changed from $(t+\tau)$ to $(t-\tau)$. In accordance with this condition, the interval of integration must be divided into two parts: $(0,\tau)$ and (τ,∞), and we obtain

$$M_0(\tau)=\frac{1}{\tau}\left\{\int_0^\tau\left[\int_{\tau-t}^{\tau+t}xJ(x)\,dx\right]\frac{e^{-t}}{t}\,dt+\int_\tau^\infty\left[\int_{t-\tau}^{t+\tau}xJ(x)\,dx\right]\frac{e^{-t}}{t}\,dt\right\}. \tag{28}$$

Following the equality (6), we write Eq. (28) in the form

$$M_0(\tau)=\frac{1}{\tau}\int_0^1\left\{\int_0^\tau\left[\int_{\tau-t}^{\tau+t}xJ(x)\,dx\right]e^{-\frac{t}{\mu}}\,\varepsilon+\int_\tau^\infty\left[\int_{t-\tau}^{t+\tau}xJ(x)\,dx\right]e^{-\frac{t}{\mu}}\,dt\right\}\frac{d\mu}{\mu^2}. \tag{29}$$

Substituting (25) and (26) into expression (29) and integrating, we obtain the identity

$$\frac{1}{\tau}\sum_{\alpha=1}^{n}C_\alpha e^{-\omega_\alpha\tau}-\frac{1}{\tau}\int_0^1\frac{Q}{\mu^2}e^{-\frac{\tau}{\mu}}\,d\mu \tag{30}$$

$$=-\frac{1}{\tau}\sum_{\alpha=1}^{n}C_\alpha e^{-\omega_\alpha\tau}\left[\lambda\int_0^1\frac{d\mu}{1-\omega_\alpha^2\mu^2}\right]-\frac{1}{\tau}\int_0^1\left[\lambda\sum_{\alpha=1}^{n}\frac{C_\alpha}{1-\omega_\alpha^2\mu^2}\right]e^{-\frac{\tau}{\mu}}\,d\mu.$$

In order to exclude the singularity in the value of μ that reduces the denominator in (30) to zero, it is necessary to require that $\omega_\alpha\mu<1$. It remains to replace the integrals over the interval (0, 1) by Gaussian sums in order to proceed to the calculated formulas of the n-th approximation, and combine terms on the left and right sides of the equation. Finally, we obtain a system of n equations

$$\lambda\sum_{\alpha=1}^{n}\frac{C_\alpha}{1-\omega_\alpha^2\mu_j^2}=\frac{Q}{\mu_j^2}\qquad(j=1,2,\ldots,n) \tag{31}$$

if we fulfill the requirement

$$\lambda\sum_{j=1}^{n}\frac{a_j}{1-\omega_\alpha^2\mu_j^2}=1, \tag{32}$$

where a_j and μ_j have their usual meaning.

The characteristic equation (32) is an algebraic equation of n-th order with respect to ω_α^2. It has 2n different nonzero roots which can be grouped in pairs $\pm\omega_\alpha(\alpha=1,2,\ldots,n)$. An analagous characteristic equation is obtained in ref. 6 in the solution of the problem of the transfer of radiation in an atmosphere with plane-parallel layers under conditions of isotropic scattering. The system of n equations (31) is sufficient to uniquely determine n unknown C_α's. The formal solution to the problem in the n-th approximation is accomplished by Eqs. (31) and (32).

Let us ascertain the consequencies of equations (31) and (32). We multiply the left and right sides of Eq. (32) by C_α and sum over the index α. Changing the order of summation with respect to the indices α and j and taking (31) into consideration, we obtain

$$\sum_{\alpha=1}^{n}C_\alpha=Q\sum_{j=1}^{n}\frac{a_j}{\mu_j^2}. \tag{33}$$

Let us examine the behavior of the average intensity of the diffuse radiation $J(\tau)$ at the origin as $\tau\to0$. The intensity is connected with $M_0(\tau)$ by Eq. (14). Replacing the second term in (26) by its approximate value, we have

$$M_0(\tau)=\frac{1}{\tau}\left[\sum_{\alpha=1}^{n}C_\alpha e^{-\omega_\alpha\tau}-Q\sum_{j=1}^{n}\frac{a_j}{\mu_j^2}e^{-\frac{\tau}{\mu_j}}\right]. \tag{34}$$

As τ goes to zero, we obtain an indeterminate form of the 0/0 type. Applying L'Hospital's rule, we find

$$\lim_{\tau\to0}M_0(\tau)=-\sum_{\alpha=1}^{n}C_\alpha\omega_\alpha+Q\sum_{j=1}^{n}\frac{a_j}{\mu_j^2}. \tag{35}$$

Expression (35) indicates that the average intensity of the diffuse radiation at the origin in the final approximation is finite and nonnegative. The latter assertion is based on the inequality $1/\mu_\alpha>\omega_\alpha$, which is a consequence of the characteristic equation (32). If there is no scattering in the medium, i.e., $\lambda=0$, then the inequality sign must be replaced by an equal sign, and we then have $M_0(0)=0$. This result agrees with theories of the properties of a nonscattering medium.

We now turn to an examination of the diffuse radiation flux $F(\tau)$, which is determined from $M_1(\tau)$ by Eq. (15). We write out the first equation of system (16)

$$\frac{1}{\sqrt{3}}\frac{d}{d\tau}\sqrt{3}M_1(\tau)=-(1-\lambda)M_0(\tau)+\lambda Q\frac{e^{-\tau}}{\sqrt{3}}. \tag{36}$$

This equation is completely general and is independent of the equation with even l on which the infinite system of equations (16) terminates; i.e., it is independent of the choice of the order of approximation. Substituting (26) into Eq. (36) and integrating over τ, we obtain

$$M_1(\tau) = (1-\lambda)\sum_{\alpha=1}^{n} C_\alpha \frac{(1+\omega_\alpha\tau)\,e^{-\omega_\alpha\tau}}{(\omega_\alpha\tau)^2} - Q\frac{e^{-\tau}}{\tau^2}. \qquad (37)$$

We see that the diffuse radiation flux consists of two parts. The first part is the total radiation flux, and the second part the direct radiation flux. We point out that in an absorbing medium, the total radiation flux diminishes as τ increases by a law which is more complex than the inverse square law. The latter, as is well known, is fulfilled in a purely scattering medium or in a vacuum.

Let us evaluate the diffuse radiation flux at the origin. As τ goes to zero in formula (37), we obtain the expression

$$(1-\lambda)\sum_{\alpha=1}^{n}\frac{C_\alpha}{\omega_\alpha^2} - Q,$$

in the numerator; this expression proves to be equal to zero. Approaching a limit again leads to an indeterminate form of the 0/0 type, which when evaluated by L'Hospital's rule, yields

$$\lim_{\tau\to 0} M_1(\tau) = \frac{\lambda}{2}\sum_{\alpha=1}^{n} C_\alpha. \qquad (38)$$

It follows from (38) that the diffuse radiation flux at the origin is in the final approximation finite and nonnegative. It can be stated on the basis of (33) that as $n \to \infty$, the diffuse radiation flux at the origin increases without limit. For a nonscattering medium ($\lambda = 0$), we obtain the natural result that $M_1(0) = 0$.

III

Let us examine the case of conservative scattering. The straightforward consequence of radiation transfer in such a medium must be the inverse square law with respect to the total flux of radiant energy. Let us prove this.

Assuming that $\lambda = 1$ and $\omega_\alpha = 0$ in (37) we approach the limit of pure scattering; in addition, when a summation is made over the index α, all of the terms vanish except the last one, which becomes indeterminate. We make use of the properties of the roots of the characteristic equation (32) to eliminate the indeterminate form. Getting rid of the denominator and grouping corresponding terms, we obtain

$$1-\lambda = \prod_{j=1}^{n} p_j^2 \prod_{\alpha=1}^{n} \omega_\alpha^2. \qquad (39)$$

Substituting (39) into (37) and approaching the limiting case of pure scattering, we have

$$\lim_{\lambda\to 1} M_1(\tau) = \prod_{j=1}^{n} p_j^2 \prod_{\alpha=1}^{n-1} \omega_\alpha^2 \frac{C_n}{\tau^2} - Q\frac{e^{-\tau}}{\tau^2}. \qquad (40)$$

We will also use the properties of the roots of the characteristic equation (32) for the limiting case $\lambda = 1$, $\omega_n = 0$; we see that

$$\prod_{j=1}^{n} p_j^2 \prod_{\alpha=1}^{n-1} \omega_\alpha^2 = \sum_{j=1}^{n} a_j p_j^2 = \frac{1}{3}. \qquad (41)$$

As a result, we find for the function $M_1(\tau)$

$$M_1(\tau) = \frac{C_n}{3\tau^2} - Q\frac{e^{-\tau}}{\tau^2}. \qquad (42)$$

It will be shown that in this case the coefficient C_n, expressed in terms of the power of source Q, is independent of the number of the approximation n and equals 3. We write the system of equations (31) for the case of the conservative problem. Multiplying each of the equations of the system by the corresponding products $a_j\mu_j^2$ and summing over the index j, we obtain

$$\sum_{j=1}^{n} a_j p_j^2 \sum_{\alpha=1}^{n-1} \frac{C_\alpha}{1-\omega_\alpha^2 p_j^2} + C_n \sum_{j=1}^{n} a_j p_j^2 = Q\sum_{j=1}^{n} a_j.$$

Changing the order of summation in the first term and making use of the characteristic equation (32) for the particular case $\lambda = 1$, we demonstrate that the first term is equal to zero. On the other hand, since

$$\sum_{j=1}^{n} a_j = 1, \quad \sum_{j=1}^{n} a_j p_j^2 = \frac{1}{3},$$

we have

$$\frac{1}{3} C_n = Q,$$

and our statement is proved. Substituting C_n in (42), we obtain

$$M_1(\tau) = Q\frac{1-e^{-\tau}}{\tau^2}. \qquad (43)$$

Making use of (2), (5), and (15), we go over to the diffuse radiation flux

$$F(\tau) = \frac{Q\Phi}{4\pi r^2}(1-e^{-\alpha\rho\tau}) \qquad (44)$$

and finally obtain the total radiation flux

$$F_\Phi(r) = \frac{Q\Phi}{4\pi r^2}. \qquad (45)$$

Relationships (44) and (45) are accurate for approximations of any order. Hence it can be concluded that (44) and (45) are correct relationships. These relationships are obvious, but the fact that they are obtained from a solution of the Milne problem for a sphere can serve to some degree as a criterion of internal consistency among the fundamental premises and conditions which are assumed in the theory and those used in the course of the solution.

Thus the inverse square law is strictly fulfilled with regard to the total radiation flux in a purely scattering atmosphere. Inasmuch as $1/\alpha\rho = l$, is the mean free path with respect to scattering for radiation of frequency ν, we see that for distances from the source of the order of several path lengths, the role of direct radiation becomes insignificant, and the diffuse radiation flux which falls off as $1/r^2$ takes on decisive importance. If $r \ll l$, the diffuse radiation flux varies as $1/r$ and increases without limit toward the center as $r \to 0$, regardless of the order of approximation.

We find the average radiation intensity in the conservative case from equation (26), assuming that in this equation, $\omega_n = 0$.

$$M_0(\tau) = \frac{1}{\tau}\left[\sum_{\alpha=1}^{n-1} C_\alpha e^{-\omega_\alpha\tau} + C_n - Q\frac{e^{-\tau}}{\tau}\right]. \qquad (46)$$

As before, we see that the average diffuse radiation intensity at the origin is in the final approximation finite and nonnegative.

It is worthy of note that $M_0(\tau)$ depends on the order of the approximation n in both the nonconservative case and in the case of a purely scattering medium. In addition to this, the function $M_0(\tau)$ is finite at the origin for finite n in both cases. It must be assumed that this condition has a close connection with the relationship that

was established in ref. 6 between the order of the approximation and the multiplicity of the radiation scattering. A similar condition occurs for the flux in the nonconservative case.

We have seen that the source function, the average intensity, and the radiation flux can be described analytically to any order of approximation. This is not the case, however, for an analytical representation of the distribution function of radiation intensity with respect to direction. An expression for the intensity $I(\tau, \mu)$ can be obtained to any degree of approximation by substituting (25) into the solution (8); however the integrals remaining inside the summation sign are not used in the final form. A calculation of the quantity of radiation arriving at a given point within the limits of any finite solid angle also requires the application of numerical methods of integration.

We have confined ourselves to the spherical indicatrix of scattering solely for the sake of simplicity. Generalization of the problem to the case of an arbitrary indicatrix of scattering does not introduce any essential difficulties if it is assumed that the indicatrix can be expanded in a series of Legendre polynomials.

In conclusion, I should like to express my gratitude to M. A. El'yashevich for suggesting the topic and discussing these results.

REFERENCES

1. V. A. Ambartsumyan, Byull. Erev. Astron. Obs. No. 6 (1945).
2. S. Chandrasekhar, Astrophys. J. 101, 1 (1945).
3. R. Marshak, Phys. Rev. 71, 7 (1947).
4. O. I. Leipunskii, "Gamma-izluchenie atomnogo vzryva" (The Gamma Radiation of Atomic Explosions). Atomizdat, 1959.
5. M. Krook, Astrophys. J. **122**, No. 3 (1955).
6. S. Chandrasekhar, "Perenos luchistoi energii" (The Transfer of Radiant Energy). Izd. Inostrannoi Lit., Moscow, 1953.
7. V. I. Smirnov, "Kurs vysshei matematiki" (A Course in Higher Mathematics), Vol. III. Gosudarst. Izd. Fiz. Mat. Lit., Moscow, 1958.

PRINCIPLES OF THE THEORY OF THE SYNTHESIS OF COATED ABSORBING LAYERS

P. G. Kard

Received 28 November 1959

Optical layers are investigated which consist of a number of absorbing layers separated by nonabsorbing interlayers. Necessary and sufficient conditions are found for the composition of the system in order that the transmitted light be maximized. The number, location, thickness, and optical parameters of the absorbing layers are assumed to be prescribed, whereas the conditions for the coating are related to the nonabsorbing interlayers. It is shown that the effect of the coating depends only on the properties of the absorbing layers, and a simple relation is found for this dependence.

INTRODUCTION

It was recently shown by the author[1] that the notion of a conjugate system is very useful in the theory of absorbing layers. Two systems of layers are said to be conjugate to each other if their corresponding layers have the same thicknesses and the refractive indices of the corresponding layers (including the terminating media) of the two systems are complex conjugates of each other. The direction of the incident light is assumed to be normal to the layer system.

Using the concept of the conjugate system the following formulas have been derived in ref. 1. (The second of Eqs. (1), which was known previously, is quoted here for the sake of completeness.)

$$\left.\begin{aligned} a' &= -\delta^*, \\ b' &= b, \end{aligned}\right\} \tag{1}$$

$$b\delta^* - a\delta^* = 1, \tag{2}$$

$$\left.\begin{aligned} a &= a_1 b_2 e^{i\chi} + a_2 b_1^* e^{-i\chi}, \\ b &= b_1 b_2 e^{i\chi} + a_2 a_1^* e^{-i\chi}. \end{aligned}\right\} \tag{3}$$

In these formulas

$$\left.\begin{aligned} a &= \frac{r}{d}, \\ b &= \frac{1}{d}, \end{aligned}\right\} \tag{4}$$

where r and d are the amplitude coefficients of reflection and transmission respectively of the system. In this paper we will denote by R, D, and A the energy coefficients of reflection, transmission, and absorption, respectively. An asterisk indicates a conjugate complex quantity, the sign ~ a conjugate coating, and quantities which refer to the case of light incident from the reverse side are marked with a dash. In Eqs. (3), which represent an improvement of the equations derived by Vlasov, the indices 1 and 2 refer to the first and second layers which are separated by an absorbing or transparent interlayer. Furthermore, for normal incidence,

$$\chi = knh \tag{5}$$

where k is the wave number in vacuum and n and h are the refractive index and thickness, respectively, of the intermediate layer.

Equations (1), (2), and (3) are valid without any limitations (assuming, of course, that all media are isotropic) and the terminating media as well as the layers can be absorbing. However, in this paper it will be assumed that the front medium and the backing are both nonabsorbing.

In addition to Eqs. (1), (2), and (3), we also need here certain results which are derived from them in another paper[2] of the author.

1. The quantities

$$b\tilde{b}^* - a\tilde{a}^* - 1 = \frac{A}{D} \equiv K \tag{6}$$

and

$$\tilde{a}b - a\tilde{b} \equiv Ue^{i\beta} \tag{7}$$

are independent of the properties of the front medium and of the portion of the layer system which is located between the front medium and the first absorbing layer. The indicated quantities are determined by the properties of only the portion of the system which starts with the first absorbing layer (inclusive) and also of the backing.

2. The quantity

$$P \equiv \frac{1}{2}(K + \bar{K}) \qquad (8)$$

depends only on the properties of the portion of the system which is located between the first and last absorbing layers and includes all absorbing layers together with the interspersed nonabsorbing interlayers. This quantity does not depend on the properties of the outer nonabsorbing layers or on the properties of the front medium or the backing. It is also independent of the direction of light incidence, i.e.,

$$P' = P. \qquad (9)$$

For future use it is convenient to introduce a quantity φ defined by

$$\cosh\varphi = 1 + P. \qquad (10)$$

FORMULATION OF THE PROBLEM

Assume that the terminating media and the absorbing skeleton of the layer system are given. By the latter term we mean the succession of absorbing layers with fixed values for the thicknesses and refractive indices. We number this succession with indices 1, 2, ..., N, going in the direction from the front medium to the backing. Each of these layers, according to Eqs. (8) and (10), is characterized by the quantities P_i and φ_i (i = 1, 2, ..., N) which depend on the properties of the given layer only. It can be readily shown[3] that

$$\cosh\varphi_i = \frac{\gamma_i^2\cosh 2\beta_i + \varkappa_i^2\cos 2\alpha_i}{\gamma_i^2 + \varkappa_i^2}, \qquad (11)$$

where $\eta_i - i\varkappa_i$ is the refractive index of the i-th layer, h_i is its thickness, and

$$\left.\begin{aligned}\alpha_i &= k\gamma_i h_i,\\ \beta_i &= k\varkappa_i h_i.\end{aligned}\right\} \qquad (12)$$

The problem consists in filling in with nonabsorbing layers all spaces between the individual layers of the skeleton and also between the last layer and the backing in such a way as to minimize the quantity A/D. It is also necessary to find this minimum value of A/D, as well as the necessary and sufficient conditions for its realizability. The formulated problem is thus a problem of the synthesis of coated absorbing layers.

DEFINITIONS

We separate out in the layer system N interlayers (one for each of the interspaces between the layers of the skeleton and one for the interspace between the last layer and the backing) from the total number of nonabsorbing interlayers. We denote these interspace layers with the indices 1, 2, ..., N, in such a way that the i-th interspace layer follows after the i-th absorbing layer. It is convenient here to assume that the last (i.e., N-th) interspace layer is adjacent to the N-th layer of the skeleton, although the location of the other interspace layers can be arbitrarily chosen. In addition to these prescribed layers there can be additional nonabsorbing layers in the interspaces between the layers of the framework. The scheme of the system is shown in the accompanying figure. The entire system is thus subdivided by the interspace layers into N + 1 subsystems. In each of the first N subsystems there is one absorbing layer (designated with the same index) surrounded by nonabsorbing (generally, multilayer) interlayers. The (N + 1)-th subsystem is entirely nonabsorbing.

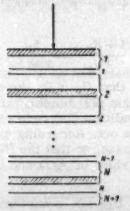

A group of subsystems superposed one on top of the other with the indices i, i + 1, ... k − 1, k, together with the interspace layers between them will be designated as the ik-th subsystem (this subsystem lies between the (i − 1)-th and k-th interspace layers). Thus, the "subsystem" which coincides with the entire system should be designated by the indices 1, N + 1. These indices, however, will be left out. The k-th subsystem will occasionally be denoted as the (kk)-th.

All quantities related to the subsystems (those already introduced as well as those to be defined below) will be designated by the same indices as the corresponding subsystems. For example, a_{i1}, $\bar{a}_{23}$, a'_{i}, b_{12}, K_{23}, $\bar{K}_{12}$, U'_{2}, σ_3, φ_{13}, etc. As was already pointed out previously the quantities P and φ for each of the subsystems do not depend on the properties of its nonabsorbing boundary layers.

We introduce a new quantity

$$S \equiv \frac{1}{2}(K - \bar{K}), \qquad (13)$$

so that

$$\left.\begin{aligned}K &= P + S,\\ \bar{K} &= P - S.\end{aligned}\right\} \qquad (14)$$

and

$$\left.\begin{aligned}\bar{P} &= P,\\ \bar{S} &= -S.\end{aligned}\right\} \qquad (15)$$

We observe that $S > 0$ always, since $K > 0$ and $\bar{K} < 0$ (see ref. 2).

Furthermore, let

$$\left.\begin{aligned}a &= |a|\,e^{i\alpha},\\ b &= |b|\,e^{i\beta}\end{aligned}\right\} \qquad (16)$$

and (by analogy with Eq. (5))

$$\alpha_i = k\eta_i h_i, \quad i = 1, 2, \ldots N. \qquad (17)$$

Since only the magnitude of φ is determined by Eq. (10) we assume that

$$\varphi > 0, \quad \bar{\varphi} = -\varphi < 0. \qquad (18)$$

We also recall one of the relations derived in ref. 2, namely,

$$S^2 - U^2 = P(P + 2) = \sinh^2\varphi. \qquad (19)$$

SOLUTION OF THE PROBLEM

We first consider the layer system as a combination of the (1N)-th and (N + 1)-th subsystems. In ref. 2 it was shown that the minimum value of K, given by

$$K_{\min.} = e^{\gamma_{1N}} - 1, \tag{20}$$

is obtained for such a combination when

$$\cos(2\alpha_N + \sigma_{1N} - \mu_{N+1} + \nu_{N+1}) = -1 \tag{21}$$

and

$$\frac{1 + R_{N+1}}{D_{N+1}} = \frac{S_{1N}}{\sinh\gamma_{1N}}. \tag{22}$$

It is here assumed that $U_{1N} \neq 0$. However, if $U_{1N} = 0$, Eq. (20) and condition (22) remain valid (except that in view of Eq. (19) condition (22) reduces to $R_{N+1} = 0$) and condition (21) drops out. According to Eqs. (10) and (19), $K_{\min} = K_{1N}$ in this case, so that the (N + 1)-th subsystem does not affect the value of A/D and is therefore superfluous.*

*Besides, the case $U_{1N} = 0$ is not feasible since this requires that also $U_N = 0$ (see Eq. (39) below). However, this is incompatible with our choice for the position of the N-th interspace layer.

A further problem is the determination of the minimum value of φ_{1N}.

Equation (20) does not determine $K_{\min}$ explicitly. It only reduces the problem to the determination of the minimum value of φ_{1N}. We will therefore consider now the (1N)-th subsystem.

Using Eqs. (8), (10), and (18) we observe that

$$K = 2(\cosh\gamma_{1N} - 1) - (e^{\gamma_{1N}} - 1),$$

that is,

$$K = e^{\gamma_{1N}} - 1. \tag{23}$$

Consequently, according to Eq. (13), $S = \sinh\varphi_{1N}$, or since $\varphi_{1N} = \varphi$,

$$\left.\begin{aligned} S &= \sinh\gamma, \\ U &= 0. \end{aligned}\right\} \tag{24}$$

We will now determine the minimum value of φ_{1N}. This is equivalent to the minimization problem of P_{1N}. To solve this problem we will consider the (1N)-th subsystem as a combination of the (1, N − 1)-th and the N-th subsystems. Applying Eq. (3) to this case and taking Eq. (1) into account we obtain

$$\left.\begin{aligned} a_{1N} &= a_{1,N-1} b'_N e^{i\alpha_N} - b^*_{1,N-1} a'_N e^{-i\alpha_N - \gamma_{N-1}}, \\ b_{1N} &= b_{1,N-1} b'_N e^{i\alpha_N} - a^*_{1,N-1} a'_N e^{-i\alpha_N - \gamma_{N-1}} \end{aligned}\right\} \tag{25}$$

Using Eq. (6) we can now calculate P_{1N}. Taking Eq. (7) into account we find that

$$P_{1N} = -1 + \frac{1}{2}(K_{1,N-1} + 1)(K'_N + 1) + \frac{1}{2}(K_{1,N-1} + 1)(K'_N + 1) - U_{1,N-1} U'_N \cos(2\alpha_{N-1} + \sigma_{1,N-1} + \sigma'_N). \tag{26}$$

Using Eqs. (9), (10), (14), and (19) this equation can be rewritten as

$$\cosh\gamma_{1N} = \cosh\gamma_{1,N-1}\cosh\gamma_N + S_{1,N-1} S'_N - \sqrt{S^2_{1,N-1} - \sinh^2\gamma_{1,N-1}}\sqrt{S'^2_N - \sinh^2\gamma_N}\cdot\cos(2\alpha_{N-1} + \sigma_{1,N-1} + \sigma'_N). \tag{27}$$

We must find the minimum value of φ_{1N}. If $U_{1,N-1} \neq 0$ and $U'_N \neq 0$ we must obviously set

$$\cos(2\alpha_{N-1} + \sigma_{1,N-1} + \sigma'_N) = 1. \tag{28}$$

Moreover, $\cosh\varphi_{1N}$ depends on $S_{1,N-1}$ and S'_N and on $\varphi_{1,N-1}$ and φ_N. According to Eq. (11), the latter quantity is fixed. We assume also that $\varphi_{1,N-1}$ is temporarily fixed and we will find the minimum of $\cosh\varphi_{1N}$ with respect to $S_{1,N-1}$ and S'_N. Corresponding calculations give (using Eq. (28))

$$\frac{S_{1,N-1}}{\sinh\gamma_{1,N-1}} = \frac{S'_N}{\sinh\gamma_N}, \tag{29}$$

from which, according to Eq. (19), it also follows that

$$\frac{U_{1,N-1}}{\sinh\gamma_{1,N-1}} = \frac{U'_N}{\sinh\gamma_N} \tag{30}$$

and

$$\frac{U_{1,N-1}}{S_{1,N-1}} = \frac{U'_N}{S'_N}. \tag{31}$$

Assuming conditions (28) and (29) to be fulfilled, we find that

$$\cosh\gamma_{1N} = (\cosh\gamma_{1N})_{\min.} = \cosh\gamma_{1,N-1}\cosh\gamma_N + \sinh\gamma_{1,N-1}\sinh\gamma_N,$$

that is,

$$\gamma_{1N} = (\gamma_{1N})_{\min.} = \gamma_{1,N-1} + \gamma_N. \tag{32}$$

The same result is also obtained in the case when $U_{1,N-1} = 0$ or $U'_N = 0$. The minimization of P_{1N} requires that if one of these quantities is equal to zero the other quantity must also be equal to zero. Consequently, the condition (29) and the equivalent conditions (30) and (31) also remain valid. However, condition (28) is in this case superfluous.

The value of φ_N in Eq. (32), in view of Eq. (11), is fixed. Consequently, the problem of determining $(\varphi_{1N})_{\min}$ can again be reduced (by a recursion relation) to the same problem with a smaller number of layers. Repeating the above reasoning N − 2 times and adding all the results we find that

$$\frac{A}{D} = \left(\frac{A}{D}\right)_{\max.} = e^{\gamma_1 + \gamma_2 + \ldots + \gamma_N} - 1, \tag{33}$$

if firstly,

$$\left.\begin{aligned} U_{1k}[\cos(2\alpha_k + \sigma_{1k} + \sigma'_{k+1}) - 1] &= 0, \\ k &= 1, 2, \ldots N-1, \\ U_{1N}[\cos(2\alpha_N + \sigma_{1N} - \mu_{N+1} + \nu_{N+1}) + 1] &= 0, \end{aligned}\right\} \tag{34}$$

and, secondly,

$$\left.\begin{aligned} \frac{S_{1k}}{\sinh\gamma_{1k}} &= \frac{S'_{k+1}}{\sinh\gamma_{k+1}}, \quad k = 1, 2, \ldots N-1, \\ \frac{S_{1N}}{\sinh\gamma_{1N}} &= \frac{1 + R_{N+1}}{D_{N+1}}, \end{aligned}\right\} \tag{35}$$

where

$$\left.\begin{aligned} \gamma_{1k} &= \gamma_1 + \gamma_2 + \cdots + \gamma_k, \\ k &= 1, 2, \ldots N. \end{aligned}\right\} \tag{36}$$

Equations (33), (34), (35), and (36) contain the complete solution of the problem. We note that (35) can also be rewritten in the form

$$\left.\begin{aligned} \frac{U_{1k}}{\sinh\gamma_{1k}} &= \frac{U'_{k+1}}{\sinh\gamma_{k+1}}, \quad k = 1, 2, \ldots N-1, \\ \frac{U_{1N}}{\sinh\gamma_{1N}} &= \frac{2\sqrt{R_{N+1}}}{D_{N+1}}. \end{aligned}\right\} \tag{37}$$

SOME TRANSFORMATIONS

The solution found in the preceding Section can be rewritten in a more simple form, namely, in a form in

which the conditions for the coating are expressed only in terms of quantities related to the subsystems with only one absorbing layer (and thus designated by a single index).

First we wish to make the following remark. When $U_{1k} = 0$ (and $U'_{k+1} = 0$) the phases σ_{1k} and σ'_{k+1} lose any meaning (see Eq. (7)), that is, they can assume arbitrary values. Consequently, even if we cannot now impose any conditions on the thickness of the k-th layer, we can formally assume that the relations

$$\left.\begin{aligned} &\cos(2\alpha_k + \sigma_{1k} + \sigma'_{k+1}) = 1, \\ &k = 1, 2, \ldots N-1, \\ &\cos(2\alpha_N + \sigma_{1N} - \mu_{N+1} + \nu_{N+1}) = -1 \end{aligned}\right\} \tag{38}$$

are fulfilled. It is only necessary to keep in mind that the above conditions imposed on the thicknesses of the layers have a real meaning only when $U_{1k} \neq 0$.

We will now determine

$$U_{1,k+1}e^{i\sigma_{1,k+1}} = a_{1,k+1}b_{1,k+1} - a_{1,k+1}\delta_{1,k+1}$$

(k = 1, 2, ... N − 1), considering the (1, k + 1)-th subsystem as a combination of the (1k)-th and (k + 1)-th subsystems. Using, in accordance with Eq. (3), the relations

$$a_{1,k+1} = a_{1k}b_{k+1}e^{i\alpha_k} + a_{k+1}\delta^*_{1k}e^{-i\alpha_k},$$

$$b_{1,k+1} = b_{1k}b_{k+1}e^{i\alpha_k} + a_{k+1}a^*_{1k}e^{-i\alpha_k},$$

and corresponding relations for $\tilde{a}_{1,k+1}$ and $\tilde{b}_{k+1}$ and substituting these relations in the foregoing formula, we find that

$$\begin{aligned} U_{1,k+1}e^{i\sigma_{1,k+1}} &= (b_{1k}b^*_{1k} - a_{1k}a^*_{1k})a_{k+1}b_{k+1} - (\delta_{1k}b^*_{1k} - a_{1k}a^*_{1k}) \\ &\times a_{k+1}\delta_{k+1} + b_{k+1}\delta_{k+1}(a_{1k}b_{1k} - a_{1k}\delta_{1k})e^{2i\alpha_k} \\ &+ a_{k+1}a_{k+1}(a^*_{1k}b^*_{1k} - a^*_{1k}\delta^*_{1k})e^{-2i\alpha_k} \\ &= (1 + K_{1k})a_{k+1}b_{k+1} - (1 + K_{1k})a_{k+1}\delta_{k+1} + b_{k+1}\delta_{k+1}U_{1k}e^{i(2\alpha_k+\nu_k)} \\ &+ a_{k+1}a_{k+1}U_{1k}e^{-i(2\alpha_k+\nu_k)}. \end{aligned}$$

Now

$$e^{i(2\alpha_k+\nu_k)} = e^{-i\mu'_{k+1}}$$

and

$$\frac{U_{1k}}{\sinh\gamma_{1k}} = \frac{U'_{k+1}}{\sinh\gamma_{k+1}}.$$

Considering also Eqs. (10) and (14) we obtain

$$\begin{aligned} U_{1,k+1}e^{i\sigma_{1,k+1}} &= \cosh\gamma_{1k}U_{k+1}e^{i\sigma_{k+1}} + S_{1k}(a_{k+1}b_{k+1} + a_{k+1}\delta_{k+1}) \\ &+ \frac{\sinh\gamma_{1k}}{\sinh\gamma_{k+1}}[b_{k+1}\delta_{k+1}(a''_{k+1}b'_{k+1} - a''_{k+1}\delta''_{k+1}) + \\ &+ \sigma_{k+1}a_{k+1}(a'_{k+1}b'_{k+1} - a'_{k+1}\delta'_{k+1})]. \end{aligned}$$

Using Eqs. (1) and (9) this gives

$$\begin{aligned} U_{1,k+1}e^{i\sigma_{1,k+1}} &= \cosh\gamma_{1k}U_{k+1}e^{i\sigma_{k+1}} + S_{1k}(a_{k+1}b_{k+1} + a_{k+1}\delta_{k+1}) \\ &+ \frac{\sinh\gamma_{1k}}{\sinh\gamma_{k+1}}[a_{k+1}b_{k+1}(1 + K'_{k+1}) - a_{k+1}\delta_{k+1}(1 + K'_{k+1})] \\ &= \cosh\gamma_{1k}U_{k+1}e^{i\sigma_{k+1}} + S_{1k}(a_{k+1}b_{k+1} + a_{k+1}\delta_{k+1}) \\ &+ \frac{\sinh\gamma_{1k}\operatorname{ch}\gamma_{k+1}}{\sinh\gamma_{k+1}}U_{k+1}e^{i\sigma_{k+1}} - \frac{\sinh\gamma_{1k}}{\sinh\gamma_{k+1}}S'_{k+1}(a_{k+1}b_{k+1} + a_{k+1}\delta_{k+1}). \end{aligned}$$

In view of Eq. (35) the terms containing S_{1k} and S'_{k+1} cancel out and we obtain, finally,

$$\frac{U_{1,k+1}e^{i\sigma_{1,k+1}}}{\sinh\gamma_{1,k+1}} = \frac{U_{k+1}e^{i\sigma_{k+1}}}{\sinh\gamma_{k+1}} \tag{39}$$

It thus follows that, firstly,

$$\left.\begin{aligned} \frac{S_{1,k+1}}{\sinh\gamma_{1,k+1}} &= \frac{S_{k+1}}{\sinh\gamma_{k+1}}, \\ \frac{U_{1,k+1}}{\sinh\gamma_{1,k+1}} &= \frac{U_{k+1}}{\sinh\gamma_{k+1}}, \end{aligned}\right\} \tag{40}$$

and, secondly,

$$\sigma_{1,k+1} = \sigma_{k+1}, \tag{41}$$

where the last relation can be assumed to hold also in the case $U_{1,k+1} = U_{k+1} = 0$.

The relations in Eq. (40) hold for all $k < N$. Comparing them with relations (35) and (37), we find that

$$\left.\begin{aligned} \frac{S_k}{\sinh\gamma_k} &= \frac{S'_{k+1}}{\sinh\gamma_{k+1}}, \quad k < N \\ \frac{S_N}{\sinh\gamma_N} &= \frac{1 + R_{N+1}}{D_{N+1}} \end{aligned}\right\} \tag{42}$$

and

$$\left.\begin{aligned} \frac{U_k}{\sinh\gamma_k} &= \frac{U'_{k+1}}{\sinh\gamma_{k+1}}, \quad k < N, \\ \frac{U_N}{\sinh\gamma_N} &= \frac{2\sqrt{R_{N+1}}}{D_{N+1}}. \end{aligned}\right\} \tag{43}$$

In an analogous way relations (38) assume the form

$$\left.\begin{aligned} &\cos(2\alpha_k + \sigma_k + \sigma'_{k+1}) = 1, \quad k < N, \\ &\cos(2\alpha_N + \sigma_N - \mu_{N+1} + \nu_{N+1}) = -1. \end{aligned}\right\} \tag{44}$$

We have thus shown that the conditions (35) and (38) for minimizing light absorbtion can be reduced to the equations (42) and (44). Conversely, one can derive the conditions (35) and (38) from Eqs. (42) and (44). Indeed, when k = 1 conditions (35) and (38) and Eqs. (42) and (44) coincide. But it was shown that Eqs. (35) and (38) may be transformed into Eqs. (40) and (41). However, the latter Eqs. for k = 1, together with Eqs. (42) and (44) for k = 2, result in Eqs. (35) and (38) for k = 2. Thus, passing successively from k to k + 1, one readily obtains Eqs. (35) and (38) from Eqs. (42) and (44).

DISCUSSION OF THE RESULTS

We have found necessary and sufficient conditions for the synthesis of coated absorbing layers with a prescribed skeleton. These conditions are given by Eqs. (42) and (44). From the relations (42) one obtains the equivalent relations (43), and in (44) only those relations have any meaning for which σ_k is determined (that is, $U_k \neq 0$). Obviously, all conditions for the coated layers can be, in principle, readily satisfied, since Eqs. (44) determine the thicknesses of the interspace layers and in each of the relations (42) with $k < N$ the left-hand side of the equations depends only on the properties of the layers located behind the k-th absorbing layer down to the k-th interspace layer (inclusive), whereas the right-hand side depends only on the properties of the layers located in front of the (k + 1)-th absorbing layer up to the k-th interspace layer (inclusive). Thus, each of the relations (42) (with $k < N$) depends only on the properties of the layers lying in a single interspace between the layers of the skeleton and can be satisfied by a proper choice of the parameters of this interlayer.

Condition (42) with k = N can be satisfied by a proper choice of the parameters of the layers located between the N-th layer of the skeleton and the backing.

In spite of the fact that the conditions (42) and (44) are not only sufficient but also necessary they still leave much freedom, since the value of the ratio $S_k/\sinh\varphi_k$ in (42) can be chosen in a great variety of ways. Coated absorbing layers can thus be synthesized to satisfy a great variety of conditions as to their optical properties. This question, however, will not be discussed in the present paper.

If conditions (42) and (44) are satisfied, then the ratio A/D has a minimum which is determined by Eq. (33). When the absorbing layers are sufficiently thin so that the sum $\varphi_1 + \varphi_2 + \ldots + \varphi_N$ is sufficiently small, then, approximately,

$$\left(\frac{A}{D}\right)_{min} = \gamma_1 + \gamma_2 + \ldots + \gamma_N,$$

or, in view of Eqs. (11) and (12),

$$\left(\frac{A}{D}\right)_{min} = \frac{8\pi^2}{\sqrt{3}} \cdot \frac{\sum_{i=1}^{N} \varkappa_i \gamma_i h_i^2}{\lambda^2}, \qquad (45)$$

where λ is the wavelength of the light in vacuum.

The practical value of the method discussed in this paper consists in the possibility of applying it to a number of actual problems. As an example, one can take the synthesis of coated interference filters with metallic reflecting surfaces. The discussed theory can in this case be applied equally as well when the number of reflecting layers is more than two as it can in the simplest case of two reflecting layers.

REFERENCES

1. P. G. Kard, Opt. i Spektr. 9, 95 (1960), Optics and Spectroscopy 9, 49 (1960).
2. P. G. Kard, Izvest. Akad. Nauk SSSR, Ser. Fiz.-Mat. i Tekh. nauk (in press).
3. P. G. Kard, Opt. i Spektr. 9, 248 (1960), Optics and Spectroscopy 9, 129 (1960).

OPTICAL SYSTEMS WITH ENHANCED RESOLVING POWER

A. I. Kartashev

Received 31 March 1959

Two new methods of optical image formation are described which under some conditions enable resolving powers to be attained that are higher than those obtained by the usual methods of observation of optical images.

It is well known that it is impossible to design and construct optical systems whose resolving power exceeds certain limiting values determined by the physical nature of light. Some new ways of obtaining optical images are described in this article.

Let the object (Fig. 1) be in the plane S in the object space and let it be projected by the optical system N into the plane S′ in the image space. Let us consider a portion A of the object consisting of the elements $a_1, a_2, a_3, \ldots, a_n$.

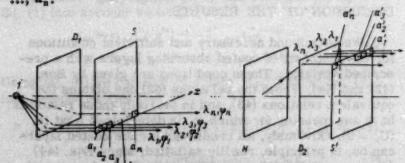

Fig. 1

The presence of such elements is equivalent to some given intensity distribution in the direction of the x-axis in the plane S.

If an equal light distribution is found in the image plane S′ the image and the object are said to be equal. When the images of the different elements $a_1, a_2, a_3, \ldots$, are smaller than the width of the first diffraction maximum the conclusions about the structure of the objective become less reliable. However, the structure of the image in this case can be determined using the following methods: we assign to each element of the object $a_1, a_2, \ldots$ a specific value of some quantity, for instance, of wavelength λ or path difference φ. A schematic diagram of such a system is shown in Fig. 1. Light from the source 1 passes through a dispersing system D_1 which enables the object S to be illuminated in such a way that a definite value of the wavelength $\lambda_1, \lambda_2, \ldots$ or path difference $\varphi_1, \varphi_2, \ldots$ corresponds to each of the elements $a_1, a_2, \ldots$. The series of elements $a_1, a_2, \ldots$ in the plane S can be regarded as an intensity distribution I in the x-direction, i.e., $I = f_1(x)$. The introduction of a dispersing system D introduces an additional condition according to which a wavelength λ corresponds to every point with the coordinate x, i.e., $\lambda = f_2(x)$, and hence for each value of λ there will be a corresponding value of the intensity:

$$I = F(\lambda). \qquad (1)$$

Here the intensity has been expressed as a function of wavelength and the coordinate x has been eliminated. The transference of this function into the image space is then carried out not by the usual method of optical imaging, but with the aid of a second dispersing system D_2 in which a definite wavelength λ corresponds to each point in the plane S′ with a coordinate x′.

From Eq. (1) it follows that for each value of λ there is a corresponding value of the intensity I, namely, that value which pertains to the point with the coordinate x in the object plane S. Thus, for each point x in the object plane with an intensity I there will be a corresponding point x′ in the image plane with a corresponding value of the intensity. We shall call such an image a "dispersion" image in contrast to the usual type of image.

Let us imagine an object placed at any desired long distance away from the optical system; all that can be done is to reproduce discrete parts of the image. The conception of the resolving power of the new optical systems is different from the conception applied to the usual optical systems. It must be noted that in every individual case the resolving power of the whole system will be determined by the resolving power of the first dispersing element. The increase (in resolving power) that we shall apply rationally is determined by the properties of this system. The above reasoning also holds for the case when the second function is given by the relationship $\varphi = f_2(x)$.

Let us assume that white light from the source 1 (Fig. 2) is projected by the condensing lens 2 onto the slit 3 of a spectroscope and that a spectrum is formed in the focal plane of the lens 4. The object, which consists of alternating transparent and opaque lines, is placed in the plane of this spectrum. Therefore, the intensity distribution in the spectrum changes in accordance with the change in the optical density of the object along the direction of the spectrum.

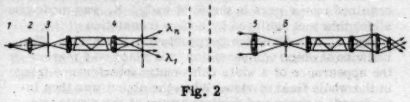

Fig. 2

The beam of light now coming from the object will possess a spectral composition determined by the elements of the object. A scattering medium could even be placed between the object and the observing system as long as the minimum amount of light necessary for its visual or photographic observation arrives at the observing system.

This scattering medium is represented by broken lines in Fig. 3. Part of the scattered light is condensed by the lens 5 onto the slit of the analyzing spectral apparatus 6 which can be a spectroscope or a spectrograph. The spectrum obtained in this way will be crossed by dark lines whose location will correspond to the opaque lines in the object. Thus a pattern is formed in the image plane of the spectrum of the analyzing apparatus which can be called an "image." This "dispersion" image differs in character from the images obtained with conventional optical systems, but is similar to a television image. The linear magnification of such a system is determined only by the ratio of the linear dispersions of the analyzing and dispersing systems. The resolving power in this case depends on the width of the entrance slit of the projecting dispersing system and the resolving power of the analyzing apparatus.

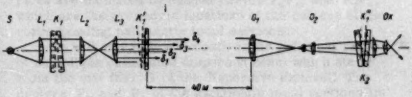

Fig. 3

In the case examined above the image is synthesized with the aid of two dispersing systems without which one generally cannot conceive the formation of an image. By developing the concept of a similar method of image synthesis one can design an optical system which has two simultaneous functions, namely: an objective forms a conventional image and this image is supplemented by obtaining an additional dispersion image which supplies details within the area of the first diffraction maximum which are not resolved by the objective on account of its limited aperture. Let us assume that the conventional optical system has a resolving power which permits the observation of individual elements of the object separated from one another by a distance greater than 1. However, in reality the object has a finer structure and in this element there are smaller elements a_1 to a_n. When using the conventional method of observation all the intermediate details of the object will not be observed as they do not emerge from the area of the first diffraction maximum. Out of the total number m of details in the object one can observe only a limited number of details, m/n. By employing the above-mentioned principles one can improve the performance of such an optical system whilst preserving the geometrical entrance parameters (the diameter of the entrance pupil or the aperture of the objective).

Figure 3 shows a schematic diagram of the second setup in which the principle of image formation proposed above is put into practive. An interference system is used here which assigns some certain value of the phase to every element of the object, in place of the dispersing element which assigned a certain wavelength to every element.

Let the object be a grating with alternating light and dark lines. The grating is illuminated by a source of white light S and a condensing lens L_1. An interference wedge K_1 is placed in the path of the beam and its image K_1' is formed by lenses L_2 and L_3 in the plane of the grating. The interference wedge consists of two glass flats whose internal surfaces are coated with reflecting layer systems with a high reflection coefficient (about 90%). The flats make a small angle with one another so that a wedge-shaped air gap is formed between them. The position of the wedge with respect to the grating is such that its edge is parallel to the lines of the grating.

Several coherent light rays which underwent multiple reflections in the wedge will, with such a method of illumination, emerge from each transparent part of the grating. Each element of the object (for instance, every transparent line) differs from its neighbor by reinforcing out of a large number of light rays a ray with a different path difference $\delta_1, \delta_2, \delta_3, \ldots$ etc. The phase change of the light rays is given by the relationship

$$\Delta\varphi_1 = \frac{\delta_1}{\lambda} - k$$

where k is a whole number. The phase change varies periodically over the field of view and has the same values at those points of the objects where the path differences of the light rays in the wedge differ by λ.

The object in such a system will send out light rays whose phase changes will be different over the extent of a linear section 1; the relationship of 1 to the wedge angle is given by the expression $\gamma = \lambda/21$.

Let the object which is illuminated in this way be imaged by the optical system O_1–O_2 (Fig. 3) in the plane K_1''. It is necessary for the linear resolving power of this system to be equal to the distance 1 if two adjacent interference orders are not to fall into one and the same diffraction maximum. Then elements which have the same phase change, but whose path differences differ by not less than λ, will fall into different diffraction maxima. In order to show the actual intensity distribution of the object within the area of the first diffraction maximum it is sufficient to place a wedge in the image plane which is similar to the first wedge. When this is done interference will take place. White light interference can be observed when the path differences $\delta_1, \delta_2, \delta_3, \ldots$ etc., associated with the points of the first wedge are equal to the path dif-

ferences at the corresponding points of the second wedge. Such a situation will exist when the parts of wedges K_1 and K_2 at which the rays undergo equal path differences are conjugate with one another.

The nature of the intensity distribution in an interference field in the case of multiple reflections, shown in Fig. 4 (curve III), is quite different from the diffraction intensity distribution, and the boundaries of the image of each individual element of the object will now be determined not by the width of the diffraction maximum (curve II) but by the width of the interference maximum. The resolving power of the system is increased by the above by a factor of $l/\Delta p$ where l is a distance equal to the separation between interference maxima and to the width of the diffraction maximum and Δp is the width of the interference maximum. The width of the latter is smaller the higher the reflection coefficient of the reflecting layers on the surfaces of the wedges. This ratio can achieve values between 10 and 20 which correspondingly increases the resolving power of the system by 10 to 20 times in comparison with conventional systems.

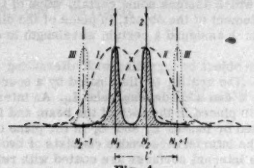

Fig. 4

The setup shown schematically in Fig. 3 was assembled for the experimental verification of the above considerations. A grating with a line separation of $a = 0.2$ mm and placed at a distance of 40 meters from the observing system served as the object. The wedge K_1 whose image was formed in the plane of the grating by the lenses L_2 and L_3 had an angle of $\gamma = 1'$. The field was illuminated with a white light source.

The observation was carried out using a telescope with an objective of 25 mm diameter. The theoretical resolving power of such a system is equal to 0.000,028, or, in linear dimensions, 1.1 mm in the object plane. The image produced by the telescope objective was examined with a microscope of $\times$ 600 magnification. Under these conditions the resolving power of the system was small and the image of the object was a washed-out field (Fig. 5a): the individual lines of the grating were not resolved.

Fig. 5

The analyzing system—the wedge K_2—had an angle $\gamma' = 3'$ and was placed in the focal plane of the eyepiece in such a way that a compensation of the path differences acquired by the rays in the first wedge K_1 was made possible; this was achieved by a slow translation of the wedge K_2 in a direction perpendicular to its edge. The instance at which compensation took place was marked by the appearance of a white achromatic interference fringe in the whole field of view. When the object was then introduced, a sharp and distinct image of the grating appeared with a distribution of lines in the field similar to that in the original (Fig. 5).

In this manner one could observe an "interference image" of elements of the object within the area of the first diffraction maximum. The image was supplemented with details which could not be seen when observing with conventional optical systems with an entrance pupil of the same diameter. The angular resolving power of all systems proved to be several times larger than that of the corresponding conventional systems but only in the direction corresponding to the direction of the dispersion.

The methods of optical image formation described above establish a basis for the construction of new optical systems with significantly increased observation potentialities.

ON THE PROPERTIES OF THE FOCAL SURFACES OF MIRROR SPECTROGRAPHS

S. A. Khrshanovskii

Received 27 November 1959

Properties of theoretical focal surfaces of spectrographic optical systems with a spherical camera mirror are investigated. The character of the changes in the shape of the focal curves as a function of the relative position of the dispersing element is investigated. Simple relations are found which permit one to follow the behavior of the central (i.e., working) portion of the investigated curves.

The focal surface of a spectrograph is the aggregate of the sharpest monochromatic images of the entrance slit. The shape of the focal surfaces depends very strongly on the type and parameters of the optical system and departs to a lesser or higher degree from a plane.[1] This is very inconvenient in the case of spectrographs. The shape of the focal surfaces depends strongly on the form of the dispersive system[2] and a sufficiently flat field often cannot be obtained in lens spectrographs even when multicomponent camera objectives of the photographic type are used. This problem has been solved in a relatively simple way only for a one-prism instrument with a mirror-lens objective.[3]

A flat field cannot generally be obtained in systems with a concave spherical diffraction grating; it is assumed that the spectrum is, in these cases, focused on a cylindrical surface which is formed by the astigmatic meridional focal sections. This assumption enables one to reduce the investigation of the properties of a focal surface to the study of the two-dimensional curve which is given by the intersection of the focal surface with the principal meridional plane of the system. This method can also be applied to plane-grating mirror spectrographs, which are gaining widespread use. In some of the systems described in the literature the focal surface is very curved,[4,5] in others a quite flat spectrum was obtained, but within relatively narrow limits.[6-9]

In the present paper an account is given of the results of an investigation of the properties of focal curves for systems of the type specified.

In Fig. 1 the meridional cross section of a common mirror spectrograph is shown. The dispersing element P is illuminated by a collimated beam of white light coming from the entrance slit, located on the axis of the system. We assume that after reflection from the surface O_pOO_q of the concave spherical camera mirror the collimated oblique dispersed beams with the principal rays GO_qF_q ... GOF_0 ... GO_pF_p converge in the image space to form astigmatic focal surfaces. In Fig. 1 these surfaces are indicated by dashed curves F_0F_m and F_0F_s, which are the grometric locations of the centers of the corresponding astigmatic focal sections.

We will now follow the path of the principal ray GO_pF_p of an oblique collimated dispersed beam which starts from the exit face G of the dispersive element. The centers F_m and F_s of the astigmatic focal sections lie on the reflected (at the point O) extension of this principal ray at the distances*

*For simplicity here and in the rest of the paper the indices p and q for the angles i, θ, and φ are left out.

$$\overline{O_pF_m} = \frac{R\cos i}{2} \text{ and } \overline{O_pF_s} = \frac{R}{2\cos i}$$

Described in a different way, the point F_m lies on the periphery of the circle $O_pF_mF_\varphi$ which crosses the radius $CO_p = R$ in the middle, and the point F_s lies on the straight line $F_\varphi F_s$ which is tangent to the above circle at the point F_φ. The formation of the astigmatic focal curves, to which we will in future refer as meridional (F_0F_m) and sagittal (F_0F_s), respectively, can be graphically visualized as follows. Each of the two points $F_m(x_m, y_m)$ and $F_s(x_s, y_s)$ moves along its respective curve during a certain complex motion, namely, simultaneously with the rotation of the normal CO_p and the rigidly coupled to it circle O_pF_φ about the point C (which results in a change of the angles

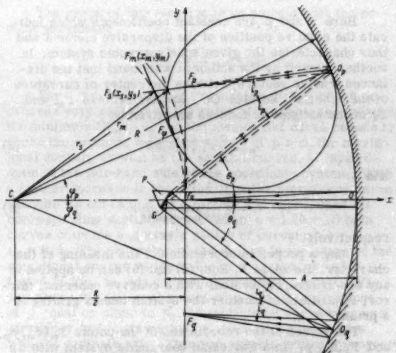

Fig. 1. Simplified schematic of a spectrograph with a concave camera mirror. P is the dispersing element (a prism or a plane diffraction grating); R is the radius of curvature of the spherical mirror O_pO_q; i_p and i_q are the angles of incidence and reflection, respectively, of the dispersed beams; θ_p and θ_q are the inclinations of the angles of these beams with the principal normal CO; φ_p and φ_q are the angles formed by the marginal normals CO_p and CO_q with the principal normal CO; F_0 is the paraxial focal point; A is the distance between the center of the camera mirror and the center of the exit face of the dispersing system; $F_pF_0F_q$ is the Gaussian image plane of the optical system of the spectrograph; $F_m(x_m, y_m)$ and $F_s(x_s, y_s)$ are the centers of the astigmatic focal sections; r_m and r_s are the radius vectors of the focal curves F_m and F_s; F_0x and F_0y are the axes of a Cartesian coordinate system with its origin at the point F_0.

θ and i), the point F_m moves along the circle O_pO_φ, and the point F_0 along the tangential line $F_\varphi F_s$.

From Fig. 1 it is seen that

$$\theta = \varphi + i \tag{1}$$

and

$$\sin i = c \sin \theta = (1 - p) \sin \theta, \tag{2}$$

where

$$c = \frac{R - A}{R} \tag{3}$$

and

$$p = 1 - c = \frac{A}{R}. \tag{4}$$

Here c and p are constant coefficients which indicate the relative position of the dispersive element and thus characterize the given spectrographic system. In another paper[10] by the author it was found that the distances (radius vectors) between the center of curvature of the spherical surface OO_p and the centers F_m and F_s of the astigmatic focuses are given by

$$r_m = \frac{R}{2} \sqrt{1 + 3c^2 \sin^2 \theta} \tag{5}$$

and

$$r_s = \frac{R}{2} \cdot \frac{1}{\sqrt{1 - c^2 \sin^2 \theta}}. \tag{6}$$

respectively.

Using a proper interpretation of the meaning of the characteristic angle θ, Eqs. (5) and (6) can be applied to any spectrographic system with a concave spherical mirror, regardless of whether the system uses a grating or a prism.

The values of the coordinates of the points $F_m(x_m, y_m)$ and $F_s(x_s, y_s)$ in a Cartesian coordinate system with its origin coinciding with the paraxial focus F_0 can be expressed by the following parametric equations:[10]

$$x_m = \frac{R}{2 \cos i} [\sin^2 i \cos (2i - \theta) + (\cos \theta - \cos i)], \tag{7}$$

$$y_m = \frac{R}{2 \cos i} [\sin \theta - \sin^2 i \sin (2i - \theta)], \tag{8}$$

$$x_s = \frac{R}{2 \cos i} (\cos \theta - \cos i), \tag{9}$$

$$y_s = \frac{R}{2 \cos i} \sin \theta. \tag{10}$$

The astigmatic difference measured along the principal ray O_pF_s is equal to

$$\Delta t = \frac{R}{2} \sin i \tan i. \tag{11}$$

From an examination of the equations (7)-(11) and an analysis of the corresponding graphs one can detect some interesting properties of the investigated focal curves.

All the basic formulas previously derived contain the radius R of the spherical mirror as a constant. It is therefore possible to normalize all quantities with respect to the radius R. Thus we define

$$X_m = \frac{x_m}{R}; \quad X_s = \frac{x_s}{R}; \tag{12}$$

$$Y_m = \frac{y_m}{R}; \quad Y_s = \frac{y_s}{R} \text{ etc.} \tag{13}$$

This enables us to make very general deductions about the properties of the investigated focal curves and also to obtain universal equations which can readily be applied to particular cases.

It is found that the shape of the curves depends to a great extent on the position of the dispersive element with respect to the camera objective. This position is characterized by the quantity p (or c). We will now investigate this important dependence and its consequences.

It is obvious that each of the two curves is symmetrical with respect to the axis of abscissas. It is therefore sufficient to examine only one of the branches of each curve, as for example, the one with positive values of the ordinates Y_m and Y_s.

Figure 2 shows sets of the upper branches of the meridional and sagittal curves calculated for different values of p (or c).* We observe the sharp differences in the rate and character of the changes in the shape of the different curves.

*The range of values for p (or c) is chosen so as to apply to cases most often found in real spectrographs.

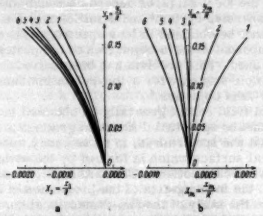

Fig. 2. The dependence of the shape and location of the astigmatic sagittal (a) and meridional (b) focal curves on the position of the exit face of the dispersing system. Values of the parameters p and c: curve 1—0.250, 0.750; curve 2—0.312, 0.688; curve 3—0.426, 0.574; curve 4—0.467, 0.533; curve 5—0.500, 0.500; curve 6—0.583, 0.417.

The abscissas X_s of points of the sagittal curves can assume only negative values. They always lie in the region to the left of the Gaussian image plane. The curvature of the sagittal curves changes relatively slowly with increase in the numerical value of p; the sign of the curvature remains the same as that of the camera mirror. The character of the changes in the shape and relative position of the central portion of the meridional curves is more complex. From Fig. 2a it is seen that as the value of p increases the meridional curve changes its curvature very rapidly and passes over from the right side of the coordinate system into the left side, approaching more and more closely the sagittal curve. It can be shown that in the investigated spectrographic systems the real focal curves, at least in their central portion, practically coincide with, or very nearly duplicate, the corresponding meridional curves. It is therefore very important to investigate closely the meridional curves. The shape of a few different meridional curves is shown in Fig. 3a in a much larger range than previously (in Fig. 2). The intrinsic properties of the meridional curves for practically used variations of mirror spectrographs[4] are best followed by an examination of curve I, which corresponds to p = 0.25 (A = R/4). We observe that this curve is initially on the right-hand side of the coordinate system and relatively quickly departs from the ordinate

axis Y_m; then, after a bend at the point $F_m(X_m, Y_m)$ always, sooner or later, crosses the ordinate axis at a point $F_{m_0}(O, Y_{m_0})$ and passes over to the left-hand plane of the coordinate system. In order to get an idea of the shape of this meridional curve and also the degree of the departure of its working portion from the ordinate axis, it is necessary and often also sufficient to know the value of the following quantities: the ordinate Y_{m_0}, the maximum abscissa X_m (indicated in the figure by arrowheads), and corresponding ordinate Y_m. We will now determine these quantities.

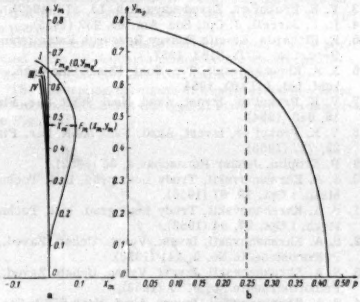

Fig. 3. Graphs of the functions (a), $Y_m = f(X_m)$ and (b), $Y_{m_0} = f(p)$. $p = (3 - \sqrt{3})/3 = 0.42265$, $c = \sqrt{3}/3$.

When $X_m = 0$ the value of the radius-vector is obviously given by

$$r_m = \sqrt{\frac{R^2}{4} + y_{m_0}^2}. \tag{14}$$

Using Eqs. (5) and (2) we find from this that the absolute value of the ordinate of the crossover point F_{m_0} is

$$y_{m_0} = \frac{\sqrt{3}}{2} R \sin i_0, \tag{15}$$

and the normalized value if

$$Y_{m_0} = \frac{y_{m_0}}{R} = \frac{\sqrt{3} Z_0}{2}, \tag{16}$$

where

$$Z_0 = \sin^2 i_0. \tag{17}$$

Now, setting to zero the right-hand side of Eq. (7) and using Eqs. (2) and (17) the quadratic equation

$$Z_0^2 - \frac{4c - 3}{4c^2} Z_0 - \frac{3c^2 - 1}{4c^2} = 0, \tag{18}$$

is obtained. The solution of this equation enables us to clarify the relation between the value of the divergence angle i_0 of the beams and the position of the dispersing element which is characterized by the parameter c. For calculations and for investigating this relationship graphically, the relation $c = f(Z_0)$, which can be derived from Eq. (18), will be found to be useful.

Using Eqs. (16), (18) and (3), it is possible to evaluate the value of Y_{m_0} for a given value of p and thus to plot a graph of $Y_{m_0} = f(p)$ (see Fig. 3b) from which it is possible to visualize the rate at which the point F_{m_0} moves along the ordinate axis as the parameter p is changed. In Fig. 3 the same scale is chosen for the ordinates Y_m and Y_{m_0} in the graphs of the functions $Y_m = f(X_m)$ (Fig. 3a) and $Y_{m_0} = f(p)$ (Fig. 3b). Using both graphs simultaneously it is thus readily possible to find for given values of p the crossover points F_{m_0} on the ordinate axis of Fig. 3a. This is illustrated with dashed lines in Fig. 3 for the case $p = 0.25$.

The maximum value of X_m of the meridional curve for a given value of p can be found from the discovered simple relation

$$X_m^{\frac{2}{3}} + p^{\frac{2}{3}} = p_0^{\frac{2}{3}}. \tag{19}$$

The graph of this function is an astroid with the constant parameter

$$p_0 = \frac{3 - \sqrt{3}}{3} = 0.42265.$$

For $p = p_0$ the value of the maximum X_m, which decreases very rapidly as the value of p increases, reaches its minimum ($X_m = 0$) and the meridional curve ceases to cross the ordinate axis. For values of $p \geq p_0$ the meridional curves, as well as the sagittal curves, always remain in the left-hand side of the coordinate system. With a further increase in the value of p the meridional curve changes its curvature very rapidly and approaches the corresponding sagittal curve. When $p = 1$ ($A = R$) both curves coincide and have a radius of curvature $r = r_m = r_s = R/2$. The character of the change in the shape of the meridional curves as the value of p increases is illustrated in Fig. 3a, where four meridional curves (I-IV) are shown for different values of p (or c). For values of p equal or close to p_0 the meridional curve becomes straighter and in its central portion almost coincides with the ordinate axis. This remarkable inherent property of uncorrected (in the commonly adopted meaning of the word) mirror systems of the investigated type permits one to design instruments with a practically flat field.

The value of the parameter $p = 0.42465$ was in its time found by using the third order aberration theory in connection with the design of spectrographs with flat fields.[7,8] As far as the determination of the shape of the focal surface is concerned, the third order theory is useful only in a limited number of cases, for example, when in the so-called vertical-symmetrical scheme[11,13] a relatively small central portion of the image (i.e., spectrum) is used. However, when the image length is considerable or when side portions of the field are used (as for example, in the so-called horizontal spectrographs[11,13] and others) a very careful investigation of the shape of the focal curves is required in order to determine the optimum optical parameters of a given system. This is now made possible with the help of the exact formulas developed in this paper. The analysis of many different types of spectrographic systems with the help of these formulas enables us to make certain conclusions and recommendations.

The meridional curves for values of p equal to 0.425 and 0.415 (one of which crosses the ordinate axis, the other not) are both close to each other and they both depart very little from the ordinate axis. We may thus consider the region of p between these values as the "flat field zone," in any case for a central image of length $2Y_m \leq 0.1 - 0.15$. In systems with a small depth of focus the effect of the residual curvature of the meridional curve is stronger, and in these cases the permissible length of the "flat" image must be chosen as the lower of the indicated limits.

It should be emphasized that the stated numbers characterize only conditions for obtaining a relatively flat field. They do not, however, give any indication of whether an image of a given length is usable or not from a point of view of the image quality at the edge of the field. The actual use of images of considerable length, even within the indicated range of values of p, can be limited by the gradual growth of the size of the scattering spot with increasing divergence angles i. It might be useful in this case to use two or more flat photographic plates placed alongside each other and a number of plates inclined with respect to the Gaussian image plane and to each other.[14] Using in this case slightly higher values of p (compared with the values indicated above), one can increase the length of the useful image without any deterioration in its image quality. By further increasing p(A) it is possible to obtain quite long images of good quality. However, this is accompanied by a strong curvature of the focal surface and necessitates the use of curved photographic plates.

The displacement of the central portion of the meridional curve (F_pF_m in Fig. 1) with the change in the value of the parameter p can be reduced to a rotation about the paraxial focal point F_p. A measure of the angle of this rotation is the increment ΔX_m for a given ordinate Y_m. We have

$$\Delta X_m = 6cY_m^2 \Delta p, \qquad (20)$$

where $\Delta p = \Delta A/R$ is the increase in the value of the parameter p.

Equation (20) permits one, in particular, to estimate the permissible error in the setting of the dispersing element with respect to the camera mirror, taking the depth of focus of the given system into account; that is, to formulate requirements for a proper alignment setup.

The correctness of the conclusions reached is supported by the presence of well performing instruments and setups as well as by a number of performed preliminary experiments.[11,14]

REFERENCES

1. O. Mielenz, Optik 16, 500 (1959).
2. O. Plaskett, Astrophys. J. 59, 65 (1924).
3. V. K. Prokof'ev, Zavodskaya Lab. 13, 175 (1947).
4. R. F. Jarrell, J. Opt. Soc. Am. 45, 259 (1955).
5. E. Richards, Atomic Energy Research Establishment, Report No. C/R, 2163, 1957.
6. S. A. Khrshanovskii, Tez. dokl. IZ nauchno-tekh. konf. Izd. LITMO, 1954.
7. V. K. Prokof'ev, Izvest, Akad. Nauk SSSR, Ser. Fiz. 18, 643 (1954).
8. V. K. Prokof'ev, Izvest, Akad. Nsuk SSSR, Ser. Fiz. 22, 737 (1958).
9. P. Króplin, Jenaer Rundschau 4, 66 (1959).
10. S. A. Khrshanovskii, Trudy Leningrad. Inst. Tochnoi Mekh. i Opt. 19, 97 (1956).
11. S. A. Khrshanovskii, Trudy Leningrad. Inst. Tochnoi Mekh. i Opt. 27, 94 (1958).
12. S. A. Khrshanovskii, Izvest. Vyssh. Ucheb. Zaved., Priborostroenie No. 5, 141 (1958).
13. S. A. Khrshanovskii, Izvest. Vyssh. Ucheb. Zaved., Priborostroenie No. 6, 72 (1958).
14. S. A. Khrshanovskii, Izvest. Akad. Nauk SSSR, Ser. Fiz. 23, 1100 (1959).

SHORT COMMUNICATIONS

A NEW BAND IN THE ABSORPTION SPECTRUM OF POLYCRYSTALLINE LAYERS OF CADMIUM SULFIDE

T. Ya. Soera and V. V. Serdyuk

Received 11 August 1959

Polycrystalline layers of cadmium sulfide attract attention as objects of investigation because of their unusual photoelectric properties. Photoresistors of CdS possess a high integral sensitivity. The spectral distribution of the photosensitivity of this semiconductor has a sharp maximum in the 500-520 mμ region.[1] Investigations of the absorption spectra of cadmium sulfide together with photoresistance measurements have been carried out by many authors on both single crystals and polycrystalline samples. In the majority of cases it was noted that the wavelength of the natural absorption edge coincides with the wavelength for maximum photosensitivity.[2]

The intense investigation of cadmium sulfide from an optical standpoint began when a complicated structure was discovered in the natural absorption edge. The structure was attributed to excitons.[3] This resulted in widespread acceptance of the exciton theory of photoconductivity. According to this theory, the appearance of electrons in the conduction band is associated with the annihilation of excitons. However, several recent optical investigations[4] have shown that the complicated structure of the natural absorption edge of CdS is connected with defects of the crystal lattice, and is strongly affected by crystal deformation, as well as other external factors. Some papers[5] have noted the strong influence of the state of the surface of the crystal on the spectral distribution of photoconductivity.

All of these facts can be explained without the aid of the exciton mechanism. References 6 and 7 suggest that the photoconductivity of cadmium sulfide arises as a result of the ionization of metal impurity atoms which exist in the lattice of the semiconductor.

Experimental facts existing at the present time do not permit one to make a final choice between the exciton and impurity mechanisms of photoconductivity. With respect to the exciton mechanism, it is particularly necessary to note ref. 8 where it is shown that neutral particles, which can only be electron-hole pairs, take part in the first stages of the transport of the photocurrent in crystals.

It is interesting to note that the photosensitivity of polycrystalline samples (vaporized layers) of cadmium sulfide is very weak immediately after preparation. A

short initial heating of the layer in air sharply increases the photosensitivity.[1] In this connection, it would be interesting to show by optical means the role of thermal treatment of the layers, and to connect changes of the absorption spectra with changes of the photosensitivity.

The present investigation is a study of the influence of thermal treatment on the absorption spectra of polycrystalline layers of cadmium sulfide. Bright yellow, nonluminescent cadmium sulfide powder was used as a starting material. This powder was volatilized in vacuum and sublimed onto a glass substrate. The layers had thicknesses of the order of 10^{-6} cm, i.e., they were so thin that interference effects did not distort the absorption pattern.

Measurements of the absorption spectra were performed on an SF-4 quartz photoelectric spectrophotometer at 5 or 2.5 mμ intervals from 400-600 mμ.

The absorption spectrum of a polycrystalline layer of cadmium sulfide had the typical form for this material (see Fig. 1,a).

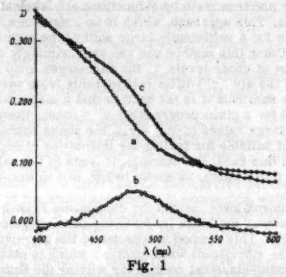

Fig. 1

After the layer is heated in air at 300°C for 5 min, a selective increase of the absorption in the 430-540 mμ region (see Fig. 1,b) is observed. In the absorption spectrum of a layer of cadmium sulfide, a broad band appears near 485 mμ. This band is easily detected if one subtracts the first curve from the second (see Fig. 1,c).

In order to exclude the possible influence of atmospheric oxygen on the formation of the new absorption band, we measured the absorption spectra of CdS layers heated to the same temperature in vacuum. In this case, as with heating in air, the appearance of additional absorption in the same spectral region was observed. Consequently, it is a thermal effect, and not oxygen, which plays the essential role in the appearance of an additional band in the cadmium sulfide absorption spectrum.

It is possible to assume that during the heating of a CdS layer the stoichiometric equilibrium in the crystalline lattice of the material is disturbed because of the escape of sulfur, which is the more volatile component of the compound. This results in an excess of the metal, which can produce additional absorption. The correctness of this assumption is verified by the fact that heating of a CdS layer in sulfur vapor does not lead to excessive absorption in the indicated region of the spectrum.

Attempts were undertaken to deposit a thin film of metallic cadmium over a layer of cadmium sulfide. However, the anticipated selective increase in absorption in the 430-540 mμ region was not observed. This probably indicates that the excess metal which appears in a semiconductor layer after heating is not found on the surface of the layer.

We prepared samples containing a known excess of metallic cadmium. This was done by keeping the CdS powder at 300°C in vacuum for several minutes before evaporating it. This treatment changed the color of the powder from bright yellow to a reddish brown. After the initial heating, the powder was vaporized by the usual method. The absorption spectrum obtained from the layer was measured; a layer prepared from unheated cadmium sulfide was used as a control. The results of the experiment are given in Fig. 2,a.

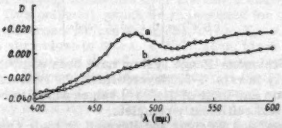

Fig. 2

In the short wavelength part of the spectrum, the layer with the cadmium impurity absorbed less than the control sample, which is explained by its smaller thickness. However, in the 460-540 mμ region, the absorption of this sample increases sharply, and it begins to absorb more than the "pure" layer. For comparison, the absorption spectrum of a "pure" sample of CdS of the same thickness, measured relative to the standard sample, is shown in the same figure (Fig. 2,b). This experiment shows that the new band in the absorption spectrum of CdS is not connected with structural changes of the layer during thermal treatment, since this band is also contained in the absorption spectrum of a sample which has not been heated, but contains a known excess of cadmium atoms.

These considerations indicate that the new band appearing in the absorption spectrum of polycrystalline layers of CdS as a result of heating is metallic in nature. Heating of the preparation leads to "cracking" of the semiconductor layer, which can be observed in a microscope with a magnification of the order of 1000. This "cracking" leads to a sharp increase in the resistance of the layer after thermal treatment, as has also been noted by many other authors. It is probable that a deposition of metallic atoms also occurs along the cracks which are formed. These deposited atoms form centers which are responsible for the appearance of additional light absorption in the 430-540 mμ region.

REFERENCES

1. B. T. Kolomiets, Doklady Akad. Nauk SSSR 33, 561 (1952).
2. E. F. Gross and M. L. Belle, Zhur. Tekh. Fiz. 25, 948 (1955).
3. E. F. Gross, B. S. Razbirin, and M. A. Yakobson, Zhur. Tekh. Fiz. 27, 1149 (1957).
4. V. L. Broude, O. S. Pakhomova, and A. F. Prikhot'ko, Opt. i Spektr. 2, 323 (1957);
V. L. Broude, V. V. Eremenko, and E. I. Rashba, Ukrain. Fiz. Zhur. 2, 96 (1957).
5. E. A. Sal'kov, G. A. Fedorus, and M. K. Sheinkman, Fiz. Tver. Tela. 1, 579 (1959).
6. K. V. Shalimova and I. V. Karpenko, Nauch. Doklady Vysshei Shkoly Radiotekh. i Elektron. 2 (1958).
7. K. V. Shalimova and I. V. Karpenko, Nauch. Doklady Vysshei Shkoly Radiotekh. i Elektron. 3 (1958).
8. M. Balkansky, R. D. Waldron, Phys. Rev. 112, No. 1 (1958).

THE FRANCK-CONDON FACTORS FOR THE SCHUMANN-RUNGE BAND SYSTEM IN THE OXYGEN MOLECULE

I. T. Yakubov

Received 12 November 1959

Franck-Condon factors

$$q(v'v'') = \left[\int_0^\infty \psi'_{v'}(r)\,\psi''_{v''}(r)\,dr\right]^2 \qquad (1)$$

for the Schumann-Runge system have been computed previously in refs. 1-5. Nevertheless, the literature does not contain any table of $q(v', v'')$ values which is both reliable and sufficiently complete.

Pillow[1] and Weniger and Herman, in their calculations, used somewhat modified versions of the "distorted wave functions" method. This method, which is based on the use of harmonic oscillator wave functions, is very rough and does not give reliable results even for small values of v.

Jarmain et al.[2] used their own "mean α" method,* which is based on a substitution of some mean α_{mean} for the constants α_1 and α_2 of upper and lower electron states in Morse potentials

$$U = D\,[1 - e^{-\alpha(r - r_e)}]^2 \qquad (2)$$

In this case, the quantity $q(v', v'')$ is quite easy to compute. However, as v increases, the potential curves, which are distorted by the introduction of α_{mean}, deviate more and more from the true ones; this leads to a corresponding distortion of the wave functions, and the error increases. In order to use the computation formulas obtained in ref. 6 for large values of $(v' + v'')$, the α_{mean} values were chosen as follows in ref. 3:

$$\alpha_{mean} = \frac{\ln\left[\frac{x_{e1}}{x_{e2}}\left(\frac{\alpha_2}{\alpha_1}\right)^2\right]}{r_{e1} - r_{e2}}. \qquad (3)$$

For the case of the Schumann-Runge system, where α_1 and α_2 differ by 23%, this choice of the mean value of α considerably distorts the lower potential curve, while the upper one remains practically unchanged. For example, the coordinate of the turning point of the $v'' = 11$ level of the distorted potential coincides with that of the $v'' = 10$ level of the true function U(r). In the calculation of an overlap integral of rapidly oscillating vibrational wave functions, such a displacement can lead to an error of hundreds of percent.

The authors in ref. 3 used the so-called "r_s-shift" to correct their results. It should be noted, however, that from the computational point of view this idea is difficult to carry out directly because one must find the r_s-shift for each pair of v', v'' values. Simplifications which permit us to use this method in practice are valid only for small values of $(v' + v'')$, when the shift is small; i.e., the correction to $q(v', v'')$ is also small. However, for large values of $(v' + v'')$, the use of r_s-shift is invalid because the original assumption is no longer valid. In view of the above discussion, we doubt the reliability of the $q(v', v'')$ values obtained by Jarmain et al., which they classify as satisfactory values.

Losev[4] computed $q(v', v'')$ values with the help of the "Strela"* computer. He used exact solutions of the Schrödinger equation with a Morse potential. The solutions were expressed in terms of generalized Laguerre polynomials. However, since the number of significant figures which disappeared in subtractions in the process of calculation rapidly exceeded the capacity of the computer, Losev's table is confined to the values $v' + v'' \leq 8$-9, and obviously is not sufficient. Nevertheless, the values of $q(v', v'')$ obtained in ref. 4 for small $(v' + v'')$ are undoubtedly accurate.

Keck et al. replaced the vibrational wave functions of the lower electron state by δ-functions at classical turning points. This approach, which is no longer new,[5] is applicable for a sufficiently large shift of the potential curves. Using this method one can approximately determine a set of upper levels v' for each lower level v'' such that the $q(v', v'')$ differ considerably from zero. Using the sum rule it is not hard to find a mean value of $q(v'v'')$ for a given progression $v'' = \text{const}$. However, even for large values of $r_{s1} - r_{s2}$, the above approximation is not suitable for finding the intensities of separate bands. In this case, for example, it leads to the value $q(5.11) = 0.016$ which, as shown below, has an error of 200-300%.

An approximate method for calculating Franck-Condon factors for large $(v' + v'')$ has been suggested previously.[7] This method makes use of the asymptotic form of the vibrational wave function, which is obtained using a quasi-classical method for solving the Schrödinger equation with the Morse potential. Monotonic segments are approximated by monotonic segments of the harmonic oscillator wave functions chosen in a certain way. This method is free from the drawbacks present in the "average α" method, and does not lose significant figures in the process of computation.

We applied the method described in ref. 7 to a calculation of the Franck-Condon factors in the Schumann-Runge system. Since quasi-classical functions are not satisfactory for $v \leq 3$, exact functions of the Morse oscillator were computed for $v' = 3$ and 2. For $v' = 0$ and 1, distorted harmonic oscillator functions, which can be constructed without much difficulty, are quite acceptable. We obtained these functions using the Pillow method, with the corrections to this method cited in ref. 7. Results of this calculation are given in the table.

Franck-Condon Factors for the Schumann-Runge Band System of the Oxygen Molecule

v' \ v''	6	7	8	9	10	11	12	13	14	15	16	17	18	19	20
0	0.000	0.004	0.012	0.028	0.054	0.087	0.123	0.155	1.171	0.165	0.127	0.065	0.024	0.006	0.003
1	0.010	0.025	0.042	0.059	0.097	0.095	0.057	0.009	0.001	0.026	0.079	0.117	0.130	0.117	0.077
2	0.026	0.052	0.068	0.077	0.051	0.021	0.000	0.027	0.057	0.069	0.039	0.000	0.020	0.087	0.125
3	0.041	0.067	0.064	0.040	0.012	0.005	0.033	0.056	0.037	0.000	0.027	0.059	0.052	0.021	0.000
4	0.073	0.068	0.039	0.007	0.007	0.043	0.058	0.023	0.013	0.048	0.055	0.026	0.003	0.048	0.073
5	0.073	0.049	0.008	0.003	0.032	0.041	0.011	0.005	0.033	0.050	0.001	0.020	0.054	0.044	0.000

In order to compare data obtained by different methods, the figure* shows both our Franck-Condon factors

*The author is grateful to S. A. Losev for making his results available to him prior to publication.

*In the figure, the Franck-Condon factors belonging to one progression are connected by a smooth curve. This

construction gives a clear picture of the regular change in $q(v', v'')$ and makes it easy to find which of the individual values of these quantities are wrong.

for the progressions $v' = 0$ and 3, and those given in refs. 3 and 4.

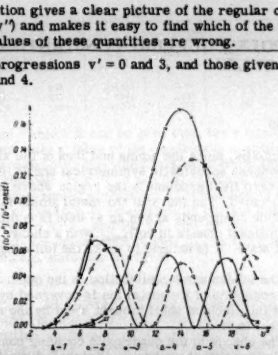

Comparison of Franck-Condon factors calculated by different methods. v'-value: 1—3: $v' = 3$; 4—6: $v' = 0$. Method of calculation: 1, 4—ref. 4; 2, 5—ref. 3; 3, 6—this paper.

The figure shows good agreement of our $q(v', v'')$ values with Losev's data and a sharp increase in error when the "mean α" method is used, leading to entirely incorrect values for large v''.

In addition, a direct check was carried out on the validity of the above arguments in connection with the results of ref. 3. Starting with the parameters of the potential curves distorted by the introduction of α_{mean}, we computed two $q(v', v'')$ values using the method suggested in ref. 7. It turned out that $q(13.0) = 0.095$ and $q(19.0) = 0.070$. These numbers are very close to the corresponding quantities obtained in ref. 3 (see the figure). The source of error in the "mean α" method therefore lies in the initial data, which are distorted when α_{mean} is introduced. Since results obtained for the $v' = 0$ progression are used to calculate the $q(v', v'')$ values of the remaining three progressions (ref. 6), the discrepancy increases. Thus, the "mean α" method cannot be applied to the case of the Schumann-Runge system because of the marked difference in values of α_1 and α_2. It should be mentioned that the estimates of the accuracy of the Franck-Condon factors calculation using the "mean α" method made in ref. 3 for other band systems are also too high.

Our calculation of Franck-Condon factors was carried out on the assumption that the Morse potential in which the initial parameters are B_e, $\omega_e X_e$, and ω_e gives a good approximation to the experimental curve U(r). This assumption must be verified for large values of v. It is well known that the Hulbert-Hirschfelder potential gives a good approximation to the experimental potential curves of various molecules over the entire energy range.[9] This potential, which we constructed for $X^3\Sigma_g^-$ using 5 spectroscopic constants (B_e, ω_e, $\omega_e X_e$, α_e, and D_e),[10] is very close to Morse's U(r). Thus, for example, the turning points of the $v'' = 17$ ($r > r_e$) level for the Morse and Hulbert-Hirschfelder potentials (in the latter case, $\omega_e Y_e$ and $\omega_e Z_e$ are taken into account in calculating the energy of the level) differ by 6×10^{-3} A. This is less than 0.05 of the last maximum in the wave function $\psi^{v''=17}(r)$ and gives rise to a small error, which is around 10% for q(3, 17), for example.

The author is grateful to L. M. Biberman who supervised this investigation.

REFERENCES

1. M. Pillow, Proc. Phys. Soc. **A63**, 940 (1950).
2. C. Weniger and R. Herman, J. phys. radium **15**, 428 (1954).
3. P. Fraser, W. Jarmain, and R. Nichols, Astrophys. J. **119**, 286 (1954).
4. S. A. Losev, Nauch. Doklady Vysschei Shkoly Fiz.-Mat. Nauki No. 5 (1958).
5. I. Keck, J. Camm, B. Kivel, and T. Wentink, Ann. Phys. **7**, 1 (1959).
6. P. Fraser and W. Jarmain, Proc. Phys. Soc. **A66**, 1145, 1153 (1953).
7. L. M. Biberman and I. T. Yahubov, Opt. i Spektr. **8**, 294 (1960), Optics and Spectroscopy **8**, 155 (1960).
8. V. N. Soshnikov, Opt. i Spektr. **6**, 315 (1959), Optics and Spectroscopy **6**, 203 (1959).
9. H. Hulbert and J. Hirschfelder, J. Chem. Phys. **9** 61 (1941).
10. G. Herzberg, Astrophys. J. **108**, 163 (1948).

INFLUENCE OF VIBRATIONS ON THE QUADRUPOLE COUPLING CONSTANTS IN ALKALI HALIDE MOLECULES

A. G. Makhanek

Received 8 January 1960

Study of the influence of vibrations on the magnitude of the quadrupole coupling constants in alkali halide molecules plays an important role both in the interpretation of experimental microwave data and for the understanding of intramolecular processes. In nearly-ionic compounds, such as the diatomic alkali halide molecules, these influences are particularly marked. For example, the quadrupole coupling constant of the Cl^{35} atom in the KCl molecule changes by almost a factor of 10 on going from the zeroth to the third vibrational level (see Table 1).

Table 1

Molecule	Atomic nucleus	$\frac{eQq}{h}$ (Mc) v = 0	v = 1	v = 2	v = 3
KCl	K^{39} [7]	−5.656 ± 0.006	−5.622 ± 0.006	−5.571 ± 0.008	−5.511 ± 0.008
KCl	Cl^{35} [7]	−0.040	−0.075 ± 0.010	−0.237 ± 0.010	−0.393 ± 0.010
KBr	K^{39} [8]	−5.003 ± 0.003	−4.984 ± 0.003	−4.915 ± 0.003	—
KBr	Br^{79} [8]	+10.244 ± 0.006	+11.244 ± 0.006	+12.204 ± 0.006	—
KF	K^{39} [9]	−7.928	−7.816	−7.744	−7.668
RbCl	Rb^{85} [10]	−52.675 ± 0.005	−52.306 ± 0.030	−51.903 ± 0.040	—
RbCl	Cl^{35} [10]	+0.744 ± 0.009	+0.812 ± 0.013	+0.870 ± 0.017	—
NaI	I^{127} [11]	−259.87 ± 0.00	−264.52 ± 0.65	−267.58 ± 0.40	−271.03 ± 0.02
LiBr	Br^{79} [11]	+37.20 ± 0.45	—	—	—
NaBr	Br^{79} [11]	+58 ± 2	—	—	—

Molecule	LiF	LiCl	LiBr	LiJ	NaF	NaCl	NaBr	NaJ
Atomic nucleus [11]	Li^7	Li^7	Li^7	Li^7	Na^{23}	Na^{23}	Na^{23}	Na^{23}
$\left\langle \frac{eqQ}{h} \right\rangle$ (Mc)	+0.408	+0.192	+0.184	+0.172	−8.12	−5.40	−4.68	−3.88

The field gradients ($q = \partial^2 v/\partial z^2$) in the region where the nuclei of the metal and halogen atoms are located, as well as their dependence on the vibrational state, are governed by many factors, which makes a theoretical investigation considerably more difficult. Nevertheless, close analysis provides a possibility of separating the fundamental contributions to the field gradient.

The matter is comparatively simple with the halogens. In ref. 1 it has been shown that, for covalently bonded halogens, the magnitude of the contribution to the electric field gradient is almost entirely determined by the missing p-electron in the outer shell of the atom. It is therefore natural to consider that the magnitudes of the quadrupole coupling constants of the halogens are governed principally by that small portion of covalent bond character which exists in alkali halide compounds. The fact that this contribution is fundamental is particularly conspicuous for such molecules as NaI, LiBr, NaBr (see Table 1), in which (in view of the low electronegativity of Br and I) there is a significant fraction of an uncompensated p-electron.

It follows from Table 1 that the quantity $eqQ_{halogen}$ varies strongly with the change in vibrational state. Duchesne supposed, in refs. 2-4, that the change in $eqQ_{halogen}$ is governed by an increase in the portion of covalent bond character with an increase in the vibrational state, and he obtained an approximate empirical formula for the dependence of $eqQ_{halogen}$ on the vibrational state.

The considerable magnitude of the quadrupole coupling constants of the metal atoms is very difficult to explain. Actually, since the atoms and ions of the alkali metals possess spherically symmetrical shells, one would expect a zero field gradient in the region where the nucleus is located. The fact that the metal atoms in the alkali halide compounds are in an s-state is confirmed by the insignificant change in eqQ_{metal} with a change in vibrational state. It is natural to make the following assumptions.

1. The fundamental contribution to the quadrupole coupling constants of the metal ion is governed by a distortion of the electron shell brought about by the halogen ion adjacent to it.

2. The change in the quadrupole coupling constants of the halogens with the vibrational state is brought about principally by an increase in the portion of covalent bond character.

Starting from these assumptions, we shall consider that the electric field gradient in the region where the nuclei of the metal atoms are located is an analytic function of the small (in comparison with the dimensions of the ion) distortions:

$$q(z) = q_0 + q_1 z + q_2 z^2 + \dots \qquad (1)$$

We shall set the magnitude of the distortion proportional to the force acting, i.e.,

$$z \sim \frac{e(1-u_p)}{r^2}, \qquad (2)$$

where u_p is the fraction of an uncompensated p-electron in the halogen atom and r the internuclear distance.

In consequence of the vanishing of the field gradient for free atoms ($r \to \infty$) of the alkali metals, $q_0 \equiv 0$. Then, considering that the rotational constant

$$B_v = B_e - \alpha_e\left(v+\frac{1}{2}\right) + \gamma_e\left(v+\frac{1}{2}\right)^2 + \dots,$$

where $B_v \sim \langle 1/r^3 \rangle_v$ and $B_e \sim 1/r_e^3$, and neglecting terms in z^2 and higher, the dependence of eqQ_{metal} on the vibra- may be represented in the following form:

$$\langle eqQ_{metal} \rangle_v = \frac{\sigma}{r_e^3}\left[1 - \frac{\alpha_e}{B_e}\left(v+\frac{1}{2}\right)\right](1-u_p), \qquad (3)$$

where σ is a constant for the atom of a given metal in all its halide molecules.

In this case, the average value of eqQ_{metal} in a given vibrational and rotational state is expressed thus:

$$\langle eqQ_{metal} \rangle_{v,J} = \frac{\sigma}{r_e^3}\left[1 - \frac{\alpha_e}{B_e}\left(v+\frac{1}{2}\right) - 4\left(\frac{B_e}{\omega_e}\right)^2 J(J+1)\right](1-u_p). \qquad (3a)$$

The results obtained with the help of formula (3) for K^{39} in KCl and KBr and for Rb^{85} in RbCl, on substituting the experimental values of σ, α_e, B_e, and u_p into it, are presented in Table 2. Comparison of these results with the experimental data (Table 1) gives evidence of satisfactory agreement. Certain deviations are possibly brought about by the fact that a number of effects have not been taken into account, such as, for example, the distortion of the electron shell of the halogens.

Table 2

Molecule	Atomic nucleus	$\frac{eQ}{h}$ (Mc) v=0	v=1	v=2	v=3
KCl	K^{39}	− 5.656	− 5.619	− 5.576	−5.534
KBr	K^{39}	− 4.994	− 4.953	− 4.932	—
RbCl	Rb^{85}	−52.675	−52.323	−51.983	—

From Table 1 it can be seen that, for a number of molecules, only a value of the quadrupole coupling constant averaged over the vibrations is experimentally known. However, in refs. 5 and 6 it has been shown that the very pronounced asymmetry in line shape in the presence of quadrupole interaction in certain molecules especially for $Na^{23}Cl$ and $Rb^{87}Cl$, may be explained by assuming that the dependence of eqQ_{metal} on the vibrational and rotational state has the form

$$\langle eq'Q_{metal} \rangle = eq'Q + eq^{(J)}QJ(J+1) + eq^{(v)}Q_v. \qquad (4)$$

where $\bar{q}$, q^J, and q^v are constants independent of the vibration and rotation of the molecule. Here the signs of the quantities $eq^{(v)}Q$ and $eq^{(J)}Q$ are opposite to the sign of the quantity $e\bar{q}Q$. For $Na^{23}Cl$ the quantity $eq^{(v)}Q/\hbar$ is approximately equal to 0.09 Mc. Evaluation of this quantity according to formula (3) leads to the value 0.054 Mc.*

*u_p is set equal to $u_{p_{NaCl}}$.

For $RB^{87}Cl$ the quantities $eq^{(v)}Q/\hbar$ and $eq^{(J)}Q/\hbar$ equal respectively 0.230 ± 0.050 Mc and 12 ± 2 cycles.

From (3) and (3a), the following values of these constants are obtained: 0.166 Mc and 10 cycles. From refs. 5 and 6 it follows that the quantity $eq^{(J)}Q/\hbar$ for the $Na^{23}F$ molecule equals 32 cycles. Calculation according to formula (3a) leads to the value 29.5 cycles. The agreement may be considered satisfactory if we take account of the approximate character of formula (4) and of the fact that the methods of measurement are indirect. For the halide compounds of the atoms Na^{23} and Li^7, the dependence of the quantity eqQ_{metal} on $\langle 1/r^3 \rangle$, as expressed by formula (3), is well confirmed, as can be seen by comparison of Tables 1 and 3.*

*Average values of σ_{Li} and σ_{Na} calculated from the experimental data were used in the calculations.

Table 3

Molecule	LiF	LiCl	LiBr	LiJ	NaF	NaCl	NaBr	NaI
Atomic nucleus	Li^7	Li^7	Li^7	Li^7	Na^{23}	Na^{23}	Na^{23}	Na^{23}
$\left\langle \frac{eQ}{h} \right\rangle$ (Mc)	+0.413	+0.215	+0.185	+0.152	−8.52	−5.18	−4.61	−3.92

In conclusion, I take the opportunity of expressing my thanks to M. A. El'yashevich for his interest in the work and his valuable counsel.

REFERENCES

1. C. H. Townes and A. L. Shawlow, "Microwave spectroscopy." New York, 1955.
2. J. Duchesne, J. Chem. Phys. 25, 369 (1956).
3. J. Duchesne, J. Chem. Phys. 20, 1804 (1952).
4. J. Duchesne, Nuovo cimento, Suppl. 9, 270 (1952).
5. W. A. Nierenberg and N. Ramsey, Phys. Rev. 72, 1075 (1947).
6. H. J. Zeiger and D. I. Bolef, Phys. Rev. 85, 789, 799 (1952).
7. Ch. A. Lee, B. P. Fabricand, R. O. Carlson, and I. I. Rabi, Phys. Rev. 91, 1395 (1953).
8. B. P. Fabricand, R. O. Carlson, Ch. A. Lee, and I. I. Rabi, Phys. Rev. 91, 1403 (1953).
9. L. Grabner and V. Hughes, Phys. Rev. 79, 819 (1950).
10. J. W. Trishka and R. Braunstein, Phys. Rev. 96, 968 (1954).
11. A. Honig, M. Mandel, M. L. Stitch, and C. H. Townes, Phys. Rev. 96, 629 (1954).

STUDY OF MOLECULAR INTERACTION IN p-DICHLOROBENZENE NEAR THE FREEZING POINT

A. A. Aivazova and I. A. Gorbatov

Received 8 February 1960

The thermal motion of molecules in a liquid is a source of the formation of distinct groups of local order. It is known that in liquids at temperatures near the freezing point, molecules oscillate about an equilibrium position. However, these equilibrium positions are not rigorously fixed--they fluctuate intermittently. If the probability of "existence" of a molecule in a potential well is proportional to $e^{u/kT}$, where u is the depth of the potential well and the time of "existence" in a given equilibrium state is equal to[1]

$$\tau = \tau_0 e^{\frac{u}{kT}}.$$

Hence, the relaxation time is determined by the state of the liquid and, particularly, by the temperature.

It is of interest to study the nature of the thermal motion of molecules in a liquid near the freezing point. With this in mind, we studied the change in line width for Rayleigh scattering, in a temperature range near the freezing point. The distribution of intensity in the scattering curve is determined by Leontovich's formula.[2]

$$I = I_0 \frac{1}{1 + \tau^2 \Delta\omega^2},$$

where I_0 is the maximum intensity, τ is the relaxation time of anisotropy, and $\Delta\omega$ is the distance from the center of the line to a point where the intensity falls from I_0 to I.

In the present work, Vuks'[3] method of determining relaxation times was used, but photoelectric recording was employed in place of photographic photometry.

The investigation was carried out using a diffraction spectrometer DFS-4 with a grating of 1200 lines/mm. A mercury vapor lamp PRK-2, operating under normal conditions, served as a light source. The line recording was made with a slit of 0.25 cm^{-1} (the inlet and outlet slits of the monochromator were the same), at a standard

slit width of the instrument, in the region 4358 A, equal to 0.15 cm^{-1}. This permitted the correction for the width of the slit to be neglected in calculating the true line contour. In order to obtain adequate resolution, we made changes in the design of the instrument, which produced a scanning rate of nearly 1 A/min. The operational stability of the light source was controlled with a photocell.

Much attention was given to purification of the substance. We used the method of repeated vacuum distillation. A light filter ZhS-4 was used to prevent decomposition of the substance by ultraviolet light.

The relaxation time was calculated according to the width of the 4358 A line at a height corresponding with the 4347 A line. We did not study the more remote part of the curve because of overlapping with the curves of adjacent lines.

p-Dichlorobenzene was selected for the investigation since its molecules are not dipolar, which eliminates the possible effect of an additional orientating interaction. Also, this substance possesses a convenient melting (52.9°C) for investigation.

The results of the measurements of relaxation times are presented in Fig. 1. From the figure, it is evident that from 90 to 65°C the experimental points lie on a straight line. This indicates that the dependence of τ on T is well expressed by Frenkel's formula. The value of the activation energy u, which is determined by the slope of the plot, is equal to 4.4 kcal/mol; the period of rotary oscillation $\tau_0 = 0.012 \times 10^{-12}$ sec. From 65 to 60°C, a decrease of relaxation times with temperature is observed. The change of slope is indicative of changes occurring in the liquid.

In refs. 4-6, an anomaly in the temperature dependence of refractive index, heat capacity, viscosity, electrical conductivity etc. is observed in a certain temperature range, significantly remote from the freezing point (of the order of 10°). Such anomalies have been treated as due to structural changes, associated with the configuration of the molecules.[7]

It appears that such a change is caused by an increase of molecular interaction in the observed temperature range. In all probability, the change of molecular interaction is reflected by the anomalous behavior of the relaxation times of anisotropy observed in this work. We think that such a change may be caused by two factors: either by a change in local ordering or by a change in the structural configuration of the molecules.

Both types of change must have an effect on the intensity of scattering. Therefore, we studied the relative intensity of the scattered light in the stated temperature range.

The dependence of I_{rel} on T is given in Fig. 2. It is readily apparent that, in this instance, an anomaly is observed and its maximum is slightly displaced in comparison with the maximum of relaxation times. This difference may be explained in the following manner: the intensity of scattered light is one of the parameters most sensitive to change in the properties of a substance. This change probably starts at 70°C and takes place in a temperature range of 6° to 7°C. Also, the maximum value of the intensity of scattered light occurs at maximum heterogeneity of a substance, and the minimum value of the relaxation times of anisotropy is observed at the moment of completion of the process of change.

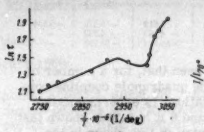

Fig. 1

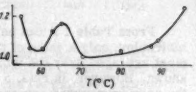

Fig. 2

Fig. 1. The relation of temperature to relaxation times of anisotropy of p-dichlorobenzene.
Fig. 2. Temperature dependence of relative intensity of scattered light for p-dichlorobenzene.

Considering that the intensity of the scattered light depends on the refractive index, we made measurements of the latter, in the same temperature range, with an Abbé refractometer. It was found (Fig. 3) that the refractive index displays an anomaly in the same range as the relaxation time. It is evident, therefore, that the anomalous behavior of the scattering intensity does not depend on the refractive index in this range.

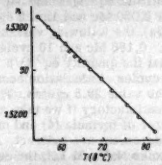

Fig. 3. The dependence of the refractive index of p-dichlorobenzene on temperature.

In conclusion, we are extremely grateful to B. M. Nosenko for constant interest in the work and for valuable advice.

REFERENCES

1. Ya. I. Frenkel', "Kineticheskaya teoriya zhidkosti" (Kinetic Theory of Liquids). 1945.
2. M. A. Leontovich, J. Phys. USSR 4, 499 (1941).
3. M. V. Vuks, Doklady Akad. Nauk SSSR 109, 5 (1956).
4. F. T. Nechai, Uchenye Zapiski Belorussk. Univ. 41 (1958).
5. F. T. Nechai, Zhur. Fiz. Khim. 31, 165 (1957).
6. S. S. Urazovskii, Zhur. Fiz. Khim. 23, 1423 (1949).
7. S. S. Urazovskii, "Molekulyarny polimorfizm" (Molecular Polymorphism). Izd. Akad. Nauk USSR, 1951.

ANALYSIS OF THE NUCLEAR MAGNETIC RESONANCE SPECTRUM OF $A_3B_2X_2$ GROUPS

V. I. Glazkov

Received 26 March 1960

The high resolution NMR spectra obtained from compounds possessing several magnetically equivalent groups, whose chemical shifts are of the same order of magnitude as the indirect spin-spin interaction between the nuclei of the different groups, have very complex structure. Therefore, to determine chemical shifts and spin-spin interaction constants from the spectral analysis it becomes necessary to calculate the energy levels and transition probabilities under the influence of the small radio frequency perturbation.

In this work we present the analysis of the spectrum of the $A_3B_2X_2$ type group (according to the classification by Pople[1]), an example of which may be given by the NMR spectrum of the molecule $(CH_3CH_2CH_2)_2O$. The analysis of this spectrum is of great interest, since it affords a means for the analysis of the spectra of more complex compounds containing the group of nuclei $A_3B_2X_2$. The complete Hamiltonian of the system is given by

$$\mathcal{H} = \mathcal{H}^0 + \mathcal{H}^1, \quad \mathcal{H}^0 = \sum_i g_i H_i I_z(i), \quad \mathcal{H}^1 = \sum_{i<j} J_{ij} I(i)\, I(j),$$

there g_i is the gyromagnetic nuclear constant, H_i, the magnetic field around the nucleus, I_i, the z component of the spin angular momentum, I(i) the angular momentum vector, and J_{ij} the spin-spin interaction constant between the nuclei i and j.

The computational analysis of the spectrum of the A_3B_2 group was made according to Pople's method.[1] The wave functions were formed from the products of the wave functions of A_3 and B_2 groups.[2] The wave functions of the group A_3 are

$$\alpha\alpha\alpha, \quad \frac{(\alpha\alpha\beta + \alpha\beta\alpha + \beta\alpha\alpha)}{\sqrt{3}}, \quad \frac{(\beta\beta\alpha + \beta\alpha\beta + \alpha\beta\beta)}{\sqrt{3}},$$

$$\beta\beta\beta, \quad \frac{(\alpha\alpha\beta + \alpha\beta\alpha - 2\beta\alpha\alpha)}{\sqrt{6}}, \quad \frac{(\alpha\alpha\beta - \alpha\beta\alpha)}{\sqrt{2}}, \quad \frac{(\beta\beta\alpha + \beta\alpha\beta - 2\alpha\beta\beta)}{\sqrt{6}}, \quad \frac{(\beta\beta\alpha - \beta\alpha\beta)}{\sqrt{2}},$$

and of the group B_2

$$\alpha\alpha, \quad \frac{(\alpha\beta + \beta\alpha)}{\sqrt{2}}, \quad \frac{(\alpha\beta - \beta\alpha)}{\sqrt{2}}, \quad \beta\beta.$$

The rules of Corio[3] were used besides the other well-known rules for the calculation of matrix elements. The energy levels and the wave functions were found by the solution of the secular equations. The calculated spectrum of the A_3B_2 group was found to be in good agreement with the data of Garvey and Slomp.[4]

The calculation of the X_2 group spectrum was made by Anderson's method.[5] The transition frequencies were calculated from the formula

$$\omega = \omega_X + J_{BX} m_B + \frac{J_{BX}^2}{2(\omega_X - \omega_B)} \{I_B(I_B+1) - m_B(m_B+1) + 2m_X m_B\},$$

and intensities, with the help of the expression

$$(I_X - m_X + 1)(I_X + m_X)\left\{1 - \frac{2J_{BX}}{\omega_X - \omega_B} m_B\right\},$$

where ω_X, ω_B are frequencies for the nuclei of X_2 and B_2 groups respectively; I_X, I_B are the total spin quantum numbers of the X_2 and B_2 groups; m_X, m_B are their projections; and J_{BX} is the constant of spin-spin interaction between the groups X_2 and B_2.

The calculated frequencies and intensities of X_2 group are in good agreement with experiment. The perturbation of the frequency ω_{AB} of the A_3B_2 group by the interaction with the X_2 group was treated by first order perturbation theory. The frequency was determined from $\omega_{AB} + J_{BX} m_X$.

The ratio of the intensities is 1:2:1. The interaction constants J_{AB} and J_{BX} were taken to be positive. The determination of the relative signs of the J_{AB} and J_{BX} constants may be made by taking into consideration the perturbation of the ω_{AB} frequency by X_2 in the second order approximation, provided the spectrum is sufficiently resolved. As an example, we made an analysis of the spectra of the $CH_3CH_2CH_2Br$ and $(CH_3CH_2CH_2)_2O$ molecules from the catalog of Humble Oil and Refining Company. The calculated and experimental spectra are in good agreement with the values of spin-spin interaction constants and chemical shifts shown in the table.

Compound	$\nu_{CH_3-CH_2}$ (cps)	$\nu_{CH_2-CH_2}$ / $\nu_{CH_2-CH_3}$ (cps)	$J_{CH_3-CH_2}$ (cps)	$J_{CH_2-CH_2}$ (cps)	$J_{CH_2-CH_3}$ / $J_{CH_3-CH_3}$	$J_{CH_2-CH_2}$ (cps)
$CH_3CH_2CH_2Br$	25.1 ± 1.5	0.27 ± 0.02	7 ± 0.5	45.7	0.137	6.26
$(CH_3CH_2CH_2)_2O$	18.6 ± 1.5	0.38 ± 0.02	7 ± 0.5	53.3	0.11	5.8

REFERENCES

1. J. A. Pople, W. G. Schneider, and H. J. Bernstein, Can. J. Chem. 35, 65 (1957).
2. H. M. McConnell, A D McLean, and C. A. Reilly, J. Chem. Phys. 23, 1152 (1955).
3. P. L. Corio, J. Chem. Phys. 29, 682 (1958).
4. B. R. McGarvey and G. Slomp, J. Chem. Phys. 30, 1586 (1959).
5. W. Anderson, Phys. Rev. 102, 151 (1956).

THE POLARIZABLE POINT LATTICE APPROXIMATION IN THE THEORY OF IMPURITY CENTERS IN IONIC CRYSTALS

I. V. Abarenkov

Received 4 April 1960

A rigid point lattice approximation has been widely used[1,2] for some time for calculations on the simplest impurity centers—color centers in alkali halide crystals. This approximation, attractive in its simplicity, makes it possible to explain some general regularities in the properties of color centers (for example Mollwo's[2] relation). However it is impossible to determine many characteristics of centers such as the width of absorption and emission lines, Stokes' displacement, etc., by the rigid point lattice approximation, since it ignores lattice vibrations. Apparently the rigid point lattice approximation is adequate only for impurity centers with small radii, and only in cases where the charge of the impurity center is the same as the charge of the ion it replaces.

Another approximation, which we will call the polarizable point lattice approximation, is presented below in general outline. It is just as simple as the rigid point lattice approximation but takes the movement of ions into account. A detailed exposition of the method as it applies to F centers in alkali halide crystals will be published in the Bulletin of the Leningrad State University. Some data on this method can also be found in ref. 3.

Let us consider a crystal with impurity centers as a system consisting of n electrons and N nuclei. The wave function of such a system $\Psi(r_1, \ldots, r_n, R_1, \ldots, R_N)$ must satisfy the equation

$$(H_1 + H_2 + H_3)\Psi = E\Psi, \tag{1}$$

where

$$H_1 = -\sum_{i=1}^{n} \frac{\hbar^2}{2m} \Delta_{r_i},$$

$$H_2 = -\sum_{p=1}^{N} \frac{\hbar^2}{2M_p} \Delta_{R_p},$$

$$H_3 = \sum_{i,\, k=1}^{n} \frac{e^2}{|r_i - r_k|} + \sum_{p,\, q=1}^{N} \frac{Z_p Z_q e^2}{|R_p - R_q|} - \sum_{i=1}^{n} \sum_{p=1}^{N} \frac{Z_p e^2}{|r_i - R_p|}.$$

It is expedient to solve this problem in the adiabatic approximation, i.e., to represent the wave function of the system in the form

$$\Psi_{an}(r_1, \ldots, r_n, R_1, \ldots, R_N) = \Psi_a(r_1, \ldots, r_n | R_1, \ldots, R_N)\, \Phi_{an}(R_1, \ldots, R_N),$$

where

$$(H_1 + H_2)\Psi_a = E_a(R_1, \ldots R_N)\Psi_a, \tag{2}$$

$$(H_2 + E_a(R_1, \ldots R_N))\Phi_{an} = E_{an}\Phi_{an}. \tag{3}$$

A knowledge of the explicit form of the function $\Psi_a(r_1, \ldots, r_n | R_1, \ldots, R_N)$ is not required for calculating a number of the energy characteristics of the impurity centers (such as the optical absorption and emission spectra, dissociation energy, etc.). This only requires a knowledge of the adiabatic potential E_a, which is usually obtained by solving Eq. (2) approximately. However, an approximate value of $E_a(R_1, \ldots, R_N)$—the energy of the system with stationary nuclei—can be determined from any of the models of the system under consideration. If the model used is physically correct, then the value E_a obtained in this way will correspond to some function Ψ_a which is an approximate solution of Eq. (2). Proceeding by this method and plotting E_a, we learn that the system in question consists of impurity centers and a series of almost closed subsystems—of ions.

Let us consider the various components of E_a separately. We define the energy of the impurity center and the main part of the interaction energy of the impurity center with the crystal as the energy of the impurity center in a field of point charges which are located at the sites of the nuclei of the corresponding ions. This energy is the eigenvalue of the equation

$$\left(H - \sum_{i=1}^{n'} \sum_{p=N'+1}^{N} \frac{e_p}{|r_i - R_p|} + \sum_{p=1}^{N'} \sum_{q=N'+1}^{N} \frac{e_p e_q}{|R_p - R_q|}\right) \times \Psi_a(r_1, \ldots, r_{n'} | R_1, \ldots, R_N) = E_a^{(2)}(R_1, \ldots, R_N)\Psi_a(r_1, \ldots, r_{n'} | R_1, \ldots, R_N), \tag{4}$$

where H is the Hamiltonian operator of the free impurity center, e_p denotes the charge of ion p, n′ if the number of electrons, and N′ is the number of impurity center nuclei.

Hereafter, we will use the atomic system of units. The energy of the ions constituting the crystal can be found from perturbation theory, taking the functions corresponding to free ions as the zero approximation functions. In this connection, we make use of the fact that the ions are almost closed subsystems. We represent this energy, which depends on the coordinates of the ions, as the sum of a certain constant term which is of no interest here, a first order term related to the interaction energy of the ions (given by Eq. (4)), and a second order term related to the interaction energy of the ions with each other and with impurity centers. The first order term represents the average value of the interaction energy computed from the free ion functions. This value can be represented[4] in the form

$$E^{(1)}(R_{N'+1}, \ldots, R_N) = \frac{1}{2} \sum_{p,\, q=N'+1}^{N} [W_1(R_p - R_q) + W_2(R_p - R_q)]. \tag{5}$$

where $W_1(R_p - R_q)$ is the Coulomb interaction energy of the ions p and q as point charges of value e_p and e_q, and $W_2(R_p - R_q)$ is an additional term which can be considered as a repulsion energy of the ions p and q.

The term which is quadratic in the interaction energy is written approximately, considering only the Coulombic interaction (i.e., the small exchange term is neglected), and assuming that the electrostatic field strength produced in the region occupied by the ion p by all of the remaining ions and impurity centers is constant and equal to B_p—the strength of the field produced in the center of

the ion p by point charges and impurity centers. Then this term can be represented in the form

$$E_a^{(2)}(R_{N'+1}, \ldots, R_N) = -\frac{1}{2}\sum_{p=N'+1}^{N} \alpha_p E_p^2, \qquad (6)$$

where the polarizability of the ion p is designated by α_p.

Thus for the adiabatic potential we finally obtain

$$E_a = E^{(1)} + E_a^{(2)} + E_a^{(3)}. \qquad (7)$$

The adiabatic potential (7) corresponds to the following model of the impurity centers: the crystal consists of "point ions" which are characterized by a charge e_p, a mass M_p, and a polarizability α_p, equal to the charge, mass, and polarizability of the ion in question. The usual coulomb forces and certain repulsive forces act between the "point ions." In addition to this, point dipoles are formed in each "point ion" by the action of the electric field. N' "point ions" are removed from a crystal of this kind and are replaced by impurity centers.

Knowing the adiabatic potential E_a, we can solve Eq. (3) and determine all of the energy characteristics of the impurity centers that concern us. Computations were carried out for the simplest impurity centers—F centers in alkali halide crystals—using the method stated above. The characteristics of an F center in an NaCl crystal at 0°K, which were obtained as a result of these calculations are shown in the Table. It also turned out that the luminescence should not be polarized above 20°K.

Energy characteristic	Calculated	Experiment
Absorption band maximum	2.3	2.7
Emission band maximum	1.0	1.1
Half-width of the absorption band	0.2	0.3
Dissociation energy of the ground state	2.6	—
Dissociation energy of the excited state	0.5	0.3

Note: All values are given in ev.

The results of the calculations for the F centers—the impurity center in which the influence of the crystal is strongest—show that the polarizable point lattice approximation apparently makes it possible to correctly determine the basic characteristics of the impurity center.

The author takes this opportunity to express his profound gratitude to M. I. Petrashen' for many discussions of this work.

REFERENCES

1. B. Gourary and F. Adrian, Phys. Rev. 105, 1180 (1957); B. Gourary and P. Luke, Phys. Rev. 107, 960 (1957); B. Gourary, Phys. Rev. 112, 337 (1958).
2. I. V. Abarenkov, Izvest. Akad. Nauk SSSR, Ser. Fiz. 22, 1320 (1958); I. V. Abarenkov, Vestnik Leningrad. Gosudarst. Univ. No. 22, 14 (1958).
3. I. V. Abarenkov, Kand. diss., Leningrad. Gosudarst. Univ., 1959.
4. P. O. Löwdin, Thesis, Uppsala, 1948.

THE LUMINESCENCE OF THALLOUS CHLORIDE

V. A. Sokolov and N. A. Tolstoi

Received 16 April 1960

1. At the present time there is very little information available on the luminescence of thallium chloride [1-4] and the various theories about the nature of this luminescence[2-4] are contradictory. In this connection it seemed of interest to conduct an investigation of the luminescence of thallous chloride on monocrystalline specimens in a controlled environment (for example, in an inert-gas atmosphere or in vacuum). In the present communication we present a few results of work along these lines.

The monocrystals were grown by means of a modified Stockbarger technique[5,6] in sealed Pyrex ampoules. The initial preparation of thallous chloride was first submitted to a double recrystallization in distilled water of high purity ($\sigma \approx 10^{-6}$ ohm^{-1}cm^{-1}). Before growing the crystals, the purified powder was heated in vacuum at 200-220°C for 3-4 hr in order to assure the complete removal of all traces of water. The specimens for investigation were sawn out of the monocrystals obtained (weight about 100 gm) and had the dimensions 1.5 × 10 × 15 mm. They were polished on flannel in a saturated aqueous solution of thallous chloride and then dried in vacuum at 110°C for three or four hours.

All work with thallous chloride, beginning with the preliminary purification of the powder and ending with the preparation of the specimens, was carried out in red light ($\lambda > 600$ mμ). Luminescence measurements were conducted by transmitted light. Hg 365 mμ radiation, isolated by means of a glass filter from the radiation of a SVDSh-250 lamp, was used for excitation. The spectral energy distribution was recorded with the aid of a UM-2 monochromator, an FEU-22 photomultiplier, and an M-95 microammeter. During the measurements the samples were kept in an atmosphere of pure helium. The thermal treatment of the crystals was conducted in darkness in all cases.

2. The measurements showed that a monocrystal of thallous chloride, cooled after growing to a temperature below −100°C, has a blue luminescence band with a maximum near 460 mμ and a half-width of about 55 mμ (see Fig. a, curve 1). If the temperature is lowered further, the intensity of the luminescence increases. The long wavelength side of the luminescence has a more gentle slope than the short wavelength side and changes to a slowly declining "tail."

3. Prolonged exposure of the sample to 365 mμ mercury radiation at a temperature below −150°C does not change the emission. However, exposure to the same light at higher temperatures leads to a reduction in the intensity of the blue luminescence throughout the whole band. (The luminescence measurement was always conducted at liquid nitrogen temperature.) Curve 2 in Fig. a represents the luminescence of the specimen after exposure to 365 mμ radiation for 10 sec at room temperature (during which the illumination on the surface of the specimen was of the order of 0.05 watt/cm^2). It is easy to see that the intensity of luminescence decreased sev-

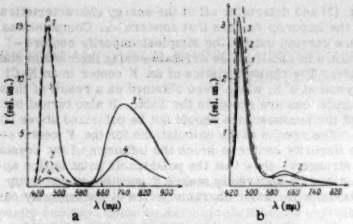

Luminescence of monocrystals of thallous chloride at liquid nitrogen temperature.
a: Curve 1—before exposure; curve 2—same sample after exposure to 365 mμ light at room temperature for 10 sec; curve 3—after heating a monocrystal at 250°C in helium atmosphere under a pressure of 1 mm Hg; curve 4—the same sample after exposure to 365 mμ light at room temperature for a few seconds.
b: curve 1—deformed crystal; curve 2—the same sample after remaining in the dark at room temperature for 14 hr; curve 3—the same sample after heating in an atmosphere of pure helium at 100°C for 15 min.

eralfold after exposure. Measurements of luminescence intensity I as a function of the time t of exposure to 365 mμ radiation showed that I decreases with increasing t according to the hyperbolic law

$$I = \frac{I_0}{(1 + At)},$$

where I_0 is the initial intensity and A is a constant that depends on the intensity of the exposure.

In a parallel measurement of the transmission of Hg 436 mμ radiation by the sample, it was established that the transmission did not change significantly in this region of the spectrum after exposure, and hence the weakening of the luminescence cannot be explained by any kind of "filter" effect. Apparently, the change in luminescence on exposure is a consequence of the appearance of quenching centers or the destruction of existing luminescence centers. Since the thallium halides are somewhat similar to the silver halides in their photochemical properties, one cannot eliminate the possibility that the change of luminescence intensity on exposure is associated with the appearance of pre-centers or sub-centers[7] of a latent image, which can also act as centers for the quenching of luminescence. If this is so, then luminescence can serve as a method of control for the formation and disappearance of these centers.

4. The decrease in luminescence intensity on exposure is a reversible process: When the exposed sample is kept in the dark, the luminescence almost regains its former intensity; the re-establishment proceeds with greater speed as the temperature is raised. At temperature lower than −150°C the rate of recovery is close to zero.

5. After the samples are heated to 250-350°C in a dry atmosphere of pure helium at a pressure of 1-10 mm Hg, the intensity of the blue band diminishes and a wide red band appears, with a maximum near 740 mμ. Both the diminution in intensity of the blue band and the increase in intensity of the red band are favored by prolonged heating.

The heat treatment of the crystal is accompanied by two processes: partial sublimation of the sample and the loss of chlorine. Grinding and polishing the surface of a crystal having both emission bands, while markedly weakening the intensity of the band at 740 mμ, does not eliminate it entirely. This suggests that the band mentioned occurs as a result of the loss of chlorine from the crystal. It should be noted that upon heating unexposed monocrystalline samples of TlCl (previously annealed in vacuum at 150°C for 3 hr) at temperatures near the melting point (390-400°C) in an atmosphere of dry air, the luminescence band with a maximum near 740 mμ does not appear. This result contradicts refs. 3 and 4.

On exposure of samples characterized by the two luminescence bands to 365 mμ radiation, the intensity of both bands decreases the intensity of the blue band falling considerably more rapidly. In Fig. a, curve 3 corresponds to the luminescence of the sample before exposure, curve 4, after exposure. In the case shown, the intensity of the blue luminescence peak decreases fifteenfold, whereas the intensity of the red peak decreases only 2.6 fold.

6. The luminescence spectrum of monocrystalline TlCl changes after plastic deformation. In Fig. b, curve 1 shows the luminescence spectrum of a monocrystalline sample submitted to plastic deformation (stress about 80 atm for 10 sec; crystal compressed between two parallel Pyrex plates). As can be seen from the figure, this is accompanied by the appearance of an orange emission band with a maximum near 620 mμ, while the intensity of the blue band decreases. If the deformed crystal is then kept in the dark for several hours (at 20°C), the intensity of the orange luminescence decreases and that of the blue increases (curve 2 in Fig. b).

7. The results presented point toward the following conclusions:

(a) The blue luminescence of TlCl is inherent in the pure crystal and occurs as a consequence of structural defects, the number of which depends on the thermal history of the specimen.

(b) With suitable treatment of the crystal, it is possible to observe several long wavelength luminescence bands. One of these, with its maximum near 620 mμ, is associated with the appearance of mechanical defects during plastic deformation. The other, whose maximum is in the 740 mμ region, occurs as a result of a chlorine deficiency in the crystal.

(c) Exposure to ultraviolet light at temperatures above −150°C and heating in darkness have opposite effects on the luminescent intensity of the crystal. This result also contradicts refs. 3 and 4. It is possible that the re-establishment of the luminescent intensity of exposed samples which occurs when they are kept in the dark at and above room temperature occurs as a results of the destruction of quenching centers.

The present short communication has presented the preliminary results of our systematic investigation of the luminescence properties of thallous chloride. We propose to give further details in subsequent publications.

REFERENCES

1. J. T. Randall, Trans. Faraday Soc. 35, 6 (1939).
2. H. Gobrecht and F. Becker, Z. Physik 5, 553 (1953).
3. A. S. Vysochanskii, Kand. Diss., Odessa, 1953.
4. A. S. Vysochanskii, Doklady Akad. Nauk SSSR 112, 228 (1957).
5. D. C. Stockbarger, J. Opt. Soc. Am. 39, 731 (1949).
6. G. Bakli, "Rost. kristallov" (Crystal Growth). Izd. Inostrannoi Lit., Moscow 1954.
7. J. W. Mitchell, Rep. Progr. Phys. 20, 433 (1957), (Russian translation in: Uspekhi Fiz. Nauk 67, 294 (1959).

OPTIMUM CONDITIONS FOR THE MEASUREMENT OF THE WIDTH OF ABSORPTION BANDS

G. G. Petrash

Received 31 March 1960

It is known that the accuracy of measurements of absorption band parameters is a function of conditions under which the spectrum was recorded (i.e., the width of the monochromator slit, the rate of scanning), of the thickness of layer of the substance under investigation, or of the magnitude of the absorption (see ref. 1). When the optical density and the width of absorption bands are being measured simultaneously, it is interesting to compute the error of the bandwidth determination, find optimum conditions for this measurement, and then compare these with the optimum conditions for the measurement of optical density.

We shall consider here only the case of small systematic errors and assume that no idealization is to be employed. We shall use an equation derived in ref. 2 which gives a first approximation to the shape of an observed band h(λ),

$$h(\lambda) = \varphi(\lambda) + \varphi''(\lambda)\{aS^2 + b\tau^2v^2\}. \qquad (1)$$

Here, $\varphi(\lambda)$ is the true distribution; S is the width of the instrument function, assumed to depend on the slit width only, and slit widths assumed to be kept equal; τ and v are, respectively, the time constant of the recording system and the velocity of scanning; a and b are parameters, dependent on the shape of the instrument function and the shape of the transient function of the recording system, respectively.

To compare absorption bandwidth γ_x, with the optical density bandwidth γ_D, the conversion method proposed by Smirnov[3] will be used. Its mathematical expression is

$$\gamma_x = \gamma_D N(x_0). \qquad (2)$$

Here, x_0 is the absorption at the band's maximum and the $N(x_0)$ function is dependent on the shape of the absorption band. using the above relationship and assuming that the bandwidth error is negligible, we may write, as a first approximation,

$$E^2 = \frac{\overline{\Delta\gamma_D^2}}{\gamma_D^2} = L(x_0)\left[V^2(x_0)\{az^2 + by^2\}^2 + \frac{U}{y^{2r}}\right]. \qquad (3)$$

The symbols here are the same as in ref. 2, i.e.,

$$z = \frac{s}{\gamma_D}; \quad y = \frac{\tau v}{\gamma_D}; \quad u = \frac{Ev}{\gamma_D^5}$$

(the parameter E is determined by the noise level of the instrument); $L(x_0)$ and $V^2(x_0)$ are functions of x_0 only.

The above equation differs from that given in ref. 2 for computation of the error in optical density measurements merely by the manner in which $L(x_0)$ and $V^2(x_0)$ are expressed. Therefore, the optimum conditions for bandwidth measurements will differ from the optimum conditions for measurement of the optical density in only their dependence on x_0. The relationship between the optimum slit width and the time constant is retained, viz.,

$$\tau_{m\gamma} = \frac{S_m}{2}\sqrt{a/b}.$$

and the relationship between the optimum slit width and x_0 will be determined by the expression

$$z_m = \frac{S_m}{\gamma_D} = \left(\frac{8U}{5a^2V^2(x_0)\sqrt{a/b}}\right)^{1/9}. \qquad (4)$$

This equation is the same as used in optical density measurements, except that in the latter case V^2 is replaced by the product r^2x^2. When x_0 values are close to the optimum, computations based on the assumption that the absorption shape has a dispersed form show that this small difference between the two equations has but a little effect upon the magnitude of z_m.

On the basis of the equations derived above, and taking into consideration results obtained in ref. 2, the following might be recommended for the selection of conditions for the recording of spectra: (1) When spectra are recorded for measurements, the thickness of the sample should be such that $0.5 < x_0 < 0.7$; (2) the time constant τ and the scanning rate v should be selected so that the systematic error due to scanning is small, i.e., the product τv should be about 5 to 10 times smaller than S; (3) the optimum slit width might be computed by means of equations given in ref. 2.

When above recommendations are followed, the measurement error will be held close to a minimum value, both for the band width and for the optical density measurements.

The author wishes to use this opportunity to express his gratitude to P. A. Bazhulin for his constant interest in this work, and to V. I. Malyshev and S. G. Rautian for their valuable discussion of results.

REFERENCES

1. S. G. Rautian, Uspekhi Fiz. Nauk **66**, 475 (1958).
2. G. G. Petrash, Opt. i Spektr. **6**, 792 (1959), Optics and Spectroscopy **6**, 516 (1959).
3. V. N. Smirnov, Vestnik Moskovsk. Univ., Ser. Mat. No. 1, 61 (1959).

OPTICAL SOCIETY *of* AMERICA

ANNOUNCEMENT OF PROGRAM AND REQUEST FOR CONTRIBUTED PAPERS

OSA-SPRING 1961 MEETING

PICK-ROOSEVELT HOTEL, PITTSBURGH, PA.

THURSDAY, FRIDAY, SATURDAY, MARCH 2, 3, and 4

The Spring 1961 Meeting of the Optical Society of America will be held in Pittsburgh, Pennsylvania, in part concurrently with the Pittsburgh Conference on Analytical Chemistry and Applied Spectroscopy.

INVITED PAPERS: A jointly-sponsored Symposium on the topic "New Frontiers in Optics and Spectroscopy" will be held on Thursday morning, March 2, in the Penn-Sheraton Hotel. It will consist of the following papers:

"Optical and Infrared Masers" by Charles H. Townes (of Columbia University and) Institute for Defense Analyses, 1710 H Street, N.W., Washington 6, D. C.
"Spectroscopic Studies in the Thermonuclear Field at the Oak Ridge National Laboratory" by J. R. McNally, Jr. and co-authors, Thermonuclear Div., Oak Ridge National Laboratory, Oak Ridge, Tennessee
"New Frontiers of Astronomical Optics" by A. B. Meinel, Kitt Peak National Observatory, Tucson, Arizona

There will also be Invited Papers in other areas such as "Optics in Japan", "Optical Workshop Practice", "Modern Methods of Lens Design", and possibly others.

CONTRIBUTED PAPERS: It is hoped that the Invited Papers will encourage presentation of many Contributed Papers in these areas, as well as in any other areas of interest to OSA members.

ABSTRACT FORM: To present a Contributed Paper, the author must submit the Title plus an Abstract (no longer than 200 words) on the standard Abstract Form (in duplicate, carbon copy will do) by December 29, 1960, to:

OSA Executive Office
1155 - Sixteenth Street, N. W.
Washington 6, D. C.
Attn: Mary E. Warga

INSTRUMENT EXHIBIT: One of the great advantages of meeting jointly with the Pittsburgh Conference is the large Instrument Exhibit at the Penn-Sheraton Hotel, which is held annually in connection with the latter meeting. The exhibits will cover instruments in the areas of optics, emission spectroscopy, ultraviolet, infrared, mass spectroscopy, fluorescence, spectrophotometry, as well as spectrochemical analysis. Many manufacturers use this opportunity to introduce to the scientists new designs of optical equipment. After the Symposium on Thursday morning it will be possible for OSA members to visit this Instrument Exhibit, using their OSA registration badges as permits to enter.

HOTEL ROOM RESERVATIONS: The Headquarters Hotel for the OSA members will be the Pick-Roosevelt Hotel on Penn Avenue in downtown Pittsburgh. A concurrent meeting with the Pittsburgh Conference means crowded hotel conditions. For this reason, please use the Hotel Room Reservation Card from the Pick-Roosevelt Hotel. Make your room reservation as early as possible stating that you are attending the Optical Society of America Meeting there. This will give you preference in hotel room reservations at this hotel.

REMINDER: Make hotel room reservation immediately. Remember the Christmas mail rush and send in Abstract before December 29, 1960.

MARY WARGA, Executive Secretary

FILLER MATERIAL - NOT IN RUSSIAN ORIGINAL

OPTICAL SOCIETY of AMERICA

FUTURE MEETINGS

PITTSBURGH, March 2, 3, and 4, 1961

PICK-ROOSEVELT HOTEL

A symposium, New Frontiers in Optics and Spectroscopy, jointly sponsored by OSA and the Pittsburgh Conference on Analytical Chemistry and Applied Spectroscopy, will be held March 2 in the Penn-Sheraton Hotel.

LOS ANGELES, October 18, 19, 20, 1961

BILTMORE HOTEL
Details to be announced.

WASHINGTON, D. C., March 15, 16, 17, 1962

Jointly with Inter Society Color Council and National Academy of Sciences Vision Committee. Hotel to be announced.

ROCHESTER, N. Y., October 4, 5, 6, 1962

MANGER HOTEL

There will probably be exhibits at this meeting.

Papers are now being solicited for the Pittsburgh meeting. Duplicate copies of Abstract (no longer than 200 words) and Title should be submitted by December 29 to OSA Executive Office, attention Mary E. Warga. Copies of the Abstract forms may be obtained from Dr. Warga.

Information about later meetings will be announced as soon as possible.

Executive Office
1155 Sixteenth Street, N. W.
Washington 6, D. C.

FILLER MATERIAL - NOT IN RUSSIAN ORIGINAL

OSA CHARTER FLIGHT 1961

EUROPE JULY 1961

You will have read in JOSA that OSA hopes to arrange a charter flight to Europe for the month of July 1961, for members attending the Paris and London ICO Meetings. These are:

PARIS: 5 through 8 July 1961 on OPTICAL MATERIALS, organized by the French National Committee for Optics and Professor André Maréchal

LONDON: 11 through 14 July 1961 on OPTICAL INSTRUMENTS AND TECHNIQUES, organized by a sub-committee of the British National Committee for Optics under the chairmanship of Mr. K. J. Habell

We contemplate a flight leaving New York (Idlewild) on Saturday 1st July for PARIS, and returning from LONDON Airport on Sunday July 30th to New York. Members would make their own way between Paris and London. Informal tours of laboratories in Paris and London may be arranged. It is necessary to make arrangements for such flight within the next month or two, so we need now an expression of interest (without commitment, of course) from members. Members who are interested in principle should return the bottom half of this page to the Executive Office as soon as possible, or hand it in at the Registration Desk during the course of the Boston Fall Meeting. The round trip fare—New York - Paris - London - New York—would be about $275.

MEMBERS WHO HAVE ALREADY INDICATED THEIR INTEREST
NEED NOT WRITE AGAIN

REPLY

CHARTER FLIGHTS JULY AND OCTOBER 1961

I am interested in principle in a charter flight N.Y.-Paris-London-N.Y. July 1961 ☐

Name _____ Membership No. _____

Address _____

OPTICAL SOCIETY OF AMERICA
Executive Office
1155 Sixteenth Street, N.W.
Washington 6, D. C.

FILLER MATERIAL—NOT IN RUSSIAN ORIGINAL

THE OPTICAL SOCIETY OF AMERICA

Why should you join OSA?

There is no other association of opticists in existence to promote and disseminate knowledge in this field. The Optical Society of America was organized in 1916 "to increase and diffuse the knowledge of optics in all its branches pure and applied, to promote the mutual interests of investigators of optical problems, of designers, manufacturers and users of optical instruments and apparatus of all kinds, and to encourage co-operation among them".

What about the advantages of membership?

You receive three monthly publications:

THE JOURNAL OF THE OPTICAL SOCIETY OF AMERICA: *This is the official publication of OSA*

OPTICS AND SPECTROSCOPY: *an English translation of the leading scientific journal of the USSR Academy of Sciences in this field*

PHYSICS TODAY: *as OSA is a member society of the American Institute of Physics, OSA members receive this publication**

From JOSA and OPTICS AND SPECTROSCOPY you will not only learn what your American colleagues are doing, but also discover what the Russians are working on in your field. Together these two journals publish the work of American and Russian scientists in all branches of optics and spectroscopy, including X-ray, ultraviolet, visible, infrared and microwave, filters, lens design, thin layer optics, geometric optics, electron optics, diffraction gratings, electroluminescence, wave mechanics, thermal radiation backgrounds, detectors, infrared polarizers, and their many applications in science and industry.

You will also receive announcements and programmes of all meetings (OSA holds at least two a year) and, even if you cannot attend many of these, you will know what is going on in your area. And you can submit a paper and have it given by proxy.

Who can join?

OSA invites to membership all who are interested in any branch of optics, either in research, in teaching, in optical applications, in the manufacture and distribution of optical equipment of all kinds, or in physiological and medical optics.

What are the membership dues? $13.00 per annum.

How can you join?

Write Dr. Mary E. Warga, Executive Secretary, Optical Society of America, 1155 16th Street, N. W., Washington 6, D. C., for an application form.

*OSA members may also subscribe to other AIP publications at a reduced rate.

OPTICAL SOCIETY *of* AMERICA

1155 SIXTEENTH STREET, N. W. WASHINGTON 6, D. C.

(FILLER MATERIAL - NOT IN RUSSIAN ORIGINAL)

EDITOR'S NOTE

Comments on the scientific content of the translated Russian articles published in OPTICS AND SPECTROSCOPY are invited. They should be addressed as a Letter to the Editor of the Journal of the Optical Society of America and forwarded to the Editor of that journal, Dr. W. R. Brode, National Bureau of Standards, Washington 25, D.C.

VOL. IX, NO. 3 [redacted] PTEMBER 1960

CONTENTS

(Numbers in parentheses are original Russian page numbers)

Concentration of Atoms in the Arc Plasma as Determined by the Pulse Absorption Method ..... L. D. Kondrasheva and I. V. Podmoshenskii 149 (281)

Investigation of a High-Frequency Discharge with Hydrodynamic Compression ..... Zh. Zheenbaev 152 (288)

Calculation and Interpretation of the Vibrational Spectra of Biphenyl and Some of its Deuterium Substitution Products ..... G. V. Peregudov 155 (295)

Vibrational Spectra of Unsaturated Hydrocarbons VIII. Vibrational Spectra and Rotational Isomerism of 1,3-Butadiene ..... L. M. Sverdlov and N. V. Tarasova 159 (304)

Vibrational Spectra of Aromatic Compounds VII. Characteristic Vibrations of Monosubstituted Benzenes ..... A. M. Bogomolov 162 (311)

Theory of the Vibrational Spectra of Polymers II. Torsional Skeletal Vibrations in Syndiotactic Polymer Chains ..... Yu. Ya. Gotlib 166 (319)

The Vibrational Spectra of Pyrophosphates ..... A. N. Lazarev and V. S. Aksel'rod 170 (326)

Spectroscopic Study of the Molecular Structure of Guanyl-Urea and Biuret ..... B. I. Sukhorukov and A. I. Finkel'shtein 172 (330)

Infrared Spectra of Heteropoly-Compounds and Their Structure ..... G. V. Yukhnevich 174 (335)

The Kinetics of the Concentration Depolarization of Luminescence and of the Intermolecular Transfer of Excitation Energy ..... P. I. Kudryashov, B. Ya. Sveshnikov, and V. I. Shirokov 177 (341)

Study of the Phosphorescence Lifetimes of Solutions of Organic Compounds at −196° ..... E. N. Viktorova, I. A. Zhmyreva, V. P. Kolobkov, and A. A. Saganenko 181 (349)

Influence of the Hydrogen Bond on the Probability of Internal Conversion to the Triplet Level in the Quinoline Molecule ..... V. L. Ermolaev and I. P. Kotlyar 183 (353)

An Electron Paramagnetic Resonance Investigation of the Valence Change of the Activator During Excitation of the Phosphor SrS-Eu,Sm ..... V. G. Dubinin and Z. A. Trapeznikova 187 (360)

The Kinetics of the Short-Lived Photoluminescence of Some Activated Alkali Halide Crystals ..... I. K. Vitol and I. K. Plyavin' 189 (365)

Light Absorption by Excitons in the Cu_2O Crystal II. Absence of Constant External Fields ..... S. A. Moskalenko 192 (369)

Radiation Transfer in a Homogeneous Medium for the Nonconservative Case ..... V. I. Barkov 195 (376)

Principles of the Theory of the Synthesis of Coated Absorbing Layers ..... P. G. Kard 200 (386)

Optical Systems with Enhanced Resolving Power ..... A. I. Kartashev 204 (394)

On the Properties of the Focal Surfaces of Mirror Spectrographs ..... S. A. Khrshanovskii 207 (399)

SHORT COMMUNICATIONS

A New Band in the Absorption Spectrum of Polycrystalline Layers of Cadmium Sulfide ..... T. Ya. Soera and V. V. Serdyuk 210 (407)

The Franck-Condon Factors for the Schumann-Runge Band System in the Oxygen Molecule ..... I. T. Yakubov 212 (409)

Influence of Vibrations on the Quadrupole Coupling Constants in Alkali Halide Molecules ..... A. G. Makhanek 214 (412)

Study of Molecular Interaction in p-Dichlorobenzene Near the Freezing Point ..... A. A. Aivazova and I. A. Gorbatov 215 (415)

Analysis of the Nuclear Magnetic Resonance Spectrum of $A_3B_2X_2$ Groups ..... V. I. Glazkov 217 (417)

The Polarizable Point Lattice Approximation in the Theory of Impurity Centers in Ionic Crystals ..... I. V. Abarenkov 218 (418)

The Luminescence of Thallous Chloride ..... V. A. Sokolov and N. A. Tolstoi 219 (421)

Optimum Conditions for the Measurement of the Width of Absorption Bands ..... G. G. Petrash 221 (423)